Holmium radioembolization of liver metastases

Maarten Smits

Holmium radioembolization of liver metastases
PhD thesis, Utrecht University – with a summary in Dutch

Cover: Bokeh view on downtown Chicago with Grant Park and Millennium Park as seen from South Michigan Avenue. Chicago, Illinois, U.S. Nikon D80, Nov 29th 2011

mrtnsmits@gmail.com

ISBN: 978-90-393-6067-5
Cover design: Maarten Smits
Lay-out: Roy Sanders
Printing: Printsupport4u - Meppel

Holmium radioembolization of liver metastases

Holmium radioembolisatie voor levermetastasen

(met een samenvatting in het Nederlands)

Proefschrift

ter verkrijging van de graad van doctor aan de Universiteit Utrecht
op gezag van de rector magnificus, prof.dr. G.J. van der Zwaan,
ingevolge het besluit van het college voor promoties
in het openbaar te verdedigen
op woensdag 18 december 2013
des middags te 4.15 uur

door

Maarten Leonard Johannes Smits
geboren op 24 november 1987
te Amsterdam

Promotoren:	Prof.dr. M.A.A.J. van den Bosch Prof.dr. W.P.Th.M. Mali
Co-promotoren:	Dr. J.F.W. Nijsen Dr. B.A. Zonnenberg

The research in this thesis was financially supported by:
Alexandre Suerman stipendium · Dutch Cancer Society · Dutch Technology Foundation · Stichting Beeldgestuurde Behandelingen van Kanker

Financial support for this thesis was generously provided by:
Quirem Medical · Nucletron, an Elekta company · Oldelft Benelux · Cook Medical · Guerbet Nederland B.V. · TD Medical · Surefire Medical · Mallinckrodt · Chipsoft · Covidien · Terumo Europe N.V. · Röntgenstichting Utrecht

Contents

Part II Imaging and Dosimetry

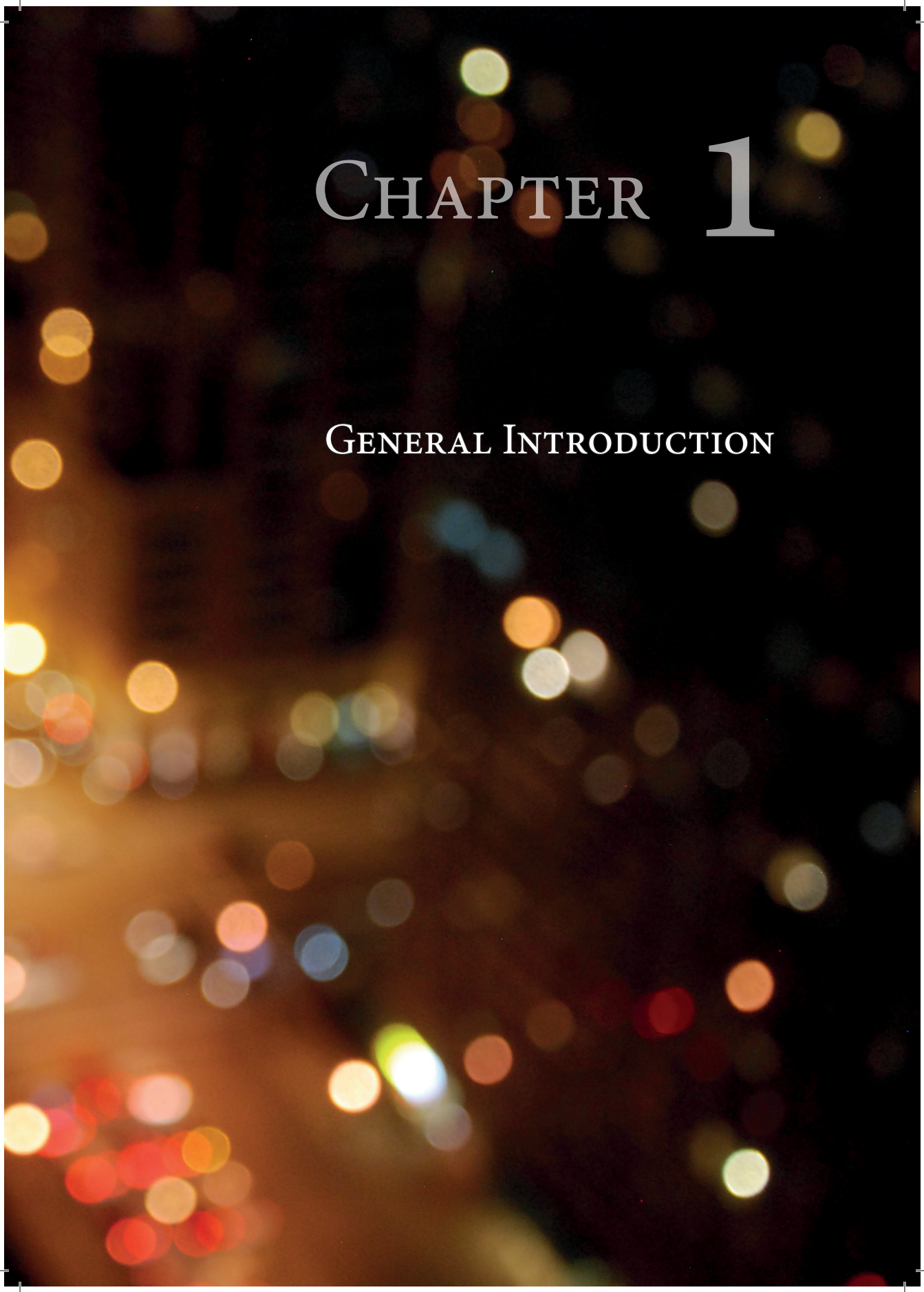

Chapter 1

General Introduction

Background, liver metastases

For many people, the liver is not the first organ that comes to mind when thinking of cancer. The most common types of cancer originate in the breast, prostate, lung and bronchus, and colorectum.[1] Cancer originating in the liver ranks 11th in the list of most frequently diagnosed cancers in the US with an estimated 30,640 new cases per year and 21,670 deaths per year in the US. The liver is even more frequently affected when looking at metastasis. Several primary tumors are known to metastasize to the liver. The liver metastases often challenge the treatment options and pose a substantial morbidity and mortality, whereas the primary tumor itself may be very well manageable. Primary tumors that commonly metastasize to the liver are colorectal carcinoma, uveal melanoma, breast carcinoma, and neuroendocrine tumors.[2,3] This thesis focuses on liver metastases in general, but it is important to note that the population of patients with liver metastases has a variety of primary tumors. There are large differences in the etiology, epidemiology and prognosis of these tumors. For this purpose, relevant information on each of these primary tumor types is provided below.

Colorectal cancer

Colorectal cancer liver metastases (CRCLM) patients constitute the majority of liver metastases patients and are therefore often chosen as the target population for studies on locoregional liver therapies.[2,3] Colorectal cancer is the fourth most frequently diagnosed cancer in the US, with an estimated incidence of 142,820 cases in 2013.[1] If the tumor remains confined to the primary site it is often curable by means of surgical resection. However, metastases arise easily with a preference to grow in the liver. A schematic overview of the treatment algorithm for patients with colorectal liver metastases is presented in *Figure 1*. At the time of diagnosis, approximately 15 – 25% of patients have liver metastases, and another 20 - 50% of patients will develop liver metastases later on during the course of disease.[4-8] The metastases are confined to the liver or are liver-dominant in approximately half of the cases.[8-10] In these patients, surgical resection is the only curative treatment option and offers a median survival of about 40 months, compared to a median survival of 18 - 24 months for chemotherapy and 6 - 12 months if patients remain untreated.[11] Unfortunately, only 15 - 25% of CRCLM patients are candidates for curative resection and another 5 - 15% can be offered adjuvant therapies such as neoadjuvant chemotherapy, radiofrequency ablation, or portal vein embolization, in order to downstage the tumor burden or increase the functional liver remnant to facilitate surgical resection.[10,12] The remainder of patients (60 - 80%) is offered palliative systemic chemotherapy.

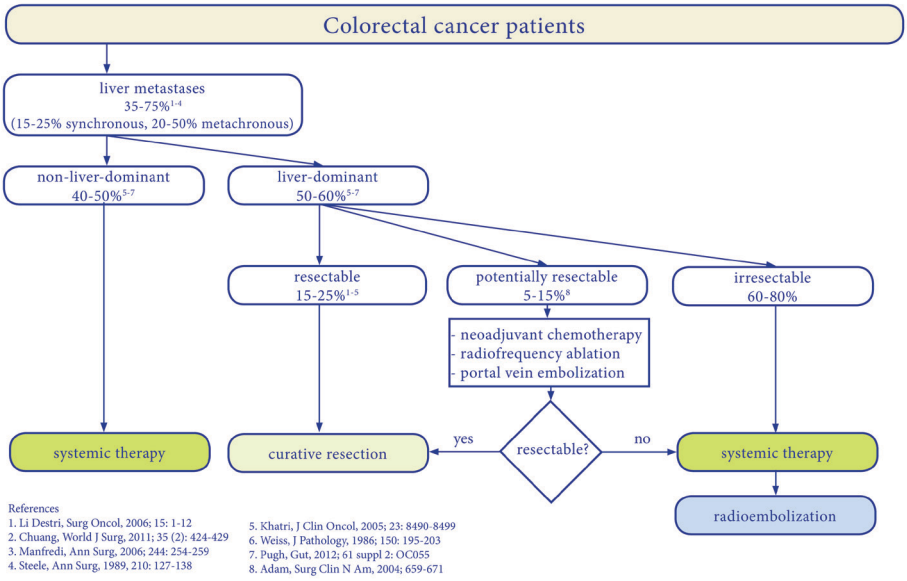

Figure 1. *Treatment algorithm for patients with liver metastases together with approximate percentages of patients following each route.*

According to the Dutch guidelines, standard first and second-line chemotherapy should consist of oxaliplatin or irinotecan-based therapy combined with fluorouracil and leucovorin.[13] Adding the vascular endothelial growth factor inhibitor bevacizumab to first line oxaliplatin-based treatment has shown little effect on tumor response or survival and is thus not recommended as standard treatment.[14] In the third line, the epidermal growth factor receptor antagonists cetuximab or panitumumab can be given to patients with wild-type KRAS gene. A schematic overview of the position of the different lines of systemic (chemo)therapy and the current position of radioembolization are presented in *Figure 2*.

Uveal melanoma

The eye is formed by three layers, of which the uvea is the middle layer. Uveal melanoma is the most common primary intraocular tumor of the eye and it represents approximately 5% of all melanoma cases.[15] Uveal melanoma can arise from melanocytes in the choroidal layer ([90]%), ciliary body (7%) or the iris (3%).[16] The liver is involved in the vast majority of patients who develop metastases from uveal melanoma and the survival of uveal melanoma patients depends largely on the presence and progression of liver metastases.[17] The median survival of patients with uveal melanoma metastasized to the liver is about 6 months.[18] The management of these patients focuses on locoregional therapies since the systemic chemotherapies used for cutaneous melanoma are

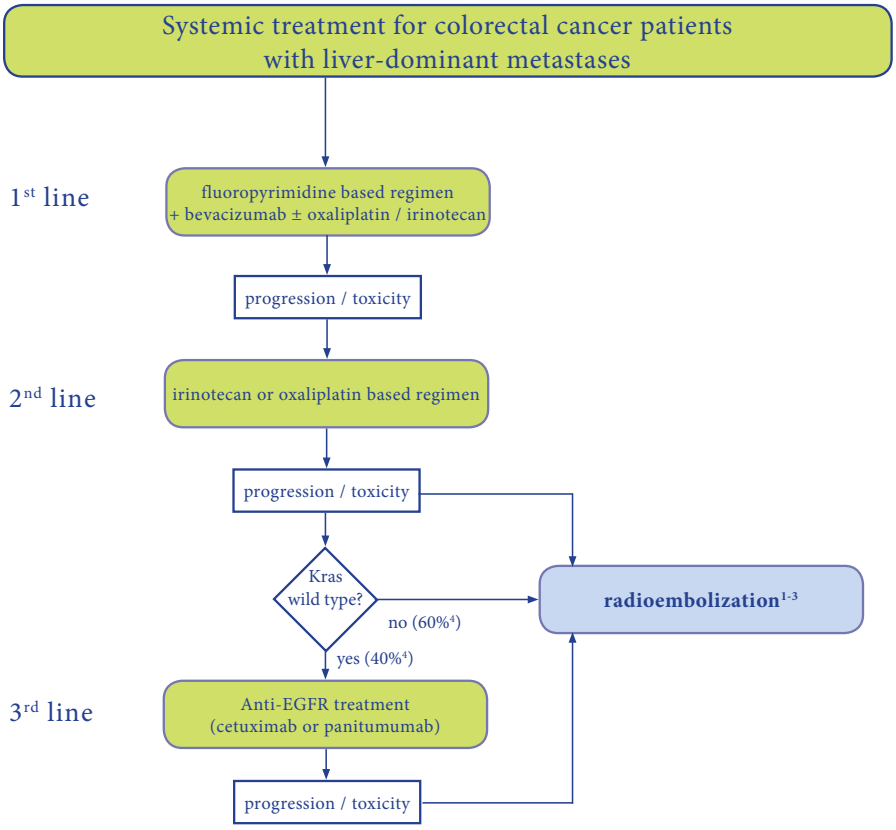

Figure 2. *Algorithm for systemic treatment (green boxes) of colorectal cancer patients displayed against the current position of radioembolization (blue box). Radioembolization is currently predominantly performed in patients who have received first and second line therapy, but radioembolization can also be performed after third line therapy. Kras = v-Ki-ras2 Kirsten rat sarcoma viral oncogene homologue gene; EGFR = epidermal growth factor receptor.*

unfortunately of little benefit for the chemoresistant uveal variant.[15,19] The tumors are, however, usually well vascularized, a feature which can be exploited by intra-vascular locoregional treatment options that will be discussed later in this chapter.

Breast cancer

Breast cancer is the most frequent type of cancer in women with an estimated incidence of 232,340 cases in the US per year.1 The liver can host metastases from breast cancer as well. In an autopsy study performed in 1973, liver metastases were found in 61% of diseased breast cancer patients.[20] At presentation, 6 - 8% of all breast cancer patients with distant metastases have metastases confined to the liver and another 26%

has metastases in the liver plus at one additional site.[21-23] The prognosis of patients with metastases confined to the liver is similar to the prognosis of colorectal liver metastases patients, with median survival ranging from 17 to 25 months.[21,22,24] Patients should be offered systemic therapy, which can consist of 1) hormonal treatment for estrogen- or progesteron-receptor positive tumors, 2) chemotherapy with a range of available drugs such as anthracycline- or taxane-based drugs, or 3) targeted therapy like trastuzumab for tumors with Her2/neu overexpression or monoclonal antibodies to inhibit vascular growth.[25] In addition, if patients are eligible, surgical resection of the liver metastases is recommended but only a minority of patients is eligible due to extent of disease. If the response of the liver metastases to systemic treatment is not adequate, locoregional treatment options such as radiofrequency ablation, chemoembolization or radioembolization may be considered.[26,27]

Neuroendocrine tumors

Approximately 10% of all liver metastases are neuroendocrine tumors.[28] The term 'neuroendocrine tumor' (NET) is used to describe tumors arising from neuroendocrine cells. A NET can be subdivided into carcinoid or islet cell tumors. The term 'carcinoid' (cancer-like) is based on the slow growth of these tumors that seems different than the typical cancerous growth. Carcinoid tumors often arise in the appendix, rectum, or small intestines. Examples of islet cell tumors are gastrinoma, insulinoma, glucagonoma, to somatostatinoma.[29] NETs can produce and release neurotransmitters and hormones into the system. Serotonin secreted by carcinoid tumors can for instance cause carcinoid syndrome including flushing and diarrhea. Effective therapy of the tumors may lead to an exacerbation of symptoms through the high-volume release of vasoactive substances during treatment. As with all types of liver metastases, neuroendocrine liver metastases should preferentially be resected, or focally treated with radiofrequency ablation. However, the majority of patients is not eligible for these curative options and are candidates for systemic therapies like somatostatin analogues (e.g. lanreotide, octreotide) or radiolabelled somatostatin analogues (*e.g.* ^{90}Y-DOTATOC, ^{90}Y-DOTATATE, ^{177}Lu-DOTATATE, or ^{131}I-MIBG).[30,31] More specifically liver-directed treatments like chemoembolization or radioembolization may be given concomitantly or after systemic treatment.[29]

Physiology and anatomy of the liver

The liver is a vital organ that performs several essential functions within the human body. The main functions are: 1) the metabolization of chemicals in the blood coming from the intestines, 2) the synthesis of several proteins and enzymes necessary for homeostatic processes such as hemostasis, 3) carbohydrate metabolism, 4) fat metabolism, 5) bile salt and cholesterol metabolism, 6) excretion of bilirubin, and 7) the storage of vital substances such as vitamin B12, iron, and copper.[32]

The blood supply of the liver is unique, consisting of blood from the portal vein and the hepatic artery. All blood leaving the intestines normally passes through the liver via the portal vein and exits the liver through the inferior vena cava. When following the branching pattern of the portal vein, the liver can be divided in eight functional segments as described by Couinaud and later modified by Bismuth (*Figure 3*).[33,34] These segments are particularly important for surgical resection but are also used in this thesis as a reference to indicate the location or distribution of lesions / particles within the liver.[35]

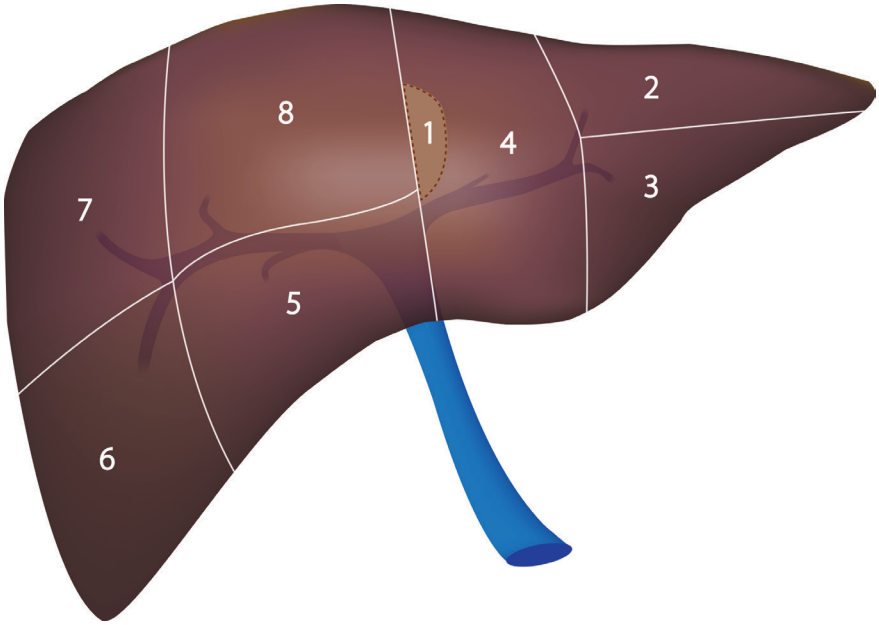

Figure 3. *Schematic representation of the liver divided into eight segments following the portal vein (in blue) branching pattern. Author's interpretation of Bismuth's adaptation of the Couinaud segmentation.*

The liver is also supplied by blood via the hepatic artery. The role of the hepatic artery in the healthy liver is limited. It is estimated that the hepatic artery is responsible for only 20% of the blood supply of the healthy liver and the other 80% of blood is supplied by the portal vein. However, the hepatic artery plays a key role when malignancies arise in the liver, since it has been demonstrated that liver metastases are fed mainly by arterial blood.[36] This effect is likely to be induced by the variety of angiogenic factors that are secreted by the tumors and stimulate angiogenesis required for tumor growth.[37]

A host for metastases

Angiogenesis is only one of the steps in the process of successful metastasis. There are many other steps that a tumor cell needs to take starting with detaching and migrating from the primary tumor, followed by intravasation into the blood or lymph vessels, extravasation at a remote site, and finally, initiation of proliferation, sustained growth and angiogenesis.[38-40] Any of these steps can go 'wrong' (from the perspective of the tumor). Once nestled at the remote location, the majority of tumor cells will not survive and many of those that do survive, fail to initiate proliferation and stay dormant instead.[41,42] There are several explanations for the relatively high frequency of metastases in the liver. First of all, the liver is perfused by a high volume of nutrient-rich blood from the portal system and there is a large number of cancer-prone organs that directly drain into the portal system. The microcirculation of the liver seems favorable for tumor cells as well. The blood flow in the liver is slow due to the extensive capillary network and regulation through Kupffer and stellate cells. In addition, the endothelium lining the sinusoids is fenestrated, lacking a basal lamina that normally shields the vessel endothelium.[43] These conditions give tumor cells a great opportunity to leave the bloodstream.[40] Furthermore, the Kupffer cells lining the sinusoids, bare several surface proteins and saccharides that support tumor cell adhesion.[44] Nevertheless, the liver also contains a large number of immune defense cells that form a defense mechanism against extravasating tumor cell.[45]

The discussion why certain organs are more prone to host metastasis than others has been going on for more than a century. Merely the key position of the liver in the portal system and large amount of blood passing through it would clarify why the liver is home to metastases so frequently, according to an outdated theory by James Ewing.[46] However, many clinical observations do not substantiate this theory. Although the position of the liver in the portal system is an obvious risk factor for catching metastases, many liver metastases originate not from the organs draining on the portal vein (*e.g.* the eye or breast). Therefore it seems likely that both the microenvironment of the liver and its role within the portal system are favorable for metastatic growth. This is in line with Paget's "seed and soil" theory, which states that the "seeding" of metastases relies

on specific tissue conditions in the "soil" of the target organ.[47] Paget compared metastasis to the seeds of a plant falling to the ground in many directions. Only a selection of these seeds grows to become new plants, depending largely on the match between the seeds and the soil where the seed lands. The original theory does not clarify why metastasis can be so different within patients with the same primary tumor. The organs affected and the rate of metastatic growth can be highly variable between patients with primary tumors from the same organ, it can even vary within a patient during the course of disease. This may in large part be due to the heterogenic genetic profile of tumor cells. Much effort is currently put into increasing the knowledge on the genetic profile of cancer.[48]

Locoregional treatment options

As earlier discussed in this chapter, liver metastases can arise from a variety of possible primary tumors with completely different biologic characteristics and metastasizing patterns. Some primary tumor types that frequently spread to the liver and the systemic therapies that should be considered for these patients have been discussed earlier in this chapter. The following paragraph provides an overview of the different locoregional treatment options for liver metastases. Whether the therapies discussed below are suited may vary largely per individual, depending on many variables like tumor type/biology/spread, medical history, availability of treatment options and patient preference.

Transplantation

Although liver transplantation seems an almost ideal solution for metastases that are confined to the liver, liver transplantation is currently not offered to patients with metastatic disease. The first successful liver transplantations in men have been performed in the late 1960's. Since then, transplant livers have been used for patients with a variety of conditions ranging from viral hepatitis to Budd-Chiari syndrome.[49] Patients with primary and secondary liver malignancies are amenable for liver transplantation as well. This came to an end in the 1990's, when survival data proved to be very low for metastatic patients, with 1- and 5-year survival rates of 62% and 18%, respectively.[50] Since then, liver transplantation is no longer reserved for metastatic patients but principally only for a selected group of patients with primary liver tumors. However, transplantation techniques have evolved over the years as well as the ability to select patients who benefit most from therapy. As a result, the 5-year survival rates after liver transplantation for any indication has improved by 20 – 30%.[51,52] The currently available imaging techniques (*e.g.* ^{18}F-FDG-PET, MRI) for example, can now detect far smaller metastases, better distinguishing true liver-limited disease from systemic disease. A

recent pilot study from Norway showed that good survival rates can be obtained for metastatic patients as well when using the current techniques.[52] The 5-year survival rate for metastatic patients in this study was 60%, which is higher than the 5-year survival rate reported after transplantation for HCC in the Scandinavian registry (57% 5-year survival rate).[51] Still, survival rates for metastasis patients were not as high as survival rates for other indications (5-year survival rates ranging from 66% for post-hepatitis C cirrhosis to 90% for autoimmune cirrhosis) and do not justify the use of the scarce donor livers for metastatic patients. Liver transplantation may perhaps become a justified option for metastatic patients in the future if better ways to improve patient selection are found or if the scarcity of donor livers is reduced. Stem cell research may in time change the field of transplantation. Recently, researchers have succeeded to regenerate hepatocytes from stem cells, a development that may eventually lead to in-vitro created donor livers.[53]

Surgical resection

Since liver transplantation is no option, surgical resection remains the treatment of choice for most liver-dominant metastases. Resection is, however, not possible in a large number of patients due to a high tumor burden, multifocality, unfavorable tumor location (near major vessels for instance), or the presence of extrahepatic metastases.[54] Various parts of the liver can be removed depending on tumor location. The resections can be classified according to the part of the liver that is removed: (bi-)segmentectomy (any segments), right/left anterior/medial/posterior sectionectomy (segments 6+7, segments 5+8, segment 4, or segments 2+3), hemihepatectomy (segments 2-4 or segments 5-8, ± segment 1), or trisectionectomy (segments 4-8 or segments 2-5+8, ± segment 1, i.e. extended hemihepatectomy).[35] It is estimated that up to 70% of the liver volume can be safely removed in patients with healthy liver parenchyma.[55] The future liver remnant – the part of the liver that will remain after resection – can take over the function of the former liver by means of hypertrophy. In many patients, however, the future liver remnant is smaller than 30%, which poses patients at risk of liver failure after surgery. Preoperative portal vein embolization can yield these patients eligible for surgical resection.[56] Portal vein embolization is mostly used for patients with metastases confined to the right liver lobe because the future liver remnant (in that case the left liver lobe) is often too small to take over the entire liver function. The procedure is aimed at embolizing the branches of the portal vein leading to the tumor-containing hemiliver whilst not interfering with the other portal vein branches. As a result, the hepatocytes in the embolized hemiliver receive less blood and will atrophy. The hepatocytes in the contralateral hemiliver receive more blood, hypertrophy and will take over the liver function from the removed part. Within weeks the liver is at full capacity and

the patient is ready for surgical resection of the embolized part. One of the downsides of portal vein embolization is that small, undetected tumor depositions in the contralateral hemiliver may be stimulated by the increased blood flow or by factors released by the embolized part of the liver, and may start to grow rapidly as well as the healthy liver.[57] To what extent this effect occurs and whether it is due to portal vein embolization is, however, still matter of debate.[58]

Ablation and embolization therapies

There is a large array of other locoregional treatment options available for liver metastases. One way to categorize these options is into ablation and embolization therapies. Radiofrequency ablation (RFA) is the most common ablative technique used for liver metastases, but other ablative therapies such as microwave ablation, irreversible electroporation, cryoablation, laser induced thermotherapy, and high-intensity focused ultrasound are used as well, albeit predominantly in experimental settings.[59] Even external radiotherapy can be considered an ablative therapy. These techniques are all based on entirely different physical concepts and will not be separately discussed in this chapter. All these therapies share a minimal invasive nature and are, in general, image-guided to direct the ablation zone to the target area and monitor the effect of ablation. The main limitation of ablative therapies are the restrictions in the maximum number and size of lesions that can be treated.

Embolization is the selective occlusion of blood vessels by administering emboli of a certain material. The types of embolization applicable to patients with liver metastases are: bland embolization, chemoembolization, radioembolization, and the previously described portal vein embolization. Occluding the blood vessels supplying a tumor was long thought to be an effective method of depriving the tumor from oxygen and nutrients in order to halt growth. However, tumors may thrive in an oxygen and nutrient-deprived environment and pure embolization (i.e. bland embolization) is, therefore, hardly advocated anymore for liver tumors.[60-62]

Transarterial chemoembolization

Transarterial chemoembolization, often abbreviated as TACE, combines embolization with the deposition of high concentrations of chemotherapeutic drugs close to the tumor. Chemotherapeutic drugs that are often used are doxorubicin (for HCC), irinotecan or oxaliplatin (for colorectal cancer metastases).[63-65] As a result, the drug concentration at the tumor is high and low in the rest of the body, theoretically increasing therapeutic efficacy and reducing toxicity. Conventional TACE is performed by administrating a chemotherapeutic agent mixed with an embolizing agent (generally lipiodol) but there are also drug-eluting beads available that combine the drug and the

embolizing particle in one. Most evidence for TACE is based on patients with HCC.[66] In the widely used Barcelona treatment algorithm for HCC, TACE is reserved for patients with intermediate stage disease.[67] The effect of treating liver metastases patients with TACE is less well studied, although the results are promising.[64,65]

Radioembolization

Radioembolization refers to a therapy in which millions of radioactive microspheres are injected into the hepatic artery combining embolization with internal radiation therapy. These microspheres have a diameter of 15-40 μm and are carried by the blood flow until they lodge at the arteriolar level. There are two types of clinically available microspheres based either on glass (Therasphere®, BTG International Ltd., London, UK) or on resin (SIR-Spheres®, SIRTeX Medical Ltd., Sydney, New South Wales, Australia). These microspheres contain yttrium-90 (^{90}Y), a radioactive element that emits beta-radiation. The beta radiation of ^{90}Y has a maximal penetration depth of approximately 11 mm and is used to selectively irradiate the tumors. Tumor selectivity is based on the previously mentioned principle that liver metastases are preferentially supplied by the hepatic artery, whereas the healthy liver is mostly supplied by the portal vein.[36] Injecting microspheres into the hepatic artery will, therefore, lead to a high concentration of radioactivity near the tumor and a lower concentration of radioactivity in the healthy liver. As such, a tumorical dose can be absorbed in the tumorous liver while the healthy liver remains functional.

The effect of ^{90}Y-radioembolization on tumor response and (progression-free) survival has been investigated in three relatively small, randomized controlled trials.[68-70] In the largest and most recent study, 46 patients with end-stage colorectal liver metastases were randomized for treatment with 5-fluorouracil with or without ^{90}Y-radioembolization. The combination arm had a significantly longer time to liver progression (4.5 vs. 2.1 months) and a non-significantly longer overall survival than the control arm (10.0 vs. 7.3 months, respectively).[68] Other studies have found promising results as well, with an estimated pooled any-response rate of 79% in patients with end-stage disease and 91% any-response rate in a first-line setting.[71]

^{90}Y-radioembolization is a minimally invasive treatment option with a relatively low amount of toxicity and complications. Toxicity consists mainly of nausea, fatigue, abdominal pain, loss of appetite and other symptoms of the so-called post-embolization syndrome.[72,73] The complication rate of ^{90}Y-radioembolization is low (<10%) and complications arise primarily when radiation arrives in non-target organs or when too much radiation arrives in the healthy liver tissue.[74-76] The main structures at risk for non-target radioembolization are the stomach, duodenum, pancreas, lungs, spleen, falciform ligament and gall bladder. A pre-treatment angiography to coil-embolize

non-target vessels together with a test-injection of technetium-99m macroaggregated albumin particles (^{99m}Tc-MAA) is used to minimize the chance of non-target deposition of ^{90}Y-microspheres.[77] ^{99m}Tc-MAA seems, however, not a perfect surrogate for microspheres when it comes to intrahepatic biodistribution assessment and lung shunt calculation (i.e. dosimetry).[78,79] The biodistribution of ^{90}Y-microspheres can be visualized indirectly through bremsstrahlung single photon emission computed tomography (SPECT) or directly through positron emission tomography (PET). Bremsstrahlung SPECT relies on the gamma radiation that is released when beta-particles are deflected. Since beta-particles have traveled up to a few millimeters before the bremsstrahlung is released, conventional ^{90}Y-bremsstrahlung SPECT is not optimal for quantitative imaging on a detailed level (e.g. tumor dosimetry). Although better results can be obtained using more elaborate reconstruction software.[80,81] ^{90}Y-PET, on the other hand, relies on the release of a 511-keV photon pair 32 times per million decays.[82] ^{90}Y-PET allows for very accurate, high resolution, quantitative imaging but is limited by the low count rate and related Poisson noise, which hinders the detection low concentrations of activity outside the liver.[83]

Holmium radioembolization

Holmium-166 poly(L-lactic acid)-microspheres (abbreviated in this thesis as ^{166}Ho-PLLA-microspheres or ^{166}Ho-microspheres) have been developed at the University Medical Center Utrecht (Utrecht, the Netherlands) as an alternative to the ^{90}Y-microspheres. Besides the high-energy beta-radiation required for tumor destruction, ^{166}Ho also emits low-energy gamma radiation, which can be used for quantitative gamma imaging.[84,85] Furthermore, the paramagnetic property of holmium can be used for magnetic resonance imaging (MRI).[86,87]

Preparation of ^{166}Ho-microspheres

Ho-PLLA-microspheres are prepared according to good manufacturing practice (GMP) guidelines in the radiopharmacy laboratory of the University Medical Center Utrecht. In short, the microspheres are synthesized using the solvent-evaporation technique by adding ^{165}Ho-acetylacetonate and poly(L-lactic acid) to a continuously-stirred chloroform solution.[88] This way, ^{165}Ho-acetylacetonate is incorporated in a matrix of poly(L-lactic acid) in the spherical shape of microspheres. Subsequently, the non-radioactive ^{165}Ho-microspheres are dried and the desired amount is packed in an irradiation vial. The vial is then neutron irradiated at the reactor institute Delft (Delft, the Netherlands, thermal neutron flux 5 x 10^{12} $cm^{-2}s^{-1}$) for several hours, depending on the desired ^{166}Ho-activity.

Preclinical studies

^{166}Ho-microspheres have come a long way since the first concept of these microspheres was conceived in the nineties. The first steps were to investigate the process of preparation and irradiation of these microspheres as well as the in-vitro stability.[88-91] Small animal models were used to establish the stability and biodistribution of ^{166}Ho-microspheres.[92] Then, the feasibility and clinical effects were studied in larger animals, with satisfactory results.[93,94] Simultaneously, the techniques for imaging the microspheres with nuclear imaging and MRI were developed and studied as well.[87,95-97] The whole process took years and a total of eight PhD-theses, based at least partially on ^{166}Ho-containing microspheres, were written at our institute.[98-105]

Clinical translation

The preclinical studies paved the way for the first study assessing ^{166}Ho-radioembolization safety in humans. The purposes of the so-called phase 1 clinical trial was to determine how much radioactivity should be given to patients, expressed as the maximum tolerated radiation dose, to provide the first data on the safety of ^{166}Ho-radioembolization, and to study the effects of ^{166}Ho-radioembolization in terms of toxicity, tumor response, survival and quality of life. Data of the phase 1 clinical trial could also be used to study dosimetry using nuclear imaging and MRI in human patients. This phase 1 HEPAR (Holmium Embolization Particles for Arterial Radiotherapy) clinical trial is the basis of this thesis.

Outline of this thesis

In this thesis, the results of the first ^{166}Ho-radioembolization treatments performed in human patients are described and related to studies on radioembolization with ^{90}Y-microspheres. The thesis is subdivided in two parts: Part I: Response and Toxicity, and Part II: Imaging and Dosimetry.

Part I. Response and Toxicity

In the first part of this thesis, clinical outcomes of radioembolization with holmium and yttrium microspheres are presented. As a first step, in Chapter 2, the outcomes: toxicity, tumor response and survival of patients treated in our center with yttrium-90 microspheres are described. These outcomes were retrospectively assessed in all consecutive patients with liver metastases who were not included in a prospective trial and were treated with radioembolization since the start of radioembolization at our center, providing a benchmark for the results of the phase 1 clinical trial.
In Chapter 3 the rationale and the study design of the phase 1 clinical trial are presented. The clinical outcomes of this trial in which we performed holmium radioemboli-

zation in patients for the first time is presented in Chapter 4. In this chapter, we present the results of the study in terms of maximum tolerated radiation dose, toxicity, tumor response, survival, and quality of life. How the results from Chapter 4 compare to the results for ^{90}Y-RE is described in Chapter 5. This chapter is based on our reply to a letter that was published in Lancet Oncology in reaction to the phase 1 clinical trial results. Chapter 6 concludes Part I of this thesis by providing an in depth analysis of quality of life and factors influencing quality of life after ^{166}Ho-RE.

Part II. Imaging and Dosimetry

A major advantage of ^{166}Ho-microspheres over ^{90}Y-microspheres lies in microsphere visualization. Chapter 7 provides an overview of the current status of imaging options and the way dosimetry is currently performed in radioembolization practices together with the latest developments in this field. In Chapter 8 we assessed the value of ^{99m}Tc-MAA to predict ^{90}Y-microsphere distribution for pre-treatment dosimetry. The value of ^{99m}Tc-MAA for treatment planning is further discussed in Chapter 9. Post-^{166}Ho-RE dosimetry is evaluated in Chapter 10. In this chapter, the post-treatment dosimetry based on MRI is compared with SPECT and estimated doses to the tumors and healthy liver are elucidated. The gamma-radiation that comes with ^{166}Ho is excellent for dosimetry but can pose radiation safety concerns as well. The radiation emitted by patients after treatment with ^{166}Ho-RE and the dose to others is presented in Chapter 11. Finally, the thesis is summarized and discussed in Chapter 12.

References

1. Siegel R, Naishadham D, Jemal A (2013) Cancer statistics, 2013. CA Cancer J Clin 63: 11-30.
2. Kasper HU, Drebber U, Dries V, Dienes HP (2005) Liver metastases: incidence and histogenesis. Z Gastroenterol 43: 1149-1157.
3. Coldwell D, Sangro B, Salem R, Wasan H, Kennedy A (2012) Radioembolization in the treatment of unresectable liver tumors: experience across a range of primary cancers. Am J Clin Oncol 35: 167-177.
4. Li Destri G, Di Cataldo A, Puleo S (2006) Colorectal cancer follow-up: useful or useless? Surg Oncol 15: 1-12.
5. Chuang SC, Su YC, Lu CY, Hsu HT, Sun LC, et al. (2011) Risk factors for the development of metachronous liver metastasis in colorectal cancer patients after curative resection. World J Surg 35: 424-429.
6. Manfredi S, Lepage C, Hatem C, Coatmeur O, Faivre J, et al. (2006) Epidemiology and management of liver metastases from colorectal cancer. Ann Surg 244: 254-259.
7. Steele G, Jr., Ravikumar TS (1989) Resection of hepatic metastases from colorectal cancer. Biologic perspective. Ann Surg 210: 127-138.
8. Pugh S, Fuller A, Rose P, Perera-Salazar R, Mellor J, et al. (2012) What is the true incidence of metachronous colorectal liver metastases? Evidence from the UK FACS trial. Gut 61: 1.
9. Weiss L, Grundmann E, Torhorst J, Hartveit F, Moberg I, et al. (1986) Haematogenous metastatic patterns in colonic carcinoma: an analysis of 1541 necropsies. J Pathol 150: 195-203.
10. Khatri VP, Petrelli NJ, Belghiti J (2005) Extending the frontiers of surgical therapy for hepatic colorectal metastases: is there a limit? J Clin Oncol 23: 8490-8499.
11. Snoeren N, van Hooff SR, Adam R, van Hillegersberg R, Voest EE, et al. (2012) Exploring gene expression signatures for predicting disease free survival after resection of colorectal cancer liver metastases. PLoS One 7: e49442.
12. Adam R, Lucidi V, Bismuth H (2004) Hepatic colorectal metastases: methods of improving resectability. Surg Clin North Am 84: 659-671.
13. (2006) Colorectal liver metastases, Dutch guideline, Version: 1.0, Oncoline, Integraal Kankercentrum Nederland.
14. (2008) Commissie BOM: Richtlijn beoordeling oncologische middelen. Medische Oncologie 6: 49-55
15. Bedikian AY (2006) Metastatic uveal melanoma therapy: current options. Int Ophthalmol Clin 46: 151-166.
16. Damato B (2006) Treatment of primary intraocular melanoma. Expert Rev Anticancer Ther 6: 493-506.
17. Bedikian AY, Kantarjian H, Young SE, Bodey GP (1981) Prognosis in metastatic choroidal melanoma. South Med J 74: 574-577.
18. Gragoudas ES, Egan KM, Seddon JM, Glynn RJ, Walsh SM, et al. (1991) Survival of patients with metastases from uveal melanoma. Ophthalmology 98: 383-389; discussion 390.
19. Albert DM, Ryan LM, Borden EC (1996) Metastatic ocular and cutaneous melanoma: a comparison of patient characteristics and prognosis. Arch Ophthalmol 114: 107-108.
20. Viadana E, Bross ID, Pickren JW (1973) An autopsy study of some routes of dissemination of cancer of the breast. Br J Cancer 27: 336-340.
21. Er O, Frye DK, Kau SW, Broglio K, Valero V, et al. (2008) Clinical course of breast cancer patients with metastases limited to the liver treated with chemotherapy. Cancer J 14: 62-68.
22. Pentheroudakis G, Fountzilas G, Bafaloukos D, Koutsoukou V, Pectasides D, et al. (2006) Metastatic breast cancer with liver metastases: a registry analysis of clinicopathologic, management and outcome characteristics of 500 women. Breast Cancer Res Treat 97: 237-244.
23. Vlastos G, Smith DL, Singletary SE, Mirza NQ, Tuttle TM, et al. (2004) Long-term survival after an aggressive surgical approach in patients with breast cancer hepatic metastases. Ann Surg Oncol 11: 869-874.
24. Atalay G, Biganzoli L, Renard F, Paridaens R, Cufer T, et al. (2003) Clinical outcome of breast cancer patients with liver metastases alone in the anthracycline-taxane era: a retrospective analysis of two prospective, randomised metastatic breast cancer trials. Eur J Cancer 39: 2439-2449.
25. (2012) Breast Cancer, Dutch guideline, version 2.0 Oncoline, Integraal Kankercentrum Nederland.

26. Diamond JR, Finlayson CA, Borges VF (2009) Hepatic complications of breast cancer. Lancet Oncol 10: 615-621.
27. Smits ML, Prince JF, Rosenbaum CE, van den Hoven AF, Nijsen JF, et al. (2013) Intra-arterial radioembolization of breast cancer liver metastases: A structured review. Eur J Pharmacol.
28. Benevento A, Boni L, Frediani L, Ferrari A, Dionigi R (2000) Result of liver resection as treatment for metastases from noncolorectal cancer. J Surg Oncol 74: 24-29.
29. Rhee TK, Lewandowski RJ, Liu DM, Mulcahy MF, Takahashi G, et al. (2008) 90Y Radioembolization for metastatic neuroendocrine liver tumors: preliminary results from a multi-institutional experience. Ann Surg 247: 1029-1035.
30. Kam BL, Teunissen JJ, Krenning EP, de Herder WW, Khan S, et al. (2012) Lutetium-labelled peptides for therapy of neuroendocrine tumours. Eur J Nucl Med Mol Imaging 39 Suppl 1: S103-112.
31. Rinke A, Muller HH, Schade-Brittinger C, Klose KJ, Barth P, et al. (2009) Placebo-controlled, double-blind, prospective, randomized study on the effect of octreotide LAR in the control of tumor growth in patients with metastatic neuroendocrine midgut tumors: a report from the PROMID Study Group. J Clin Oncol 27: 4656-4663.
32. Read AE (1972) Clinical physiology of the liver. Br J Anaesth 44: 910-917.
33. Bismuth H (1982) Surgical anatomy and anatomical surgery of the liver. World J Surg 6: 3-9.
34. Couinaud C, Delmas A, Patel J (1957) Le foie: Etudes anatomiques et chirurgicales. Masso: Paris.
35. Georgiev P, Clavien PA (2007) Liver resections. In: Clavien PA, Sarr SG, Fong Y, editors. Atlas of upper gastrointestinal and hepato-pancreatico-biliary surgery. Berlin: Springer. pp. 309-391.
36. Bierman HR, Byron RL, Jr., Kelley KH, Grady A (1951) Studies on the blood supply of tumors in man. III. Vascular patterns of the liver by hepatic arteriography in vivo. J Natl Cancer Inst 12: 107-131.
37. Folkman J, Merler E, Abernathy C, Williams G (1971) Isolation of a tumor factor responsible for angiogenesis. J Exp Med 133: 275-288.
38. Luzzi KJ, MacDonald IC, Schmidt EE, Kerkvliet N, Morris VL, et al. (1998) Multistep nature of metastatic inefficiency: dormancy of solitary cells after successful extravasation and limited survival of early micrometastases. Am J Pathol 153: 865-873.
39. Weiss L (1996) Metastatic inefficiency: intravascular and intraperitoneal implantation of cancer cells. Cancer Treat Res 82: 1-11.
40. (2011) Liver metastasis: Biology and Clinical Management; Ablin RJ, Jiang WG, editors. Dordrecht: Springer.
41. Naumov GN, Townson JL, MacDonald IC, Wilson SM, Bramwell VH, et al. (2003) Ineffectiveness of doxorubicin treatment on solitary dormant mammary carcinoma cells or late-developing metastases. Breast Cancer Res Treat 82: 199-206.
42. Cameron MD, Schmidt EE, Kerkvliet N, Nadkarni KV, Morris VL, et al. (2000) Temporal progression of metastasis in lung: cell survival, dormancy, and location dependence of metastatic inefficiency. Cancer Res 60: 2541-2546.
43. Vekemans K, Braet F (2005) Structural and functional aspects of the liver and liver sinusoidal cells in relation to colon carcinoma metastasis. World J Gastroenterol 11: 5095-5102.
44. Ishibashi H, Nakamura M, Komori A, Migita K, Shimoda S (2009) Liver architecture, cell function, and disease. Semin Immunopathol 31: 399-409.
45. Gao B, Jeong WI, Tian Z (2008) Liver: An organ with predominant innate immunity. Hepatology 47: 729-736.
46. Ewing J (1928) Neoplastic diseases. A treatise on tumors. Philadelphia: WB Saunders Company.
47. Paget S (1989) The distribution of secondary growths in cancer of the breast. 1889. Cancer Metastasis Rev 8: 98-101.
48. Fokas E, Engenhart-Cabillic R, Daniilidis K, Rose F, An HX (2007) Metastasis: the seed and soil theory gains identity. Cancer Metastasis Rev 26: 705-715.
49. Starzl TE, Groth CG, Brettschneider L, Penn I, Fulginiti VA, et al. (1968) Orthotopic homotransplantation of the human liver. Ann Surg 168: 392-415.

50. Muhlbacher F, Huk I, Steininger R, Gnant M, Gotzinger P, et al. (1991) Is orthotopic liver transplantation a feasible treatment for secondary cancer of the liver? Transplant Proc 23: 1567-1568.
51. (2009) Scandiatransplant. The Nordic Liver Transplant Registry annual report 2009. Available at: http://www.scandiatransplant.org/members/nltr/ANNUAL_REPORT_2009_FINAL.pdf/view.
52. Hagness M, Foss A, Line PD, Scholz T, Jorgensen PF, et al. (2013) Liver transplantation for nonresectable liver metastases from colorectal cancer. Ann Surg 257: 800-806.
53. Huch M, Dorrell C, Boj SF, van Es JH, Li VS, et al. (2013) In vitro expansion of single Lgr5+ liver stem cells induced by Wnt-driven regeneration. Nature 494: 247-250.
54. Strasberg S, Linehan DC (2006) Tumors of the pancreas, biliary tract and liver. ACS Surgery Principles and Practice. pp. 681-685.
55. Mullin EJ, Metcalfe MS, Maddern GJ (2005) How much liver resection is too much? Am J Surg 190: 87-97.
56. Abulkhir A, Limongelli P, Healey AJ, Damrah O, Tait P, et al. (2008) Preoperative portal vein embolization for major liver resection: a meta-analysis. Ann Surg 247: 49-57.
57. Hoekstra LT, van Lienden KP, Verheij J, van der Loos CM, Heger M, et al. (2013) Enhanced tumor growth after portal vein embolization in a rabbit tumor model. J Surg Res 180: 89-96.
58. Sakai N, Clarke CN, Schuster R, Blanchard J, Tevar AD, et al. (2010) Portal vein ligation accelerates tumor growth in ligated, but not contralateral lobes. World J Gastroenterol 16: 3816-3826.
59. Hickey R, Vouche M, Sze DY, Hohlastos E, Collins J, et al. (2013) Cancer Concepts and Principles: Primer for the Interventional Oncologist-Part II. J Vasc Interv Radiol 24: 1167-1188.
60. Liapi E, Geschwind JF (2010) Intra-arterial therapies for hepatocellular carcinoma: where do we stand? Ann Surg Oncol 17: 1234-1246.
61. Bruix J, Llovet JM, Castells A, Montana X, Bru C, et al. (1998) Transarterial embolization versus symptomatic treatment in patients with advanced hepatocellular carcinoma: results of a randomized, controlled trial in a single institution. Hepatology 27: 1578-1583.
62. Warburg O (1956) On the origin of cancer cells. Science 123: 309-314.
63. Poggi G, Quaretti P, Minoia C, Bernardo G, Bonora MR, et al. (2008) Transhepatic arterial chemoembolization with oxaliplatin-eluting microspheres (OEM-TACE) for unresectable hepatic tumors. Anticancer Res 28: 3835-3842.
64. Richardson AJ, Laurence JM, Lam VW (2013) Transarterial chemoembolization with irinotecan beads in the treatment of colorectal liver metastases: systematic review. J Vasc Interv Radiol 24: 1209-1217.
65. Liapi E, Geschwind JF (2010) Chemoembolization for primary and metastatic liver cancer. Cancer J 16: 156-162.
66. Llovet JM, Bruix J (2003) Systematic review of randomized trials for unresectable hepatocellular carcinoma: Chemoembolization improves survival. Hepatology 37: 429-442.
67. Bruix J, Sherman M, American Association for the Study of Liver D (2011) Management of hepatocellular carcinoma: an update. Hepatology 53: 1020-1022.
68. Hendlisz A, Van den Eynde M, Peeters M, Maleux G, Lambert B, et al. (2010) Phase III trial comparing protracted intravenous fluorouracil infusion alone or with yttrium-90 resin microspheres radioembolization for liver-limited metastatic colorectal cancer refractory to standard chemotherapy. J Clin Oncol 28: 3687-3694.
69. Gray B, Van Hazel G, Hope M, Burton M, Moroz P, et al. (2001) Randomised trial of SIR-Spheres plus chemotherapy vs. chemotherapy alone for treating patients with liver metastases from primary large bowel cancer. Ann Oncol 12: 1711-1720.
70. Van Hazel G, Blackwell A, Anderson J, Price D, Moroz P, et al. (2004) Randomised phase 2 trial of SIR-Spheres plus fluorouracil/leucovorin chemotherapy versus fluorouracil/leucovorin chemotherapy alone in advanced colorectal cancer. J Surg Oncol 88: 78-85.
71. Vente MA, Wondergem M, van der Tweel I, van den Bosch MA, Zonnenberg BA, et al. (2009) Yttrium-90 microsphere radioembolization for the treatment of liver malignancies: a structured meta-analysis. Eur Radiol 19: 951-959.

72. Kennedy AS, Coldwell D, Nutting C, Murthy R, Wertman DE, Jr., et al. (2006) Resin 90Y-microsphere brachytherapy for unresectable colorectal liver metastases: modern USA experience. Int J Radiat Oncol Biol Phys 65: 412-425.
73. Szyszko T, Al-Nahhas A, Tait P, Rubello D, Canelo R, et al. (2007) Management and prevention of adverse effects related to treatment of liver tumours with 90Y microspheres. Nucl Med Commun 28: 21-24.
74. Riaz A, Lewandowski RJ, Kulik LM, Mulcahy MF, Sato KT, et al. (2009) Complications following radioembolization with yttrium-90 microspheres: a comprehensive literature review. J Vasc Interv Radiol 20: 1121-1130; quiz 1131.
75. Carretero C, Munoz-Navas M, Betes M, Angos R, Subtil JC, et al. (2007) Gastroduodenal injury after radioembolization of hepatic tumors. Am J Gastroenterol 102: 1216-1220.
76. Seidensticker R, Seidensticker M, Damm R, Mohnike K, Schutte K, et al. (2012) Hepatic toxicity after radioembolization of the liver using (90)Y-microspheres: sequential lobar versus whole liver approach. Cardiovasc Intervent Radiol 35: 1109-1118.
77. Salem R, Lewandowski RJ, Sato KT, Atassi B, Ryu RK, et al. (2007) Technical aspects of radioembolization with 90Y microspheres. Tech Vasc Interv Radiol 10: 12-29.
78. Bult W, Vente MA, Zonnenberg BA, Van Het Schip AD, Nijsen JF (2009) Microsphere radioembolization of liver malignancies: current developments. Q J Nucl Med Mol Imaging 53: 325-335.
79. Elschot M, Lam MG, Nijsen JF, Smits ML, Prince JF, et al. (2013) Tc-99m-MAA overestimates the absorbed dose to the lungs in radioembolization: a quantitative evaluation in patients treated with Ho-166 microspheres. [submitted].
80. Rong X, Du Y, Ljungberg M, Rault E, Vandenberghe S, et al. (2012) Development and evaluation of an improved quantitative (90)Y bremsstrahlung SPECT method. Med Phys 39: 2346-2358.
81. Elschot M, Lam MG, van den Bosch MA, Viergever MA, de Jong HW (2013) Quantitative Monte Carlo-Based 90Y SPECT Reconstruction. J Nucl Med.
82. Selwyn RG, Nickles RJ, Thomadsen BR, DeWerd LA, Micka JA (2007) A new internal pair production branching ratio of 90Y: the development of a non-destructive assay for 90Y and 90Sr. Appl Radiat Isot 65: 318-327.
83. Elschot M, Vermolen BJ, Lam MG, de Keizer B, van den Bosch MA, et al. (2013) Quantitative comparison of PET and Bremsstrahlung SPECT for imaging the in vivo yttrium-90 microsphere distribution after liver radioembolization. PLoS One 8: e55742.
84. Elschot M, Nijsen JF, Dam AJ, de Jong HW (2011) Quantitative evaluation of scintillation camera imaging characteristics of isotopes used in liver radioembolization. PLoS One 6: e26174.
85. de Wit TC, Xiao J, Nijsen JF, van het Schip FD, Staelens SG, et al. (2006) Hybrid scatter correction applied to quantitative holmium-166 SPECT. Phys Med Biol 51: 4773-4787.
86. Seevinck PR, van de Maat GH, de Wit TC, Vente MA, Nijsen JF, et al. (2012) Magnetic resonance imaging-based radiation-absorbed dose estimation of 166Ho microspheres in liver radioembolization. Int J Radiat Oncol Biol Phys 83: e437-444.
87. Nijsen JF, Seppenwoolde JH, Havenith T, Bos C, Bakker CJ, et al. (2004) Liver tumors: MR imaging of radioactive holmium microspheres--phantom and rabbit study. Radiology 231: 491-499.
88. Zielhuis SW, Nijsen JF, de Roos R, Krijger GC, van Rijk PP, et al. (2006) Production of GMP-grade radioactive holmium loaded poly(L-lactic acid) microspheres for clinical application. Int J Pharm 311: 69-74.
89. Vente MA, Nijsen JF, de Roos R, van Steenbergen MJ, Kaaijk CN, et al. (2009) Neutron activation of holmium poly(L-lactic acid) microspheres for hepatic arterial radio-embolization: a validation study. Biomed Microdevices 11: 763-772.
90. Nijsen JF, van Steenbergen MJ, Kooijman H, Talsma H, Kroon-Batenburg LM, et al. (2001) Characterization of poly(L-lactic acid) microspheres loaded with holmium acetylacetonate. Biomaterials 22: 3073-3081.
91. Zielhuis SW, Nijsen JF, Figueiredo R, Feddes B, Vredenberg AM, et al. (2005) Surface characteristics of holmium-loaded poly(L-lactic acid) microspheres. Biomaterials 26: 925-932.

92. Nijsen F, Rook D, Brandt C, Meijer R, Dullens H, et al. (2001) Targeting of liver tumour in rats by selective delivery of holmium-166 loaded microspheres: a biodistribution study. Eur J Nucl Med 28: 743-749.

93. Vente MA, Nijsen JF, de Wit TC, Seppenwoolde JH, Krijger GC, et al. (2008) Clinical effects of transcatheter hepatic arterial embolization with holmium-166 poly(L-lactic acid) microspheres in healthy pigs. Eur J Nucl Med Mol Imaging 35: 1259-1271.

94. Vente MA, de Wit TC, van den Bosch MA, Bult W, Seevinck PR, et al. (2010) Holmium-166 poly(L-lactic acid) microsphere radioembolisation of the liver: technical aspects studied in a large animal model. Eur Radiol 20: 862-869.

95. Zielhuis SW, Seppenwoolde JH, Bakker CJ, Jahnz U, Zonnenberg BA, et al. (2007) Characterization of holmium loaded alginate microspheres for multimodality imaging and therapeutic applications. J Biomed Mater Res A 82: 892-898.

96. Zielhuis SW, Nijsen JF, Dorland L, Krijger GC, van Het Schip AD, et al. (2006) Removal of chloroform from biodegradable therapeutic microspheres by radiolysis. Int J Pharm 315: 67-74.

97. Seevinck PR, Seppenwoolde JH, de Wit TC, Nijsen JF, Beekman FJ, et al. (2007) Factors affecting the sensitivity and detection limits of MRI, CT, and SPECT for multimodal diagnostic and therapeutic agents. Anticancer Agents Med Chem 7: 317-334.

98. Vente MA (2009) Thesis: Preclinical studies on holmium-166 poly(L-lactic acid) microspheres for hepatic arterial radioembolization: Utrecht University.

99. Bult W (2010) Thesis: Holmium microparticles for intratumoral radioablation: Utrecht University.

100. Elschot M (2013) Thesis: Quantitative nuclear imaging for dosimetry in radioembolization: Utrecht University.

101. van de Maat GH (2013) Thesis: Magnetic resonance imaging in ^{166}Ho liver radioembolization: Utrecht University.

102. Seevinck PR (2009) Thesis: Multimodal imaging of holmium-loaded microsphere for internal Radiation therapy: Utrecht University.

103. Zielhuis SW (2006) Thesis: Lanthanide bearing radioactive particles for cancer therapy and multimodality imaging.

104. Nijsen JF (2001) Thesis: Radioactive holmium poly(L-lactic acid) microspheres for treatment of liver malignancies: Utrecht University.

105. Seppenwoolde JH (2004) Thesis: Magnetic Susceptibility Effects in Diagnostic and Interventional MIR: Utrecht University.

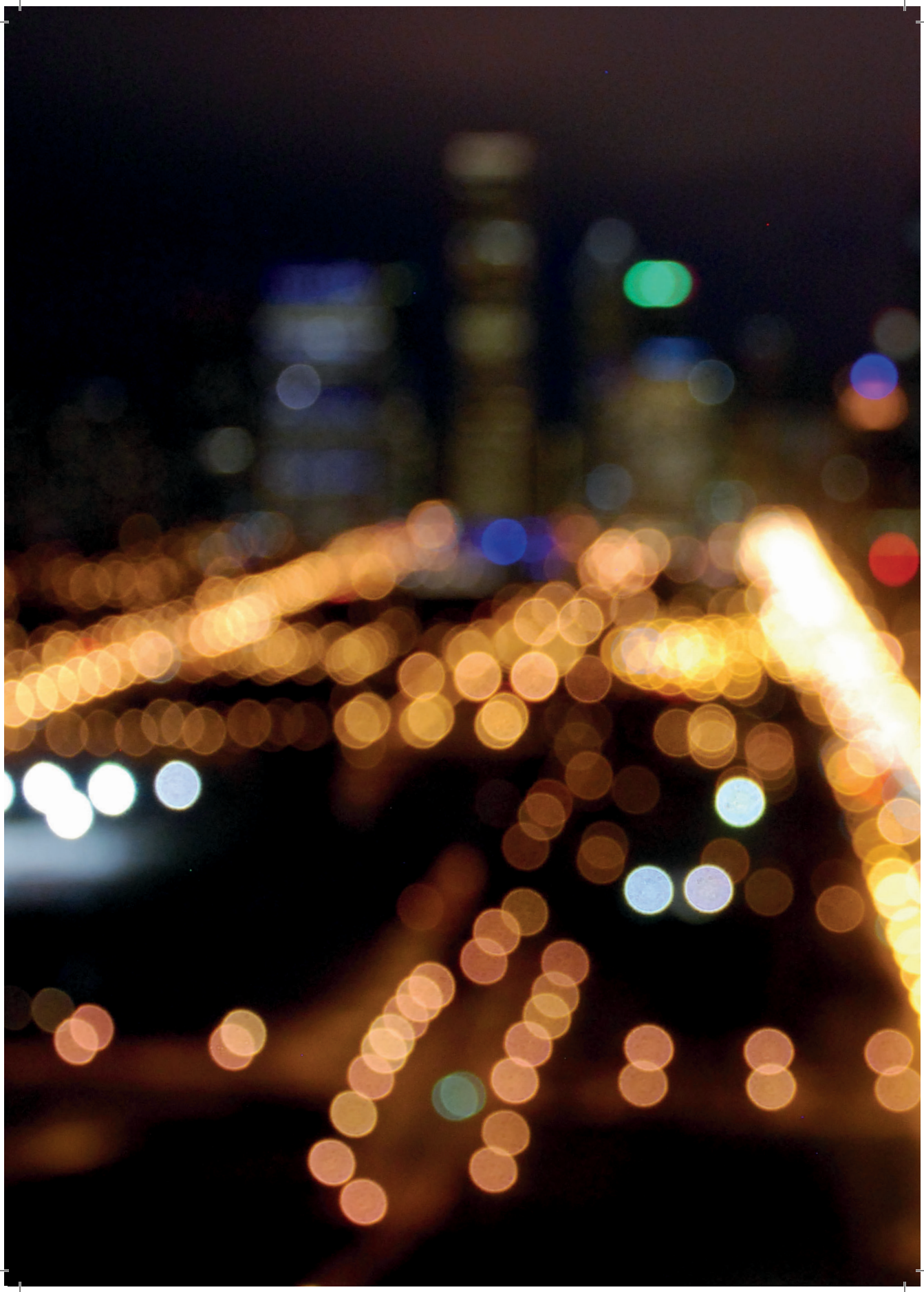

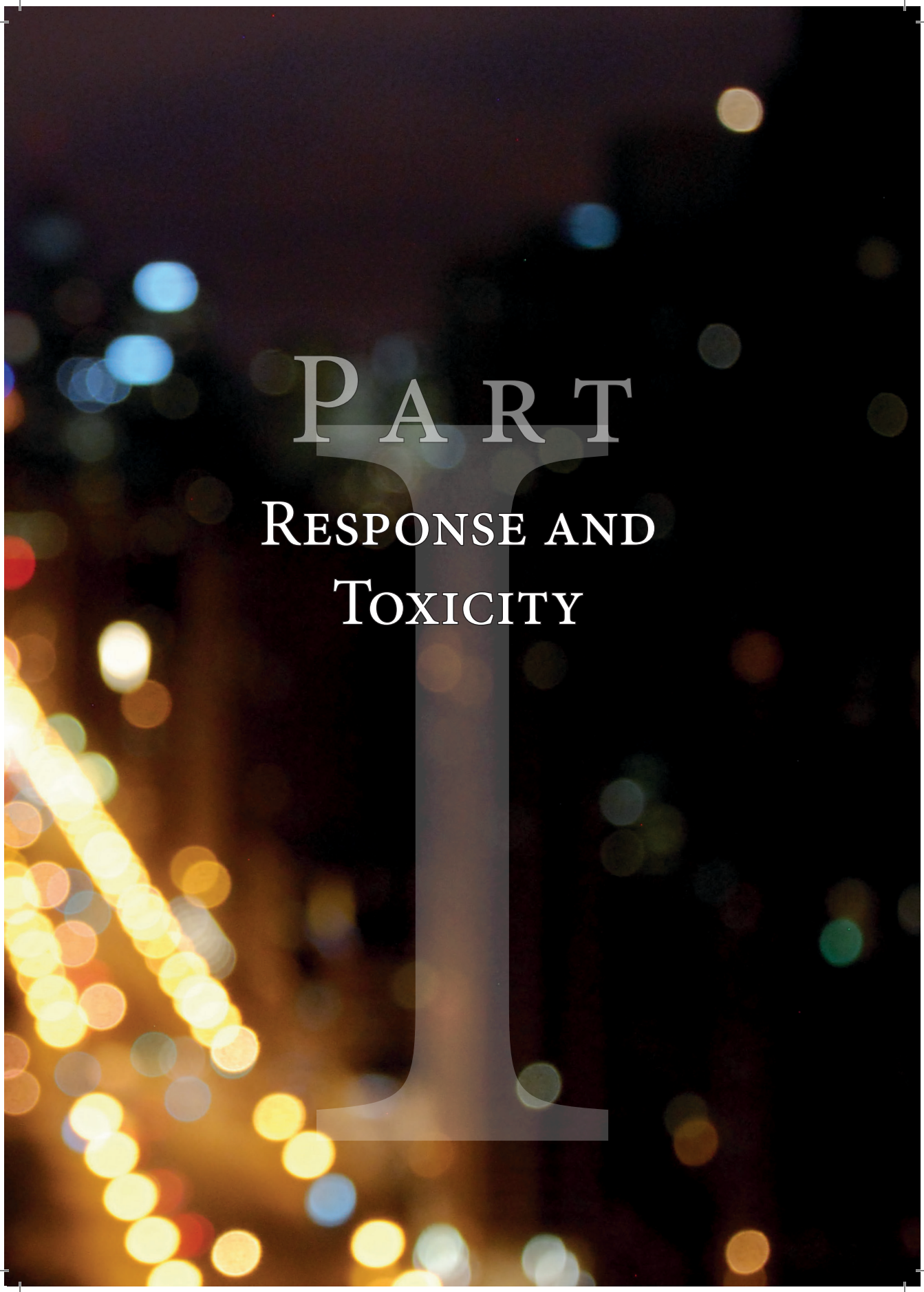

Part I

Response and Toxicity

Chapter 2

Toxicity, tumor response, and overall survival after ^{90}Y-radioembolization for unresectable liver metastases

MLJ Smits*, AF van den Hoven*, CENM Rosenbaum, BA Zonnenberg, MGEH Lam, JFW Nijsen, M Koopman, MAAJ van den Bosch
* Shared first authors

PLoS One 2013

Objective

To investigate clinical and laboratory toxicity in patients with unresectable liver metastases, treated with yttrium-90 radioembolization (^{90}Y-RE).

Methods

Patients with liver metastases treated with ^{90}Y-RE, between February 1st 2009 and March 31st 2012, were included in this study. Clinical toxicity assessment was based on the reporting in patient charts. Laboratory investigations at baseline and during a four-month follow-up were used to assess laboratory toxicity according to the Common Terminology Criteria for Adverse Events version 4.02. The occurrence of grade 3-4 laboratory toxicity was stratified according to treatment strategy (whole liver treatment in one session versus sequential sessions). Response assessment was performed at the level of target lesions, whole liver and overall response in accordance with RECIST 1.1 at 3- and 6 months post-treatment. Median time to progression (TTP) and overall survival were calculated by Kaplan-Meier analysis.

Introduction

Intra-arterial radioembolization with yttrium-90 microspheres (^{90}Y-RE) is an increasingly applied treatment option for patients with unresectable primary or secondary hepatic malignancies, refractory to systemic therapies. The treatment consists of intra-arterial administration of microspheres tagged with or containing yttrium-90 (^{90}Y), a radioisotope that emits high-energy beta radiation. In contrast to the normal liver parenchyma, which mainly relies on the portal vein, intrahepatic malignancies mainly depend on the hepatic artery for their blood supply.[1] As a consequence, these tumors can be selectively targeted by instillation of ^{90}Y-microspheres in the hepatic artery.

There is growing evidence for an overall beneficial effect of ^{90}Y-RE regarding time to progression, overall survival and quality of life in salvage patients with either primary or metastatic hepatic malignancies.[2-4] The effect of ^{90}Y-RE in terms of tumor response varies widely, with disease control rates (complete response + partial response + stable disease) ranging from 56% – 100%.[4] Given the wide variety in tumor response rates, great effort is put into optimal patient selection through the identification of prognostic factors for a favorable outcome after ^{90}Y-RE.[5-7] Improved selection may increase the efficacy of this therapy and prevent patients from futile treatment and unnecessary toxicity.

Although minimally invasive, ^{90}Y-RE is not without adverse effects. Common adverse effects

Results

A total of 59 patients, with liver metastases from colorectal cancer (n=30), neuroendocrine tumors (NET) (n=6) and other primary tumors (n=23) were included. Clinical toxicity after ^{90}Y-RE treatment was confined to grade 1-2 events, predominantly post-embolization symptoms. No grade 3-4 clinical toxicity was observed, whereas laboratory toxicity grade 3-4 was observed in 38% of patients. Whole liver treatment in one session was not associated with increased laboratory toxicity. Three-months disease control rates for target lesions, whole liver and overall response were 35%, 21% and 19% respectively. Median TTP was 6.2 months for target lesions, 3.3 months for the whole liver and 3.0 months for overall response. Median overall survival was 8.9 months.

Conclusion

The risk of severe complications or grade 3-4 clinical toxicity in patients with liver metastases of various primary tumors undergoing ^{90}Y-RE is low. In contrast, laboratory toxicity grade 3-4 can be expected to occur in more than one-third of patients without any clinical signs of radiation induced liver disease.

related to ^{90}Y-RE are symptoms of the post-embolization syndrome, comprising fatigue, nausea, vomiting, abdominal pain, loss of appetite and fever.[7-10] In general, these symptoms appear on the day of treatment and last up to three days after treatment.[11] More serious complications can occur when an excessive radiation dose is applied to non-target tissue. An excessive dose to the healthy liver parenchyma, which can be due to either a high overall administered activity or an unfavorable tumor to non-tumor activity distribution ratio, can cause radiation induced liver disease (RILD). Alternatively, distribution of microspheres in organs other than the liver could cause serious morbidity and even mortality (*e.g.* radiation pneumonitis or gastric ulceration). These severe complications occur in less than 10% of patients.[12-14]

Laboratory toxicity in terms of elevated liver function tests and liver enzymes can be expected after ^{90}Y-RE. It is important to monitor laboratory toxicity, because this may be an early indicator for RILD. Relatively little is known, however, about the normal range of laboratory toxicities following ^{90}Y-RE in patients who do not develop RILD. The primary objective of this study was to investigate clinical and laboratory toxicity in patients with liver metastases, treated with ^{90}Y-RE. Secondary objectives were assessment of tumor response and overall survival.

Materials and Methods

Patient selection

Records of all liver metastases patients who were not participating in a clinical trial and had received a pre-treatment angiographic procedure for treatment with ^{90}Y-RE at our institute between February 1st 2009 and March 31st 2012 were retrospectively analyzed. Patients that were eligible for ^{90}Y-RE had unresectable liver dominant metastases and had progressive disease under systemic treatment, or were no longer treated systemically due to contraindications. The Medical Ethics Committee of the University Medical Center Utrecht waived the need for informed-consent and approved this study.

Procedure

^{90}Y-RE was carried out over two sessions: a pre-treatment diagnostic angiography and a treatment angiography. Patients were admitted to the hospital on the evening before angiography. They received 1.5 L per 24h NaCl 0.9% intravenously for pre- and post-hydration. Pre-treatment diagnostic angiography started with selective visceral catheterization (celiac axis and superior mesenteric artery) in order to obtain an angiographic map of the patient's vascular anatomy. Specific extrahepatic vessels were coil-embolized to prevent ^{90}Y-microspheres that were injected into one of the hepatic arteries, to be distributed to visceral organs other than the liver. Arteries that were actively searched for and embolized using coils included the gastroduodenal artery, the right gastric artery, and pancreaticoduodenal vessels and any other relevant arteries depending on the patient's specific anatomy. Subsequently, 150 MBq technetium-99m-labelled macro-albumin aggregates (^{99m}Tc-MAA) were injected into the hepatic artery to simulate the ^{90}Y-microspheres distribution. Next, single photon emission computed tomography (SPECT) and planar nuclear imaging were performed. In order to assess whether part of the dose was deposited in abdominal organs other than the liver, the SPECT images were analyzed after fusion with computed tomography (CT). Planar nuclear imaging was used to calculate the lung shunt fraction; patients with a lung shunt <10% received the full dose of ^{90}Y-microspheres, when lung shunt fraction was between 10% - 15% or 15% - 20% the dose of ^{90}Y-microspheres was reduced with 20% and 40%, respectively.[15] Lung shunt fractions of >20% implied that no treatment could be given. If radioactivity was detected in non-target organs, such as pancreas, duodenum or stomach, further angiographic investigation was performed with additional coiling and/or a more distal injection position of ^{99m}Tc-MAA.[16] Patients stayed one night in the hospital for observation.

Treatment angiography was performed within two weeks after the pre-treatment angiography. Patients were readmitted to hospital the day before angiography, where they

again received pre- and post-hydration. One hour before angiography, patients received a single intravenous dose of dexamethason (10 mg) and ondansetron (8 mg). The dose of radioactive resin microspheres (SIR-Spheres®, SIRTeX, Lane Cove, Australia) for each individual patient was calculated according to the body surface area method provided by the manufacturer.[15] The tumor volume and total liver volume were calculated by volumetric assessment of CT imaging. Subsequently, the dose of ^{90}Y-microspheres was administered with the catheter tip in the hepatic artery or one of its branches, at the same position as used for the injection of ^{99m}Tc-MAA. The total liver weight (m_{liver}) was derived from CT-volumetric measurements assuming a density of 1 kg/l. The net amount of administered radioactivity (A_{net}) (prepared activity minus residual activity in administration system and catheter) was calculated. The whole liver absorbed dose (D_{liver}), assuming a homogeneous distribution and full absorption of activity in the liver, was then estimated using the following Medical Internal Radiation Dose (MIRD) committee-based formula[17]:

$$D_{liver}\left[Gy\right] = 49.38\,\frac{A_{net}\left[GBq\right]}{m_{liver}\left[kg\right]}$$

Patients received ^{90}Y-RE as a whole liver treatment in a single angiographic procedure (*i.e.* whole liver delivery), whole liver treatment in two sessions (*i.e.* sequential delivery) or as treatment of a single lobe (*i.e.* lobar treatment). In cases of sequential delivery, the aim was to perform both treatment sessions within a commonly accepted interval of 30-45 days.[11] The distribution of ^{90}Y-microspheres was assessed with either bremsstrahlung SPECT or ^{90}Y-positron emission tomography computed tomography (PET-CT). Our institution's radiation safety committee required all patients to stay in the hospital for a minimum of 12 hours after treatment.

Toxicity assessment

Post-treatment, patients reported to the outpatient clinics at intervals of approximately four weeks. At these visits, physical examination and laboratory tests were performed. The following laboratory investigations were included in our analysis in order to assess laboratory toxicity: total bilirubin, alkaline phosphatase (ALP), gamma-glutamyl transferase (GGT), aspartate aminotransferase (AST), alanine aminotransferase (ALT), albumin, hemoglobin (Hb) and white blood cell count (leukocytes). Blood samples, taken up to four weeks prior to ^{90}Y-administration and during a four months follow-up were used for toxicity analysis. Laboratory toxicity was graded according to the Common Terminology Criteria for Adverse Events (CTCAE) v4.0.[18] GGT, AST, ALT and Hb reference values were gender dependent. For each patient, baseline CTCAE grades and

maximal CTCAE grades during follow-up were determined. In addition, new toxicity or progression of baseline toxicity to a higher CTCAE grade was grouped separately and will be referred to as "new toxicity". Patients, in whom data on baseline and/or follow-up laboratory investigations were not available in our center, were excluded from the laboratory toxicity assessment. The clinical toxicity assessment was based on the reporting of periprocedural complications, treatment-related symptoms (CTCAE grade 1-2) and serious adverse events (CTCAE grade 3-4), in the patient charts.

Response assessment

Baseline imaging was performed with CT or magnetic resonance imaging (MRI) of the liver. In addition, patients with (suspected) ^{18}F-fluorodeoxyglucose (^{18}F-FDG)-avid tumors received ^{18}F-FDG-PET to assess the presence of extrahepatic metastases. Follow-up imaging was performed with CT or MRI of the liver (depending on the modality used for baseline imaging) at approximately 1, 3 and 6 months post-treatment. Response assessment was performed in accordance with the Response Evaluation Criteria in Solid Tumors (RECIST 1.1) on the level of target lesions (TL), whole liver (including non-target lesions) and overall response (including non-target lesions and extrahepatic disease) at 3 months (range 2.0 - 4.5 months) and 6 months (range 4.5 - 7.5 months) after the first ^{90}Y-RE procedure.[19] Up to five target lesions per patient were identified by an observer (either MS or CR) and the maximal cross-sectional diameter of each target lesion was subsequently measured by the other observer. Observers were blinded for the identity and characteristics of the patient; date of imaging and whether it was a baseline or follow-up scan. Data on progression of non-target lesions, new liver lesions and progression of extrahepatic disease were extracted from radiologic reports. Patients who were lost to follow-up were regarded as having progressive disease (PD) on the 'overall response level' at the time of death. Median time to progression (TTP) was calculated for all response levels per Kaplan-Meier analysis.

Survival Analysis

Overall survival was defined as the interval between the date of (first) ^{90}Y-RE treatment and the date of death or most recent contact (alive). Median overall survival (including corresponding 95% CI) was calculated through Kaplan-Meier survival-analysis. Statistical analyses were performed with SPSS Statistics 20.0 for windows (IBM SPSS, Chicago, IL). All percentages were rounded to the nearest whole number.

Results

Patients

Between February 1st 2009 and March 31st 2012, a total of 73 consecutive patients (excluding patients participating in a prospective clinical trial) with liver metastases were considered eligible for ^{90}Y-RE treatment at our institute and received a pre-treatment angiographic procedure with ^{99m}Tc MAA. A flowchart of the study design and patient treatment is presented in **Figure 1**. Fourteen patients (19%) could not be treated with ^{90}Y-RE, due to persistent extrahepatic deposition (PED) of ^{99m}Tc-MAA (*n*=11), rapidly progressive disease (*n*=2) and a lung shunt fraction exceeding twenty percent (26%, *n*=1). Fifty-nine patients received ^{90}Y-RE treatment.

Baseline characteristics of these patients are presented in *Table 1*. The majority of the patients (30/59, 51%) had colorectal cancer liver metastases, six patients (10%) had neuroendocrine tumor (NET) liver metastases, and 23 patients (39%) suffered from liver metastases from various other primary tumors.

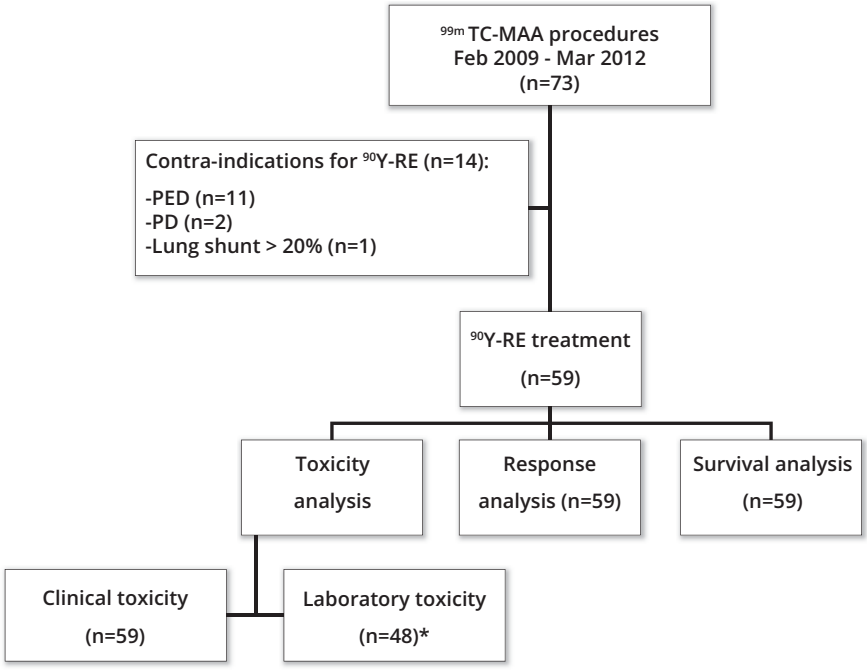

Figure 1. *Flowchart displaying treatment selection and study design. *11 patients were non-evaluable for the laboratory toxicity assessment. Abbreviations: PED = persistent extrahepatic deposition; PD = rapidly progressive disease.*

Table 1. *Baseline characteristics*

Baseline Characteristics	Value
Mean age (years)	60 ± 12
Gender	
Male	32 (54%)
Female	27 (46%)
Primary tumor	
Colorectal cancer	30 (51%)
Neuroendocrine cancer	6 (10%)
Uveal melanoma	6 (10%)
Breast cancer	5 (9%)
Esophageal cancer	2 (3%)
Gallbladder cancer	2 (3%)
Gastric cancer	1 (2%)
Pancreatic cancer	1 (2%)
Nasopharyngeal cancer	1 (2%)
Extrahepatic cholangiocarcinoma	1 (2%)
ACUP	2 (3%)
UCC	1 (2%)
GIST	1 (2%)
WHO performance score	
WHO = 0	31 (53%)
WHO = 1	14 (24%)
WHO ≥ 2	7 (12%)
Unreported	7 (12%)
Child-Pugh score	
A5-A6	53 (90%)
B7-B8	6 (10%)
Tumor burden	
< 25%	43 (73%)
≥ 25% - < 50%	11 (19%)
≥ 50%	5 (9%)
Evidence of extrahepatic metastases	
Yes	16 (27%)
No	43 (73%)

Table 1. *Continued*

Baseline Characteristics	Value
Prior treatment	
Systemic treatment	51 (86%)
Locoregional treatment	50 (85%)
Salvage versus non-salvage therapy	
Salvage therapy	41 (70%)
Non-salvage therapy	17 (29%)
Unreported	1 (2%)

Values are presented as n (percentage) or mean ± standard deviation. Percentages do not add up to 100%, due to rounding to the nearest whole number. Salvage therapy = ^{90}Y-RE after all regular treatment options have been tried. Non-salvage therapy ^{90}Y-RE, when not all treatment options have been tried yet. Abbreviations: ACUP = Adenocarcinoma of Unknown Primary; UCC = Urothelial Cell Carcinoma; GIST = Gastrointestinal Stromal Tumor; WHO = World Health Organization.

Treatment details are presented in *Table 2*. The majority of the patients received a whole liver treatment in one session (*n*=38, 64%), with a selective administration of ^{90}Y-microspheres in the left and right hepatic artery (*n*=28) or administration in the proper (*n*=9) or common hepatic artery (*n*=1). In ten patients, whole liver treatment was performed selectively in sequential sessions (*n*=10, 17%), with a median interval of 14 days (range 12-77 days) between both treatment sessions. Eleven patients received unilobar treatment (*n*=11, 19%). The mean net administered activity was 1473 MBq (standard deviation 447) with an estimated mean liver-absorbed dose of 42.0 Gy (standard deviation 14.3). Post-treatment bremsstrahlung scintigraphy or ^{90}Y-PET, revealed no extrahepatic deposition of radioactivity in any of the patients. Four patients were retreated with ^{90}Y-RE after disease progression had occurred, with a median interval of 9 months (range 5-25 months) between the first and second treatment. Median time of hospital admission was 2 days (range 1-4 days). Fifty-four patients (92%) were discharged the day after treatment. The other five patients required longer hospitalization (one or two days extra), due to comorbidities such as renal insufficiency, diabetes mellitus or heart failure.

Toxicity

Eleven patients (19%) were excluded from laboratory toxicity analysis, because data on laboratory investigations at baseline or during follow-up, within our defined intervals, were not available in our center. In the remaining 48 patients, there were values missing for some laboratory parameters, therefore the denominator was adjusted according-

Table 2. *Treatment details*

Treatment details	Value
Initial extrahepatic deposition of ^{99m}Tc-MAA	12 (20%)
Median ^{99m}Tc-MAA lung shunt fraction	6% (0-20%)
Dose reduction required in n patients	3 (5%)
Mean ^{90}Y administered activity (MBq)	1473 ± 447
Mean ^{90}Y liver absorbed dose (Gy)	42.0 ± 14.3
Whole liver treatment in one session	38 (64%)*
Selective administration (LHA & RHA)	28 (48%)
PHA	9 (15%)
CHA	1 (2%)
Whole liver treatment in sequential sessions (LHA & RHA)	10 (17%)
Lobar treatment	11 (19%)
Retreatment with ^{90}Y-RE after progression	4 (7%)
Median time to retreatment (months)	9 (5-25)

*Values are presented as n (percentage), median (range) or mean ± standard deviation. * This number includes four patients with a history of previous hemihepatectomy. Abbreviations: MBq = Megabecquerel; Gy = Gray; LHA = Left Hepatic Artery; RHA = Right Hepatic Artery; PHA = Proper Hepatic Artery; CHA = Common Hepatic Artery.*

ly when calculating incidences. CTCAE grades at baseline, maximum CTCAE grades during follow-up and corresponding new toxicity are presented in *Figure 2*. Grade 3-4 toxicity at baseline was observed for GGT (16/47, 34%) and ALP (1/47, 1%). Grade 3-4 new toxicity was observed in 18 patients (38%), including following parameters: GGT (13/47, 27%), ALP (10/27, 21%), bilirubin (1/41, 2%), AST (1/47, 2%), ALT (1/47, 2%), and albumin (1/42, 2%). In addition, the incidence of grade 3-4 new toxicity was stratified according to treatment strategy. Ten out of 28 evaluable patients (36%) who received whole liver treatment in one session had grade 3-4 new toxicity, compared to five out of ten patients (50%) who received whole liver treatment in sequential sessions, and three out of ten patients (30%) who received unilobar treatment (*Table 3*).

The following periprocedural complications were reported: allergic reaction to contrast agent (*n*=6), arterial dissection (*n*=2), nausea/vomitus during angiography (*n*=1), delayed hemostasis at the access site requiring prolonged clamping (*n*=1), inguinal hematoma at the access site (*n*=1). Complications did not prevent any patients from receiving therapy. Back pain or abdominal pain during angiography was managed with fentanyl (37% of patients, range 50-200 mcg i.v.) and/or diclofenac (35% of patients, range 50 – 125 mg i.v.).

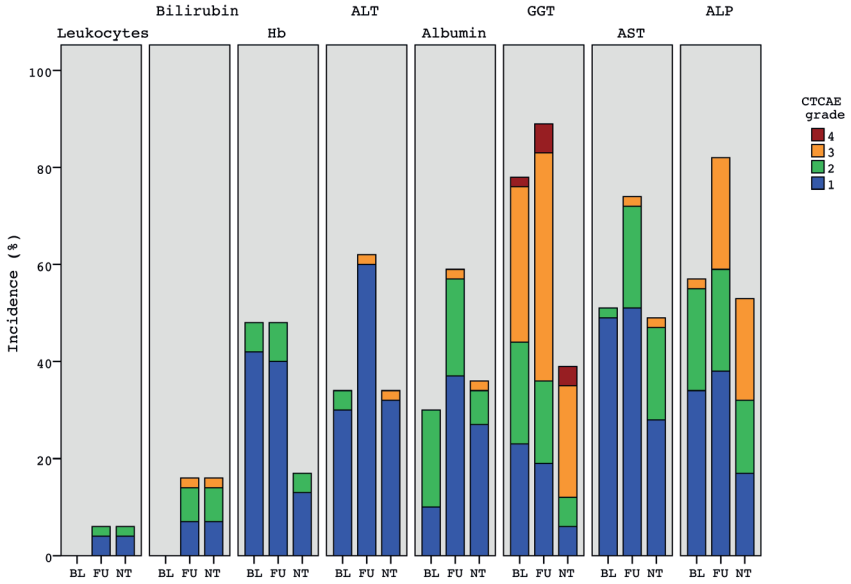

Figure 2. *Laboratory toxicity. Clustered bar-chart displaying the incidence of laboratory toxicity at baseline (BL), during follow-up (FU) and corresponding 'new toxicity' (NT) per laboratory value. CTCAE grades: blue = grade 1; green = grade 2; orange = grade 3; red = grade 4. Abbreviations: ALT = alanine amino-transferase; Hb = hemoglobin; AST = aspartate aminotransferase; AP = alkaline phosphatase; GGT = gamma-glutamyl transferase.*

Table 3. *Grade 3/4 laboratory toxicity*

Treatment strategy	Incidence of new grade 3/4 laboratory toxicity
All evaluable patients	18/48 (38%)
Whole liver treatment in one session	10/28* (36%)
Whole liver treatment in sequential sessions	5/10 (50%)
Single lobar treatment	3/10 (30%)

*Values are presented as n (percentage). * This number includes four patients with a history of previous hemi-hepatectomy.*

Clinical symptoms associated with the postembolization syndrome (CTCAE grade 1-2) were observed in the majority of the treated patients. This syndrome comprised the following symptoms (in order of frequency): fatigue and loss of appetite, pain/discomfort in the right upper abdominal quadrant requiring analgesics (paracetamol and/or diclofenac and/or morphine), nausea and vomitus, fever and general discomfort. In general, these symptoms started on the day of treatment and lasted up to two weeks after treatment. No grade 3-4 clinical toxicity was observed after ^{90}Y-RE treatment and

no serious treatment-related complications such as duodenal or gastric ulceration, radiation pneumonitis or RILD, were observed.

Response

Target lesions-, whole liver- and overall response rates and TTP (for all patients and per tumor type) at 3- and 6-months are displayed in *Table 4*. Target lesion, whole liver and overall disease control rates (complete response + partial response + stable disease) at 3-months post-treatment were 35%, 21% and 19% respectively. Corresponding disease control rates at 6-months were 25%, 13% and 12%. Median TTP for all patients was 6.2 months (95% CI 2.2-10.0) for target lesions, 3.3 months (95% CI 2.8-3.8) for the whole liver and 3.0 months (95% CI 2.4-3.5) overall.

Survival

At the time of analysis, 49 patients had died and 10 patients were still alive. Median overall survival for the entire group of patients (*n*=59) was 8.9 months (95% CI 7.2-10.6). The Kaplan-Meier survival curve is displayed in *Figure 3*. Median overall survival was 8.9 months (95% CI 6.9-10.9) for colorectal cancer liver metastases (*n*=30), 40.3 months (0-107.9) for NET metastases (*n*=6) and 7.8 months (95% CI 5.0-10.6) for other metastases (n=23) (*Figure 4*).

Table 4. *Response rates and time to progression*

	Target Lesion		Whole liver		Overall	
	3 months	6 months	3 months	6 months	3 months	6 months
CR	2 (3%)	0	2 (3%)	0	1 (2%)	0
PR	3 (5%)	3 (5%)	2 (3%)	2 (3%)	2 (3%)	1 (2%)
SD	16 (27%)	12 (20%)	9 (15%)	6 (10%)	8 (14%)	6 (10%)
PD	16 (27%)	6 (10%)	26 (44%)	16 (27%)	30 (51%)	19 (32%)
Deceased	9 (15%)	24 (41%)	9 (15%)	24 (41%)	9 (15%)	24 (41%)
NE	9 (15%)	10 (17%)	7 (12%)	7 (12%)	5 (9%)	5 (9%)
Loss FU	4 (7%)	4 (7%)	4 (7%)	4 (7%)	4 (7%)	4 (7%)
Disease control rate	35%	25%	21%	13%	19%	12%
TTP (all patients)	6.2 months (2.2-10.0)		3.3 months (2.8-3.8)		3.0 months (2.4-3.5)	
TTP (CRLM)	6.2 months (2.5-9.8)		3.0 months (2.8-3.3)		2.8 months (2.2-3.3)	
TTP (NET)	36.4 months (0-88.7)		19.0 months (0-62.0)		11.7 months (0-24.8)	
TTP (Other)	4.4 months (0.8-8.0)		3.8 months (1.9-5.5)		3.3 months (2.2-4.4)	

Values are presented as n (percentage) or median Kaplan-Meier estimate (95% confidence interval). Abbreviations: CR = Complete Response; PR = Partial Response; SD = Stable Disease; PD = Progressive Disease; NE = Non-evaluable; Loss FU = Loss to Follow-Up; TTP= Time To Progression.

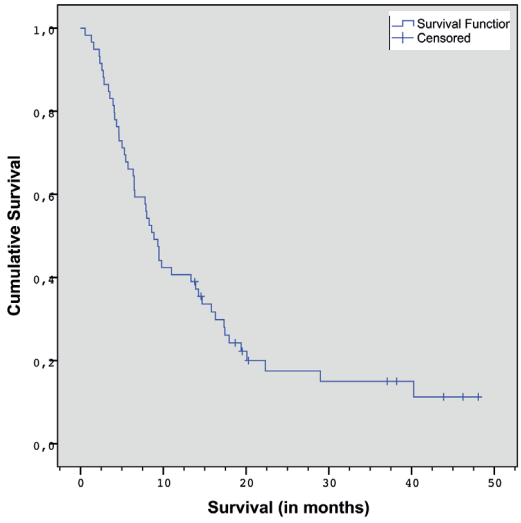

Figure 3. *Kaplan-Meier Survival curve for all 59 patients*

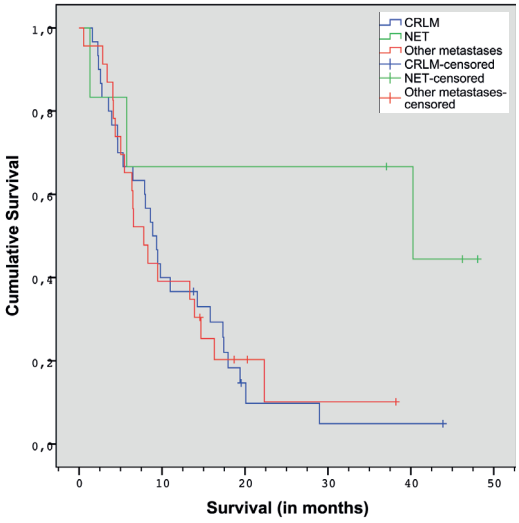

Figure 4. *Kaplan-Meier Survival curve per tumor type. The blue line represents patients with colorectal liver metastases (CRLM), the green line represents patients with neuroendocrine tumor (NET) liver metastases, and the red line represents patients with liver metastases from other primary tumors.*

Discussion

The primary objective of this study was to investigate treatment-related clinical and laboratory toxicity in patients with unresectable liver metastases, treated with ^{90}Y-RE. Secondary objectives were to assess tumor response and overall survival. Clinical toxicity was confined to grade 1-2 symptoms of the post-embolization syndrome. No RILD or other grade 3-4 clinical toxicity was observed, whereas laboratory toxicity grade 3-4 was observed in 38% of patients. In this cohort, a disease control rate of up to 35% was obtained at 3-months post-treatment, and median overall survival was 8.9 months.

Tumor response rates vary widely in the ^{90}Y-RE literature.[4] This may be explained in part by differences in methodology for response assessment. Various studies do not specify whether RECIST criteria have been followed. According to these criteria, tumor response should be differentiated in target lesion, liver and overall response.[19] In order to improve interpretability of overall response rates, studies should indicate whether patients had evidence of extrahepatic disease at baseline. Response rates are commonly divided into 3- and 6-months rates post-treatment. However, it should be clearly stated which imaging intervals are chosen to represent this 3- and 6-months measurements. In addition, it would be preferable to score target lesion response blindly, to assure objective measurements. In a comprehensive review of the ^{90}Y-RE literature, twelve studies were identified that reported a 3-month disease control rate, ranging from 63 – 100%.[4] In most of these studies, the level on which response assessment had been performed was not specified. Assuming these are whole-liver disease control rates, our 3-month disease control rate was much lower: 21%. This difference could be attributable to differences in methodology of response assessment, as mentioned above. However, less stringent patient selection criteria and the heterogeneity of our cohort, including hyper- and hypovascular liver metastases from various primary tumors, could also have attributed to lower response rates.

Toxicity due to radiation to the liver has first been described after external radiation therapy.[20,21] It was found that the liver is very sensitive to radiation and patients may develop radiation induced liver disease (RILD), months after an overdose of radiation. Histopathologically, RILD is characterized by veno-occlusive disease with congestion of the central veins and sinusoids.[21-24] The symptoms of RILD comprise fatigue, anicteric ascites, hepatomegaly, and elevated liver function tests (especially alkaline phosphatase).[23] High dose corticosteroids can be given to mitigate the course of this disease. It is however, hard to recognize RILD since it has a long latency time and many of its symptoms can also occur after non-complicated treatment with ^{90}Y-RE. A better understanding of the physiological variation of treatment-related laboratory toxicity after ^{90}Y-RE would be very helpful in discriminating early signs of RILD from transient laboratory abnormalities after treatment. Mild toxicity (grade 1-2) of liver function tests is common after ^{90}Y-RE, occurring in up to 70% of the patients.[25-27] Reported incidences of grade 3-4 toxicity are much lower and vary widely across studies. Van Hazel *et al.*[2] observed no grade 3-4 toxicity in their study, Piana *et al.*[25] found an overall incidence of 7% and Kennedy *et al.*[8] reported an incidence of up to 20.5% for ALP. In the study of Piana *et al.*, one patient died of RILD.[25] In our study we found higher incidences of laboratory toxicity, with new laboratory toxicity grade 3-4 occurring in up to 38% of the patients. However, we did not observe any serious treatment-related complications,

nor did we observe any RILD. This indicates that serious laboratory toxicity regarding transaminases and liver function tests can occur as part of the physiological reaction of the liver to ^{90}Y-RE treatment.

One of the factors complicating the interpretation of toxicity results is that abnormalities in liver function tests and transaminases could be the result of tumor progression instead of treatment-related toxicity. Moreover, results of toxicity are often incompletely reported in the ^{90}Y-RE literature. Many studies do not specify how CTCAE scores for laboratory toxicity have been determined. This could inadvertently lead to an underestimation of treatment toxicity and it limits the comparability of studies. Therefore, we aimed to report our methods and results in an unambiguous and transparent fashion. The most important limitations of this study were its retrospective design and the lack of standardization of laboratory investigations and reporting of clinical symptoms during physical examination. Therefore, our results in terms of the incidence of laboratory or clinical toxicity are likely to be underestimations of the real incidence of toxicity. Another limitation was the heterogeneity of our study population. However, this heterogenic group does reflect the typical population of patients referred for ^{90}Y-RE treatment.

Fourteen of the 73 patients (19%) who received work-up angiography did not receive ^{90}Y-RE. The majority of these patients (n=11) were not eligible because of persisting extrahepatic deposition (PED) of ^{99m}Tc-MAA. This PED rate of 11/73 (15%) is much higher than the rates reported in the literature (ranging from 0% to 10%).[16,28,29] A likely cause of the high PED rate in this study is the relative large number of proximal injection positions (*i.e.* proper or common hepatic artery). Several studies have demonstrated that extrahepatic deposition can be solved/prevented by more distal injection positions (left/middle/right hepatic artery or even more selective).[16,28,30] We have changed our current practice accordingly and we rarely perform whole liver treatments from the proper hepatic artery anymore. In addition, our center and many others increasingly use c-arm cone beam computed tomography during the pre-treatment angiography to help prevent extrahepatic distribution and identify culprit vessels.[31,32]

The whole liver approach has also been associated with increased toxicity. Seidensticker *et al.* have reported that a whole liver approach, in non-cirrhotic liver metastases patients, resulted in a higher number of liver-related CTCAE grade 3-4 events as compared to a sequential lobar approach.[14] We could not confirm this finding in our patients. In fact, the number of patients with CTCAE grade 3-4 laboratory toxicity was even lower in the whole liver approach group (36%) than in the sequential lobar group (50%). Selection bias, and confounding due to differences in baseline characteristics, may play a significant role in this matter. However, we do recognize the clinical impor-

tance, and we think that the question whether treating the whole liver at once increases toxicity, should be determined using a randomized controlled trial.
The majority of the patients (70%) treated in our cohort, received radio-embolization as salvage therapy. This illustrates that ^{90}Y-RE is still regarded as a treatment option of last resort, for patients who have unresectable and chemorefractory liver tumors. The costs of radioembolization treatment (approximately **€**11.000 for one dose of SIR-spheres plus the costs of the procedure, the involved imaging, hospitalization and follow-up) need to be weighed against the potential benefit to the patient.[33] For this purpose, prospective comparative studies evaluating survival, tumor response, and quality of life after ^{90}Y-RE are strongly warranted. In addition, it will become increasingly important to select those patients that will benefit most from this therapy. Performing radioembolization at an earlier stage in patients with liver metastases might for instance translate into improved tumor response rates and overall survival. Two large randomized controlled trials are currently ongoing, investigating the effect on overall survival (SIRFLOX study) and progression free survival (FOXFIRE study) of the addition of ^{90}Y-RE to FOLFOX (fluorouracil, leucovorin, oxaliplatin) with or without bevacizumab as first-line treatment for patients with unresectable colorectal liver metastases.[34]

Conclusion

The risk of severe complications or grade 3-4 clinical toxicity in patients with liver metastases of various primary tumors undergoing ^{90}Y-RE is low. In contrast, laboratory toxicity grade 3-4 was observed in more than one-third of the patients without any signs of RILD. This physiological reaction of liver enzymes to ^{90}Y-RE therapy may mask early signs of toxicity due to RILD.

References

1. Bierman HR, Byron RL, Jr., Kelley KH, Grady A (1951) Studies on the blood supply of tumors in man. III. Vascular patterns of the liver by hepatic arteriography in vivo. J Natl Cancer Inst 12: 107-131.
2. Van Hazel G, Blackwell A, Anderson J, Price D, Moroz P, et al. (2004) Randomised phase 2 trial of SIR-Spheres plus fluorouracil/leucovorin chemotherapy versus fluorouracil/leucovorin chemotherapy alone in advanced colorectal cancer. J Surg Oncol 88: 78-85.
3. Gray B, Van Hazel G, Hope M, Burton M, Moroz P, et al. (2001) Randomised trial of SIR-Spheres plus chemotherapy vs. chemotherapy alone for treating patients with liver metastases from primary large bowel cancer. Ann Oncol 12: 1711-1720.
4. Vente MA, Wondergem M, van der Tweel I, van den Bosch MA, Zonnenberg BA, et al. (2009) Yttrium-90 microsphere radioembolization for the treatment of liver malignancies: a structured meta-analysis. Eur Radiol 19: 951-959.
5. Dunfee BL, Riaz A, Lewandowski RJ, Ibrahim S, Mulcahy MF, et al. (2010) Yttrium-90 radioembolization for liver malignancies: prognostic factors associated with survival. J Vasc Interv Radiol 21: 90-95.
6. Chua TC, Bester L, Saxena A, Morris DL (2011) Radioembolization and systemic chemotherapy improves response and survival for unresectable colorectal liver metastases. J Cancer Res Clin Oncol 137: 865-873.
7. Sato K, Lewandowski RJ, Bui JT, Omary R, Hunter RD, et al. (2006) Treatment of unresectable primary and metastatic liver cancer with yttrium-90 microspheres (TheraSphere): assessment of hepatic arterial embolization. Cardiovasc Intervent Radiol 29: 522-529.
8. Kennedy AS, Coldwell D, Nutting C, Murthy R, Wertman DE, Jr., et al. (2006) Resin 90Y-microsphere brachytherapy for unresectable colorectal liver metastases: modern USA experience. Int J Radiat Oncol Biol Phys 65: 412-425.
9. Salem R, Thurston KG (2006) Radioembolization with 90yttrium microspheres: a state-of-the-art brachytherapy treatment for primary and secondary liver malignancies. Part 2: special topics. J Vasc Interv Radiol 17: 1425-1439.
10. Szyszko T, Al-Nahhas A, Tait P, Rubello D, Canelo R, et al. (2007) Management and prevention of adverse effects related to treatment of liver tumours with 90Y microspheres. Nucl Med Commun 28: 21-24.
11. Kennedy A, Nag S, Salem R, Murthy R, McEwan AJ, et al. (2007) Recommendations for radioembolization of hepatic malignancies using yttrium-90 microsphere brachytherapy: a consensus panel report from the radioembolization brachytherapy oncology consortium. Int J Radiat Oncol Biol Phys 68: 13-23.
12. Riaz A, Lewandowski RJ, Kulik LM, Mulcahy MF, Sato KT, et al. (2009) Complications following radioembolization with yttrium-90 microspheres: a comprehensive literature review. J Vasc Interv Radiol 20: 1121-1130; quiz 1131.
13. Carretero C, Munoz-Navas M, Betes M, Angos R, Subtil JC, et al. (2007) Gastroduodenal injury after radioembolization of hepatic tumors. Am J Gastroenterol 102: 1216-1220.
14. Seidensticker R, Seidensticker M, Damm R,

Mohnike K, Schutte K, et al. (2012) Hepatic toxicity after radioembolization of the liver using (90)Y-microspheres: sequential lobar versus whole liver approach. Cardiovasc Intervent Radiol 35: 1109-1118.

15. Sirtex (2013) SIR-Spheres Yttrium-90 Resin Microspheres Package Insert.
16. Barentsz MW, Vente MA, Lam MG, Smits ML, Nijsen JF, et al. (2011) Technical solutions to ensure safe yttrium-90 radioembolization in patients with initial extrahepatic deposition of (99m)technetium-albumin macroaggregates. Cardiovasc Intervent Radiol 34: 1074-1079.
17. Dezarn WA, Cessna JT, DeWerd LA, Feng W, Gates VL, et al. (2011) Recommendations of the American Association of Physicists in Medicine on dosimetry, imaging, and quality assurance procedures for 90Y microsphere brachytherapy in the treatment of hepatic malignancies. Med Phys 38: 4824-4845.
18. Common Terminology Criteria for Adverse Events (CTCAE) v4.0, available at http://ctep.cancer.gov.
19. Eisenhauer EA, Therasse P, Bogaerts J, Schwartz LH, Sargent D, et al. (2009) New response evaluation criteria in solid tumours: revised RECIST guideline (version 1.1). Eur J Cancer 45: 228-247.
20. Reed GB, Jr., Cox AJ, Jr. (1966) The human liver after radiation injury. A form of veno-occlusive disease. Am J Pathol 48: 597-611.
21. Lawrence TS, Robertson JM, Anscher MS, Jirtle RL, Ensminger WD, et al. (1995) Hepatic toxicity resulting from cancer treatment. Int J Radiat Oncol Biol Phys 31: 1237-1248.
22. da Silveira EB, Jeffers L, Schiff ER (2002) Diagnostic laparoscopy in radiation-induced liver disease. Gastrointest Endosc 55: 432-434.
23. Guha C, Kavanagh BD (2011) Hepatic radiation toxicity: avoidance and amelioration. Semin Radiat Oncol 21: 256-263.
24. Sempoux C, Horsmans Y, Geubel A, Fraikin J, Van Beers BE, et al. (1997) Severe radiation-induced liver disease following localized radiation therapy for biliopancreatic carcinoma: activation of hepatic stellate cells as an early event. Hepatology 26: 128-134.
25. Piana PM, Gonsalves CF, Sato T, Anne PR, McCann JW, et al. (2011) Toxicities after radioembolization with yttrium-90 SIR-spheres: incidence and contributing risk factors at a single center. J Vasc Interv Radiol 22: 1373-1379.
26. Gulec SA, Mesoloras G, Dezarn WA, McNeillie P, Kennedy AS (2007) Safety and efficacy of Y-90 microsphere treatment in patients with primary and metastatic liver cancer: the tumor selectivity of the treatment as a function of tumor to liver flow ratio. J Transl Med 5: 15.
27. Arslan N, Emi M, Alagoz E, Ustunsoz B, Oysul K, et al. (2011) Selective intraarterial radionuclide therapy with Yttrium-90 (Y-90) microspheres for hepatic neuroendocrine metastases: initial experience at a single center. Vojnosanit Pregl 68: 341-348.
28. Dudeck O, Wilhelmsen S, Ulrich G, Lowenthal D, Pech M, et al. (2012) Effectiveness of repeat angiographic assessment in patients designated for radioembolization using yttrium-90 microspheres with initial extrahepatic accumulation of technitium-99m macroaggregated albumin: a single center's experience. Cardiovasc Intervent Radiol 35: 1083-1093.

29. Smits ML, Nijsen JF, van den Bosch MA, Lam MG, Vente MA, et al. (2012) Holmium-166 radioembolisation in patients with unresectable, chemorefractory liver metastases (HEPAR trial): a phase 1, dose-escalation study. Lancet Oncol 13: 1025-1034.

30. Lam MG, Banerjee S, Louie JD, Abdelmaksoud MH, Iagaru AH, et al. (2013) Root Cause Analysis of Gastroduodenal Ulceration After Yttrium-90 Radioembolization. Cardiovasc Intervent Radiol.

31. Louie JD, Kothary N, Kuo WT, Hwang GL, Hofmann LV, et al. (2009) Incorporating cone-beam CT into the treatment planning for yttrium-90 radioembolization. J Vasc Interv Radiol 20: 606-613.

32. Heusner TA, Hamami ME, Ertle J, Hahn S, Poeppel T, et al. (2010) Angiography-based C-arm CT for the assessment of extrahepatic shunting before radioembolization. Rofo 182: 603-608.

33. Garin E, Rolland Y, Boucher E, Ardisson V, Laffont S, et al. (2010) First experience of hepatic radioembolization using microspheres labelled with yttrium-90 (TheraSphere): practical aspects concerning its implementation. Eur J Nucl Med Mol Imaging 37: 453-461.

34. Sharma RA, Wasan HS, Love SB, Dutton S, Stokes JC, et al. (2008) FOXFIRE: a phase III clinical trial of chemo-radio-embolisation as first-line treatment of liver metastases in patients with colorectal cancer. Clin Oncol (R Coll Radiol) 20: 261-263.

Chapter 3

Holmium-166 radioembolization for the treatment of patients with liver metastases: design of the phase I HEPAR trial

MLJ Smits, JFW Nijsen, MAAJ van den Bosch, MGEH Lam, MAD Vente, JE Huijbregts, AD van het Schip, M Elschot, W Bult, HWAM de Jong, PCW Meulenhoff, BA Zonnenberg

Journal of Experimental and Clinical Cancer Research 2010

Abstra

Background

Intra-arterial radioembolization with yttrium-90 microspheres (^{90}Y-RE) is an increasingly used therapy for patients with unresectable liver malignancies. Over the last decade, radioactive holmium-166 (^{166}Ho) poly(L-lactic acid) microspheres have been developed as a possible alternative to ^{90}Y-RE. Next to high-energy beta-radiation, ^{166}Ho also emits gamma-radiation, which allows for imaging by gamma scintigraphy. In addition, holmium is a highly paramagnetic element and can therefore be visualized on MRI. These imaging modalities are useful for assessment of the biodistribution and allow dosimetry through quantitative analysis of the scintigraphic and MR images. Previous studies have demonstrated the safety of ^{166}Ho-radioembolization (^{166}Ho-RE) in animals. The aim of this phase I trial is to assess the safety and toxicity profile of ^{166}Ho-RE in patients with liver metastases.

Methods

The HEPAR study (Holmium Embolization Particles for Arterial Radiotherapy) is a non-randomized, open label, safety study. We aim to include 12 to 24 patients with liver metastases of any origin, who have chemotherapy-refractory disease and who are

Background

The liver is a common site of metastatic disease. Hepatic metastases can originate from a wide range of primary tumors (e.g. colorectal-. breast- and neuroendocrine tumors).[1] It is estimated that 50% of all patients with a primary colorectal tumor will in due course develop hepatic metastases.[2] Once a primary malignancy has spread to the liver, the prognosis of many of these patients deteriorates significantly. Potentially curative treatment options for hepatic metastases consist of subtotal hepatectomy or, in certain cases, radiofrequency ablation. Unfortunately, only 20-30% of patients are eligible for these potentially curative treatment options, mainly because hepatic metastases are often multiple and in an advanced stage at the time of presentation.[3] The majority of patients are therefore left with palliative treatment options.

Palliative therapy consists primarily of systemic chemotherapy. In spite of the many promising developments on cytostatic and targeted biological agents over the last ten years, there are still certain tumor types that do not respond adequately and the long-term survival rate for patients with unresectable metastatic liver disease remains low.[4-8] Moreover, systemic chemotherapy can be associated with substantial side effects that lie in the non-specific nature of this treatment. Cytostatic agents are distributed over the entire body, destroying cells that divide rapidly, both tumor cells and healthy cells.

not amenable to surgical resection. Prior to treatment, in addition to the standard technetium-99m labelled macroaggregated albumin (^{99m}Tc-MAA) dose, a low radioactive safety dose of 60 mg ^{166}Ho-microspheres will be administered. Patients are treated in 4 cohorts of 3-6 patients, according to a standard dose escalation protocol (20 Gy, 40 Gy, 60 Gy, and 80 Gy, respectively). The primary objective will be to establish the maximum tolerated radiation dose of ^{166}Ho-microspheres. Secondary objectives are to assess tumor response, biodistribution, performance status, quality of life, and to compare the ^{166}Ho-microspheres-safety dose and the ^{99m}Tc-MAA dose distributions with respect to the ability to accurately predict microsphere distribution.

Discussion

This will be the first clinical study on ^{166}Ho-RE. Based on preclinical studies, it is expected that ^{166}Ho-RE has a safety and toxicity profile comparable to that of ^{90}Y-RE. The biochemical and radionuclide characteristics of ^{166}Ho-microspheres that enable accurate dosimetry calculations and biodistribution assessment may however improve the overall safety and efficacy of the procedure.

A relatively recently developed therapy for primary and secondary liver cancer is radioembolization with yttrium-90 microspheres (^{90}Y-RE). ^{90}Y-RE is a minimally invasive procedure during which radioactive microspheres are instilled selectively into the hepatic artery using a catheter. The high-energy beta-radiation emitting microspheres subsequently strand in the arterioles (mainly) of the tumor and a tumoricidal radiation absorbed dose is delivered. The clinical results of this form of internal radiation therapy are promising.[9,10] The only currently clinically available microspheres for radioembolization loaded with ^{90}Y are made of either glass (TheraSphere®, BTG International Ltd., London, UK) or resin (SIR-Spheres®, SIRTeX Medical Ltd., Sydney, New South Wales, Australia).

Although ^{90}Y-RE is evermore used and considered a safe and effective treatment, ^{90}Y-microspheres have a drawback: following administration the actual biodistribution cannot be optimally visualized. For this reason, ^{166}Ho-microspheres have been developed at our center.[11,12] Like ^{90}Y, ^{166}Ho emits high-energy beta particles to eradicate tumor cells but ^{166}Ho also emits low-energy (81 keV) gamma photons, which allows for nuclear imaging. As a consequence, visualization of the microspheres is feasible. This is very useful for three main reasons. Firstly, prior to administration of

the treatment dose, a small scout dose of ^{166}Ho-microspheres can be administered for prediction of the distribution of the treatment dose. This provides a theoretical advantage over ^{90}Y-RE, for which the distribution assessment depends on a scout dose of ^{99m}Tc-MAA, with a disputable distribution correlation with the actual microspheres.[13] Secondly, quantitative analysis of the nuclear images would allow assessment of the radiation dose delivered on both the tumor and the normal liver (i.e. dosimetry).[14] Thirdly, since holmium is highly paramagnetic, it can be visualized using magnetic resonance imaging (MRI). Quantitative analysis of these MRI images is also possible, which is especially useful for medium- and long-term monitoring of the intrahepatic behavior of the microspheres.[15,16]

The pharmaceutical quality of ^{166}Ho-microspheres has been thoroughly investigated and proven to be satisfactory.[17-19] Multiple animal studies have been conducted in order to investigate the intrahepatic distribution (ratio tumor-to-normal liver), the toxicity profile/biocompatibility of the ^{166}Ho-microspheres, safety of the administration procedure, and efficacy of these particles.[20-22]
Now that the preclinical phase of ^{166}Ho-RE has been successfully completed, we will start a clinical trial (the HEPAR study: Holmium Embolization Particles for Arterial Radiotherapy) in order to evaluate ^{166}Ho-RE in patients with liver metastases. The main purpose of this trial is to assess the safety and toxicity profile of ^{166}Ho-RE. Secondary endpoints are tumor response, biodistribution prediction with ^{99m}Tc-MAA versus a safety dose of ^{166}Ho-microspheres, performance status, and quality of life.

Methods

Study design

The HEPAR study is a single center, non-randomized, open label safety study. In this phase I study, a new device will be investigated, namely ^{166}Ho-microspheres for intra-arterial radioembolization for the treatment of liver malignancies. In a group of 12 to 24 patients with liver metastases, treated with increasing doses of ^{166}Ho, the device will be investigated for safety and toxicity.

Subjects

The study will include patients with liver-dominant metastases, of any histology, who cannot be treated by standard treatment options such as surgery and systemic chemotherapy, due to advanced stage of disease, significant side effects or unsatisfactory tumor response.

Medical device

Using the solvent evaporation technique, non-radioactive holmium-165 (^{165}Ho) and its acetylacetonate complex (HoAcAc) can be incorporated into the poly(L-lactic acid) matrix to form microspheres (*Figure 1*). Subsequently, the non-radioactive ^{165}Ho- microspheres can be made radioactive by neutron activation in a nuclear facility and form ^{166}Ho-microspheres. Neutron-activated ^{166}Ho has a half-life of 26.8 hours and is a beta emitter ($E_{\beta max}$ = 1.85 MeV) that also emits gamma photons (E_{γ} = 81 keV) suitable for single photon emission computed tomography (SPECT) (*Table 1*).

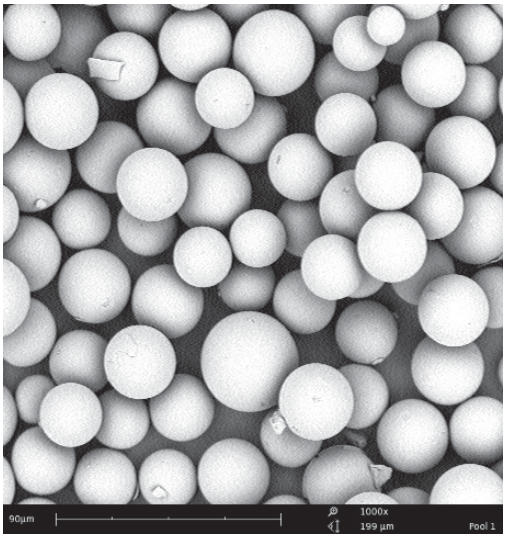

Figure 1. *Scanning electron microscope image of holmium microspheres*

Recruitment

Patients with liver metastases who agree to participate in the study must be referred to the principle investigator. The principle investigator will inform every patient and obtain his or her informed consent.

Pre-treatment work-up

Screening

A screening visit will take place at the outpatient clinic within 14 days prior to the fist angiography. During this visit, the principle investigator will run through the inclusion and exclusion criteria, conduct a physical examination, and assess the WHO performance status of the patient. Subsequently, CT, MRI, and positron emission tomography (PET) will be performed, as well as electrocardiography (ECG). PET will only be per-

Table 1. *Radionuclide and physicochemical characteristics of ^{90}Y- and ^{166}Ho-microspheres for radioembolization*

Product	^{166}Ho-PLLA-MS	SIR-Spheres®	TheraSphere®
Radionuclide	Holmium-166	Yttrium-90	
T1/2 (h)	26.8	64.2	
γ-emission (keV)	80.6 (6.7%) and 1,379.4 (0.9%)	none	
β-emission (keV)	1,774.3 (48.7%) and 1,854.9 (50.0%)	2,280.1 (100%)	
Imaging options	SPECT and MRI	Bremsstrahlung SPECT and PET	
Matrix material	PLLA	resin	glass
Density (g/ml)	1.4	1.6	3.3
Diameter (μm)	30 ± 5	32 ± 10	25 ± 10
Administered amount of particles (mg)	600	1,370	66 – 440
Administered number of particles	33,000,000	40,000,000 – 80,000,000	1,200,000 – 8,000,000
Maximal activity (GBq)	15	3	20
Activity per microsphere (Bq)	450	50	1,250 – 2,500

^{90}Y = yttrium-90; ^{166}Ho-PLLA-MS = holmium-166 poly(L-lactic acid) microspheres; MRI = Magnetic Resonance Imaging; PET = Positron Emission Tomography; SPECT = Single Photon Emission Computed Tomography

formed in FDG-avid tumors. Liver weight will be calculated, based on the liver volume measured on CT data with a density conversion factor of 1.0 g/cm^3. Relevant laboratory tests (hematology, coagulation profile, serum chemistry, tumor marker) must be documented and reviewed. All patients are asked to fill out the European Organization for Research and Treatment of Cancer (EORTC) QLQ-C30 questionnaire.[23]

Angiography

Patients will be hospitalized on the evening prior to angiography. On day 0 the patient is subjected to angiography of the upper abdominal vessels. The celiac axis and superior mesenteric artery are visualised, followed by coiling of relevant vessels, in particular branches of the hepatic artery supplying organs other than the liver, e.g. gastroduodenal artery (GDA), right gastric artery (RGA). If major arteries like the GDA or RGA cannot be successfully occluded, the patient will be withheld ^{166}Ho-RE. This procedure will be performed by a skilled and trained interventional radiologist. The catheter is introduced using the Seldinger technique. Premedication consists of a single administration of corticosteroids (dexamethason 10 mg i.v.) and antiemetics (ondansetron 8 mg i.v.). Proton pump inhibitors (pantoprazol 1 dd 40 mg) are started on the day of the intervention and prescribed for use until the end of the follow-up.

Macroaggregated albumin injection

After successful angiography and coiling of relevant vasculature is performed, a dose of ^{99m}Tc-Macroaggregated Albumin (^{99m}Tc-MAA) will be administered in the hepatic artery on the same day. The ^{99m}Tc-MAA are used to assess whether a favorable distribution of the ^{166}Ho-microspheres can be expected. The patient is subjected to planar imaging of the thorax and abdomen and SPECT of the abdomen, in order to determine the ^{99m}Tc-MAA distribution. Images will be evaluated qualitatively and quantitatively. Extrahepatic deposition of activity is a contra-indication for administration of the treatment dose. Region of interest analysis will be used to calculate lung shunting. Lung shunting should not exceed 20% of the dose ^{99m}Tc-MAA. If the amount of lung shunting cannot be reduced to <20% using standard radiological interventional techniques to decrease the shunting, the patient will not be eligible to receive a safety nor a treatment dose of ^{166}Ho-microspheres. The dose point-kernel method will be applied to the (non-homogeneous) activity distribution to calculate the absorbed dose distribution.[24] Dose-volume histograms will be generated in order to quantify the dose distribution, and the tumor to healthy tissue absorbed dose ratio will be calculated.

^{166}Ho-microspheres-safety dose

The second angiography takes place around 1 week after the first angiography but no longer than 2 weeks later. Patients will be hospitalized on the evening before treatment. They will be discharged approximately 48 hours after the intervention unless complications have occurred. Prior to the procedure, the patient is offered a tranquilizer (oxazepam 10 mg). A safety dose of ^{166}Ho-microspheres will be administered through a catheter inside the hepatic artery, at the position planned during the first intervention. The safety dose will consist of 60 mg (10% of the total amount of microspheres) ^{166}Ho-microspheres with a lower specific activity (90 Bq/microsphere) than for the treatment dose. After the safety dose, planar imaging of both the thorax and abdomen will be performed, as well as SPECT and MRI of the abdomen. Presence of inadvertent administration to the lungs or other upper abdominal organs will once more be checked for. These SPECT and MRI images will be compared with the images post ^{99m}Tc-MAA and post-treatment, regarding extrahepatic deposition of activity, percentage lung shunting, homogeneity of the dose distribution and tumor to healthy tissue absorbed dose ratio.

Treatment

^{166}Ho-microspheres-treatment dose

When the amount of lung shunting does not exceed 20% of the safety dose of ^{166}Ho-microspheres, the (complete) treatment dose of ^{166}Ho-microspheres will be administered (*Figure 2*).

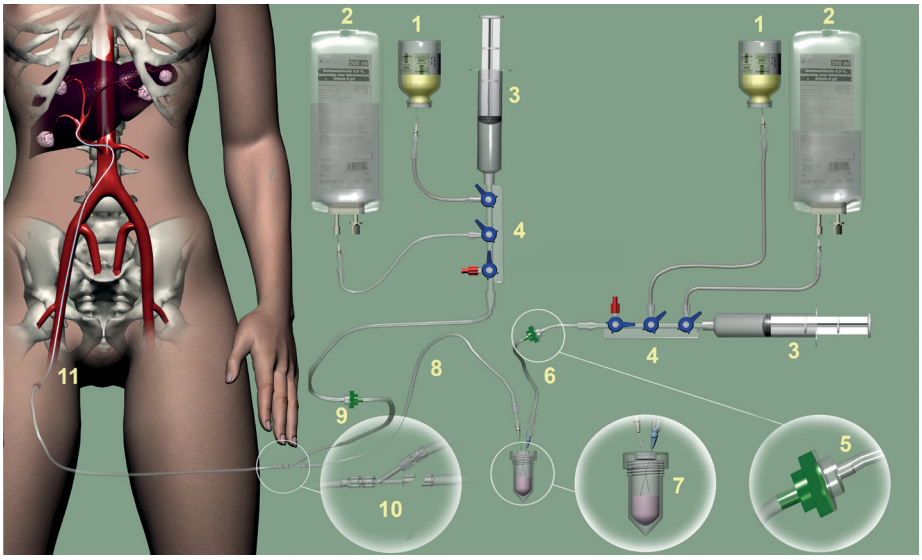

Figure 2. *Schematic overview of the administration system for ^{166}Ho-RE. The administration system consists of the following components: iodine contrast agent (Visipaque®, GE Healthcare) (1), saline solution (2), 20-ml syringe (Luer-Lock) (3), three-stopcock manifold (4), one-way valve (5), inlet line (6), administration vial containing the ^{166}Ho-microspheres (7), outlet line (8), flushing line (9), Y-connector (10) and catheter (11).*

Consecutive cohorts of 3 patients will be treated with identical amounts of microspheres (600 mg). If no toxicity ≥ grade 3 according to the Common Terminology Criteria for Adverse Events (CTCAE)[25] is observed, the next cohort of three patients will be treated at the next radiation dose level. If in one patient CTCAE ≥ grade 3 is observed in a particular cohort, the cohort will be extended to six patients.

If toxicity ≥ grade 3 is observed in two or more patients in a particular cohort, the study will be terminated because the endpoint, e.g. the maximum tolerated radiation dose, is reached. This will be reported to the Independent Ethics Committee (IEC). The dose level prior to the toxic radiation dose will become the recommended dose for efficacy studies. If an event is classified as grade 3 or 4 administration technique related, the patient will be replaced. The specific activity of the ^{166}Ho-microspheres will be increased by adapting the activation time in the nuclear reactor. The first, second, third and fourth cohort will be treated with a dose of 1.3, 2.5, 3.8 and 5.0 GBq/kg (liver weight), respectively. Assuming a homogenous uptake throughout the liver, this equals escalating radiation doses of 20 Gy, 40 Gy and 60 Gy, to a maximum dose of 80 Gy in the last cohort. A maximum of 15.1 GBq will be given to the maximum treated liver weight (inclusive the tumor tissue) of 3 kg (*Table 2*). The amount of radioactivity administered to the patient is calculated according to the following formula:

$A_{Ho\text{-}166}$ (MBq)/LW (kg) = Liver Dose (Gy)/15.87 x 10^{-3} (J/MBq)

Table 2. *Dose (Gy) and activity (MBq) relation of ^{166}Ho treatment*

	Liver weight (kg)				
	1	1,5	2	2,5	3
Liver dose (Gy)	A (MBq)	A (MBq)	A (MBq)	A (MBq)	A (MBq)
10	630	945	1260	1575	1890
20	**1260**	**1890**	**2520**	**3150**	**3780**
30	1890	2835	3780	4725	5670
40	**2520**	**3780**	**5040**	**6300**	**7560**
50	3150	4725	6300	7875	9450
60	**3780**	**5670**	**7560**	**9450**	**11340**
70	4410	6615	8820	11025	13230
80	**5040**	**7560**	**10080**	**12600**	**15120**

In bold: the four consecutive cohorts receive 1.3 GBq/kg (20 Gy), 2.5 GBq/kg (40 Gy), 3.8 GBq/kg (60 Gy) and 5.0 GBq/kg (80 Gy), respectively. As an example, a patient in the first cohort (20 Gy) with a 1.5-kg liver, will be administered a total activity of 1890 MBq

where LW is the liver weight of the patient which may be determined using CT, MRI or ultrasound, and where 15.87 x 10^{-3} (J/MBq) is the activity-to-dose conversion factor for ^{166}Ho.[22]

Radiation exposure rate

During the hospitalization in week 1 the radiation exposure rate will be measured from 1 m distance at t = 0, 3, 6, 24, and 48 hours following ^{166}Ho-microspheres administration. Patients will not be discharged from the hospital until the dose equivalent is less than 90 μSv/h measured from 1 m distance.

Follow-up

All patients are followed over a period of 12 weeks after treatment with weekly visits at the outpatient clinic. During each visit, data is collected by physical examination, WHO performance status assessment and laboratory examination (hematology, coagulation profile, serum chemistry and [if applicable] tumor marker). Adverse events are monitored. In addition, patients are asked to fill out the EORTC questionnaires in the 6th and 12th week post-treatment. CT and (in case of ^{18}F-FDG-avid tumors) PET are performed in the 6th and 12th week post-treatment and MRI is performed in the 1st and the 12th week post-treatment (*Figure 3*).

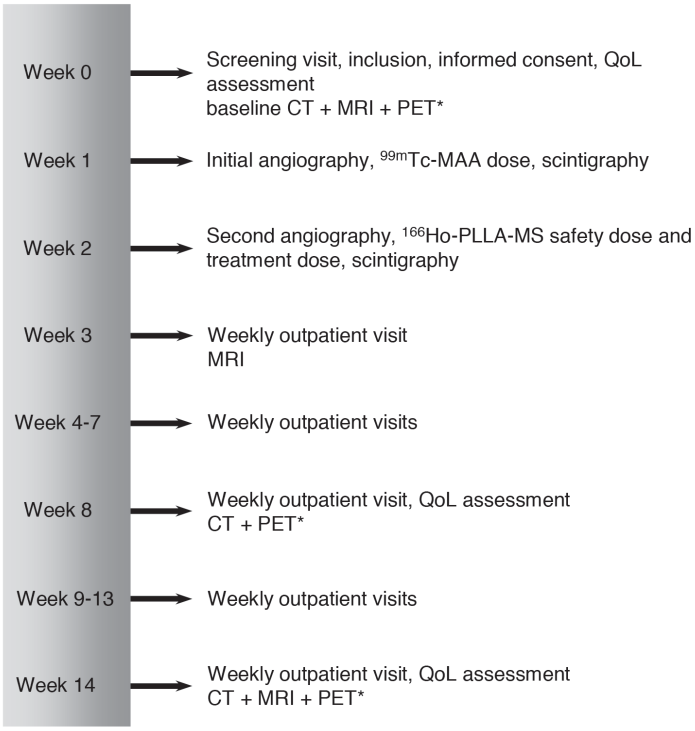

Figure 3. *Timeline for study participants. QoL = quality of life; CT = computed tomography; MRI = magnetic resonance imaging; PET = positron emission tomography; ^{166}Ho-PLLA-MS = holmium-166 poly(L-lactic acid) microspheres. * only in ^{18}F-FDG-avid tumors*

Holmium content

Pooled urine samples will be collected from 0-3 hours, 3-6 hours, 6-24 hours and 24-48 hours post-^{166}Ho-microspheres administration. In the 6th and 12th week post treatment, pooled 24-hours urine will be collected for measurement of holmium content. The date and time of the start and the end of the collection period, the volume and whether the collection was complete or not, will be noted in the case record form. During the hospitalization in week 1, blood will be drawn for measuring the holmium content in the blood at t = 0, 3, 6, 24, and 48 hours following ^{166}Ho-microspheres administration.[19]

Primary objective

The primary objective of this study is to establish the safety and toxicity profile of treatment with ^{166}Ho-microspheres. This profile will be established using the CTCAE v3.0 methodology and will be used to determine the maximum tolerated radiation dose.

Any of the following events which are considered possibly or probably related to the administration of ^{166}Ho-microspheres will be considered a serious adverse event during the 12 weeks follow-up period:

- Grade 3-4 neutropenic infection (absolute neutrophil count < 1.0 x 10^9/L) with fever > 38.3°C,
- Grade 4 neutropenia lasting > 7 days,
- Grade 4 thrombocytopenia (platelet count < 25.0 x10^9/L),
- Grade 3 thrombocytopenia lasting for > 7 days,
- Any other grade 3 or 4 toxicity (excluding expected AST/SGOT, ALT/SGPT elevation, elevated bilirubin and lymphopenia) possibly related to study device, using CTCAE v3.0.
- Any life threatening event possibly related to the study device: events as a consequence of inadvertent delivery of ^{166}Ho-microspheres into non-target organs like the lung (radiation pneumonitis), the stomach and duodenum (gastric/duodenal ulcer or perforation), the pancreas (radiation pancreatitis), and liver toxicity due to an excessive radiation dose ("radiation induced liver disease" [RILD][10]).

The hematological and biochemical adverse events as well as RILD will be considered dose-limiting toxicity.

Secondary objectives

Secondary objectives are to evaluate tumor response, performance status, biodistribution, quality of life and to compare the accuracy of the ^{99m}Tc-MAA scout dose with a safety dose of ^{166}Ho-microspheres, in predicting microsphere distribution of the treatment dose. Tumor response will be quantified using CT of the liver scored according to Response Evaluation Criteria in Solid Tumors guidelines (RECIST 1.1).[26] Tumor viability will be assessed by PET, depending on tumor type. In addition, the antitumoral effect will be assessed by relevant tumor markers responses if applicable (*i.e.* carcinoembryonic antigen [CEA] in colorectal carcinoma and chromogranin A [CgA] for neuroendocrine tumors). Biodistribution is assessed using quantitative SPECT and MRI. Urine and blood samples will be screened for presence of ^{166}Ho-microspheres or fragments of ^{166}Ho-microspheres. Performance status is assessed using WHO performance status criteria. Quality of life (QoL) is evaluated using the EORTC questionnaire QLQ-C30 with colorectal liver metastases module QLQ-LMC21. Finally, the accuracy of the ^{166}Ho-microspheres-safety dose in predicting the distribution of the treatment dose is compared with the accuracy of the ^{99m}Tc-MAA. Quantitative SPECT analysis will be performed using the scatter correction method described by De Wit *et al.*.[14]

Safety profile

From the literature on ^{90}Y-RE, it is known that several treatment related effects can occur in radioembolization. As long as the patient is treated with the correct technique, which includes that no excessive radiation dose be delivered to any organ, the common adverse events after receiving radioactive microspheres are fever, abdominal pain, nausea, vomiting, diarrhea and fatigue (*i.e.* post-embolization syndrome).[10,27,28] These effects are in general self-limiting within 1 to 2 weeks, and may be up to grade 3 or 4 (CTCAE v3.0) without direct clinical relevance. Based on the preclinical studies, a similar safety profile is expected for ^{166}Ho-RE.[21,22]

Escape medication

Patients will receive oral analgesics (paracetamol up to 4000 mg/24 h) for relief of fever and pain after the administration of microspheres. To reduce nausea and vomiting, patients will receive anti-emetics (ondansetron up to 3 dd 8 mg) during the first 24 hours after administration of the treatment dose. In the case of persisting nausea, metoclopramid (up to 300 mg/24 h) will be used. Patients suffering from diarrhea will receive loperamide (up to 16 mg/24 h). The vascular contrast agent jodixanol (Visipaque®) may cause renal insufficiency in poorly hydrated patients. All patients will therefore be hydrated. This consists of 1.5 l NaCl 0.9% both prior to and post angiography. Inadvertent delivery of microspheres into organs such as the lungs, stomach, duodenum, pancreas, and gallbladder is associated with serious side effects. To reduce toxicity of the radioactive microspheres in patients with excessive extrahepatic deposition of ^{166}Ho-microspheres, the cytoprotective agent amifostine (Ethyol®, up to 200 mg/m^2 for 7 days) may be administered intravenously.

Statistical considerations

Descriptive statistics (n, mean, standard deviation, median, minimum and maximum) will be calculated for each quantitative variable; frequency counts by category will be made for each qualitative variable. Interim analysis will be performed after every 3 patients. Inclusion of patients in the next cohort will be performed if the Independent Data Monitoring Committee (IDMC) has scrutinized the toxicity data and given permission to proceed.

Two sets of study data will be evaluated: the primary objective will be evaluated in the full analysis set (FAS). The FAS is defined as the set of data generated from the included patients who received at least the safety dose. The secondary objectives will be evaluated in both FAS and per-protocol set (PPS). The PPS is defined as the set of data generated from the included patients who complied with the protocol.

Monitoring

The IDMC will perform a safety review after each series of treatments of three consecutive patients. The IDMC members have no conflict of interest with the sponsor because they are not involved in the study, nor are they receiving funds. The IDMC will work according to standard operating procedures and will receive reports on a regular basis on all toxicity CTCAE ≥ grade 3 reported for this trial. Recruitment will not be interrupted unless otherwise requested by the chairman of the IDMC. The responsibilities of the IDMC include:

- minimize the exposure of patients to an unsafe therapy or dose
- make recommendations for changes in study processes where appropriate
- endorse continuation of the study
- inform the institutional IEC in the case of toxicity CTCAE ≥ grade 3 and/or when the well-being of the subjects is jeopardized

Ethical considerations

The study will be conducted according to the principles of the Declaration of Helsinki (version 9.10.2004) and in accordance with the Medical Research Involving Human Patients Act (WMO), the requirements of International Conference on Harmonization - Good Clinical Practice. The study protocol has been approved by the IEC and by the institutional Radiation Protection Committee.

Discussion

The HEPAR trial is a phase I study to evaluate the safety and toxicity profile of ^{166}Ho radioembolization. Secondary endpoints are tumor response, biodistribution assessment, performance status, quality of life and comparison of the biodistributions of the ^{99m}Tc-MAA-scout dose and the ^{166}Ho-microspheres-safety dose. With regard to the method of administration, *viz.* through a catheter placed in the hepatic artery, the in-vivo characteristics (no significant release of radionuclide), and the mechanism of action (local irradiation of the tumor), ^{166}Ho-microspheres constitute a device analogous to the ^{90}Y microspheres, which are currently applied clinically. ^{166}Ho-microspheres only differ in the radioisotope and the device matrix that are used. In a toxicity study on ^{166}Ho-RE in pigs, it has been demonstrated that (healthy) pigs can withstand extremely high liver absorbed doses, at least up to 160 Gy.[22] During these animal experiments, only very mild side effects were seen: slight and transitory inappetence and somnolence, which may well have been associated with the anesthetic and analgesic agents that had been given and not necessarily with the microsphere administration. It is plausible that this low toxicity profile is caused by the inhomogeneous

distribution of ^{166}Ho within the liver after intra-arterial injection, as was observed on MRI and SPECT images. The current study will investigate whether a similar distribution pattern can also be observed in human subjects and whether this inhomogeneous distribution is concentrated around the tumor sites.

Hepatic arterial injection with ^{99m}Tc-MAA and subsequent scintigraphic imaging is widely used to predict the biodistribution of ^{90}Y microspheres, prior to the actual radioembolization procedure. Its accuracy can however be disputed. In our center, we have observed that patients with a borderline lung shunt fraction of 10% to 19%, as calculated using the ^{99m}Tc-MAA images (approximately 24% of all patients, all of whom were instilled a by 50% reduced amount of radioactivity), had no signs of lung shunting on post-^{90}Y-RE Bremsstrahlung images. In these cases, it seems that the ^{99m}Tc-MAA-scan had false-positively predicted extrahepatic spread. This may be explained by the fact that ^{99m}Tc-MAA differs in many aspects from the microspheres that are used. Shape, size, density, in-vivo half-life, and number of ^{99m}Tc-MAA particles do not resemble the microspheres in any way.[13,29] In addition, free technetium that is released from the MAA particles can disturb the (correct) assessment of extrahepatic spread. We hypothesize that a small safety dose with low-activity ^{166}Ho-microspheres will be a more accurate predictor of distribution than ^{99m}Tc-MAA. The unique characteristics of ^{166}Ho-microspheres, in theory, allow a more accurate prediction of the distribution with the use of scintigraphy and MRI. In this study, we chose to perform both an injection with ^{99m}Tc-MAA and administration of a safety dose of ^{166}Ho-microspheres. The respective distributions of the ^{99m}Tc-MAA and the ^{166}Ho-microspheres-safety dose will be compared with the distribution of the treatment dose of ^{166}Ho-microspheres by quantitative analysis of the scintigraphic images.

Both commercially available ^{90}Y-microspheres products are approved by the Food and Drug Administration (FDA) and European Medicines Agency as a medical device and not as a drug. Radioactive microspheres are a medical device since these implants do not achieve any of their primary intended purposes through chemical action within or on the body and are not dependent upon being metabolized for the achievement of their primary intended purpose. In accordance with the definition of a medical device by the FDA and in analogy with the ^{90}Y-microspheres, we consider the ^{166}Ho-microspheres to be a medical device.[30] The Dutch medicine evaluation board has discussed this issue (13 July 2007) and has concluded that the microspheres are indeed to be considered a medical device.

One important issue concerning the resin-based SIR-Spheres® is the relatively high number of particles instilled (>1,000 mg), since this may sometimes be associated with macroscopic embolization as observed during the fluoroscopic guidance.[27,31] Several authors have reported stasis of flow during administration of resin microspheres

and were forced to end the procedure prematurely because of the risk of backflow, hence extrahepatic deposition of a part of the dosage.[27,32,33] The specific activity of the ^{166}Ho-microspheres is considerably higher than that of the resin microspheres (≤450 and 50 Bq/microsphere, respectively). However, in order to obtain an equivalent absorbed dose, the total amount of radioactivity of the administered microspheres in ^{166}Ho-radioembolization needs to be 3 times higher than in ^{90}Y-radioembolization, due to the shorter physical half-life of ^{166}Ho. Even so, compared with the resin ^{90}Y-microspheres, considerably less microspheres (≤600 mg) are required in ^{166}Ho-radioembolization to obtain an equivalent radiation dose, which results in a lower risk of stasis or backflow during administration.[9,28] Another issue is that ^{90}Y- microspheres can not be visualized under fluoroscopy during injection. Manufacturers of resin ^{90}Y-microspheres state that their microspheres are to be administered with water for injection alternated with non-ionogenic contrast.[34] As a result, the operating physician cannot detect stasis or backflow of microspheres until he has switched from injecting microspheres to injecting the contrast agent. Holmium-microspheres, on the contrary, are administered in a mixture of 50% saline and 50% non-ionogenic contrast under constant fluoroscopic imaging, which ensures constant control over the microspheres during injection.[35] However, continuous fluoroscopic imaging during microsphere administration may comprise an increased radiation dose delivered to the patient, specifically the abdominal skin, during the procedure.

If this phase I trial provides sufficient data to prove that ^{166}Ho-microspheres has an acceptable safety and toxicity profile, further studies will be needed. The next step will be an efficacy study in a larger number of patients. The primary endpoints of that study will be tumor response and survival.

Acknowledgements

The authors thank Ms. Tjitske Bosma (clinical research coordinator, University Medical Center Utrecht) for her contribution to the study design and coordination, and Mr. Remmert de Roos for his assistance in the preparation of the microspheres. This study was financially supported by the Dutch Cancer Society (KWF Kankerbestrijding), under grant UU2009-4346.

References

1. Choti MA, Bulkley GB (1999) Management of hepatic metastases. Liver Transpl Surg 5: 65-80.
2. Russell AH, Tong D, Dawson LE, Wisbeck W (1984) Adenocarcinoma of the proximal colon. Sites of initial dissemination and patterns of recurrence following surgery alone. Cancer 53: 360-367.
3. Bennett JJ, Cao D, Posner MC (2005) Determinants of unresectability and outcome of patients with occult colorectal hepatic metastases. J Surg Oncol 92: 64-69.
4. van Laarhoven HW, Punt CJ (2004) Systemic treatment of advanced colorectal carcinoma. Eur J Gastroenterol Hepatol 16: 283-289.
5. Bengtsson G, Carlsson G, Hafstrom L, Jonsson PE (1981) Natural history of patients with untreated liver metastases from colorectal cancer. Am J Surg 141: 586-589.
6. Zuckerman DS, Clark JW (2008) Systemic therapy for metastatic colorectal cancer: current questions. Cancer 112: 1879-1891.
7. Lee JJ, Chu E (2007) An update on treatment advances for the first-line therapy of metastatic colorectal cancer. Cancer J 13: 276-281.
8. Golfinopoulos V, Salanti G, Pavlidis N, Ioannidis JP (2007) Survival and disease-progression benefits with treatment regimens for advanced colorectal cancer: a meta-analysis. Lancet Oncol 8: 898-911.
9. Vente MA, Hobbelink MG, van Het Schip AD, Zonnenberg BA, Nijsen JF (2007) Radionuclide liver cancer therapies: from concept to current clinical status. Anticancer Agents Med Chem 7: 441-459.
10. Salem R, Thurston KG (2006) Radioembolization with yttrium-90 microspheres: a state-of-the-art brachytherapy treatment for primary and secondary liver malignancies: part 3: comprehensive literature review and future direction. J Vasc Interv Radiol 17: 1571-1593.
11. Nijsen JF, Zonnenberg BA, Woittiez JR, Rook DW, Swildens-van Woudenberg IA, et al. (1999) Holmium-^{166} poly lactic acid microspheres applicable for intra-arterial radionuclide therapy of hepatic malignancies: effects of preparation and neutron activation techniques. Eur J Nucl Med Mol Imaging 26: 699-704.
12. Nijsen JF, van Steenbergen MJ, Kooijman H, Talsma H, Kroon-Batenburg LM, et al. (2001) Characterization of poly(L-lactic acid) microspheres loaded with holmium acetylacetonate. Biomaterials 22: 3073-3081.
13. Bult W, Vente MA, Zonnenberg BA, Van Het Schip AD, Nijsen JF (2009) Microsphere radioembolization of liver malignancies: current developments. Q J Nucl Med Mol Imaging 53: 325-335.
14. de Wit TC, Xiao J, Nijsen JF, van het Schip FD, Staelens SG, et al. (2006) Hybrid scatter correction applied to quantitative holmium-^{166} SPECT. Phys Med Biol 51: 4773-4787.
15. Seppenwoolde JH, Nijsen JF, Bartels LW, Zielhuis SW, van Het Schip AD, et al. (2005) Internal radiation therapy of liver tumors: qualitative and quantitative magnetic resonance imaging of the biodistribution of holmium-loaded microspheres in animal models. Magn Reson Med 53: 76-84.

16. Nijsen JF, Seppenwoolde JH, Havenith T, Bos C, Bakker CJ, et al. (2004) Liver tumors: MR imaging of radioactive holmium microspheres--phantom and rabbit study. Radiology 231: 491-499.

17. Zielhuis SW, Nijsen JF, de Roos R, Krijger GC, van Rijk PP, et al. (2006) Production of GMP-grade radioactive holmium loaded poly(L-lactic acid) microspheres for clinical application. Int J Pharm 311: 69-74.

18. Zielhuis SW, Nijsen JF, Dorland L, Krijger GC, van Het Schip AD, et al. (2006) Removal of chloroform from biodegradable therapeutic microspheres by radiolysis. Int J Pharm 315: 67-74.

19. Zielhuis SW, Nijsen JF, Krijger GC, van het Schip AD, Hennink WE (2006) Holmium-loaded poly(L-lactic acid) microspheres: in vitro degradation study. Biomacromolecules 7: 2217-2223.

20. Nijsen F, Rook D, Brandt C, Meijer R, Dullens H, et al. (2001) Targeting of liver tumour in rats by selective delivery of holmium-^{166} loaded microspheres: a biodistribution study. Eur J Nucl Med 28: 743-749.

21. Zielhuis SW, Nijsen JF, Seppenwoolde JH, Bakker CJ, Krijger GC, et al. (2007) Long-term toxicity of holmium-loaded poly(L-lactic acid) microspheres in rats. Biomaterials 28: 4591-4599.

22. Vente MA, Nijsen JF, de Wit TC, Seppenwoolde JH, Krijger GC, et al. (2008) Clinical effects of transcatheter hepatic arterial embolization with holmium-^{166} poly(L-lactic acid) microspheres in healthy pigs. Eur J Nucl Med Mol Imaging 35: 1259-1271.

23. Aaronson NK, Ahmedzai S, Bergman B, Bullinger M, Cull A, et al. (1993) The European Organization for Research and Treatment of Cancer QLQ-C30: a quality-of-life instrument for use in international clinical trials in oncology. J Natl Cancer Inst 85: 365-376.

24. Bolch WE, Bouchet LG, Robertson JS, Wessels BW, Siegel JA, et al. (1999) MIRD pamphlet No. 17: the dosimetry of nonuniform activity distributions--radionuclide S values at the voxel level. Medical Internal Radiation Dose Committee. J Nucl Med 40: 11S-36S.

25. Trotti A, Colevas AD, Setser A, Rusch V, Jaques D, et al. (2003) CTCAE v3.0: development of a comprehensive grading system for the adverse effects of cancer treatment. Semin Radiat Oncol 13: 176-181.

26. Eisenhauer EA, Therasse P, Bogaerts J, Schwartz LH, Sargent D, et al. (2009) New response evaluation criteria in solid tumours: revised RECIST guideline (version 1.1). Eur J Cancer 45: 228-247.

27. Sato K, Lewandowski RJ, Bui JT, Omary R, Hunter RD, et al. (2006) Treatment of unresectable primary and metastatic liver cancer with yttrium-90 microspheres (TheraSphere): assessment of hepatic arterial embolization. Cardiovasc Intervent Radiol 29: 522-529.

28. Kennedy AS, Coldwell D, Nutting C, Murthy R, Wertman DE, Jr., et al. (2006) Resin 90Y-microsphere brachytherapy for unresectable colorectal liver metastases: modern USA experience. Int J Radiat Oncol Biol Phys 65: 412-425.

29. Rao SN, Basu SP, Sanny CG, Manley RV, Hartsuck JA (1976) Preliminary x-ray investigation of an orthorhombic crystal form of human plasma albumin. J Biol Chem 251: 3191-3193.

30. U.S. Food and Drug Administration: Device Regulation and Guidance.

31. Vente MA, Wondergem M, van der Tweel I, van den Bosch MA, Zonnenberg BA, et al. (2009) Yttrium-90 microsphere radioembolization for the treatment of liver malignancies: a structured meta-analysis. Eur Radiol 19: 951-959.

32. Murthy R, Nunez R, Szklaruk J, Erwin W, Madoff DC, et al. (2005) Yttrium-90 microsphere therapy for hepatic malignancy: devices, indications, technical considerations, and potential complications. Radiographics 25 Suppl 1: S41-55.

33. Popperl G, Helmberger T, Munzing W, Schmid R, Jacobs TF, et al. (2005) Selective internal radiation therapy with SIR-Spheres in patients with nonresectable liver tumors. Cancer Biother Radiopharm 20: 200-208.

34. SIRTeX Medical Inc. SIRTeX medical training manual. TRN-US-03, 40.

35. Vente MA, de Wit TC, van den Bosch MA, Bult W, Seevinck PR, et al. (2010) Holmium-^{166} poly(L-lactic acid) microsphere radioembolisation of the liver: technical aspects studied in a large animal model. Eur Radiol 20: 862-869.

Chapter 4

Holmium-166 radioembolization: results of a phase 1, dose escalation study in patients with unresectable, chemorefractory liver metastases *the HEPAR trial*

MLJ Smits, JFW Nijsen, MAAJ van den Bosch, MGEH Lam, MAD Vente, WPThM Mali, AD van het Schip, BA Zonnenberg

Lancet Oncology 2012

Abstra

Background

The efficacy of radioembolization for the treatment of liver tumors depends on the selective distribution of radioactive microspheres to tumorous tissue. The distribution of holmium-166 (^{166}Ho) poly(L-lactic acid) microspheres can be visualised in vivo by both single-photon-emission CT (SPECT) and MRI. In this phase 1 clinical trial, we aimed to assess the safety and the maximum tolerated radiation dose (MTRD) of ^{166}Ho-radioembolization in patients with liver metastases.

Methods

Between Nov 30, 2009, and Sept 19, 2011, patients with unresectable, chemorefractory liver metastases were enrolled in the Holmium Embolization Particles for Arterial Radiotherapy (HEPAR) trial. Patients were treated with intra-arterial ^{166}Ho-radioembolization in cohorts of three patients, with escalating aimed whole-liver absorbed doses of 20, 40, 60, and 80 Gy. Cohorts were extended to a maximum of six patients if dose-limiting toxicity occurred. Patients were assigned a dose in the order of study entry, with dose escalation until dose-limiting toxicity was encountered in at least two patients of a dose cohort. Clinical or laboratory toxicities were scored according to the National Cancer Institute's Common Terminology Criteria for Adverse Events version 3.0. The primary endpoint was the MTRD. Analyses were per protocol. This study is registered with ClinicalTrials.gov, number NCT01031784.

Findings

15 patients underwent ^{166}Ho-radioembolization at doses of 20 Gy (n=6), 40 Gy (n=3), 60 Gy (n=3), and 80 Gy (n=3). Mean estimated whole-liver absor-

Introduction

Radioembolization using yttrium-90 (^{90}Y) microspheres is increasingly used to selectively target liver metastases as first-line or salvage treatment in patients with unresectable hepatic tumors.[1,2] The rationale behind this treatment is that blood from the hepatic artery flows preferentially to malignancies, whereas healthy liver parenchyma is mainly perfused by blood from the portal vein. Microspheres injected into the hepatic artery will therefore selectively target tumorous tissue, whereas the healthy liver tissue is spared. Recent research has focused on quantitative imaging for dosimetry to ensure optimum deposition of radioactive microspheres in the tumorous tissue.[3,4] Holmium-166 poly(L-lactic acid) (^{166}Ho-PLLA) microspheres that can be seen on imaging with multiple modalities have been developed at University Medical Center Utrecht (Utrecht, Netherlands) for quantitative in-vivo imaging. In addition to emitting

bed doses were 18 Gy (SD 2) for the 20 Gy cohort, 35 Gy (SD 1) for the 40 Gy cohort, 58 Gy (SD 3) for the 60 Gy cohort, and 73 Gy (SD 4) for the 80 Gy cohort. The 20 Gy cohort was extended to six patients because of the occurrence of dose-limiting toxicity in one patient (pulmonary embolism). In the 80 Gy cohort, dose-limiting toxicity occurred in two patients: grade 4 thrombocytopenia, grade 3 leucopenia, and grade 3 hypoalbuminemia in one patient, and grade 3 abdominal pain in another patient. The MTRD was identified as 60 Gy. The most frequently encountered laboratory toxicities (including grade 1) were lymphocytopenia, hypoalbuminemia, raised alkaline phosphatase, raised aspartate aminotransferase, and raised gamma-glutamyltransferase, which were all noted in 12 of 15 patients. Stable disease or partial response regarding target lesions was achieved in 14 of 15 patients (93%, 95% CI 70–99) at 6 weeks and nine of 14 patients (64%, 95% CI 39–84) at 12 weeks after radioembolization. Compared with baseline, the average global health status and quality of life scale score at 6 weeks after treatment had decreased by 13 points (p=0.053) and by 14 points at 12 weeks (p=0.048). In all patients, technetium-99m (^{99m}Tc)-macroaggregated albumin SPECT, ^{166}Ho scout dose SPECT, and ^{166}Ho treatment dose SPECT showed similar patterns of the presence or absence of extrahepatic deposition of activity.

Interpretation

^{166}Ho-radioembolization is feasible and safe for the treatment of patients with unresectable and chemorefractory liver metastases and enables image-guided treatment. Clinical ^{166}Ho-radioembolization should be done with an aimed whole-liver absorbed dose of 60 Gy.

beta-radiation for tumor destruction, ^{166}Ho-microspheres emit gamma radiation and are paramagnetic, which makes them visible on both single photon emission CT (SPECT) and MRI, enabling use of dosimetry and personalized patient treatment.[5,6] Using these microspheres, assessment of whether the tumor distribution was strictly intrahepatic and whether each tumor has received an adequate dose can be done shortly after treatment. If not, additional treatment can be provided to previously non-targeted tumors. We previously reported the safety, efficacy, and imaging properties of ^{166}Ho-PLLA-microspheres in both in-vitro and in-vivo studies.[7-11] In this phase 1 clinical trial, we aimed to assess the safety and maximum tolerated radiation dose (MTRD) of ^{166}Ho-radioembolization in patients with unresectable and chemorefractory liver metastases to identify the starting dose for further studies and clinical treatment.

Methods

Patients

Between Nov 30, 2009, and Sept 19, 2011, patients with unresectable, chemorefractory liver metastases were enrolled in the phase 1 Holmium Embolization Particles for Arterial Radiotherapy (HEPAR) dose- escalation study of intra-arterial ^{166}Ho-radioembolization. The study design has been published previously.[12] Patients were included in the study if they complied with the following inclusion criteria: presence of liver-dominant, unresectable, chemorefractory liver metastases of any primary tumor; age 18 years or older; an estimated life expectancy of over 3 months; WHO performance status score 0–2; at least one measurable lesion of at least 10 mm on CT; and a negative pregnancy test for women. Patients with impaired hematological function (leucocytes $<4.0\times10^9$ cells per L and platelet count $<150\times10^9$/L), impaired renal function (serum creatinine >185 μmol/L), impaired cardiac function (relevant morphological changes on electrocardiography or New York Heart Association classification of heart disease score ≥2), impaired hepatic function (alanine aminotransferase [ALT], aspartate aminotransferase [AST], or alkaline phosphatase over five times the upper limit of normal, or serum bilirubin over 1.5 times the upper limit of normal), patients who had received chemotherapy or abdominal surgery over the previous 4 weeks, those with incompletely healed surgical incisions, and those with contraindications for MRI were excluded from study treatment.

All patients provided written informed consent before enrolment. Ethical approval for this study was obtained from the institutional review board and the study was undertaken in accordance with the Declaration of Helsinki. An independent data monitoring committee assessed study results and patient safety at interim analyses, which were organized after every third patient who received treatment had completed at least 6 weeks of follow-up. Inclusion of patients could only continue after approval from the independent data monitoring committee.

Procedures

^{166}Ho-PLLA-microspheres were produced at University Medical Center Utrecht according to good manufacturing practice guidelines, as described previously.[13-15] For each patient, a scout dose of 60 mg and a treatment dose of 540 mg of ^{165}Ho-PLLA-microspheres were packed in high-density polyethylene vials (Posthumus Plastics, Beverwijk, Netherlands) and these vials were irradiated separately in the nuclear facility of the Reactor Institute Delft (Delft University of Technology, Delft, Netherlands). Upon arrival at the University Medical Center Utrecht (Utrecht, Netherlands), the amount of radioactivity of both doses of microspheres was measured in a dose calibrator (VDC-

404, Veenstra Instrumenten, Joure, Netherlands) and a quality check (particle integrity assessment by light microscopy and particle size measurement) was done on a sample of the treatment dose of microspheres.

The calculations of the amount of radioactivity for this dose-escalation study were done using a method derived from the medical internal radiation dosimetry (MIRD) pamphlet number 17.[16] This method is widely used for ^{90}Y-dosimetry.[17] The amount of administered ^{166}Ho-radioactivity was calculated using the aimed whole-liver absorbed dose (20, 40, 60, or 80 Gy) and the liver weight, as described previously.[12] The liver volume was measured on contrast-enhanced CT images with Volumetool[18] assuming a tissue density for liver tissue of 1.00 g/cm^3.[19] Whole-liver absorbed doses were calculated assuming homogeneous distribution of the administered activity and complete absorption of the dose in the liver, using the following formula:

$$\frac{A_{Ho166}(MBq)}{LW\ (kg)} = liver\ dose\ (Gy) \times 63\left(\frac{MBq}{J}\right)$$

Where A_{Ho166} is the administered activity, *LW* is the liver weight, and *liver dose* is the aimed whole-liver absorbed dose.

All patients underwent triphasic contrast-enhanced abdominal CT at study entry to estimate the intrahepatic tumor burden at baseline. Patients were admitted to hospital on the evening before each angiography session. All patients received 1.5 L NaCl 0.9% per intravenous cannula 12 h before angiography to optimize hydration status. 1 h before angiography, patients were given an intravenous dose of corticosteroids (dexamethasone 10 mg) and anti-emetics (ondansetron 8 mg) for prophylaxis of post-embolization syndrome. The technical procedures for ^{166}Ho-radioembolization did not differ substantially from routine procedures for ^{90}Y-radioembolization.[20] Briefly, a detailed map of the vasculature supplying the liver and the surrounding organs was obtained. Subsequently, the hepatic artery was carefully skeletonized by means of coil embolization of all vessels originating from the hepatic artery that could lead to deposition of activity in non-target organs such as the intestines and pancreas. Subsequently, technetium-99m (^{99m}Tc)-macro-aggregated albumin (MAA; 150 MBq, 0.8 mg, TechneScan LyoMaa, Mallinckrodt Medical, Petten, Netherlands) was administered, followed by planar nuclear imaging and SPECT or SPECT-CT to calculate the fraction of the ^{99m}Tc-MAA shunting to the lungs and to ensure that the remaining activity was distributed exclusively to the liver. If the lung shunt fraction of ^{99m}Tc-MAA was less than 20% and no extrahepatic deposition of ^{99m}Tc-MAA was detected, a second angiography was done within 2 weeks. During this second angiography, a scout dose of ^{166}Ho-microspheres

(250 MBq) was administered from the same catheter position as where ^{99m}Tc-MAA was injected during the work-up angiography and SPECT or SPECT-CT, plus, in some patients, MRI, were done. Administration of ^{166}Ho-microspheres was always done using a dedicated administration system.[21] By this system, the vial was flushed with a saline solution mixed with contrast agent, bringing the microspheres in suspension and forcing them to exit the administration system and flow into the microcatheter. Flushing occurred in a pulsatile manner at an overall rate of about 0.2–0.4 mL/s. This way, 10–20 mL of contrast and saline mixture was injected. During injection, fluoroscopy was used at regular intervals to check for any stasis or backflow. The ^{166}Ho-microspheres-scout dose was used as an extra predictor for the distribution of the ^{166}Ho-microspheres treatment dose to increase the overall safety of the procedure and to allow assessment of distribution. At present, ^{99m}Tc-MAA is used for this purpose, although its validity as a predictor for intrahepatic microsphere distribution is uncertain.[22,23] MAA particles differ substantially from ^{90}Y-microspheres and ^{166}Ho-microspheres in size, amount, density, and shape.[23] To overcome these differences, we hypothesized that the distribution of microspheres for radioembolization can be best predicted with a scout dose of the same microspheres. If no extrahepatic ^{166}Ho-microspheres were detected, a treatment dose of ^{166}Ho-microspheres was injected under angiography on the same day. After each administration, the net delivered activity was calculated by measuring the residual activity in the administration system and the dose vial. Abdominal SPECT or SPECT-CT and MRI for distribution assessment of the treatment dose were done 3–5 days after treatment.

Patients were treated in consecutive cohorts of three patients according to a standard phase 1 3+3 dose-escalation protocol.[24] The aimed whole-liver absorbed dose of ^{166}Ho was increased per cohort from 20 to 40, 60, and then 80 Gy, respectively. A cohort was extended to six patients if dose-limiting toxicity was found in one of the initial three patients. If dose-limiting toxicity was found in two patients of a given dose cohort, the MTRD was classed as the preceding dose.

Follow-up consisted of physical examinations, clinical chemistry assessments (including electrolytes, renal and liver function tests, minerals, and relevant tumor markers) and hematological tests every week, for the duration of 12 weeks, and triphasic contrast-enhanced abdominal CT, ^{18}F-fluorodeoxyglucose (^{18}F-FDG) PET, and MRI at 6 and 12 weeks after treatment. CT was used for response assessment and spleen volumetry. Quality of life (QoL) was assessed by the European Organization for Research and Treatment of Cancer QLQ-C30 and QLQ-LMC21 questionnaires at baseline and at 6 and 12 weeks after treatment. All urine from 0 to 24 h after treatment was collected and blood was sampled after treatment for holmium content measurement with inductively

coupled plasma mass spectrometry. Any clinical or laboratory toxicity was scored according to the National Cancer Institute's Common Terminology Criteria for Adverse Events (CTCAE) version 3.0. For each parameter, the highest CTCAE grade was recorded during follow-up. Dose-limiting toxicity was defined as any toxicity exceeding grade 2 that was deemed definitely, probably, or possibly related to the administration of ^{166}Ho-microspheres, with the exception of raised liver enzymes, hyperbilirubinemia, raised lactate dehydrogenase, or lymphocytopenia.

The primary objective of this dose-escalation study was to identify the MTRD, defined as the highest aimed whole-liver absorbed dose, up to 80 Gy, at which fewer than two patients exhibited dose-limiting toxicity. Secondary objectives were assessment of overall toxicity using CTCAE, tumor response assessment on triphasic contrast-enhanced abdominal CT according to the Response Evaluation Criteria in Solid Tumors version 1.1,[25] QoL assessment, and visualization of the biodistribution of ^{166}Ho-microspheres by SPECT and MRI.

Statistical analysis

We calculated descriptive statistics of means and SDs for continuous variables and frequencies and percentages per category for categorical variables. 95% CIs for proportions were calculated using the Wilson score method without continuity correction. We compared changes in global health status and QoL scale by a two-tailed paired-samples *t*-test. All objectives were assessed in the per-protocol analysis set, defined as the data from all patients who received ^{166}Ho-microspheres (treatment dose). We used SPSS software version 15.0 (SPSS, Chicago, IL, USA) for all analyses. This study is registered with ClinicalTrials.gov, number NCT01031784.[12]

Role of the funding source

The sponsors of the study had no role in study design, data collection, data analysis, data interpretation, writing of the manuscript, or the decision to submit for publication. The corresponding author (BZ) had full access to all the data in the study and had final responsibility for the decision to submit for publication.

Results

27 patients were enrolled on an intention-to-treat basis, 12 of whom were excluded from treatment during work-up because of excessive extrahepatic metastases (*n*=2), recurrent extrahepatic deposition of ^{99m}Tc-MAA (*n*=2), vascular anatomy impeding whole-liver treatment (*n*=5), and laboratory values matching exclusion criteria (*n*=3). Table 1 lists the demographic data of the 15 patients who underwent ^{166}Ho-radioembolization. The primary tumor types were ocular melanoma (median liver in-

volvement 22%, range 2–43%), colorectal carcinoma (median liver involvement 24%, range 4–52%), cholangiocarcinoma (median liver involvement 14%, range 8–20%), and breast carcinoma (liver involvement 10%). During the angiographic procedures, the following arteries were embolized with coils: gastroduodenal artery (*n*=14), right gastric artery (*n*=4), and unidentified intestinal branches arising from the hepatic arteries (*n*=2). ^{166}Ho-microspheres were injected in the proper hepatic artery (*n*=6), the left and right hepatic artery (*n*=5), the right hepatic artery (*n*=2), the left hepatic artery (*n*=1), and the common hepatic artery (*n*=1). The mean total administered ^{166}Ho activity (scout plus treatment dose) per consecutive dose cohort is shown in *Table 1*, as are the mean estimated whole-liver absorbed doses per cohort. At time of injection, the mean activity of the scout dose was 224 MBq (SD 52) and the activity of the treatment dose was 2343 MBq (SD 1035) for the 20 Gy cohort, 3930 MBq (1121) for the 40 Gy cohort, 7839 MBq (1365) for the 60 Gy cohort, and 7854 MBq (1893) for the 80 Gy cohort, corresponding to an injected amount of microspheres of 47 mg (SD 11) for the scout dose and 474 mg (50) for the treatment dose, which resulted in a total amount of injected microspheres of 521 mg (58). No stasis or reflux of contrast agent occurred during administration of microspheres.

Table 1. *Baseline characteristics and treatment details per dose cohort*

	All patients (*n*=15)	20 Gy (*n*=6)	40 Gy (*n*=3)	60 Gy (*n*=3)	80 Gy (*n*=3)
Demographics					
Sex					
Male	9	5	2	2	0
Female	6	1	1	1	3
Age (years)	55 (38 - 87)	52 (38 - 59)	50 (43 - 61)	57 (45 - 87)	63 (48 - 67)
WHO performance status					
0	13	5	3	2	3
1	2	1	0	1	0
Baseline global health status / quality of life scale*	75.6 ± 12.4	79.2 ± 7.0	66.7 ± 8.3	83.3 ± 23.6	72.2 ± 17.3
Tumor type (primary)					
Ocular melanoma	6	4	1	0	2
Colorectal carcinoma	6	2	1	2	0
Cholangiocarcinoma	2	0	0	1	1
Breast carcinoma	1	0	1	0	0
Liver volume (ml)	2,071 ± 599	2,234 ± 756	1,884 ± 530	2,236 ± 498	1,771 ± 497

Table 1. *Continued*

	All patients (*n*=15)	20 Gy (*n*=6)	40 Gy (*n*=3)	60 Gy (*n*=3)	80 Gy (*n*=3)
Liver involvement					
Exact percentage	14 (2 - 52)	19 (4 - 43)	12 (2 - 25)	20 (13 - 52)	8 (2 - 43)
0% - 25%	10	4	2	2	2
25% - 50%	4	2	1	0	1
>50%	1	0	0	1	0
No. of tumors per patient	5 (1 - 21)	7 (1 - 19)	4 (2 - 21)	4 (3 - 5)	4 (3 - 10)
Site of disease					
Unilobar	4	1	1	2	0
Bilobar	11	5	2	1	3
Evidence of extrahepatic metastases					
Yes	6	4	0	1	1
No	9	2	3	2	2
Previous therapies					
Systemic treatment	11	5	3	2	1
Locoregional treatment	5	1	2	1	1
Treatment details					
Lung shunt					
^{99m}Tc-MAA lung shunt fraction (%)	7.2 ± 2.7	7.2 ± 2.8	8.3 ± 5.0	9.3 ± 3.2	6.2 ± 1.7
Activity					
Prepared ^{166}Ho-activity (MBq)	5,415 ± 2,928	2,750 ± 1,056	4,671 ± 1,119	8,453 ± 1,283	8,450 ± 2,127
Remaining ^{166}Ho-activity in administration system (MBq)	329 ± 201	218 ± 77	526 ± 253	355 ± 216	330 ± 246
Net administered ^{166}Ho-activity (MBq)	5,085 ± 2,876	2,532 ± 1,039	4,145 ± 1,161	8,099 ± 1,378	8,120 ± 1,900
Absorbed dose					
Aimed whole-liver absorbed dose (Gy)**	44 ± 24	20	40	60	80
Actual whole-liver absorbed dose (Gy)**	40 ± 23	18 ± 2	35 ± 1	58 ± 3	73 ± 4

Data are median (range), means ± SD, or counts. WHO = world health organization; ^{99m}Tc-MAA = technetium-99m macro-aggregated albumin; ^{166}Ho = holmium-166

** As measured with the European Organization for Research and Treatment of Cancer's QLQ-C30 questionnaire*

***Estimated dose assuming homogeneous distribution of the administered activity and complete absorption of the dose in the liver*

Table 2. *Adverse events CTCAE grade >1 stratified per dose cohort*

	Adverse events and adverse event grade per patient															Total (*n*=15)	
	20 Gy (*n*=6)						40 Gy (*n*=3)			60 Gy (*n*=3)			80 Gy (*n*=3)			Any grade	
Consecutive patient number	#1	#2	#3	#4	#5	#6	#7	#8	#9	#10	#11	#12	#13	#14	#15	Count	%
Hematologic																	
Leukopenia	-	-	-	-	-	-	-	-	-	-	-	-	2	3*	-	2	13%
Lymphocytopenia	3	2	-	2	2	2	-	2	-	2	2	2	3	3	2	12	80%
Thrombopenia	-	-	-	-	-	-	-	-	-	2	-	-	-	4*	-	2	13%
Nonhematologic																	
Albumin	2	-	2	-	-	-	-	-	-	2	-	-	2	3*	-	5	33%
Alkaline phosphatase	-	-	2	-	-	-	-	-	2	-	-	2	2	2	2	6	40%
ALT	-	-	-	-	-	2	-	-	-	-	-	2	2	-	3	4	27%
AST	-	-	-	-	-	-	-	2	-	-	-	2	2	3	2	5	33%
Bilirubin	-	-	-	-	-	-	-	-	-	-	-	-	-	4	-	1	7%
Gamma-glutamyltransferase	-	3	3	2	3	3	2	2	2	-	3	3	3	-	3	12	80%
Lactate dehydrogenase	-	3	2	-	-	-	-	-	2	-	-	-	-	3	-	4	27%
Phosphate	-	-	-	-	-	-	-	-	-	-	-	2	-	-	-	1	7%
Clinical																	
Abdominal pain	2	2	-	-	-	-	2	-	-	2	2	-	3*	2	2	8	53%
Allergic contrast reaction	-	-	-	-	-	-	-	-	-	-	2	-	-	-	-	1	7%
Anorexia	-	-	-	-	-	-	-	-	-	-	-	-	2	-	-	1	7%
Ascites	-	-	-	-	-	-	-	-	-	2	-	-	-	-	-	1	7%
Constipation	-	-	-	-	-	-	-	-	-	-	-	-	2	-	-	1	7%
Dizziness	2	-	-	-	-	-	-	-	-	-	-	-	-	-	-	1	7%
Fatigue	2	-	-	-	-	-	-	-	-	-	-	-	-	-	-	1	7%
Flank pain	2	2	-	-	-	-	-	-	-	-	-	-	-	-	-	2	13%

Table 2. *Continued*

	Adverse events and adverse event grade per patient															Total	
	20 Gy						40 Gy			60 Gy			80 Gy			(*n*=15)	
	(*n*=6)						(*n*=3)			(*n*=3)			(*n*=3)			Any grade	
Clinical																	
Headache	-	2	-	-	-	-	-	-	-	-	-	-	-	-	-	1	7%
Nausea	-	2	-	-	-	-	2	-	-	-	-	-	2	-	-	3	20%
Peripheral edema	-	-	-	-	-	-	-	-	-	-	-	-	-	3	-	1	7%
Pulmonary embolism	3*	-	-	-	-	-	-	-	-	-	-	-	-	-	-	1	7%
Transpiration, nocturnal	-	-	2	-	-	-	-	-	-	-	-	-	-	-	-	1	7%
Vomitus	-	2	-	-	-	-	2	-	-	-	2	-	-	-	-	3	20%
Total count	7	8	5	2	2	3	4	3	3	5	5	6	11	10	6		

*Toxicity is given in CTCAE grade per patient. * Dose-limiting toxicity*
ALT = Alanine transaminase; AST= Alanine aminotransferase; CTCAE = Common Terminology Criteria for Adverse Events

Table 2 summarizes the grade 2–5 events that were recorded during the study. At 12 weeks after treatment, splenic growth had occurred in ten of 15 patients (67%; mean increase 17% [SD 22]). The mean amount of holmium excreted in the urine during the first 24 h after treatment was less than 0.5% of the total administered amount of Ho. At 3 h after treatment, the mean amount of free holmium in the blood was 0.08%/L of the total administered amount of ^{166}Ho.
The first cohort (20 Gy) was extended to six patients because of the occurrence of dose-limiting toxicity in one patient (pulmonary embolism). Despite this event, dose escalation was continued since there were no dose-limiting toxicities in the other patients in this cohort. All other dose-limiting toxicities occurred in two patients in the final cohort (80 Gy). The first patient (patient 13), who was already on morphine for abdominal pain before treatment, was readmitted to the hospital 3 days after treatment with complaints of progressive abdominal pain. The pain was managed with intravenous morphine (6 mg/h). The scheduled SPECT-CT 3 days after treatment revealed extrahepatic deposition of a small amount of activity, located around the duodenum and the head of the pancreas. Amylase and lipase concentrations were normal and endoscopy 6 days after treatment showed no ulceration of the gastric or duodenal wall. The patient reported that the pain gradually regressed to baseline 4 weeks after treatment.
The second patient (patient 14) experienced grade 4 thrombocytopenia, grade 3 leucopenia, and grade 3 hypoalbuminemia. The hematological dose-limiting toxicity in conjunction with increasing serum bilirubin concentrations and ascites in this patient led us to suspect radiation-induced liver disease.[26] High-dose corticosteroids (prednisolone 30 mg two times per day) were given for this indication. Unfortunately, this patient died shortly after study completion (15 weeks after radioembolization). Autopsy showed no typical radiation-induced pathological changes. The entire liver was occupied by micrometastases and there was extensive metastatic colonization of the lungs and the abdominal cavity. We therefore rejected the diagnosis of radiation-induced liver disease. Aside from the aforementioned findings, there were no life-threatening morbidities or deaths during the 12-week follow-up period. According to the study protocol, the study was stopped after the 80 Gy cohort and the MTRD was identified as 60 Gy.
Overall, the most frequently encountered laboratory toxicities (including grade 1) were lymphocytopenia, hypoalbuminemia, raised alkaline phosphatase, raised AST, and raised gamma-glutamyltransferase, which were encountered in 12 of 15 patients (80%); anemia and raised ALT in ten of 15 patients (67%), and monocytosis, thrombocytopenia, and hyperammonemia in nine of 15 patients (60%). *Figure 1* shows liver enzyme concentrations and hematological parameters over time, separated by patients with and without progressive disease. Both biochemical and hematological toxicities were most prominent in patients with progressive liver disease. Abdominal pain and nau-

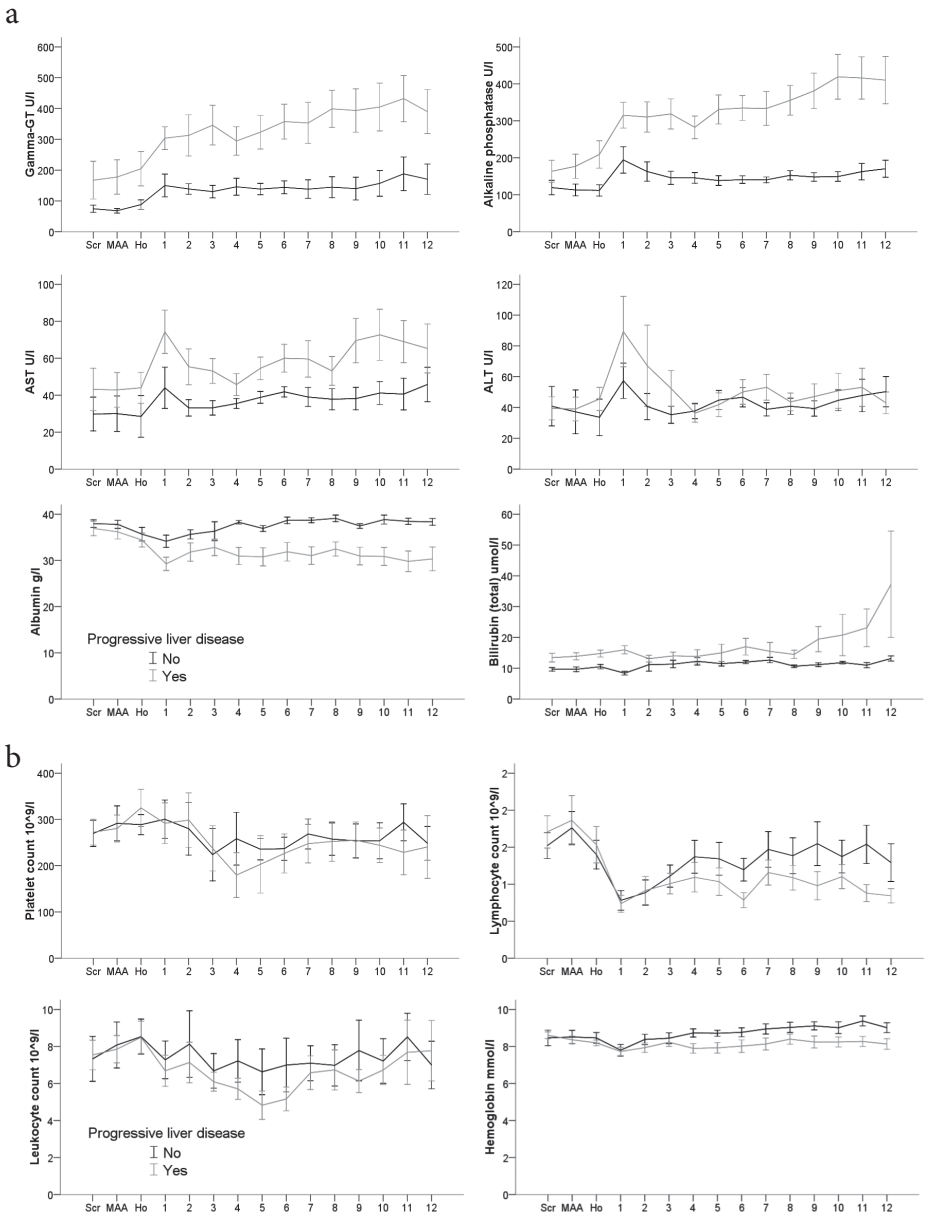

Figure 1. *Liver enzymes serum levels (a) and hematological parameters levels (b) measured weekly for patients with progressive disease (gray line) and patients with no progressive disease (black line) in the liver (observed at 12-week follow-up). All serum level values are mean ± 1 SE. ALT = alanine aminotransferase; AST = aspartate aminotransferase; Ho = lab measurement 1 day prior to ^{166}Ho-microsphere treatment; MAA = lab measurement 1 day prior to ^{99m}Tc-MAA administration; Scr = lab measurement at screening visit*

sea were the most frequently experienced clinical toxicities, each reported by 12 of 15 patients (80%), followed by other characteristic post-embolization symptoms such as fatigue (nine patients; 60%), anorexia (eight patients; 53%), vomiting (seven patients; 47%), and fever (six patients; 40%). Other clinical toxicity that could not be associated with post-embolization syndrome also occurred. This toxicity was either related to the procedure (allergic reaction to the radiopaque contrast agent used, back pain due to lying on the angiography table) or to extrahepatic tumor progression (headache, polydipsia, and shoulder pain).

In all patients, ^{99m}Tc-MAA SPECT, ^{166}Ho scout dose SPECT, and ^{166}Ho treatment dose SPECT showed similar patterns of the presence or absence of extrahepatic deposition of activity. In the patient who was readmitted for abdominal pain with extrahepatic deposition of activity on ^{166}Ho treatment dose SPECT, extrahepatic deposition of activity was initially not recognized on the ^{99m}Tc-MAA SPECT and ^{166}Ho scout dose SPECT images. A culprit vessel was retrospectively identified that was not recognized during angiography. The amount of extrahepatic activity, as estimated by quantitative SPECT, was less than 2% of the total administered dose (117 MBq). *Figure 2* shows an example of how the intrahepatic distribution of ^{166}Ho-microspheres was visualized with SPECT and MRI.

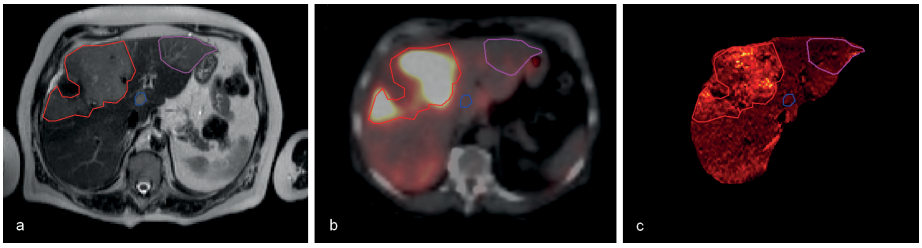

Figure 2. *Intrahepatic visualization of ^{166}Ho-microspheres. T2-weighted MRI of the liver in a patient with several ocular melanoma liver metastases, outlined by colored regions of interest (panel a). Post radioembolization, the distribution of ^{166}Ho-PLLA-microspheres within the liver is visualized with the use of SPECT (panel b) and R2*-weighted MRI (panel c). From panels b and c, it is clear that the largest tumor (red outline), received a substantial proportion of the administered activity. However, the small tumor in the caudate lobe (blue outline) and the larger tumor in the left liver lobe (pink outline) received a far smaller proportion of activity. This example illustrates how the imaging capabilities of ^{166}Ho-PLLA-microspheres allow treatment optimization. Optimal treatment in this patient would imply additional, more selective, treatment of the two sub-optimally treated tumors.*

Table 3 shows tumor responses at 6 and 12 weeks after treatment. At 6 weeks follow-up, 14 of 15 patients (93%, 95% CI 70–99) exhibited stable disease or partial response, and one of 15 patients (7%, 1–30) had progressive disease in the target lesions. At 12 weeks follow-up, nine of 14 patients (64%, 95% CI 39–84) exhibited stable disease or partial response, and five of 14 patients (36%, 16–61) had progressive disease in the

target lesions. One patient, who had terminal disease and was told it would become fatal within weeks, declined the 12-week scan and so could not be assessed for 12-week target lesions response. When extrahepatic disease was also taken into account (overall response), 13 patients (87%) had progressive disease 12 weeks after treatment. Tumor marker concentrations (assessable in ten of 15 patients) increased by more than 50% in four of ten patients (40%) at the 12-week follow-up (*Figure 3*).

Table 3. *Tumor response post radioembolization per holmium-166-radioembolization dose received*

		All patients (*n*=15)		20 Gy (*n*=6)		40 Gy (*n*=3)		60 Gy (*n*=3)		80 Gy (*n*=3)	
		TLR	OR	TLR	OR	TLR	OR	TLR*	OR	TLR	OR
6-weeks post ^{166}Ho-RE	PR	1 (7%)	1 (7%)	1	1	0	0	0	0	0	0
	SD	13 (87%)	7 (47%)	4	1	3	2	3	1	3	3
	PD	1 (7%)	7 (47%)	1	4	0	1	0	2	0	0
12-weeks post ^{166}Ho-RE	PR	1 (7%)	1 (7%)	1	1	0	0	0	0	0	0
	SD	8 (57%)	1 (7%)	3	0	2	1	2	0	1	0
	PD	5 (36%)	13 (87%)	2	5	1	2	0	3	2	3

*OR = overall response; PD = Progressive disease; PR = Partial response; SD = Stable disease; TLR = target lesion response; * One patient refused week-12 follow-up imaging, overall response was progressive due to new brain metastases*

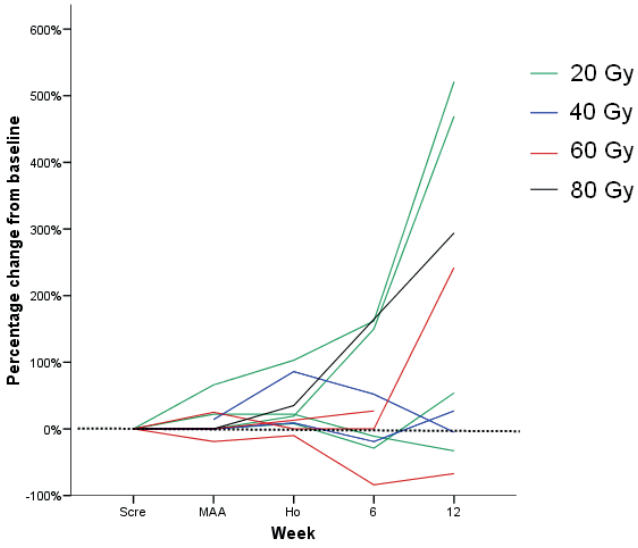

Figure 3. *Course of tumor markers during follow-up. The course of tumor markers was evaluable in 10/15 patients (CEA (n = 7), CA 19-9 (n = 2), S-100 (n = 1)). Baseline values were set to 0 and follow-up values were expressed in percentage change from baseline. CA 19-9 = carbohydrate antigen 19-9; CEA = carcinoembryonic antigen; Ho = lab measurement 1 day prior to ^{166}Ho-microsphere administration; MAA = lab measurement 1 day prior to ^{99m}Tc-MAA administration; S-100 = S-100 protein; Scre = lab measurement at screening visit*

QoL could be fully assessed in all patients except for one (patient 11) who failed to fill out the questionnaire at baseline and at 12 weeks after treatment. Compared with baseline, the mean global health status and QoL scale score at 6 weeks after treatment had decreased by 13 points (from 75.6, 95% CI 68.4–82.8, to 62.5, 49.2–75.8; two-tailed significance p=0.053) and by 14 points at 12 weeks to a mean score of 61.9 (46.8–78.0; two-tailed significance p=0.048). The decrease in global health status and QoL score was numerically greatest in patients with progressive disease. The mean decrease over the first 6 weeks in patients with progressive liver disease was 18.8 points compared with 5.6 points for non-progressive patients (p=0.31). Over the 12 weeks of follow-up, this difference was smaller (16.7 points *vs.* 9.7 points, respectively; p=0.63).

Discussion

In this phase 1 study, 60 Gy of ^{166}Ho was identified as the MTRD. Radioembolization for liver metastases is traditionally done in a salvage setting when standard treatments have failed. In this specific population, 80 Gy was not tolerable. We therefore chose to use a dose of 60 Gy in the ongoing HEPAR phase 2 clinical trial. The mean whole-liver absorbed dose with ^{166}Ho-radioembolization in the 60 Gy cohort was about two times the mean whole-liver absorbed dose that is delivered by ^{90}Y-radioembolization with resin microspheres (SIR-Spheres, SIRTeX Medical, Lane Cove, Australia) when the empirical or body surface area method is used.[1] Clinically, this higher dose might be an advantage, since a higher absorbed dose at the tumor level might lead to an increased response. Even though 60 Gy is a high dose for the liver, the actual dose to the tumor is thought to be substantially higher.[27] 60 Gy is the radiation dose absorbed by the liver if all energy from the administered activity is homogeneously absorbed by the liver. In reality, there is a preferential deposition of activity in tumorous regions, causing much higher absorbed doses in those regions while mostly sparing the healthy liver parenchyma.

Toxicity after ^{166}Ho-radioembolization was mainly confined to symptoms associated with post-embolization syndrome.[29] These symptoms include fatigue, nausea, vomiting, abdominal pain, fever, and anorexia. The mean global health status and QoL scale score decreased significantly at 12 weeks after treatment. This decrease was numerically greatest in patients with progressive liver disease, although it was not significantly greater than in patients without progressive liver disease.

Biochemical toxicity, consisting of grade 1–2 increases in ALT, AST, and bilirubin serum concentrations, grade 1–2 hypoalbuminemia, and grade 1–3 increase of gamma-glutamyltransferase and lactate dehydrogenase concentrations, was in line with the toxicity reported for ^{90}Y-radioembolization.[29,30]

During the first 2 weeks after treatment, we noted a peak in liver enzyme concentrations. This peak was probably a result of injury to the liver caused by the radiation or the embolic component of radioembolization, or both. Late laboratory toxicity (>2 weeks after treatment), both biochemical and hematological, was most severe in patients with progressive liver disease. This finding is most probably a result of disease progression rather than radiation toxicity.

The fraction of systemically spread holmium was low and hematological toxicity was mild in this study. Thrombocytopenia, which was present in 60% of patients after ^{166}Ho-radioembolization, might be related to the concomitant finding that the spleen volume had increased in ten of 15 patients (mean increase 17%). Hypersplenism might affect the number of circulating platelets since the spleen functions as a platelet filter.[31] Increased spleen size is also a side-effect of ^{90}Y-radioembolization, with mean increases of 23–41% at 3 months after treatment.[32-34]

The most important limitations of this phase 1 study were the small number of patients and the unequal distribution of sex, liver involvement, liver volume, and tumor type across the dose cohorts. Furthermore, this study was done in metastatic patients only. Patients with primary liver tumors constitute a distinct group on their own. A phase 1 study of the use of ^{166}Ho-radioembolization in this patient group is needed, with a particular focus on the toxicity of ^{166}Ho-radioembolization in cirrhotic patients and patients with portal vein thrombosis.

^{166}Ho-microspheres are produced in a non-profit environment and are not yet commercially available. The short neutron-activation time for ^{165}Ho (up to 6 h for low-flux reactors and up to 1 h for high-flux reactors),[14,35] which we think is a major cost-determining step, renders it suitable for commercial exploitation. ^{166}Ho-microspheres might change the manner that radioembolization is done in three ways. First, by using a scout dose of ^{166}Ho-microspheres, the medical team undertaking radioembolization will be able to assess the pre-treatment SPECT and MRI results to calculate a specific image-based treatment dose and hence ascertain optimum treatment. Based on the distribution of the scout dose, the treatment dose can then be adjusted so that the tumorous tissue receives the highest possible dose without exceeding the MTRD of the healthy liver tissue. Second, after treatment, the actual dose distribution could be assessed by the same methods to confirm the success of the planned treatment (*ie.* post-treatment dosimetry). Third, ^{166}Ho-microspheres could also be administered under real-time MRI guidance, with direct visualization of the distribution of microspheres (*ie.* per-treatment dosimetry).[36]

Acknowledgments

This research project was funded by the Dutch Cancer Society (KWF Kankerbestrijding), under grant UU2009-4346 and by the Technology Foundation STW under grant 6069. MLJS is supported by a University Medical Center Utrecht Alexandre Suerman MD/PhD grant. We thank T Bosma for coordinating the study and collecting study data; R de Roos for preparing the microspheres; M Sarilar, M Blaauw, D J de Vries, R J Linssen, and H T Wolterbeek of the Reactor Institute Delft, Delft University of Technology (Delft, Netherlands) for irradiating the microspheres; and W Bult for coordinating the inductively coupled plasma mass spectrometry measurements, which were done at the University Medical Center Groningen (Groningen, Netherlands).

Research in context

We developed holmium-166 poly(L-lactic acid) (^{166}Ho-PLLA)-microspheres because radioembolization practices can benefit from a microsphere that can been seen on multimodal imaging and that has optimum properties for both treatment and imaging.[3,4] Holmium was deemed to be suitable for this purpose because of its high-energy beta-radiation and low-energy gamma-radiation emission on nuclear imaging.[5,6] Coincidentally, we discovered that the magnetic susceptibility of holmium was also excellent for quantitative imaging with MRI. Findings from a meta-analysis on yttrium radioembolization[28] showed that both primary and secondary tumors respond well to yttrium radioembolization with little toxicity.

However, treatment of these tumors would benefit from methods for quantitative imaging to ensure optimum deposition of radioactive microspheres in the tumorous tissue to improve patient outcome. The imaging possibilities of yttrium microspheres are insufficient for this purpose. Previous laboratory and animal studies have shown positive results regarding the safety, efficacy, and imaging properties of ^{166}Ho-PLLA-microspheres.[7-11] We therefore did a phase 1 clinical trial in patients. Findings from this trial show that ^{166}Ho-PLLA-microspheres can be translated from a laboratory invention to a device that can be used in human beings.

Interpretation

Our findings show that ^{166}Ho-radioembolization at a dose of 60 Gy is a feasible and safe treatment option for patients with unresectable, chemorefractory liver metastases. Quantitative imaging can now be used to personalize and improve patient treatment. The efficacy of ^{166}Ho-radioembolization will be investigated in the ongoing Holmium Embolization Particles for Arterial Radiotherapy phase 2 trial.

References

1. Kennedy AS, McNeillie P, Dezarn WA, Nutting C, Sangro B, et al. (2009) Treatment parameters and outcome in 680 treatments of internal radiation with resin ^{90}Y-microspheres for unresectable hepatic tumors. Int J Radiat Oncol Biol Phys 74: 1494-1500.
2. Hendlisz A, Van den Eynde M, Peeters M, Maleux G, Lambert B, et al. (2010) Phase III trial comparing protracted intravenous fluorouracil infusion alone or with yttrium-90 resin microspheres radioembolization for liver-limited metastatic colorectal cancer refractory to standard chemotherapy. J Clin Oncol 28: 3687-3694.
3. Gates VL, Esmail AA, Marshall K, Spies S, Salem R (2011) Internal pair production of ^{90}Y permits hepatic localization of microspheres using routine PET: proof of concept. J Nucl Med 52: 72-76.
4. Wissmeyer M, Heinzer S, Majno P, Buchegger F, Zaidi H, et al. (2011) ^{90}Y Time-of-flight PET/MR on a hybrid scanner following liver radioembolization (SIRT). Eur J Nucl Med Mol Imaging 38: 1744-1745.
5. Nijsen JF, Seppenwoolde JH, Havenith T, Bos C, Bakker CJ, et al. (2004) Liver tumors: MR imaging of radioactive holmium microspheres--phantom and rabbit study. Radiology 231: 491-499.
6. de Wit TC, Xiao J, Nijsen JF, van het Schip FD, Staelens SG, et al. (2006) Hybrid scatter correction applied to quantitative holmium-166 SPECT. Phys Med Biol 51: 4773-4787.
7. Vente MA, Nijsen JF, de Wit TC, Seppenwoolde JH, Krijger GC, et al. (2008) Clinical effects of transcatheter hepatic arterial embolization with holmium-166 poly(L-lactic acid) microspheres in healthy pigs. Eur J Nucl Med Mol Imaging 35: 1259-1271.
8. Nijsen F, Rook D, Brandt C, Meijer R, Dullens H, et al. (2001) Targeting of liver tumor in rats by selective delivery of holmium-166 loaded microspheres: a biodistribution study. Eur J Nucl Med 28: 743-749.
9. Zielhuis SW, Nijsen JF, Figueiredo R, Feddes B, Vredenberg AM, et al. (2005) Surface characteristics of holmium-loaded poly(L-lactic acid) microspheres. Biomaterials 26: 925-932.
10. Zielhuis SW, Nijsen JF, Krijger GC, van het Schip AD, Hennink WE (2006) Holmium-loaded poly(L-lactic acid) microspheres: in vitro degradation study. Biomacromolecules 7: 2217-2223.
11. Zielhuis SW, Nijsen JF, Seppenwoolde JH, Bakker CJ, Krijger GC, et al. (2007) Long-term toxicity of holmium-loaded poly(L-lactic acid) microspheres in rats. Biomaterials 28: 4591-4599.
12. Smits ML, Nijsen JF, van den Bosch MA, Lam MG, Vente MA, et al. (2010) Holmium-166 radioembolization for the treatment of patients with liver metastases: design of the phase I HEPAR trial. J Exp Clin Cancer Res 29: 70.
13. Nijsen JF, van Het Schip AD, van Steenbergen MJ, Zielhuis SW, Kroon-Batenburg LM, et al. (2002) Influence of neutron irradiation on holmium acetylacetonate loaded poly(L-lactic acid) microspheres. Biomaterials 23: 1831-1839.
14. Nijsen JF, Zonnenberg BA, Woittiez JR, Rook DW, Swildens-van Woudenberg IA, et al. (1999) Holmium-166 poly lactic acid microspheres ap-

plicable for intra-arterial radionuclide therapy of hepatic malignancies: effects of preparation and neutron activation techniques. Eur J Nucl Med Mol Imaging 26: 699-704.

15. Zielhuis SW, Nijsen JF, de Roos R, Krijger GC, van Rijk PP, et al. (2006) Production of GMP-grade radioactive holmium loaded poly(L-lactic acid) microspheres for clinical application. Int J Pharm 311: 69-74.
16. Bolch WE, Bouchet LG, Robertson JS, Wessels BW, Siegel JA, et al. (1999) MIRD pamphlet No. 17: the dosimetry of nonuniform activity distributions--radionuclide S values at the voxel level. Medical Internal Radiation Dose Committee. J Nucl Med 40: 11S-36S.
17. Dezarn WA, Cessna JT, DeWerd LA, Feng W, Gates VL, et al. (2011) Recommendations of the American Association of Physicists in Medicine on dosimetry, imaging, and quality assurance procedures for ^{90}Y microsphere brachytherapy in the treatment of hepatic malignancies. Med Phys 38: 4824-4845.
18. Bol GH, Kotte AN, van der Heide UA, Lagendijk JJ (2009) Simultaneous multi-modality ROI delineation in clinical practice. Comput Methods Programs Biomed 96: 133-140.
19. (1989) International Commission on Radiation Units and Measurements. Tissue substitutes in radiation dosimetry and measurement, ICRU Report 44. Bethesda, MD.
20. Salem R, Lewandowski RJ, Sato KT, Atassi B, Ryu RK, et al. (2007) Technical aspects of radioembolization with ^{90}Y microspheres. Tech Vasc Interv Radiol 10: 12-29.
21. Vente MA, de Wit TC, van den Bosch MA, Bult W, Seevinck PR, et al. (2010) Holmium-166 poly(L-lactic acid) microsphere radioembolization of the liver: technical aspects studied in a large animal model. Eur Radiol 20: 862-869.
22. Dhabuwala A, Lamerton P, Stubbs RS (2005) Relationship of 99m-technetium labelled macroaggregated albumin (^{99m}Tc-MAA) uptake by colorectal liver metastases to response following Selective Internal Radiation Therapy (SIRT). BMC Nucl Med 5: 7.
23. Bult W, Vente MA, Zonnenberg BA, Van Het Schip AD, Nijsen JF (2009) Microsphere radioembolization of liver malignancies: current developments. Q J Nucl Med Mol Imaging 53: 325-335.
24. Lin Y, Shih WJ (2001) Statistical properties of the traditional algorithm-based designs for phase I cancer clinical trials. Biostatistics 2: 203-215.
25. Eisenhauer EA, Therasse P, Bogaerts J, Schwartz LH, Sargent D, et al. (2009) New response evaluation criteria in solid tumors: revised RECIST guideline (version 1.1). Eur J Cancer 45: 228-247.
26. Guha C, Kavanagh BD (2011) Hepatic radiation toxicity: avoidance and amelioration. Semin Radiat Oncol 21: 256-263.
27. Campbell AM, Bailey IH, Burton MA (2001) Tumor dosimetry in human liver following hepatic yttrium-90 microsphere therapy. Phys Med Biol 46: 487-498.
28. Vente MA, Wondergem M, van der Tweel I, van den Bosch MA, Zonnenberg BA, et al. (2009) Yttrium-90 microsphere radioembolization for the treatment of liver malignancies: a structured meta-analysis. Eur Radiol 19: 951-959.

29. Kennedy AS, Coldwell D, Nutting C, Murthy R, Wertman DE, Jr., et al. (2006) Resin 90Y-microsphere brachytherapy for unresectable colorectal liver metastases: modern USA experience. Int J Radiat Oncol Biol Phys 65: 412-425.

30. Piana PM, Gonsalves CF, Sato T, Anne PR, McCann JW, et al. (2011) Toxicities after radioembolization with yttrium-90 SIR-spheres: incidence and contributing risk factors at a single center. J Vasc Interv Radiol 22: 1373-1379.

31. Aster RH (1966) Pooling of platelets in the spleen: role in the pathogenesis of "hypersplenic" thrombocytopenia. J Clin Invest 45: 645-657.

32. Moroz P, Anderson JE, Van Hazel G, Gray BN (2001) Effect of selective internal radiation therapy and hepatic arterial chemotherapy on normal liver volume and spleen volume. J Surg Oncol 78: 248-252.

33. Nosher JL, Ohman-Strickland PA, Jabbour S, Narra V, Nosher B (2011) Changes in liver and spleen volumes and liver function after radioembolization with yttrium-90 resin microspheres. J Vasc Interv Radiol 22: 1706-1713.

34. Jakobs TF, Saleem S, Atassi B, Reda E, Lewandowski RJ, et al. (2008) Fibrosis, portal hypertension, and hepatic volume changes induced by intra-arterial radiotherapy with 90yttrium microspheres. Dig Dis Sci 53: 2556-2563.

35. Vente MA, Nijsen JF, de Roos R, van Steenbergen MJ, Kaaijk CN, et al. (2009) Neutron activation of holmium poly(L-lactic acid) microspheres for hepatic arterial radio-embolization: a validation study. Biomed Microdevices 11: 763-772.

36. Seppenwoolde JH, Bartels LW, van der Weide R, Nijsen JF, van het Schip AD, et al. (2006) Fully MR-guided hepatic artery catheterization for selective drug delivery: a feasibility study in pigs. J Magn Reson Imaging 23: 123-129.

Chapter 5

The evolution of radioembolization

MLJ Smits, JFW Nijsen, MAAJ van den Bosch, BA Zonnenberg

Lancet Oncology 2012

Maurizio Cosimelli[1] outlined the ongoing evolution of radioembolization in response to our phase 1 study.[2] Cosimelli stated that the evidence for effectiveness of radioembolization with ^{90}Y-microspheres cannot be directly translated to radioembolization with ^{166}Ho-microspheres because of differences in toxic effects (80% of patients treated with ^{166}Ho-radioembolization had increases gamma-glutamyl transpeptidase concentrations and lymphocytopenia) and radionuclide properties (shorter half-life of ^{166}Ho [26.8 h] than ^{90}Y [64.2 h]). When assessing the toxic effects of radioembolization, studies with similar designs should be compared. In our phase 1 study, extensive biochemical and hematological analysis were done every week during follow-up. Similar studies have, unfortunately, not been published for ^{90}Y-radioembolization. Nevertheless, abnormalities in biochemical and hematological analyses are not unique to ^{166}Ho-radioembolization and have been reported after ^{90}Y-RE as well.[3-5] Lymphocytopenia is thought to be caused by irradiation of blood passing through the liver, which is a logical side effect of radioembolization.[3,6] Release of gamma-glutamyl transpeptidase - a sign of bilio-canicular injury - was highest in patients with progressive liver disease and their plasma levels kept rising from baseline to the end of follow-up, which suggests that these abnormalities might have been largely caused by tumor progression.

The short half-life of ^{166}Ho leads to deposition of a radiation dose in a shorter time than with ^{90}Y, which might or might not be favorable for tumor destruction. However, we think that it is far more important that an adequate amount of microspheres, and thereby an adequate absorbed dose, is given to each tumor. Still too often, patients with liver metastases treated with radioembolization (either with ^{90}Y or ^{166}Ho) have a part of a tumor, or a part of the liver with several lesions, that receive little or no activity, because of the heterogeneous intrahepatic distribution of the microspheres. Tumors receiving no to little activity will probably not respond to treatment, irrespective of the decay time of the radionuclide.

A dose-response relation on tumor level has not been fully established for ^{90}Y-radioembolization to date, mainly due to the lack of an accurate method for dosimetry, requiring quantitative assessment of the biodistribution of the microspheres. We therefore believe that these questions can be best solved by using quantitative imaging technology such as MRI, positron emission tomography, or and single photon emission CT for each patient treated with radioembolization. Furthermore, we should investigate whether in patients with incomplete tumor targeting on biodistribution imaging, retreatment of the incompletely targeted tumors will increase tumor response and survival. If so, post-treatment dosimetry and retreatment could become standard practice for radioembolization in patients with hepatic cancers.

References

1. Cosimelli M (2012) The evolution of radioembolization. Lancet Oncol 13: 965-966.

2. Smits M, Nijsen JF, van den Bosch MA, Lam MG, Vente MA, et al. (2012) Holmium-166 radioembolization in patients with unresectable, chemorefractory liver metastases (HEPAR trial): a phase 1, dose-escalation study. Lancet Oncol 13: 1025-1034.

3. Ibrahim SM, Lewandowski RJ, Sato KT, Gates VL, Kulik L, et al. (2008) Radioembolization for the treatment of unresectable hepatocellular carcinoma: a clinical review. World J Gastroenterol 14: 1664-1669.

4. Arslan N, Emi M, Alagoz E, Ustunsoz B, Oysul K, et al. (2011) Selective intraarterial radionuclide therapy with Yttrium-90 ($Y-^{90}$) microspheres for hepatic neuroendocrine metastases: initial experience at a single center. Vojnosanit Pregl 68: 341-348.

5. Carr BI, Metes DM (2012) Peripheral blood lymphocyte depletion after hepatic arterial ^{90}Yttrium microsphere therapy for hepatocellular carcinoma. Int J Radiat Oncol Biol Phys 82: 1179-1184.

6. Neff RD, Cassen B (1968) Relative radiation sensitivity of circulating small and large lymphocytes. J Nucl Med 9: 402-405.

Chapter 6

Quality of life in liver metastases patients treated with holmium-166 radioembolization

MLJ Smits, JF Prince, AA Pronk, JFW Nijsen, BA Zonnenberg,
MGEH Lam, MAAJ van den Bosch

Submitted

Abstra

Purpose

To evaluate the adverse effect of intra-arterial holmium-166 radioembolization (^{166}Ho-RE) on quality of life (QoL) in patients with liver metastases.

Materials and Methods

Patients with unresectable and chemorefractory liver metastases were treated with ^{166}Ho-RE in a dose-finding phase 1 trial. The European Organisation for Research and Treatment of Cancer QLQ-C30 and LMC21 questionnaires were used to evaluate QoL at baseline, at six and at twelve weeks after treatment. The course of the global health status/QoL and symptom and functioning scales were analysed. Patients were categorized into responders and non-responders according to RECIST criteria based on CT imaging at 12 weeks post treatment. Outcomes between subgroups were compared.

Results

Fifteen patients received ^{166}Ho-RE and filled out the questionnaires with a compliance of 96%. The mean global health status/QoL decreased after ^{166}Ho-RE from 75.6 to

Introduction

Intra-arterial radioembolization is mostly applied as a palliative treatment option for patients with liver metastases who are not or no longer candidates for partial liver resection and/or first or second line chemotherapy.[1,2] When proposing palliative treatment options to patients with liver metastases, physicians tend to focus on survival benefit, and the consequences in terms of quality of life are often not discussed.[3] Studies have shown, however, that 82 - 95% of patients with advanced cancer value quality of life (QoL) at least as much as survival benefit.[3,4] Therefore, it is important for decision making for the individual patient that data on QoL are available for all palliative therapies. Radioembolization is a locoregional treatment option for patients with malignancies in the liver during which radioactive microspheres are administered via the hepatic artery. Radioembolization with yttrium-90 microspheres has been shown to lead to an increased progression-free survival and a non-significantly prolonged overall survival, accompanied by primarily short-term toxicity in patients with advanced colorectal carcinoma liver metastases.[5,6] The effect of ^{90}Y-RE on QoL is less well-studied and the evidence is sparse in the literature.

Holmium-166-poly(L-lactic acid) (^{166}Ho) microspheres have been developed as an alternative to the currently used yttrium-90 (^{90}Y) microspheres. The main advantage of ^{166}Ho-microspheres is the ability to be visualised in-vivo by SPECT and MRI, which

62.5 points at 6 weeks (p=0.053) and to 61.9 points at 12 weeks (p=0.048). The biggest drop in functioning scales was observed in physical, social and role functioning. The most prominent symptoms were fatigue, appetite loss, pain, dyspnea and insomnia. Scores for global health status/QoL, functioning and symptoms worsened the most for non-responders.

Conclusion

In this phase 1 study, QoL deteriorated moderately after ^{166}Ho-RE. Tumor progression may be an important factor in QoL since the deterioration was largest in non-responders.

enables quantitative biodistribution imaging.[7,8] We performed a phase 1 trial in order to investigate the safety and toxicity profile of ^{166}Ho-RE.[9] The purpose of the current study was to evaluate the adverse effect of ^{166}Ho-RE on QoL in these patients.

Materials and Methods

Patients and study design

Patients with unresectable, chemorefractory liver metastases of any primary tumor type were included in the HEPAR phase 1 trial. In this trial, the maximum tolerated radiation dose was the endpoint of the study and was determined to be 60 Gy to the whole liver.[9] QoL was assessed in these patients as well and was used for the current study. Patients had to be at least 18 years of age, have an estimated life expectancy of over 3 months, a WHO performance status score of 0-2, at least one measurable lesion of at least 10 mm on CT and a negative pregnancy test for women. Patients were not allowed to have an impaired hematological function (leucocytes $<4.0x10^9$ cells/L and platelet count $<150x10^9$/L), an impaired renal function (serum creatinine >185 µmol/L), an impaired cardiac function (relevant morphological changes on electrocardiography or New York Heart Association classification of heart disease score ≥2), an impaired hepatic function (alanine aminotransferase [ALT], aspartate aminotransferase [AST], or

alkaline phosphatise over five times the upper limit of normal, or serum bilirubin over 1.5 times the upper limit of normal), received chemotherapy or abdominal surgery over the previous 4 weeks, incompletely healed surgical incisions or contraindications for MRI. Patients were enrolled in cohorts of three to six patients, scheduled to receive escalating radiation doses to the liver as calculated by aimed whole-liver radiation absorbed doses of 20 Gy, 40 Gy, 60 Gy, and 80 Gy. All cohorts consisted of three patients and were extended in case dose-limiting toxicity occurred in one of the three patients. If dose-limiting toxicity occurred in two out of three patients in one cohort, the primary study endpoint was reached, and the maximum tolerated radiation dose would be set at the dose of the preceding cohort. The institutional review board approved this study and all patient provided written informed consent. This study was registered at clinicaltrials.gov, number NCT01031784. A more detailed description of the study design and the main study results have been published elsewhere.[9,10]

Treatment procedures

Patients first received a work-up angiography during which a catheter was placed in the hepatic artery via the femoral artery. Any vessels arising from the hepatic artery or its branches and leading tot non-target organs such as the stomach or intestines, were coil-embolized. Then, approximately 150 MBq of technetium-99m-labelled macroalbumin aggregates (^{99m}Tc-MAA) was administered as a surrogate for the ^{166}Ho-microspheres. Patients were allowed to receive ^{166}Ho-microspheres if on post-^{99m}Tc-MAA-scintigraphy and SPECT, ^{99m}Tc-MAA was exclusively distributed to the liver with a lung shunt fraction <20%. Subsequently, a second angiography session was planned in which a scout dose (60mg, 250 MBq) of ^{166}Ho-microspheres was administered at the same injection position as for ^{99m}Tc-MAA injection directly followed by SPECT and MRI. The treatment dose of ^{166}Ho-microspheres (540 mg, varying activities depending on liver volume) was then injected the same afternoon, followed by SPECT and MRI a few days afterwards.

Quality of life assessment

The QoL in patients was assessed using the validated European Organisation for Research and Treatment of Cancer QLQ-C30 version 3.0 and QLQ-LMC21 questionnaires at baseline and at six and twelve weeks after treatment.[11] From the questionnaires a Global Health Status / Quality of Life (GHS/QoL) scale, five functioning scales and twenty-two symptom scales were derived. All scales can range in scores from 0 to 100, where a high score on the GHS/QoL or functioning scales represents a high degree of GHS/QoL or functioning, and a high score on the symptoms scale represents a high level of symptomatology. The functioning scales are: physical functioning, role functio-

ning, emotional functioning, cognitive functioning and social functioning. The symptom scales are: fatigue, nausea and vomiting, pain, dyspnea, insomnia, appetite loss, constipation, diarrhea, financial difficulties (QLQ-C30); and eating, activity/vigour, pain, emotional problems, weight loss, taste, dry mouth, sore mouth/tongue, peripheral neuropathy, jaundice, contact with friends, talking about feelings, and sex life (QLQ-LMC21).

Response assessment

Patients were categorized into responders (stable disease, partial response, or complete response in the liver) and non-responders (progressive disease in the liver). Response was scored according to the Response Evaluation Criteria in Solid Tumors (RECIST) v.1.1 on CT at 12-weeks follow-up.

Scoring and statistical analysis

Scoring of the questionnaires was performed according to the scoring manual provided by the EORTC.[12] Corrections for missing values in a scale composite of multiple questions were performed by using the average of the known values for the respective scale. Interpretation of changes in scores took place according to an anchor-based interpretation according to which a change of 5-10 points is 'little' change, >10-20 'moderate' change, and >20 'very much'/'severe' change.[13] A change <5 points was interpreted as neglectable change. The GHS/QoL scale was used as an indicator of overall QoL. Descriptive statistics (average score, standard deviation, percentage) were used to describe the scores on the GHS/QoL, functioning and symptom scales. Changes in GHS/QoL scores during follow-up were tested for statistical significance by a two-tailed paired-sample t-test. SPSS was used for all analyses (version 20, IBM corporation, Somers, NY).

Results

Fifteen patients underwent ^{166}Ho-RE for the treatment of liver metastases. Baseline characteristics are listed in *Table 1*. The primary tumor types were ocular melanoma (n=6), colorectal carcinoma (n=6), cholangiocarcinoma (n=2), and breast carcinoma (n=1). The first dose cohort (20 Gy) consisted of six patients and the other dose cohorts (40, 60, and 80 Gy) consisted of three patients each. Six patients had partial response or stable disease in the liver at 12-weeks follow-up (responders) and nine patients had progressive disease (non-responders).

Table 1. *Demographics*

Baseline Characteristics	Value
Mean age (years)	55 (38-87)
Gender	
Male	9
Female	6
Primary tumor	
Ocular melanoma	6
Colorectal carcinoma	6
Cholangiocarcinoma	2
Breast carcinoma	1
WHO performance score	
WHO = 0	13
WHO = 1	2
Tumor burden	
< 25%	10
≥ 25% - < 50%	4
≥ 50%	1
Evidence of extrahepatic metastases	
Yes	6
No	9
Prior treatment	
Systemic treatment	11
Locoregional treatment	5
Treatment and follow-up	
Aimed whole liver absorbed dose	
20 Gy	6
40 Gy	3
60 Gy	3
80 Gy	3
Tumor response	
Responders*	6
Non-responders*	9

*Values are presented as n or median (range). WHO = World Health Organization. *Response defined as partial response or stable disease in the liver as assessed on CT at 12-weeks post treatment*

Compliance

In total, the 15 patients were asked to fill a total of 45 questionnaires, of which 43 were handed in (compliance 96%). One patient failed to fill out the questionnaire both at baseline and 12 weeks after treatment and this patient was therefore excluded from the analyses. Of the 42 questionnaires that were analyzed, each comprising 51 questions, 2 questions were left blank (missing items 2/2142, 0.1%). Baseline questionnaires were collected on average 2.1 (SD 0.4) weeks before treatment. Follow-up questionnaires were handed in on average 5.9 (SD 0.1) weeks and 12.1 (SD 0.2) weeks after treatment.

Table 2. *EORTC scores*

	Baseline score	Score 6-weeks post treatment	Anchor-based interpretation of change	Score 12-weeks post treatment	Anchor-based interpretation of change
Global health status / QoL	75.6 ± 12.4	62.5 ± 23.1	moderate	61.9 ± 26.1	moderate
Functioning scales					
Physical functioning	90.5 ± 11.3	81.4 ± 20.9	little	73.3 ± 26.7	moderate
Role functioning	78.6 ± 22.1	60.7 ± 35.6	moderate	65.5 ± 34.9	moderate
Emotional functioning	80.4 ± 22.6	78.6 ± 21.6	neglectable	76.2 ± 21.1	neglectable
Cognitive functioning	90.5 ± 12.6	86.9 ± 16.2	neglectable	83.3 ± 18.5	little
Social functioning	88.1 ± 15.2	69.1 ± 29.9	moderate	76.2 ± 25.9	moderate
Symptom scales (QLQ-C30)					
Fatigue	27.0 ± 18.3	37.3 ± 26.4	little	42.1 ± 35.5	moderate
Nausea and vomiting	4.8 ± 7.8	10.7 ± 15.5	little	15.5 ± 23.1	little
Pain	11.9 ± 20.1	23.8 ± 31.8	moderate	27.4 ± 25.1	moderate
Dyspnoea	4.8 ± 12.1	14.3 ± 28.4	little	21.4 ± 24.8	moderate
Insomnia	14.3 ± 21.5	14.3 ± 21.5	no change	19.1 ± 21.5	little
Appetite loss	4.8 ± 12.1	19.1 ± 31.3	moderate	28.6 ± 28.9	severe
Constipation	14.3 ± 25.2	9.5 ± 27.5	neglectable	9.5 ± 15.6	neglectable
Diarrhoea	11.9 ± 21.1	4.8 ± 12.1	little	7.1 ± 14.2	little
Financial difficulties	9.5 ± 20.4	11.9 ± 21.1	neglectable	11.9 ± 21.1	neglectable
Symptom scales (LMC-21)					
Eating	6.0 ± 10.6	23.8 ± 27.5	moderate	33.3 ± 34.6	severe
Fatigue	18.3 ± 18.3	36.5 ± 27.7	moderate	42.1 ± 38.8	severe
Pain	10.3 ± 14.1	26.2 ± 27.1	moderate	24.6 ± 23.1	moderate
Emotional problems	29.2 ± 24.2	21.4 ± 13.8	little	33.3 ± 24.9	neglectable

Table 2. *Continued*

	Baseline score	Score 6-weeks post treatment	Anchor-based interpretation of change	Score 12-weeks post treatment	Anchor-based interpretation of change
Weight loss	7.1 ± 19.3	14.3 ± 21.5	little	9.5 ± 27.5	neglectable
Taste	0	14.3 ± 31.3	moderate	21.4 ± 24.8	severe
Dry mouth	2.4 ± 8.9	11.9 ± 16.6	little	11.9 ± 21.1	little
Sore mouth/tongue	0	0	no change	0	no change
Peripheral neuropathy	4.8 ± 12.1	0	little	2.4 ± 8.9	neglectable
Jaundice	0	0	no change	0	no change
Contact with friends	0	7.1 ± 26.7	little	9.5 ± 27.5	little
Talking about feelings	7.1 ± 19.3	0	little	9.5 ± 20.4	neglectable
Sex life	21.4 ± 36.1	40.5 ± 35.0	moderate	45.2 ± 42.6	severe

Values are presented mean ± standard deviation. QLQ-C30 = 30-questions questionnaire for quality of life in cancer patients; QLQ-LMC21 = additional 21-questions questionnaire for colorectal cancer patients; QoL = quality of life

Global health status / quality of life

The mean GHS/QoL score at 6 weeks after treatment had decreased 'moderately' by 13.1 points (from 75.6 to 62.5, p=0.053) compared to baseline. After 12 weeks the QoL score had decreased 'moderately' compared to baseline, by 13.7 points to a mean score of 61.9 (p=0.048) (*Table 2*). The decrease in GHS/QoL score was higher in non-responders than in responders: 18.8 *vs.* 5.6 points at 6 weeks (p=0.31) and 16.7 *vs.* 9.7 points at 12 weeks post treatment (p=0.63), respectively (*Figure 1*).

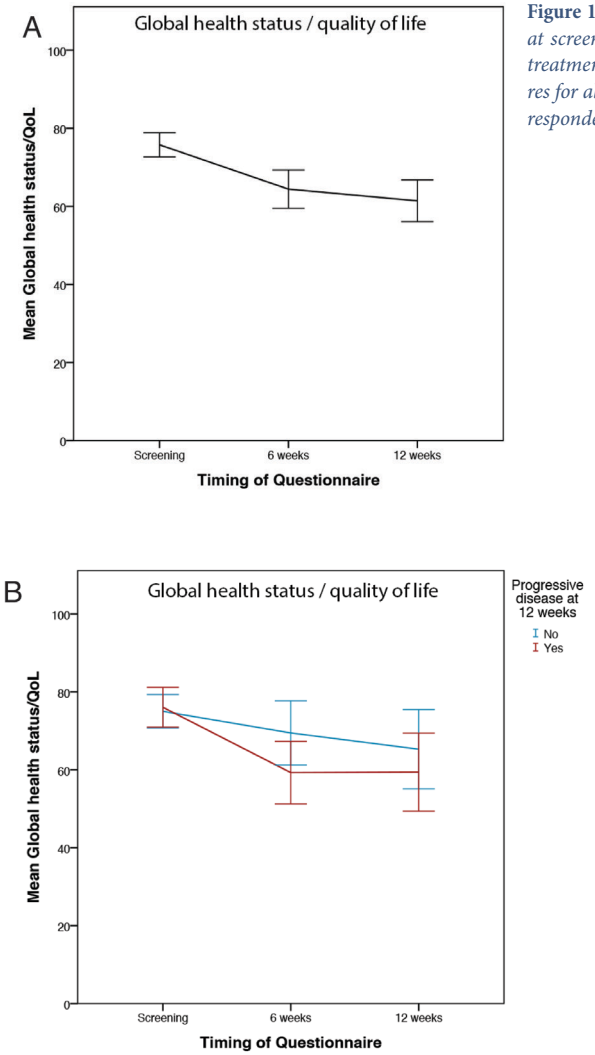

Figure 1. *Course of quality of life (QoL) scores at screening, and at six and twelve weeks post treatment. Global health status(GHS)/QoL scores for all patients (a); GHS/QoL scores split for responders and non-responders (b).*

Functioning and Symptom scales

Mean scores for all functioning scales decreased during follow-up (*see Table 2*). Physical functioning, role functioning and social functioning were the most affected functions, with mean scores decreasing 'moderately' by 9.1, 17.9, and 19.0 points at 6 weeks, and by 17.2, 14.1 and 11.9 points at 12 weeks, respectively. Cognitive and emotional functioning score decreased little during follow-up. In analogy, the mean scores for nearly all symptom scales increased (more symptomatology). Patients did report less constipation and diarrhea. None of the patients reported any sore mouth/tongue or jaundice. There were no severe changes in symptom scales at 6 weeks. Mean scores worsened 'severely' at 12 weeks for appetite loss (+23.8 points), eating (+27.3 points), fatigue (+23.8 points), taste (+21.4 points) and sex life (+23.8 points). Mean scores for all other symptoms changed 'neglectably', 'little' or 'moderately' (*Table 2*). The course of the scores for GHS/QoL, functioning and symptom scales are presented in *Figure 2*.

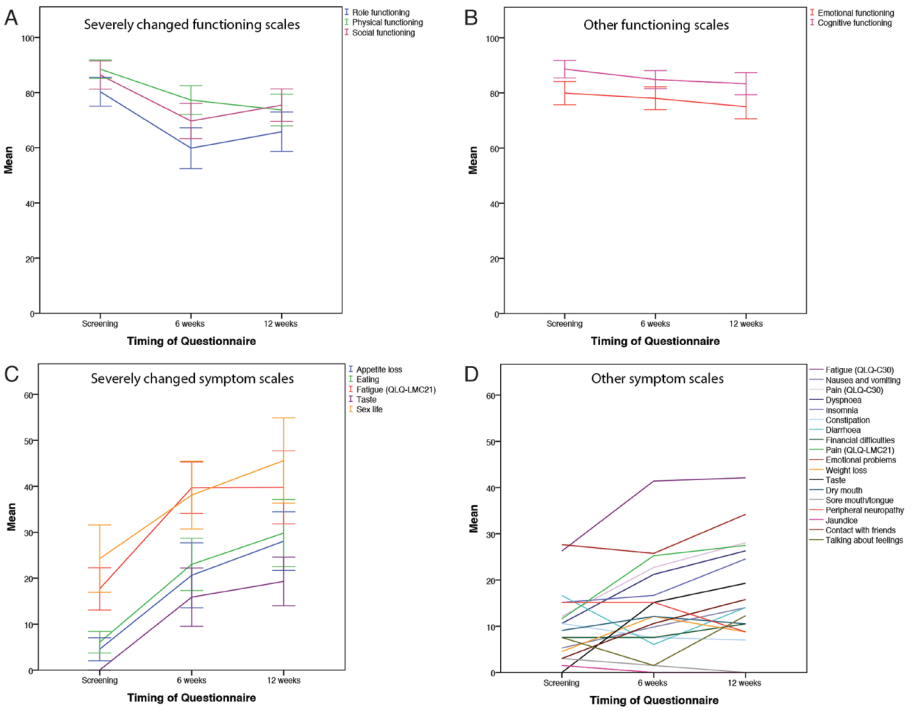

Figure 2. *Course of severely changed functioning scores (a) and non-severely changed functioning scores (b); Course of severely changed symptom scores (c) and non-severely changed symptom scores (d).*

Discussion

This study showed that the GHS/QOL of advanced liver metastases patients decreased moderately after treatment with ^{166}Ho-RE. This decrease was most prominent in patients with progressive liver disease.

The GHS/QoL score was used as a general measure of QoL. The GHS/QoL score is based on two questions and the other 49 questions (on which functioning and symptom scores are based) may help to determine why GHS/QoL scores changed. In this study, physical functioning, role functioning and social functioning were the most affected functioning scales. These functioning scales comprised questions assessing whether patients were limited in activities like walking/eating/dressing/washing/performing strenuous activities (physical functioning), performing hobbies or other daily activities (role functioning), and whether the physical condition or treatment interfered with their family life or social activities (social functioning). Factors other than the treatment itself can influence these scores. Social functioning, for instance, may be affected by the instructions for radiation safety. Patients are instructed to keep a safe distance to family and relatives for the first days after treatment. Participation in this clinical trial with intensive monitoring and follow-up imaging may have influenced functioning as well. Patients had to come to the outpatient clinic every week and received multiple MRI, CT, SPECT and PET scans, which poses a significant time, psychological, and physical burden, possibly reflected in the decreased role functioning scores. It is therefore plausible that the drop in GHS/QoL will be less when ^{166}Ho-RE is offered in regular clinical practice instead of in a research setting.

The results of this phase I study showed that the toxicity profile of ^{166}Ho-RE was similar to that of ^{90}Y-RE, with a high incidence of post-embolization symptoms such as abdominal pain, nausea, fatigue, anorexia, vomiting, and fever. It is interesting to note that the questionnaire scores for typical post-embolization symptoms like nausea/vomiting and pain were only little or moderately changed, while fatigue, sex life and symptoms involved with eating (appetite loss, eating, taste) were the most affected symptoms. This knowledge can help to better inform patients on what to expect from therapy. Furthermore, in order to improve QoL after radioembolization in the future, we think it is important to interview patients to determine what caused their QoL to decrease and how they experienced the treatment and the follow-up period. For this reason, our department is now developing a patient survey addressing all these questions.

To compare our results to earlier studies (using ^{90}Y-RE), we searched for literature on QoL in patients treated with ^{90}Y-RE to use as a benchmark for our results (*Table 3*). Seven studies presented data on QoL after ^{90}Y-RE.[6,14-19] The study by Mancini *et al.* was disregarded because it presented data from the same patient cohort as Cosimelli *et*

al.[14,15] Of the four studies in which patients received ^{90}Y-RE as a stand-alone treatment, QoL worsened in one, improved in two, and 'did not worsen' in another study. The only two studies that provided QoL-scores were performed in patients with hepatocellular carcinoma.[18,19] Steel *et al.* used the Functional Assessment of Cancer Therapy-Hepatobiliary (Fact-Hep) questionnaire and found no clinically significant difference in QoL after three or six months between hepatic artery infusion of chemotherapy (cisplatin) or ^{90}Y-microspheres (Therasphere®) in patients with hepatocellular carcinoma.[19] Overall health-related quality of life decreased from 77.2 points at baseline to 74.5 points three months after ^{90}Y-RE, and 47.3 points after six months. Salem *et al.* used the Fact-Hep questionnaire as well, and found an increase of health-related QoL in patients with hepatocellular carcinoma from 80.4 points to 84.3 points four weeks after ^{90}Y-RE.[18] Cosimelli *et al.* measured QoL using the EORTC QLQ-C30 and CR38 in 14 patients out of 50 patients treated with ^{90}Y-RE for metastatic colorectal cancer.[14] The authors reported that the QoL was not adversely affected by radioembolization but provide no further details. Kalinowski *et al.* described ^{90}Y-RE in nine neuroendocrine liver metastases patients in whom QoL was assessed at three-monthly intervals using the EORTC QLQ-C30 and LMC-21.[16] The authors report a statistically significant increase in QoL after six months.

In two studies, patients with metastasized colorectal carcinoma were randomized to either chemotherapy or chemotherapy and ^{90}Y-RE. Gray *et al.* performed a randomized controlled trial in which a total of 74 patients with metastatic colorectal carcinoma were randomized to ^{90}Y-RE plus hepatic artery chemotherapy (HAC) with floxuridine or solely HAC.[17] QoL was assessed using an 11-question linear analogue self-assessment questionnaire. In a second randomized controlled trial, 21 patients with colorectal liver metastases were treated with chemotherapy (fluorouracil/leucovorin) or chemotherapy plus ^{90}Y-RE.[6] QoL was self-assessed by patients using the Functional Living Index Cancer questionnaire and clinicians assessed patient well-being using the Spitzer index. Both studies found no difference in QoL between the study arms.

Radioembolization for patients with colorectal cancer liver metastases is currently predominantly applied in an end-stage setting, where it may compete with third-line options like the epidermal growth factor receptor (EGFR) antibodies cetuximab and panitumumab. Knowing the effect of these antibody-treatments on QoL may be important for choosing between these options. In a landmark study on cetuximab, the mean GHS/QoL score as measured with the EORTC QLQ-C30 questionnaire decreased only by 0.5 and 3.6 points at 8 and 16 weeks after cetuximab treatment, respectively.[20] This decrease is less than seen after ^{166}Ho-RE, although it must be noted that the questionnaire compliance in this study was only 81% at 8 weeks and 67% at 16 weeks. There are no

studies comparing the effect of RE and anti-EGFR treatment on QoL. The studies that compared RE with third-line chemotherapy found no difference between arms in the effect on QoL[6,17] or a better QoL in patients treated with RE (*Table 3*).[19]

Based on the available literature, the decrease in QoL after ^{166}Ho-RE found in this study is in line with results from studies on ^{90}Y-RE. There are several limitations to our study. Since this was a phase one clinical trial in which patients were treated with ^{166}Ho-RE according to a dose escalation protocol, the total number of patients was limited, there was no control group, and the aimed whole liver absorbed doses varied in order to find the optimal dose. This study should therefore be interpreted as a first reconnaissance of the effects of ^{166}Ho-RE in humans. Furthermore, in current study we decided only to look at differences in QoL for two categories of patients, *i.e.* responders and non-responders, since these categories showed very different results regarding laboratory toxicity as well and the small number of patients hindered analysis of more categories.[9] The EORTC QLQ-C30 questionnaire was used because it has been validated in many settings and languages and is often used for measuring QoL in radioembolization studies (*see Table 3*).[11,21] In addition to the QLQ-C30 as a universal questionnaire for cancer patients, all patients were asked to fill out the LMC21 module. Although this module has been validated in patients with colorectal liver metastases (only 40% of this study's population) we think this questionnaire provides valuable information about the symptomatology in the patients with liver metastases from other primaries as well.

More knowledge about the influence of ^{166}Ho-RE on QoL is important for several reasons. Above all, we think it is important to use this information to better inform patients about what to expect from ^{166}Ho-RE and help them to make a well-informed choice between all the available palliative treatment options. Second, since the decrease in GHS/QoL was largest in patients with progressive disease, QoL seems to be related to other outcomes like tumor response, progression-free survival and survival. We hypothesize that finding ways to improve tumor response after RE, for instance by assuring that an adequate amount of radioactivity arrived in all tumors, may therefore have a positive effect on QoL.

In conclusion, patients treated with ^{166}Ho-RE experienced a moderately decreased health-related QoL at 6 and 12 weeks after treatment. QoL decreased most in patients with progressive disease. These results are in line with available data on QoL after ^{90}Y-RE.

		Author	Treatment arm	Control arm	n (Y-RE / other)	Primary tumor(s)	Questionnaires
Solely Y-RE	No control arm	Cosimelli et al.	Y-RE		14[b]	Colorectal	QLQ C30, QLQ LMC21 QLQ CR38
		Kalinowski et al.	Y-RE		9	Neuroendocrine	QLQ C30, QLQ LMC21
	Control arm	Salem et al.	Y-RE	TACE	29 / 27	HCC	FACT-Hep
		Steel et al.	Y-RE	CP	14 / 14	HCC	FACT-Hep
Y-RE + chemo		Gray et al.	Y-RE & 5-FU	5-FU	36 / 34	Colorectal	Self Assessment Scale
		Van Hazel et al.	Y-RE & 5-FU/LV	5-FU/LV	11 / 10	Colorectal	FLIC questionnaire, Spitzer index
		Smits et al.[f]	Ho-RE		15	Colorectal ocular melanoma cholangiocarcinoma breast	QLQ C30, QLQ LMC21

Y-RE = Yttrium-90 radioembolization, HADs = Hospital Anxiety and Depression Scale, NS = Not specified, 5-FU = Fluorouracil, LV = Leucovorin, NR = not reported, CP = Cisplatin, TACE = Transarterial Chemoembolization, HCC = Hepatocellular carcinoma, Ho-RE = Holmium-166 radioembolization

Values presented as mean, values in parentheses are SD, in brackets 95% CI

a displayed for Y-RE, b of 50 included patients 14 were evaluated for QoL, c values were read out from a graph, d original data of 2 weeks not published, e calculated from difference, f this study

Scale range	Baseline[a]	4 weeks	6 weeks	3 months	6 months	9 months	12 months	Outcome
								QoL was not adversely affected
0-100	50[c]			66	58	50	58	QoL temporarily improved with statistical significance
0-180	80,4 (2.76)	84,28 (2,96)[e]						No significant difference between arms
0-180	77.2 (17.4)			74,5 (18.6)	47,3 (23.8)			Patients treated with Y-RE had significantly better QoL at 3 months than in the control arm, no significant difference at 6 months
								No significant difference, in both arms QoL tended to improve
								No significant difference between arms
0-100	75.6 [68.4-82.8]		62.5 [49.2-75.8]	61.9 [46.8-78.0]				Decrease in QoL greatest in patients with progressive disease

References

1. Vente MA, Wondergem M, van der Tweel I, van den Bosch MA, Zonnenberg BA, et al. (2009) Yttrium-90 microsphere radioembolization for the treatment of liver malignancies: a structured meta-analysis. Eur Radiol 19: 951-959.
2. Khatri VP, Chee KG, Petrelli NJ (2007) Modern multimodality approach to hepatic colorectal metastases: solutions and controversies. Surg Oncol 16: 71-83.
3. Meropol NJ, Weinfurt KP, Burnett CB, Balshem A, Benson AB, 3rd, et al. (2003) Perceptions of patients and physicians regarding phase I cancer clinical trials: implications for physician-patient communication. J Clin Oncol 21: 2589-2596.
4. Meropol NJ, Egleston BL, Buzaglo JS, Benson AB, 3rd, Cegala DJ, et al. (2008) Cancer patient preferences for quality and length of life. Cancer 113: 3459-3466.
5. Hendlisz A, Van den Eynde M, Peeters M, Maleux G, Lambert B, et al. (2010) Phase III trial comparing protracted intravenous fluorouracil infusion alone or with yttrium-90 resin microspheres radioembolization for liver-limited metastatic colorectal cancer refractory to standard chemotherapy. J Clin Oncol 28: 3687-3694.
6. Van Hazel G, Blackwell A, Anderson J, Price D, Moroz P, et al. (2004) Randomised phase 2 trial of SIR-Spheres plus fluorouracil/leucovorin chemotherapy versus fluorouracil/leucovorin chemotherapy alone in advanced colorectal cancer. J Surg Oncol 88: 78-85.
7. van de Maat GH, Seevinck PR, Elschot M, Smits ML, de Leeuw H, et al. (2012) MRI-based biodistribution assessment of holmium-166 poly(L-lactic acid) microspheres after radioembolisation. Eur Radiol.
8. Smits ML, Elschot M, Van Den Bosch MA, van de Maat GH, van het Schip AD, et al. (2013) Imageable radioactive holmium-166 microspheres for treatment of liver malignancies: *in vivo* dosimetry based on SPECT and MRI. Journal of Nuclear Medicine *[in press]*.
9. Smits ML, Nijsen JF, van den Bosch MA, Lam MG, Vente MA, et al. (2012) Holmium-166 radioembolisation in patients with unresectable, chemorefractory liver metastases (HEPAR trial): a phase 1, dose-escalation study. Lancet Oncol 13: 1025-1034.
10. Smits ML, Nijsen JF, van den Bosch MA, Lam MG, Vente MA, et al. (2010) Holmium-166 radioembolization for the treatment of patients with liver metastases: design of the phase I HEPAR trial. J Exp Clin Cancer Res 29: 70.
11. Blazeby JM, Fayers P, Conroy T, Sezer O, Ramage J, et al. (2009) Validation of the European Organization for Research and Treatment of Cancer QLQ-LMC21 questionnaire for assessment of patient-reported outcomes during treatment of colorectal liver metastases. Br J Surg 96: 291-298.
12. (2001, http://groups.eortc.be/qol/manuals) European Organization for Research Treatment of Cancer. QLQ-C30 Scoring manual. 3rd ed.
13. Osoba D, Rodrigues G, Myles J, Zee B, Pater J (1998) Interpreting the significance of changes in health-related quality-of-life scores. J Clin Oncol 16: 139-144.
14. Cosimelli M, Golfieri R, Cagol PP, Carpanese L, Sciuto R, et al. (2010) Multi-centre phase II clinical trial of yttrium-90 resin microspheres

alone in unresectable, chemotherapy refractory colorectal liver metastases. Br J Cancer 103: 324-331.

15. Mancini R, Carpanese L, Sciuto R, Pizzi G, Golfieri R, et al. (2006) A multicentric phase II clinical trial on intra-arterial hepatic radiotherapy with ^{90}yttrium SIR-spheres in unresectable, colorectal liver metastases refractory to i.v. chemotherapy: preliminary results on toxicity and response rates. In Vivo 20: 711-714.
16. Kalinowski M, Dressler M, Konig A, El-Sheik M, Rinke A, et al. (2009) Selective internal radiotherapy with Yttrium-90 microspheres for hepatic metastatic neuroendocrine tumors: a prospective single center study. Digestion 79: 137-142.
17. Gray B, Van Hazel G, Hope M, Burton M, Moroz P, et al. (2001) Randomised trial of SIR-Spheres plus chemotherapy vs. chemotherapy alone for treating patients with liver metastases from primary large bowel cancer. Ann Oncol 12: 1711-1720.
18. Salem R, Gilbertsen M, Butt Z, Memon K, Vouche M, et al. (2013) Increased Quality of Life Among Hepatocellular Carcinoma Patients Treated with Radioembolization, Compared with Chemoembolization. Clin Gastroenterol Hepatol.
19. Steel J, Baum A, Carr B (2004) Quality of life in patients diagnosed with primary hepatocellular carcinoma: hepatic arterial infusion of Cisplatin versus 90-Yttrium microspheres (Therasphere). Psychooncology 13: 73-79.
20. Au HJ, Karapetis CS, O'Callaghan CJ, Tu D, Moore MJ, et al. (2009) Health-related quality of life in patients with advanced colorectal cancer treated with cetuximab: overall and KRAS-specific results of the NCIC CTG and AGITG CO.17 Trial. J Clin Oncol 27: 1822-1828.
21. Aaronson NK, Ahmedzai S, Bergman B, Bullinger M, Cull A, et al. (1993) The European Organization for Research and Treatment of Cancer QLQ-C30: a quality-of-life instrument for use in international clinical trials in oncology. J Natl Cancer Inst 85: 365-376.

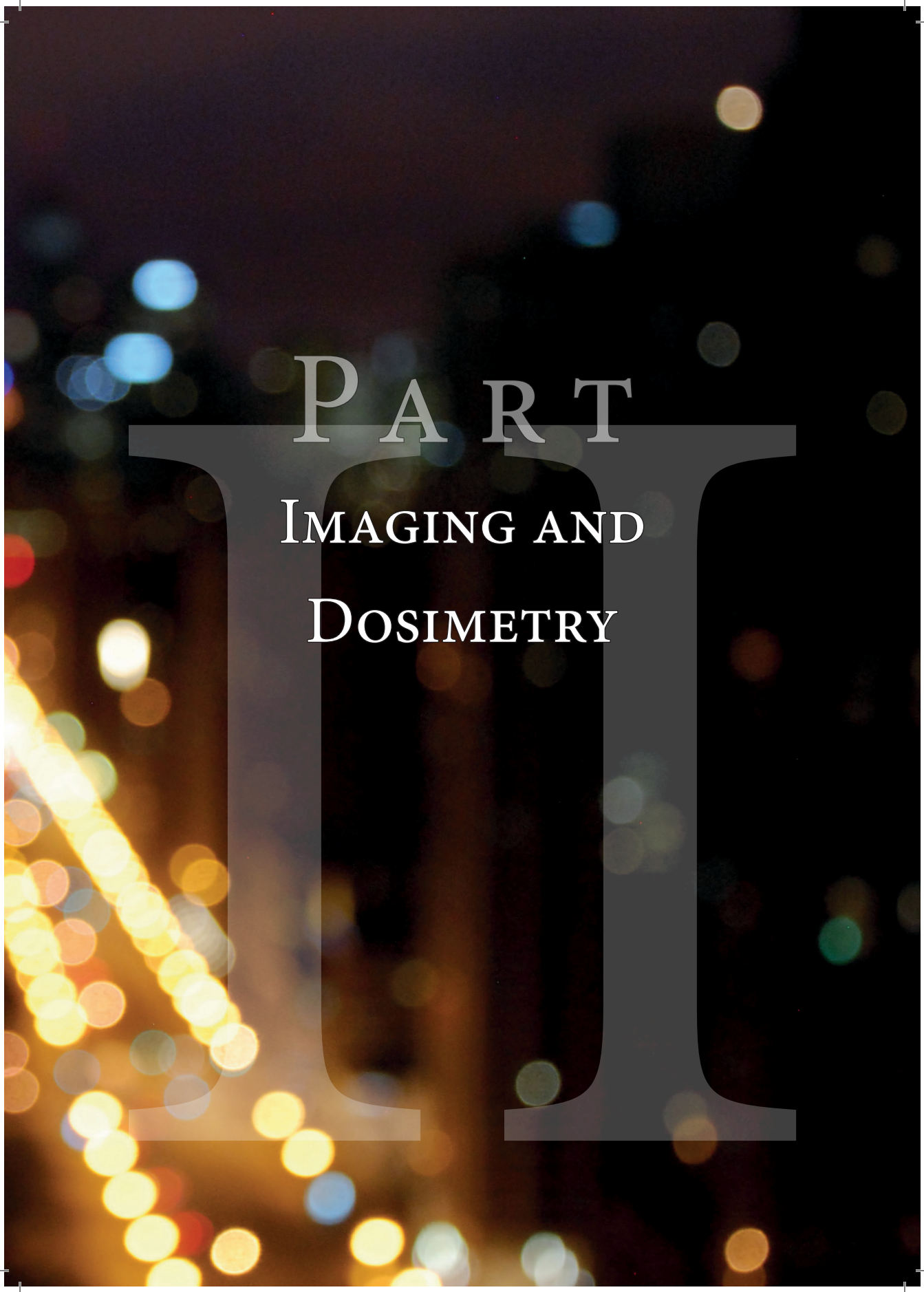

Part II

Imaging and Dosimetry

Chapter 7

Developments in radioembolization dosimetry

MLJ Smits, M Elschot, JFW Nijsen, HWAM de Jong,
MAAJ van den Bosch, MGEH Lam

Manuscript draft

While the worldwide treatment of liver malignancies with yttrium-90 radioembolization (^{90}Y-RE) is rapidly growing, methods for calculating the activity to be administered are largely based on empirical toxicity and efficacy analyses, rather than organ-specific dosimetry. At the same time, it is recognized that treatment planning based on proper dosimetry is of vital importance for the optimization of RE. The heterogeneous and often clustered intra-hepatic biodistribution of millions of point-source radioactive particles poses a challenge for dosimetry. Several studies found a relationship between absorbed doses and treatment outcome, with regard to both toxicity and efficacy. This should ultimately lead to improved patient selection and individualized treatment planning. New calculation methods, imaging techniques and a new generation microspheres for image-guided RE all contribute to these improvements. The aim of this review is to give insight in the latest and most important developments on RE dosimetry, and give future directions on patient selection, individualized treatment planning and study designs.

Introduction

Yttrium-90 (^{90}Y) radioembolization (RE) is an established treatment modality for chemotherapy resistant, unresectable liver malignancies.[1-3] The radioisotope ^{90}Y (average beta energy 0.93 MeV; half-life 2.67 days; maximum tissue range 11 mm) is either labeled to resin microspheres (SIR-Spheres®, Sirtex Medical Limited, Lane Cove, Australia) or incorporated in glass microspheres (TheraSphere®, BTG International Ltd., London, UK). After injection in the hepatic artery these microspheres lodge in the capillaries around the tumors and deliver high local radiation absorbed doses, while largely sparing the normal liver parenchyma.[4]

^{90}Y activity calculation is largely based on empirical grounds only. Although the safety and efficacy of RE using these methods have been sufficiently proven, the observed toxicity in some patients, and the lack of response in other patients, challenge their validity. It is crucial for optimal treatment to be able to predict the absorbed dose to the tumor and the absorbed dose to the healthy liver. This knowledge should lead to individualized treatment planning and improved patient selection.

Image-based dosimetry may be performed before the actual treatment, during treatment, or after treatment. The timing of dosimetry has different implications for the key factors of accurate image-based dosimetry, which include the used device, the imaging technique and the calculation methods. Substantial progress has been made in each of

these areas over the last years. The aim of this review is to summarize current status, limitations, developments and future directions for radioembolization dosimetry.

Pre-treatment dosimetry

Scout dose

Before every RE procedure, a preparatory angiography is performed to map the anatomy of the patient, to coil-embolize non-target vessels arising close to the injection site, and to administer a scout dose.[5] Since ^{90}Y emits no direct gamma-radiation it is less suitable for low activity scout dose imaging. Relatively high activity is needed to accurately quantify the ^{90}Y biodistribution. Instead, the surrogate technetium-99m macroalbumin aggregates (^{99m}Tc-MAA) are used for this purpose, and single photon emission computed tomography (SPECT) combined with CT is the preferred modality to determine the exact intra- and extrahepatic biodistribution of ^{99m}Tc-MAA. Its use is three fold. First it is used to exclude any extrahepatic deposition of activity in organs other than the lungs, second it can be used to calculate the hepatopulmonary shunt as a percentage of the administered activity, and third, its intrahepatic biodistribution may be used for treatment planning.[6]

A ^{99m}Tc-MAA scout dose is currently the preferred method to exclude extrahepatic deposition in non-target organs such as the stomach, duodenum or pancreas. Extrahe-

patic distribution can also be detected on c-arm CT. The benefit of using c-arm CT is that the extrahepatic distribution can be corrected immediately and no additional angiographies are needed to coil-embolize the culprit vessel. For this reason, some centers ceased to rely on ^{99m}Tc-MAA to exclude extrahepatic deposition and coil-embolize non-target vessels during the treatment angiography, right before microsphere injection. The advantage is that vessels can then be coil-embolized shortly before treatment, which decreases the chance of formation of new non-target collaterals.[7] ^{99m}Tc-MAA is then merely used to predict the lung shunt fraction.

Calculation of the hepatopulmonary shunt is performed in every patient in order to exclude the deposition of a toxic amount of activity in the lungs, which can lead to radiation pneumonitis.[8,9] The accuracy of ^{99m}Tc-MAA in this aspect is however uncertain. A recent study showed that the lung shunt fraction for radioembolization is largely overestimated, even on ^{99m}Tc-MAA-SPECT.[10] As a result, many patients receive an unjustified dose reduction or don't receive treatment at all. For this reason and other reasons, there are ongoing efforts to develop surrogate particles other than ^{99m}Tc-MAA, which are discussed later on in this article.

If the ^{99m}Tc-MAA scout dose confirms a patient's eligibility for RE (*i.e.* no extrahepatic deposition of ^{99m}Tc-MAA and an acceptable lung shunt fraction), the scout dose may also be used for treatment planning. Some centers deny RE to patients whenever the activity concentration in the tumor is low in comparison with non-tumorous areas. The rationale behind this strategy is that this means less treatment benefit and an increased risk of liver toxicity.[11,12] The different methods for activity planning and the role of intrahepatic biodistribution of ^{99m}Tc-MAA for activity planning are discussed below.

Activity planning: BSA method

In early clinical studies, the used activity ranged between 2 – 3 GBq depending on the metastatic tumor load (the so-called 'empirical' method), but this method was soon abandoned after clinically observed toxicity.[13] A patient with a large metastatic tumor load but a small overall liver size developed radioembolization-induced liver disease (REILD). The 'body surface area (BSA)' method was subsequently developed to overcome this problem, because it is known that BSA correlates with liver volume and thus the administered activity could be corrected for liver volume without the need for assessing the liver volume on cross-sectional imaging.[14] This is currently the preferred method for calculating the prescribed activity in patients with multiple liver metastases who are treated with resin microspheres.[15,16]

The standard BSA formula for resin microspheres is based on BSA and liver tumor involvement, and the fraction of the total liver volume involved by tumor:[16]

Eq. 1 $$Prescribed\ activity\ (GBq)\ =\ (BSA\ (m^2) - 0.2) + \frac{tumor\ involvement\ (\%)}{100}$$

In the case of a significant shunt to the lungs the prescribed activity is reduced (10 – 15% shunt fraction; 20% activity reduction; 15 – 20% shunt fraction: 40% activity reduction; > 20% shunt fraction: no treatment). The BSA method leads to considerable inter-patient variation in absorbed doses. While BSA may be related to liver weight in healthy persons, this is not necessarily the case in patients with liver tumors. As a result, treatment planning according to the BSA-based method (*Eq. 1*) leads to inconsistent liver absorbed doses. Large patients with small livers will receive relatively high doses on the liver and vice versa (*Figure 1*).

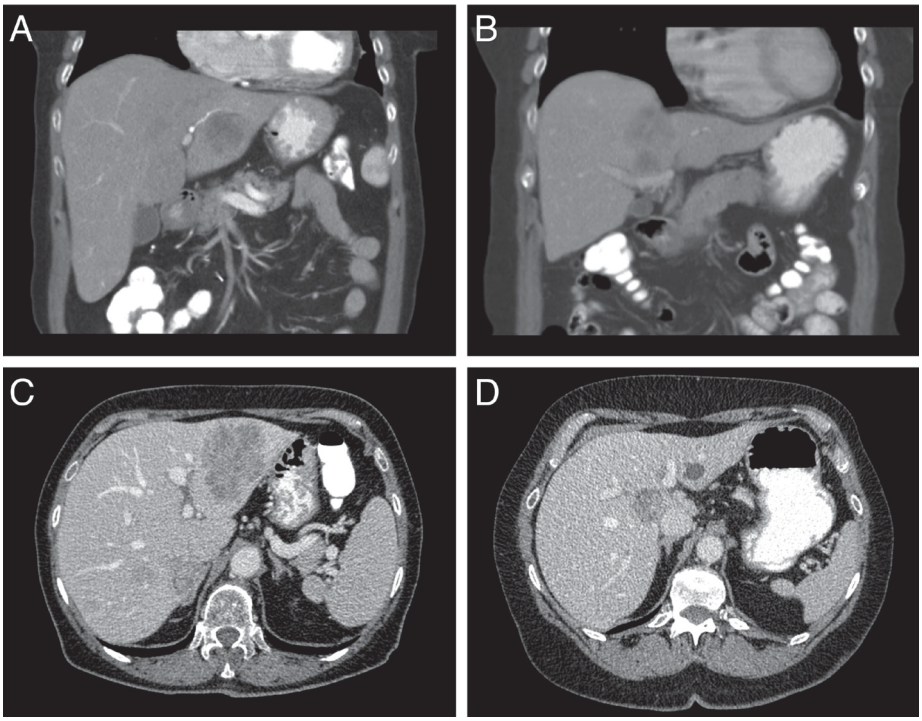

Figure 1. *The BSA-based activity calculation method does not take the target volume into account, leading to a wide variation in absorbed target doses. A small patient (BSA 1.62) with a large liver (1963 mL)(A and C) versus a large patient (BSA 2.02) with a small liver (1558 mL)(B and D). The former patient (panel A and C) received 1554 MBq resulting in a mean target absorbed dose of 40 Gy, while the latter patient (panel B and D) received 1872 MBq resulting in a mean target absorbed dose of 60 Gy.*

Activity planning: MIRD method

Activity calculation for glass microspheres is based on an estimation of the mean absorbed dose in the target liver volume.[17] It uses a simplified calculation method derived from the MIRD equations for dose calculation.[18] An absorbed dose of 50 Gy per GBq per kilogram tissue is used with assumptions of homogeneous intrahepatic microsphere distribution and absorption of all the administered activity and energy in the liver, using the following formula:

Eq. 2 $$Prescribed\ activity\ (GBq) = \frac{Desired\ dose\ (Gy) \times M_{Target}\ (kg)}{50\ (J/GBq)}$$

where M_{Target} is the mass of the target volume. The desired dose may range from 80 – 120 Gy depending on the clinical judgment of the treating physician. The lung dose should not exceed 30 Gy (or 50 Gy for repeated treatment), which, with the above mentioned assumptions and an assumed lung mass of 1 kg, is equivalent to an absolute hepatopulmonary shunt of approximately 600 MBq of ^{90}Y-microspheres.[17,19]

The method used for glass microspheres (*Eq. 2*) is based on estimations of this whole liver absorbed dose.[17] The treating physician may prescribe an amount of activity based on a desired absorbed dose, which depends on the patient's clinical status. Although this seems to be scientifically sound, the intrahepatic biodistribution varies per patient and thus the dose to tumor and healthy liver can vary between patients as well. The method (*Eq. 2*) is particularly useful for so-called radiation lobectomy.[20] Patients with extensive disease in a limited part of the liver may be treated with supra-therapeutic absorbed doses to a limited target volume that will ablate both the tumor and the normal liver parenchyma within that target volume, while sparing the untreated part of the liver.

The large majority of treatment centers use these two methods, depending on the microspheres used. Glass microspheres are mostly used to target only a part of the liver, whereas resin microspheres are more frequently used to target the entire liver.[21] Furthermore, the number of the resin microspheres is higher, and the specific activity is lower, than glass microspheres.[22] It is not fully understood whether this leads to a different mechanism of action (*i.e.* more embolic effect) than that of glass microspheres, with possibly a different tolerance for radiation. It has been recognized that especially the BSA method has some distinct disadvantages because it artificially limits the injected activity between 1-3 GBq, and because the desired activity in cases of high hepatopulmonary shunting is adjusted empirically using standard reference tables provided by the manufacturer.[23] Both methods fail to account for the absorbed dose to the tumor and the normal liver compartment and therefore lack a sound scientific basis.

Activity planning: Partition model

A huge step forward with regard to dosimetry was the development of the 'partition' method.[24-26] This method involves selecting safe absorbed doses to the normal liver and lung and implanting the maximum activity that does not exceed these limits. The tumor and normal liver compartments are in general delineated on anatomical imaging modalities, and the anticipated activity in these compartments is calculated on scout dose SPECT imaging using ^{99m}Tc-MAA, which is injected during preparatory angiography 1 – 2 weeks prior to treatment. The ratio between the activity concentrations in the tumor and normal liver compartments ($R_{T/N}$) is calculated as:

Eq. 3 $$R_{T/N} = \frac{A_{Tumor}\ (GBq)/M_{Tumor}\ (kg)}{A_{Normal\ liver}\ (GBq)/M_{Normal\ liver}\ (kg)}$$

where A is the activity in GBq and M is the mass of the compartment in kg. Subsequently the prescribed activity may be calculated as:

Eq. 4 $$Prescribed\ activity\ (GBq) = \frac{D_{Normal\ liver}\ (Gy) \times R_{T/N} \times M_{Tumor}\ (kg) + M_{Normal\ liver}\ (kg)}{50\ (J/GBq) \times (1 - LSF)}$$

where $D_{Normal\ liver}$ is the maximum desired absorbed dose to the normal liver in Gy, $R_{T/N}$ follows from *Eq. 3*, and LSF is the lung shunt fraction. The partition method is derived from the glass microspheres method (*Eq. 2*). Importantly, it adjusts for the difference between absorbed dose to the tumor and the normal liver (T/N). The partition model may unfortunately only be used in highly selected patients with a low number of well-delineated tumors, which constitute a mere minority of patients with liver metastasis.[15,16] Therefore, the partition model is still not routinely used today.[15,16]

Several studies have sought to validate the partition model by investigating the relationship between the amount of ^{99m}Tc-MAA-activity in the tumor(s) and the tumor response or survival after treatment. *Table 1* provides an overview of the literature on this matter. The results of these studies are heterogeneous: four studies found some kind of relationship between dose and response and three studies found no or a very weak relationship. Part of the heterogeneity in study outcomes is the inconsistency in the methods used to quantify activity distribution and the volume of the compartments. One study even used a volume of interest drawn over a 'normal' region to extrapolate the found values and calculate the dose on the entire healthy liver.[27] Combining the limited number of available studies on this matter, there is no convincing evidence that there is a strong dose-response relationship based on ^{99m}Tc-MAA-activity in the tumor(s), especially not for metastatic patients.

Table 1. *Studies evaluating pre-treatment tumor dosimetry and dose-response relationship.*

Study design and methods	Dhabuwala *et al.*, 2005	Gulec *et al.*, 2007
No. patients	58	40
Primary tumor	CRCLM	CRCLM (n=15), NET (n=10), HCC (n=5), breast cancer (n=4), lung cancer (n=2), ovarian cancer (n=1)
Treatment	^{90}Y-RE, resin microspheres, via laparotomy	^{90}Y-RE, resin microspheres
Method for activity planning	Empirical method	Empirical or BSA method
Modality used for dosimetry	^{99m}Tc-MAA planar scintigraphy	^{99m}Tc-MAA SPECT
Modality for response assessment	CT and CEA values in blood	CT, 3 months post therapy
Response evaluation method	Self-defined criteria	RECIST
Toxicity evaluation method	n.a.	CTCAE v.3
Study outcomes		
Tumor dose, median (range) or mean ± SD	n.r.	121.5 ± 85.6 Gy
Normal liver dose, median (range) or mean ± SD	n.r.	17.2 ± 18.6 Gy
T/N ratios, median (range)	n.r.	n.r. (2.9 - 15.4)
Dose-response relationship	-	+/-
	T/N ratio correlated poorly with CEA levels (r^2= 0.004)	Responders had a median tumor dose of 107.8 Gy and nonresponders 76.9 Gy
Dose-survival relationship	-	n.a.
	No significant difference in survival between patients with high or low ^{99m}Tc-MAA tumor uptake	
Dose-toxicity relationship	n.a.	-
		liver function tests abnormalities did not correlated with liver dose

** as calculated from Table 1 in Campbell et al. ** probably overlapping patient cohorts between Chiesa et al., and Mazzaferro et al. ***Tumor threshold dose >205 Gy and healthy liver dose <120 Gy. BSA = body surface area; ^{90}Y = yttrium-90; RE = radioembolization; n.r. = not reported; SPECT = single photon emission computed tomography; PET = positron emission tomography; FDG = fluorodeoxyglucose; SUV = standardized uptake value; WHO = world health organization; RECIST = response evaluation criteria in solid tumors; EASL = European association for the study of the liver; CTCAE = common terminology criteria for adverse events; n.a. = not applicable; T/N ratio = tumor-to-non-tumor ratio; ^{99m}Tc-MAA = technetium-99m macroalbumin aggregates; CEA = carcinoembryonic antigen.*

Table 1. *Continued I.*

Flamen *et al.*, 2008	Campbell *et al.*, 2009	Ulrich *et al.*, 2013
8	12	66
CRCLM	CRCLM	CRCLM
^{90}Y-RE, resin microspheres	^{90}Y-RE, resin microspheres	^{90}Y-RE, resin microspheres
BSA method	n.r.	n.r.
^{99m}Tc-MAA SPECT	^{99m}Tc-MAA SPECT	^{99m}Tc-MAA SPECT
^{18}F-FDG-PET	^{18}F-FDG-PET, approx. 3 months post therapy	MRI, 6 weeks and 3 months post therapy
Total lesion glycolysis	Mean SUV	RECIST v1.1
n.a.	n.a.	n.a.
37 ± 25 Gy	150 Gy (85 - 340 Gy)*	n.r.
mean 27 Gy, 95% CI 22-33 Gy	35 Gy (23 - 53 Gy)*	n.r.
n.r.	4.2 (2.9 - 9.4)*	n.r.
-	+/-	-
T/N ratio >1 indicated tumor response (89% sensitivity and 65% specificity). Poor linear relation between tumor dose and response (r^2= 0.26)	Dose and response correlated with linear coefficients (r) ranging from 0.43 - 0.60	Response to ^{90}Y was independent of ^{99m}Tc-MAA uptake in the tumor. Tendancy towards inverse relationship.
n.a.	n.a.	n.a.
n.a.	n.a.	n.a.

Table 1. *Continued II.*

Study design and methods	Garin *et al.*, 2013	Mazzaferro *et al.*, 2013
No. patients	71	52
Primary tumor	HCC	HCC
Treatment	^{90}Y-RE, glass microspheres	^{90}Y-RE, glass microspheres
Method for activity planning	Mean absorbed liver dose 120 ± 20 Gy and lung dose <30 Gy or boosting method***	Mean absorbed liver dose 120 and lung dose <30 Gy
Modality used for dosimetry	^{99m}Tc-MAA SPECT/CT	^{99m}Tc-MAA SPECT
Modality for response assessment	CT, every 3 months	
Response evaluation method	EASL	RECIST, WHO and EASL
Toxicity evaluation method	CTCAE v.4	n.a.
Study outcomes		
Tumor dose, median (range) or mean ± SD	342 ± 116 Gy (responding lesions) and 191 ± 89 Gy (non-responding lesions)	387 Gy (24 - 1,478 Gy)
Normal liver dose, median (range) or mean ± SD	76 ± 35 Gy	n.r.
T/N ratios, median (range)	n.r.	n.r.
Dose-response relationship	+	+
	Tumor dose of >205 Gy indicated tumor response (100% sensitivity and 90% accuracy)	Correlation between response and tumor dose (r = 0.60). Tumor dose of >500 Gy indicated response (AUC 0.78)
Dose-survival relationship	+	n.a.
	Median survival was 23.2 months (if tumor dose >205 Gy) vs. 11.5 months (<205 Gy), tumor dose correlated with survival p=0.04	
Dose-toxicity relationship	+	+
	Healthy liver dose ≥ 120 Gy and hepatic reserve <30% is predictive of toxicity (p<0.0001)	A healthy liver dose of >70 indicates liver decompensation (75% sensitivity and 75% specificity)**

** as calculated from Table 1 in Campbell et al. ** probably overlapping patient cohorts between Chiesa et al., and Mazzaferro et al. ***Tumor threshold dose >205 Gy and healthy liver dose <120 Gy. BSA = body surface area; ^{90}Y = yttrium-90; RE = radioembolization; n.r. = not reported; SPECT = single photon emission computed tomography; PET = positron emission tomography; FDG = fluorodeoxyglucose; SUV = standardized uptake value; WHO = world health organization; RECIST = response evaluation criteria in solid tumors; EASL = European association for the study of the liver; CTCAE = common terminology criteria for adverse events; n.a. = not applicable; T/N ratio = tumor-to-non-tumor ratio; ^{99m}Tc-MAA = technetium-99m macroalbumin aggregates; CEA = carcinoembryonic antigen.*

Functional segmentation

Unfortunately, most patients presented for radioembolization have multiple tumors distributed over the whole liver, which hinders accurate segmentation of all tumors and direct registration with ^{99m}Tc-MAA distribution. A new method was recently introduced to overcome this problem.[28] This method involves a second SPECT scan after intravenous injection of ^{99m}Tc-MAA sulfur colloid (^{99m}Tc-SC; 185 MBq) directly following conventional ^{99m}Tc-MAA SPECT imaging (37 MBq). Sulfur colloid is used as a biomarker for normal hepatic reticulo-endothelial tissue, and its distribution can be visualized with a second SPECT shortly after the ^{99m}Tc-MAA SPECT. The absorbed dose to functional liver tissue is estimated by calculation of ^{99m}Tc-MAA activity in regions with ^{99m}Tc-SC uptake. Similarly, the tumor-absorbed dose is predicted by calculation of ^{99m}Tc-MAA activity in voxels without ^{99m}Tc-SC uptake. In an early feasibility study, toxicity correlated significantly with SPECT-based calculation of the absorbed dose to functional liver tissue.28 In addition, SPECT-based calculation of the tumor absorbed dose correlated with radiographic response, decrease in serum CEA and overall survival. Patients receiving a tumor absorbed dose > 55 Gy had a median survival of 32.8 months compared to 7.2 months in patients who received < 55 Gy. This method offers a physiology-based functional imaging tool for hepatic RE treatment. It appears to be a robust prognostic tool for patients with multiple tumors requiring whole-liver treatment, and may lead to improved individualized treatment planning.

Multiple injection positions

Currently only about 14% of patients is treated with a single administration in the proper or common hepatic artery. The vast majority receives treatment from two or more injection sites.[29] The prescribed activity needs to be split proportionally to the volume of the perfused areas. There are several methods for calculating these proportions. The proportional volume of the right and left liver lobe can be assessed by manual delineation on CT or MRI, dividing the activity accordingly.[30] However, this assessment is complicated by the variable vascular anatomy in the liver. For instance, the middle hepatic artery supplying segment IV, may originate from the left or the right hepatic artery.[31] The patient-specific arterial anatomy needs to be taken into account for delineation of the liver lobes. A more sophisticated method has been presented by Kao *et al.*, who developed an artery-specific method by calculating the volume of each flow area on c-arm CT with selective contrast injection from each injection position for treatment.[32] The regular use of contrast-enhanced c-arm CT during work-up angiography for RE is not only useful to determine the target volume, but also to ascertain that the tumors are sufficiently targeted.[33,34] Sections of the liver or tumors that are not supplied by the catheterized vessel can be recognized and acted upon. However, contrast reaching a tumor does not guarantee that microspheres will reach and completely cover that tumor as well.[35]

Developments in pre-treatment dosimetry

An ideal surrogate particle for pre-treatment dosimetry follows a distribution pattern that is very similar to the distribution pattern of the microspheres used for treatment. This seems not the case for ^{99m}Tc-MAA and ^{90}Y-microspheres, which may be due to differences in the size, number, density, and morphology of ^{99m}Tc-MAA and ^{90}Y-microspheres (*Figure 2*). A recent study showed that substantial differences exist between intrahepatic ^{99m}Tc-MAA distribution and subsequent ^{90}Y distribution.[36] In that study, a total of 39 procedures (225 segments according to Bismuth's modification of Couinaud's liver segmentation) in 31 patients were included for analysis (see Chapter 8 of this thesis).[36] A difference of >10%, >20% and >30% of the mean activity per mL was found in respectively 153 / 224 (68%), 97 / 224 (43%), and 72 / 224 (32%) segments. In every single ^{99m}Tc-MAA-procedure, at least 1 segment showed an under- or overestimation of 10%. The mismatch between ^{99m}Tc-MAA and ^{90}Y distribution can increase by a

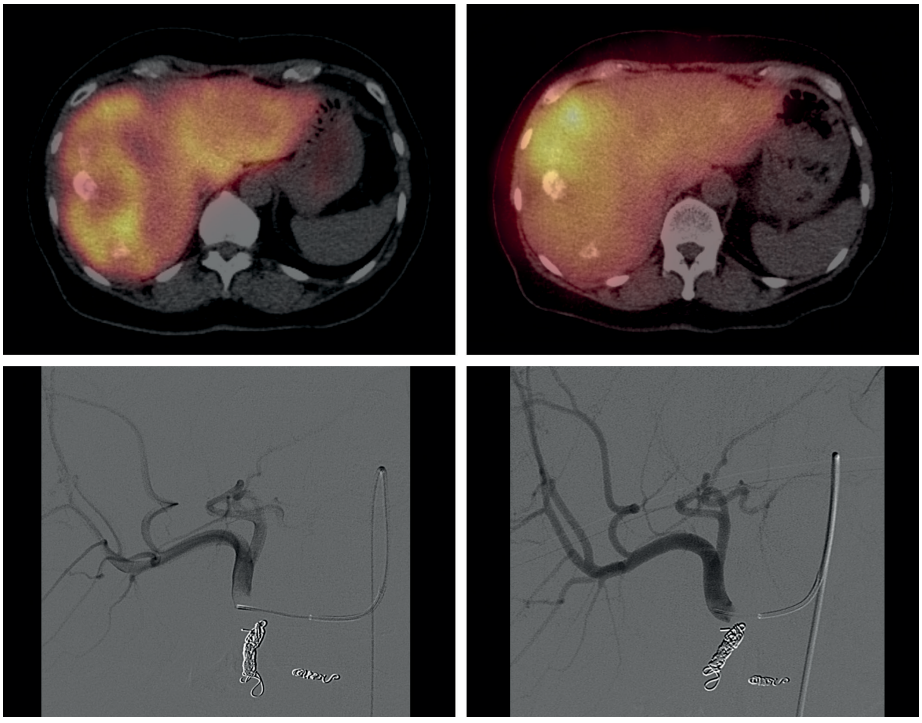

Figure 2. *Example of intrahepatic biodistribution mismatch between technetium-99m macroalbumin aggregates (A) and resin yttrium-90 microspheres (B) while the catheter positions for both injections were similar (C and D, respectively).*

mismatch in catheter tip position, by injections close to bifurcations, and by injections in the main hepatic artery.[36, 37]

Further optimization may be reached with a scout dose other than ^{99m}Tc-MAA. Differences in the size, number, density, size, and morphology between ^{99m}Tc-MAA and ^{90}Y may result in a different activity distribution.[38] The number of ^{99m}Tc-MAA particles used to predict the biodistribution (1-2 x10^5 particles) is significantly lower than the number of ^{90}Y microspheres applied (resin: 30-60 x10^6; glass: 4-5 x10^6 particles), while the density of ^{99m}Tc-MAA particles (1.1 g/mL) is lower than that of ^{90}Y microspheres (resin: 1.6 g/mL; glass: 3.3 g/mL).[39] The particle size distribution of ^{99m}Tc-MAA is such that over 90% are within 10 – 90 μm in size (mean 15 μm). No particles have a greater size than 150 μm. The average number of ^{90}Y-microspheres (typically tens of millions) outnumbers the average number of MAA particles (1-2 million). The mean size of ^{90}Y microspheres is 32 ± 10 μm, while also the morphology of the spherical ^{90}Y microspheres is considerably different than the macro-aggregated random shape of ^{99m}Tc-MAA particles.[39] The embolization effect of the much larger number of ^{90}Y-microspheres may result in flow alterations that may alter the distribution of the particles.[36,40]

Researchers have sought to develop a particle that is rheologically identical to the radioactive microspheres used for treatment. ^{99m}Tc-albumin spheres have been developed for this purpose (ROTOP-HAS microspheres B20, Rotop Pharmaka, Dresden, Germany). Just like ^{99m}Tc-MAA, these particles consist of ^{99m}Tc labeled to albumin, but are shaped spherically to better mimic the ^{90}Y-microspheres. The predictive value of these microspheres before ^{90}Y-radioembolization is currently under investigation.[41] Selwyn *et al.* developed a positron-emitting resin microsphere labeled with ^{18}F that showed promising results regarding labeling efficiency and imaging capabilities.[42] The in vivo stability was, however, insufficient with significant leaching of ^{18}F from these microspheres (15% in 45 min). Another particle that was already applied in human patients is a holmium-166 (^{166}Ho) loaded poly(L-lactic acid) microsphere. These microspheres have been developed as a new generation microspheres for image-guided radioembolization.[43] The radioisotope ^{166}Ho emits high-energy beta particles, used for tumor destruction, and gamma radiation, which allows for nuclear imaging (half-life 27 hours; gamma energy 81 keV; maximum beta energy 1.8 MeV). Holmium is also a highly paramagnetic and radiopaque metal, and as such can be visualized on MRI and CT.[44,45] Prior to administration of the therapeutic dose a small scout dose of ^{166}Ho-microspheres may be instilled to predict the distribution of the therapeutic dose. Since the particles in the scout dose are physically identical to the particles of the therapeutic dose, the biodistribution is expected to be more similar.

Post-treatment dosimetry

Although in most centers post-treatment dosimetry is not routinely performed, it may be useful for optimization of the toxicity profile and the efficacy of RE treatment. Deposition of a fraction of the total administered activity in non-target organs can lead to serious complications, such as radiation pneumonitis and gastro-intestinal ulceration.[46] Early detection of possible extrahepatic activity, *i.e.* before the patient starts to exhibit adverse effects, can therefore be life saving. Besides, the intrahepatic biodistribution may predict toxicity and the risk of developing REILD.[47,48] An unfavorable intrahepatic distribution with a relatively high radiation dose to the healthy-liver tissue (low T/N ratio) might for instance require prophylactic treatment or more intensive monitoring than patients with high T/N ratios.

Second, post-treatment dosimetry can reveal tumors that have not received the planned radiation dose and require additional targeting.[40] Pre-treatment scout dose imaging or contrast-enhanced c-arm CT imaging does not guarantee that microspheres will reach and completely cover the tumor.[35] Therefore, post-treatment dosimetry remains a valuable tool to support treatment planning in selected patients that potentially benefit from a (super-selective) second treatment with radioembolization.[49] At the same time it may prevent unacceptable toxicity whenever repeated treatment is warranted, since it has been shown that patients who receive a second treatment may have an increased risk of REILD (25%).[21]

Lastly, post-treatment dosimetry is key for establishing dose-effect and dose-toxicity relations. This information should support general understanding of the radiobiological mechanisms involved in radioembolization and may elucidate important dosimetric parameters that are related to therapy outcome. Once these parameters are known, they should be included in the pre-treatment dosimetric model for activity planning. To date, there are six studies available that have investigated dose-effect [48,50-54] and/or dose-toxicity relations [48] based on post-treatment images of the microsphere distribution (*Table 2*). Comparing the results of these studies is limited due to the large heterogeneity in terms of the number of patients, the primary tumor types, the methods of treatment, dosimetry and response assessment. Five studies reported a more or less positive dose-response relationship versus one study that did not.

Lau *et al.*, found that a tumor dose of >120 Gy indicated tumor response with an 87% sensitivity and 87% specificity in 18 hepatocellular carcinoma (HCC) patients.[51] The authors did however not use imaging for dosimetry, but instead measured activity at normal liver and tumor sites preoperatively with a beta probe. Wang *et al.* found that a tumor absorbed dose of >90.65 Gy was indicative of tumor response.[52] Radioembolization in this study was performed with phosphorus-32 microspheres in 25 HCC pa-

tients. Walrand *et al.*, who performed ^{90}Y-RE in eight colorectal carcinoma liver metastases patients, found a strong correlation between tumor absorbed dose (corrected for hemoglobin enhancement) and cell survival fraction (r=0.96).[50] The definition given for cell survival fraction was the ratio between the number of living cells just after and before the therapy. Dosimetry was performed with ^{90}Y-positron emission tomography (PET). However, this study was performed in only eight patients and four outlying tumors had to be excluded from the analysis to obtain this correlation. A fourth study, by Strigari *et al.*, with the largest number of patients (n=73 HCC patients), reported that the median tumor absorbed dose was higher for responders than for non-responders.[48] Patients with a complete and partial response according to RECIST had median tumor absorbed doses of 122 Gy and 99 Gy, respectively. Unfortunately, non-quantitative Bremsstrahlung SPECT was used for tumor dosimetry. Kao *et al.* looked at a highly selected group of tumors in 8 out of 25 patients and found that the absorbed dose to 70% of the tumor was in general >100 Gy in HCC patients compared to <100 Gy in case of incomplete response.[54] The only study that did not find a dose-response relationship was performed in metastatic patients who received ^{166}Ho-RE.[53] The number of patients in this study was relatively low (n = 15), but SPECT with a high accuracy for ^{166}Ho-microspheres was used for dosimetry.

In order to optimally establish the dose-response relationship, both dose and response should be measured as accurately as possible. Tumor dosimetry should be performed with accurate quantitative imaging methods and meticulous delineation of all tumors. Response on the other hand, is more subjective. Classic response evaluation methods based on tumor volume or size may not suffice since a lesion may remain visible after treatment even when a tumor is not metabolically active anymore.[55] Functional or metabolic parameters such as diffusion-restriction on MRI or FDG-avidity on PET may be more suitable.[55,56]

The reported minimal tumor absorbed dose to obtain response ranged between 90-120 Gy. This range, however, provides a distorted view of the real biodistribution. In reality, the absorbed dose is not homogeneously distributed in the tumor. It may be more useful to know the minimal dose to a tumor fraction needed for response. Further research using dose-volume histograms should help to establish such parameters for each tumor type and type of microsphere used. Not surprisingly, the evidence for a dose-response relationship based on post-treatment dosimetry (*Table 2*) is stronger than the evidence for a dose-response relationship based on pre-treatment dosimetry (*Table 1*).

Nuclear imaging

Quantitative assessment of ^{90}Y has long been considered impossible, due to the limited quality of the ^{90}Y Bremsstrahlung SPECT images. Recent developments in hard-

Table 2. *Studies evaluating post-treatment tumor dosimetry and dose-response relationship.*

Post treatment dosimetry Study design	Lau *et al.*, 1994	Wang *et al.*, 2010	Strigari *et al.*, 2010	Walrand *et al.*, 2012	Kao *et al.*, 2013	Smits *et al.*, 2013
No. patients	18	25	73	8	8 (selection)	15
Primary tumor	HCC	HCC	HCC	Colorectal carcinoma (n=6), Melanoma (n=2)	HCC (n=6), Cholangiocarcinoma (n=1), Adrenal GIST (n=1)	Colorectal carcinoma (n=6), Ocular melanoma (n=6), Cholangiocarcinoma (n=2), Breast carcinoma (n=2)
Treatment	^{90}Y-RE, resin microspheres, via laparotomy	^{32}P-RE + TACE	^{90}Y-RE, resin microspheres	^{90}Y-RE, microsphere type n.r.	^{90}Y-RE, resin microspheres	^{166}Ho-RE
Activity calculation	n.r.	n.r.	Body surface area method	n.r.	n.r.	Aimed whole liver absorbed doses of 20 - 80 Gy
Dosimetry	Per-operative beta probe measurements and liver biopsies	^{32}P-Bremsstrahlung SPECT	^{90}Y-Bremsstrahlung SPECT	^{90}Y-PET	^{90}Y-PET	^{166}Ho-SPECT
Modality used for assessing tumor response	CT, 2, 4, 6, and 12 months post therapy	n.r.	CT, 4-8 months post treatment	FDG-PET, 6.8 weeks (median) post treatment	n.r.	CT, 6- and 12 weeks post treatment

Table 2. *Continued I*

Post treatment dosimetry Study design	Lau *et al.*, 1994	Wang *et al.*, 2010	Strigari *et al.*, 2010	Walrand *et al.*, 2012	Kao *et al.*, 2013	Smits *et al.*, 2013
Response evaluation method	self-defined criteria	WHO	RECIST and EASL	Tumor metabolic ratio using SUV	RECIST	RECIST v1.1
Toxicity evaluation method	n.a.	n.a.	CTCAE v.4	n.a.	CTCAE v.4	n.a.
Study outcomes						
Tumor dose, median (range) or mean ± SD	n.r.	137.42 ± 56.69 Gy (63.70 - 245.00 Gy)	60.0 Gy/GBq (13.1 – 251.4 Gy/GBq)	131.3 Gy (39.6 – 172.2 Gy)*	n.r.	43.7 Gy (13.2 - 64.9 Gy)
Median normal liver dose, median (range) or mean ± SD	n.r.		18.4 Gy/GBq (3.2 – 50.0 Gy/GBq)	n.r.	n.r.	20.7 Gy (7.1 - 54.3 Gy)
T/N ratios, median (range) or mean ± SD	n.r.	3.30 ± 0.91 (1.9 - 5.8)	2.7 (1.7 - 6.0)	n.r.	n.r.	1.4 (0.9 - 2.8)
Dose-response relationship	+ Tumor dose of >120 Gy (on all tumors) indicated tumor response (87% sensitivity and 87% specificity)**	+ Tumor dose of >90.65 Gy indicates tumor response (74% sensitivity and 50% specificity)	+/- Median mean tumor dose was higher for responders than non-responders	+ Correlation between cell survival fraction and tumor dose corrected for hemoglobin enhancement factor (r = 0.96)	+ For HCC, response generally occurs at a tumor dose D_{70} of >100 Gy. Incomplete response generally at D70 <100 Gy	- Poor correlation between mean tumor dose and response (r^2=0.09 at 6 weeks and r^2=0.04 at 12 weeks)

Table 2. *Continued II*

Post treatment dosimetry Study design	Lau *et al.*, 1994	Wang *et al.*, 2010	Strigari *et al.*, 2010	Walrand *et al.*, 2012	Kao *et al.*, 2013	Smits *et al.*, 2013
Dose-survival relationship	+ Median survival was 55.9 weeks (if tumor dose >120 Gy) vs. 26.2 weeks (<120 Gy), p=0.005	+ Median survival was 21 months (if dose >90.65 Gy) vs. 12 months (if dose <90.65 Gy)	n.a.	n.a.	n.a.	n.a.
Dose-toxicity relationship	n.a.	n.a.	+ Healthy-liver-TD_{50} =52 Gy, whole-liver BED_{50}= 93 Gy	n.a.	n.a.	n.a.

*HCC = hepatocellular carcinoma; GIST = gastrointestinal stromal tumor; ^{90}Y = yttrium-90; ^{32}P = phosphorus-32; ^{166}Ho = holmium-166; TACE = transarterial chemoembolization; RE = radioembolization; n.r. = not reported; SPECT = single photon emission computed tomography; PET = positron emission tomography; FDG = fluorodeoxyglucose; SUV = standardized uptake value; WHO = world health organization; RECIST = response evaluation criteria in solid tumors; EASL = European association for the study of the liver; CTCAE = common terminology criteria for adverse events; n.a. = not applicable; T/N ratio = tumor-to-non-tumor ratio; TD_{50} = tolerance dose with 50% complication probability; BED_{50} = biologic effective dose with 50% complication probability; D_{70} = minimum dose to 70% tumor volume. * The mean tumor doses were calculated for each individual patient from the mean tumor doses and tumor volumes as reported in Table 1 of the study by Walrand et al.[50] ** Estimated sensitivity and specificity based on provided numbers in the article.*

ware and image reconstruction software, however, have paved the way for quantitative ^{90}Y-PET and ^{90}Y-Bremsstrahlung SPECT imaging.

The wide range (0 – 2.3 MeV) and continuous nature of the Bremsstrahlung photon energy spectrum complicate quantification of the local ^{90}Y activity with the reconstruction software that is currently available in the clinic [57]: the absence of a photopeak prohibits the use of simple energy window-based scatter rejection and correction techniques and hinders attenuation correction based on a single photon energy. Furthermore, compensation for penetration of high-energy photons through the collimator septa is required for accurate resolution recovery.[58] With more elaborate reconstruction software, however, quantitative ^{90}Y bremsstrahlung SPECT imaging is possible, as was demonstrated by Rong *et al.* [59] and Elschot *et al.*.[60] These methods incorporate energy-dependent models of the scatter and attenuation effects in the patient, and of the photon interactions in the collimator-detector system in the iterative reconstruction algorithm.

^{90}Y has long been considered a pure beta-emitter by the Nuclear Medicine community, despite the fact that the very low branch leading to positron emission (32 times per million decays) was already discovered in 1955.[61,62] It was not until the introduction of the latest generation of 3D PET/CT scanners with Time Of Flight (TOF) technology that the feasibility of ^{90}Y-PET was demonstrated.[40] An advantage of ^{90}Y-PET over Bremsstrahlung SPECT is that advanced correction techniques for scatter, random, and attenuation effects are clinically available and can be directly applied.[40,57,63] Moreover, PET has a higher resolution than SPECT, because a mechanical collimator is not required, which results in better quantification of the ^{90}Y activity in small lesions.[57,60] A disadvantage of ^{90}Y-PET is the very low count rate, which results in images that are prone to deterioration by Poisson noise. The minimum detectable activity on ^{90}Y-PET images was estimated to be 1 MBq ml^{-1} by Carlier *et al.*.[64] Although this is probably good enough for intrahepatic dosimetry in most patients, it impedes for instance detection of possible lung shunting on post-treatment ^{90}Y-PET images. *Figure 3* shows the intrahepatic ^{90}Y-biodistribution in a patient, visualized with ^{90}Y-Bremsstrahlung SPECT and ^{90}Y-PET, in comparison to ^{166}Ho. As mentioned before, owing to its single photon emissions, ^{166}Ho-microspheres can be imaged with conventional quantitative SPECT techniques (*Figure 3*), which enables post-treatment assessment of the absorbed dose distribution.

Other imaging modalities

Post-treatment dosimetry may also be performed by image-analysis based on physical features of the particles other than radioactivity, including magnetic properties or electron densities. A great benefit of quantitative imaging with CT or MRI is the anatomical

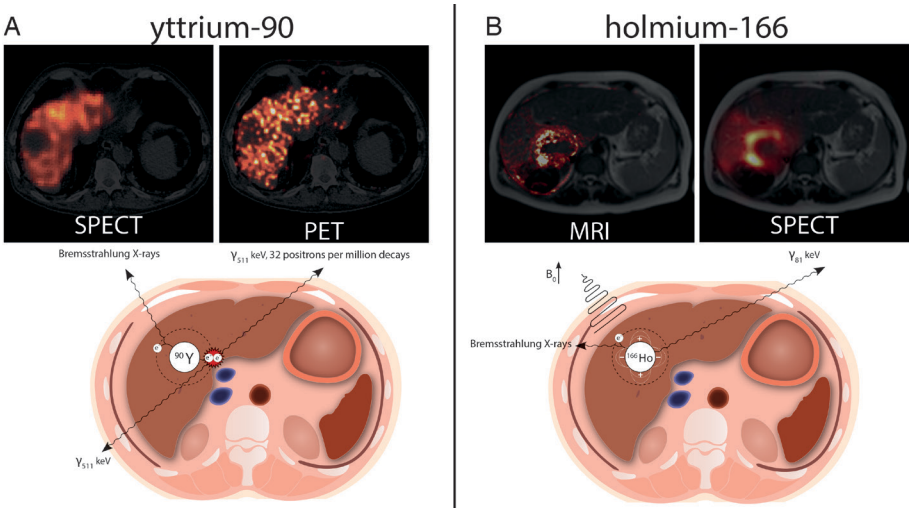

Figure 3. *Schematic illustration of the physical properties and decay of ^{90}Y (A) and ^{166}Ho (B) in the liver. The upper row displays examples of the microsphere biodistribution in the liver using ^{90}Y-SPECT (A upper left), ^{90}Y-PET (A upper right), ^{166}Ho-MRI (B upper left), and ^{166}Ho-SPECT (B upper right)*

information that comes with it. Imaging may be performed at any time, also long after treatment when the radioactivity has already decayed (for studying long term migration and stability of the microspheres). Both CT and MRI require specific microspheres that provide contrast on these images.

In contrast to ^{90}Y microspheres it is possible to quantify new generation microspheres for RE such as ^{166}Ho microspheres using CT or MRI. Quantification of ^{166}Ho microspheres with CT was demonstrated in phantom experiments [44], but, unfortunately, lacked the sensitivity for use in clinical practice. MRI is more promising in that regard due to the paramagnetic properties of the used element holmium. Quantitative analysis with MRI is especially useful for medium- and long-term monitoring of the intra-hepatic behavior of the microspheres.[45,65] A schematic overview of how the physical properties of ^{90}Y and ^{166}Ho can be used for imaging is presented in *Figure 3*. Quantitative analysis of the SPECT and MR images allows for accurate assessment of the absorbed dose on both the tumor(s) and the normal liver.[53]

Dosimetry during treatment

The greatest disadvantage of post-treatment dosimetry is that irrespective of how accurate it estimates the absorbed dose, the activity has already been administered. Dosimetry during treatment, on the other hand, would allow for on-site modifications to the treatment plan and could therefore be very beneficial. Dosimetry during RE is however

technically very challenging and has not yet been performed in patients. Two options for dosimetry during treatment involve the use of nuclear imaging and MRI.

MRI-angiography

Perhaps the best-suited modality for dosimetry during treatment is MRI. MRI can provide anatomical and functional information at a high temporal and spatial resolution with excellent soft tissue contrast. The key ingredient is a type of microsphere that provides sufficient contrast on MRI. To our knowledge, there are currently two types of microspheres for MRI-guided RE under investigation. Both particles are based on a paramagnetic element to induce susceptibility artifacts on T2*-weighted MRI. One type consists of iron-oxide incorporated in / labeled to glass microspheres.[66,67] Studies in rats and rabbits have shown that the biodistribution of these microspheres can be accurately quantified with MRI but no clinical studies have yet been performed. The second type is the ^{166}Ho-microsphere which consists of holmium integrated in a matrix of poly(L-lactic acid). In this case, holmium is used both as the contrast agent for MRI and as the radionuclide for therapy. This eliminates the need for post-labeling the microspheres with the radionuclide or contrast agent, which results in a less stable particle and requires a hot lab. These microspheres may be excellent candidates for MRI-guided RE. Its feasibility was demonstrated in an animal model.[68] However, as with all MRI-guided endovascular interventions, MRI-guided RE faces complicating factors such as a shortage of clinically available MR-compatible and trackable catheters, guide-wires and coils, limited operational space, and high costs.[69,70]

Scintigraphy-guided angiography

Three-dimensional nuclear imaging is generally not associated with real-time imaging, because the scan duration is typically in the order of 30 minutes or longer, during which the camera rotates around a presumably static object. With the localized deposition of activity that is typical for liver RE (*i.e.* high activity concentrations), however, it may be possible to acquire good quality SPECT scans in 5 to 10 minutes. This may allow for dosimetry during treatment administration in the same angiography procedure, if a SPECT/CT scanner is available in the angiography room. An advantage would be that while the catheter tip can stay in position, quantitative SPECT/CT can guide further administration of the microspheres. Real-time tracking of the microsphere distribution during administration may further enhance the possibilities of SPECT for treatment guidance. For this purpose, our institution is currently working on simultaneous X-ray fluoroscopy / scintigraphy imaging. This hybrid imaging modality would give the interventional radiologist direct feedback, more control over the procedure, and the possibility to combine scout and therapy dose in one session.

Discussion

The purpose of this paper was to show how in vivo dosimetry using quantitative imaging modalities can help to improve radioembolization practices and to give an overview of the current status and ongoing developments in this field. The currently used methods for determining the amount of activity to be delivered during radioembolization need further refinement. As a result, patients can receive a too high dose on the healthy liver or a too low dose on (a part of) the tumors. Accurately predicting the biodistribution of microspheres can help to come to the most effective and safe dose for each specific patient. Currently, biodistribution is predicted by using surrogate particles (mainly ^{99m}Tc-MAA), but these have are not very accurate, probably because of differences in particle properties but also because of the dynamic blood flow in the liver. Dosimetry during treatment is therefore ideal so that treatment can be adjusted based on real-time information of the distribution of the microspheres themselves. Performing dosimetry during treatment is unfortunately also the most challenging option since it requires new generation microspheres (*e.g.* SPIO-labeled or ^{166}Ho-microspheres) and/or new methods of performing radioembolization (*e.g.* radioembolization guided by fluoroscopy-scintigraphy-c-arm or real-time MRI), which are still in the experimental phase. Dosimetry post treatment is the most straightforward option and remains essential to confirm adequate biodistribution of microspheres after treatment as long as reliable methods for dosimetry before and during treatment are lacking.

Acknowledgments

The work of MS was supported by the Stichting Beeldgestuurde Behandeling van Kanker and by the Alexandre Suerman MD/PhD grant of the University Medical Center Utrecht.

References

1. Kennedy A, Coldwell D, Sangro B, Wasan H, Salem R (2012) Integrating radioembolization into the treatment paradigm for metastatic neuroendocrine tumors in the liver. Am J Clin Oncol 35: 393-398.
2. Sangro B, Salem R, Kennedy A, Coldwell D, Wasan H (2011) Radioembolization for hepatocellular carcinoma: a review of the evidence and treatment recommendations. Am J Clin Oncol 34: 422-431.
3. Wasan H, Kennedy A, Coldwell D, Sangro B, Salem R (2012) Integrating radioembolization with chemotherapy in the treatment paradigm for unresectable colorectal liver metastases. Am J Clin Oncol 35: 293-301.
4. Kennedy A, Coldwell D, Sangro B, Wasan H, Salem R (2012) Radioembolization for the treatment of liver tumors general principles. American journal of clinical oncology 35: 91-99.
5. Lewandowski RJ, Sato KT, Atassi B, Ryu RK, Nemcek AA, Jr., et al. (2007) Radioembolization with ^{90}Y microspheres: angiographic and technical considerations. Cardiovasc Intervent Radiol 30: 571-592.
6. Lenoir L, Edeline J, Rolland Y, Pracht M, Raoul JL, et al. (2012) Usefulness and pitfalls of MAA SPECT/CT in identifying digestive extrahepatic uptake when planning liver radioembolization. Eur J Nucl Med Mol Imaging 39: 872-880.
7. Abdelmaksoud MH, Hwang GL, Louie JD, Kothary N, Hofmann LV, et al. (2010) Development of new hepaticoenteric collateral pathways after hepatic arterial skeletonization in preparation for yttrium-90 radioembolization. J Vasc Interv Radiol 21: 1385-1395.
8. Bester L, Salem R (2007) Reduction of arteriohepatovenous shunting by temporary balloon occlusion in patients undergoing radioembolization. J Vasc Interv Radiol 18: 1310-1314.
9. Salem R, Parikh P, Atassi B, Lewandowski RJ, Ryu RK, et al. (2008) Incidence of radiation pneumonitis after hepatic intra-arterial radiotherapy with yttrium-90 microspheres assuming uniform lung distribution. Am J Clin Oncol 31: 431-438.
10. Elschot M, Lam MG, Nijsen JF, Smits ML, Prince JF, et al. (2013) Tc-99m-MAA overestimates the absorbed dose to the lungs in radioembolization: a quantitative evaluation in patients treated with Ho-166 microspheres. [submitted].
11. Sangro B, Gil-Alzugaray B, Rodriguez J, Sola I, Martinez-Cuesta A, et al. (2008) Liver disease induced by radioembolization of liver tumors: description and possible risk factors. Cancer 112: 1538-1546.
12. Flamen P, Vanderlinden B, Delatte P, Ghanem G, Ameye L, et al. (2008) Multimodality imaging can predict the metabolic response of unresectable colorectal liver metastases to radioembolization therapy with Yttrium-90 labeled resin microspheres. Phys Med Biol 53: 6591-6603.
13. Gray B, Van Hazel G, Hope M, Burton M, Moroz P, et al. (2001) Randomised trial of SIR-Spheres plus chemotherapy vs. chemotherapy alone for treating patients with liver metastases from primary large bowel cancer. Ann Oncol 12: 1711-1720.
14. Vauthey JN, Abdalla EK, Doherty DA, Gertsch P, Fenstermacher MJ, et al. (2002) Body surface

area and body weight predict total liver volume in Western adults. Liver Transpl 8: 233-240.

15. Lau WY, Kennedy AS, Kim YH, Lai HK, Lee RC, et al. (2012) Patient selection and activity planning guide for selective internal radiotherapy with yttrium-90 resin microspheres. Int J Radiat Oncol Biol Phys 82: 401-407.
16. Sirtex (2013) SIR-Spheres Yttrium-90 Resin Microspheres Package Insert.
17. Nordion (2013) Therasphere Yttrium-90 Glass Microsphere Package Insert.
18. Gulec SA, Mesoloras G, Stabin M (2006) Dosimetric techniques in ^{90}Y-microsphere therapy of liver cancer: The MIRD equations for dose calculations. J Nucl Med 47: 1209-1211.
19. Ho S, Lau WY, Leung TW, Johnson PJ (1998) Internal radiation therapy for patients with primary or metastatic hepatic cancer: a review. Cancer 83: 1894-1907.
20. Riaz A, Gates VL, Atassi B, Lewandowski RJ, Mulcahy MF, et al. (2011) Radiation segmentectomy: a novel approach to increase safety and efficacy of radioembolization. Int J Radiat Oncol Biol Phys 79: 163-171.
21. Lam MG, Louie JD, Iagaru AH, Goris ML, Sze DY (2013) Safety of Repeated Yttrium-90 Radioembolization. Cardiovasc Intervent Radiol.
22. Dezarn WA, Cessna JT, DeWerd LA, Feng W, Gates VL, et al. (2011) Recommendations of the American Association of Physicists in Medicine on dosimetry, imaging, and quality assurance procedures for ^{90}Y microsphere brachytherapy in the treatment of hepatic malignancies. Med Phys 38: 4824-4845.
23. Kao YH, Tan EH, Ng CE, Goh SW (2011) Clinical implications of the body surface area method versus partition model dosimetry for yttrium-90 radioembolization using resin microspheres: a technical review. Ann Nucl Med 25: 455-461.
24. Ho S, Lau WY, Leung TW, Chan M, Ngar YK, et al. (1996) Partition model for estimating radiation doses from yttrium-90 microspheres in treating hepatic tumours. Eur J Nucl Med 23: 947-952.
25. Ho S, Lau WY, Leung TW, Chan M, Johnson PJ, et al. (1997) Clinical evaluation of the partition model for estimating radiation doses from yttrium-90 microspheres in the treatment of hepatic cancer. Eur J Nucl Med 24: 293-298.
26. Ho S, Lau WY, Leung TW, Chan M, Chan KW, et al. (1997) Tumour-to-normal uptake ratio of ^{90}Y microspheres in hepatic cancer assessed with ^{99m}Tc-macroaggregated albumin. Br J Radiol 70: 823-828.
27. Dhabuwala A, Lamerton P, Stubbs RS (2005) Relationship of ^{99m}technetium labelled macroaggregated albumin (^{99m}Tc-MAA) uptake by colorectal liver metastases to response following Selective Internal Radiation Therapy (SIRT). BMC Nucl Med 5: 7.
28. Lam MG, Goris ML, Iagaru AH, Mittra ES, Louie JD, et al. (2013) Fusion MAA-sulfur colloid SPECT imaging for Yttrium-90 radioembolization: towards customized physiology-based dose planning. Journal of Vascular and Interventional Radiology 24: S34.
29. Powerski MJ, Scheurig-Munkler C, Banzer J, Schnapauff D, Hamm B, et al. (2012) Clinical practice in radioembolization of hepatic malignancies: a survey among interventional centers in Europe. Eur J Radiol 81: e804-811.

30. Stuart JE, Tan B, Myerson RJ, Garcia-Ramirez J, Goddu SM, et al. (2008) Salvage radioembolization of liver-dominant metastases with a resin-based microsphere: initial outcomes. J Vasc Interv Radiol 19: 1427-1433.

31. Michels NA (1966) Newer anatomy of the liver and its variant blood supply and collateral circulation. Am J Surg 112: 337-347.

32. Kao YH, Hock Tan AE, Burgmans MC, Irani FG, Khoo LS, et al. (2012) Image-guided personalized predictive dosimetry by artery-specific SPECT/CT partition modeling for safe and effective ^{90}Y radioembolization. J Nucl Med 53: 559-566.

33. Louie JD, Kothary N, Kuo WT, Hwang GL, Hofmann LV, et al. (2009) Incorporating cone-beam CT into the treatment planning for yttrium-90 radioembolization. J Vasc Interv Radiol 20: 606-613.

34. Murthy R, Mutha P, Madoff DC, Mahvash A, Erwin W (2009) Establishment of the radiation effect of yttrium-90 microspheres: role of C-arm CT. J Vasc Interv Radiol 20: 422-424.

35. Kao YH, Tan EH, Teo TK, Ng CE, Goh SW (2011) Imaging discordance between hepatic angiography versus Tc-99m-MAA SPECT/CT: a case series, technical discussion and clinical implications. Ann Nucl Med 25: 669-676.

36. Wondergem M, Smits ML, Elschot M, de Jong HW, Verkooijen HM, et al. (2013) ^{99m}Tc-Macroaggregated Albumin Poorly Predicts the Intrahepatic Distribution of ^{90}Y Resin Microspheres in Hepatic Radioembolization. J Nucl Med.

37. Jiang M, Fischman A, Nowakowski FS (2012) Segmental Perfusion Differences on Paired Tc-99m Macroaggregated Albumin (MAA) Hepatic Perfusion Imaging and Yttrium-90 (Y-^{90}) Bremsstrahlung Imaging Studies in SIR-Sphere Radioembolization: Associations with Angiography. Journal of Nuclear Medicine & Radiation Therapy 03.

38. Van de Wiele C, Maes A, Brugman E, D'Asseler Y, De Spiegeleer B, et al. (2012) SIRT of liver metastases: physiological and pathophysiological considerations. Eur J Nucl Med Mol Imaging 39: 1646-1655.

39. Bult W, Vente MA, Zonnenberg BA, Van Het Schip AD, Nijsen JF (2009) Microsphere radioembolization of liver malignancies: current developments. Q J Nucl Med Mol Imaging 53: 325-335.

40. Lhommel R, van Elmbt L, Goffette P, Van den Eynde M, Jamar F, et al. (2010) Feasibility of ^{90}Y TOF PET-based dosimetry in liver metastasis therapy using SIR-Spheres. Eur J Nucl Med Mol Imaging 37: 1654-1662.

41. (2010) Predictive Value of ^{99m}Tc- Albumin Spheres Before ^{90}Y- SIR Therapy (EXPLOSIVE), NCT01186263 http://clinicaltrials.gov/ct2/show/NCT01186263?term=explosive+^{99m}tc&rank=1.

42. Selwyn RG, Avila-Rodriguez MA, Converse AK, Hampel JA, Jaskowiak CJ, et al. (2007) 18F-labeled resin microspheres as surrogates for ^{90}Y resin microspheres used in the treatment of hepatic tumors: a radiolabeling and PET validation study. Phys Med Biol 52: 7397-7408.

43. Smits ML, Nijsen JF, van den Bosch MA, Lam MG, Vente MA, et al. (2012) Holmium-166 radioembolisation in patients with unresectable, chemorefractory liver metastases (HEPAR trial): a phase 1, dose-escalation study. Lancet

Oncol 13: 1025-1034.

44. Seevinck PR, Seppenwoolde JH, de Wit TC, Nijsen JF, Beekman FJ, et al. (2007) Factors affecting the sensitivity and detection limits of MRI, CT, and SPECT for multimodal diagnostic and therapeutic agents. Anticancer Agents Med Chem 7: 317-334.

45. van de Maat GH, Seevinck PR, Elschot M, Smits ML, de Leeuw H, et al. (2012) MRI-based biodistribution assessment of holmium-166 poly(L-lactic acid) microspheres after radioembolisation. Eur Radiol.

46. Leung TW, Lau WY, Ho SK, Ward SC, Chow JH, et al. (1995) Radiation pneumonitis after selective internal radiation treatment with intraarterial ^{90}yttrium-microspheres for inoperable hepatic tumors. Int J Radiat Oncol Biol Phys 33: 919-924.

47. Campbell JM, Wong CO, Muzik O, Marples B, Joiner M, et al. (2009) Early dose response to yttrium-90 microsphere treatment of metastatic liver cancer by a patient-specific method using single photon emission computed tomography and positron emission tomography. Int J Radiat Oncol Biol Phys 74: 313-320.

48. Strigari L, Sciuto R, Rea S, Carpanese L, Pizzi G, et al. (2010) Efficacy and toxicity related to treatment of hepatocellular carcinoma with ^{90}Y-SIR spheres: radiobiologic considerations. J Nucl Med 51: 1377-1385.

49. Chang TT, Bourgeois AC, Balius AM, Pasciak AS (2013) Treatment modification of yttrium-90 radioembolization based on quantitative positron emission tomography/CT imaging. J Vasc Interv Radiol 24: 333-337.

50. Walrand S, Lhommel R, Goffette P, Van den Eynde M, Pauwels S, et al. (2012) Hemoglobin level significantly impacts the tumor cell survival fraction in humans after internal radiotherapy. EJNMMI Res 2: 20.

51. Lau WY, Leung WT, Ho S, Leung NW, Chan M, et al. (1994) Treatment of inoperable hepatocellular carcinoma with intrahepatic arterial yttrium-90 microspheres: a phase I and II study. Br J Cancer 70: 994-999.

52. Wang XD, Yang RJ, Cao XC, Tan J, Li B (2010) Dose delivery estimated by bremsstrahlung imaging and partition model correlated with response following intra-arterial radioembolization with ^{32}P-glass microspheres for the treatment of hepatocellular carcinoma. J Gastrointest Surg 14: 858-866.

53. Smits ML, Elschot M, Van Den Bosch MA, van de Maat GH, van het Schip AD, et al. (2013) Imageable radioactive holmium-166 microspheres for treatment of liver malignancies: in vivo dosimetry based on SPECT and MRI. Journal of Nuclear Medicine [in press].

54. Kao YH, Steinberg JD, Tay YS, Lim GK, Yan J, et al. (2013) Post-radioembolization yttrium-90 PET/CT - part 2: dose-response and tumor predictive dosimetry for resin microspheres. EJNMMI Res 3: 57.

55. Wahl RL, Jacene H, Kasamon Y, Lodge MA (2009) From RECIST to PERCIST: Evolving Considerations for PET response criteria in solid tumors. J Nucl Med 50 Suppl 1: 122S-150S.

56. Cui Y, Zhang XP, Sun YS, Tang L, Shen L (2008) Apparent diffusion coefficient: potential imaging biomarker for prediction and early detection of response to chemotherapy in hepatic metastases. Radiology 248: 894-900.

57. Elschot M, Vermolen BJ, Lam MG, de Keizer B, van den Bosch MA, et al. (2013) Quantitative comparison of PET and Bremsstrahlung SPECT for imaging the in vivo yttrium-90 microsphere distribution after liver radioembolization. PLoS One 8: e55742.

58. Elschot M, Nijsen JF, Dam AJ, de Jong HW (2011) Quantitative evaluation of scintillation camera imaging characteristics of isotopes used in liver radioembolization. PLoS One 6: e26174.

59. Rong X, Du Y, Ljungberg M, Rault E, Vandenberghe S, et al. (2012) Development and evaluation of an improved quantitative (^{90})Y bremsstrahlung SPECT method. Med Phys 39: 2346-2358.

60. Elschot M, Lam MG, van den Bosch MA, Viergever MA, de Jong HW (2013) Quantitative Monte Carlo-Based ^{90}Y SPECT Reconstruction. J Nucl Med.

61. Ford K (1955) Predicted 0+ level in 40Zr^{90}. Phys Rev 98: 1516-1517.

62. Langhoff H (1961) Zum experimentellen Nachweis von Zweiquantenzerfall beim 0+–0+—Ubergang des Zr^{90}. Zeitschrift fu r Physik 164: 166-173.

63. Willowson K, Forwood N, Jakoby BW, Smith AM, Bailey DL (2012) Quantitative (^{90})Y image reconstruction in PET. Med Phys 39: 7153-7159.

64. Carlier T, Eugene T, Bodet-Milin C, Garin E, Ansquer C, et al. (2013) Assessment of acquisition protocols for routine imaging of Y-90 using PET/CT. EJNMMI Res 3: 11.

65. Seevinck PR, Seppenwoolde JH, Zwanenburg JJ, Nijsen JF, Bakker CJ (2008) FID sampling superior to spin-echo sampling for T_2^*-based quantification of holmium-loaded microspheres: theory and experiment. Magn Reson Med 60: 1466-1476.

66. Gupta T, Virmani S, Neidt TM, Szolc-Kowalska B, Sato KT, et al. (2008) MR tracking of iron-labeled glass radioembolization microspheres during transcatheter delivery to rabbit VX2 liver tumors: feasibility study. Radiology 249: 845-854.

67. Li W, Zhang Z, Guo Y, Nicolai J, Reed A, et al. SPIO-labeled ^{90}Y microspheres permit accurate quantification of macroscopic intra-hepatic biodistribution; 2013; Salt Lake City, UT.

68. Seppenwoolde JH, Bartels LW, van der Weide R, Nijsen JF, van het Schip AD, et al. (2006) Fully MR-guided hepatic artery catheterization for selective drug delivery: a feasibility study in pigs. J Magn Reson Imaging 23: 123-129.

69. Kos S, Huegli R, Bongartz GM, Jacob AL, Bilecen D (2008) MR-guided endovascular interventions: a comprehensive review on techniques and applications. Eur Radiol 18: 645-657.

70. Smits HF, Bos C, van der Weide R, Bakker CJ (1999) Interventional MR: vascular applications. Eur Radiol 9: 1488-1495.

Chapter 8

Technetium-99m-MAA poorly predicts the intrahepatic distribution of yttrium-90 microspheres in radioembolization

M Wondergem, MLJ Smits, M Elschot, HWAM de Jong, HM Verkooijen, MAAJ van den Bosch, JFW Nijsen, MGEH Lam

Journal of Nuclear Medicine 2013

In hepatic ^{90}Y radioembolization, pretreatment ^{99m}Tc-macroaggregated albumin (^{99m}Tc-MAA) nuclear imaging is used for lung shunt analysis, evaluation of extrahepatic deposition, and sometimes for treatment planning, using a partition model. A high level of agreement between pretreatment ^{99m}Tc-MAA distribution and final ^{90}Y-microsphere distribution is assumed. The aim of this study was to investigate the value of pretreatment ^{99m}Tc-MAA SPECT to predict intrahepatic post-treatment ^{90}Y-microsphere distribution.

Materials and Methods

Volumes of interest (VOIs) were delineated on pretreatment contrast-enhanced CT or MR images according to Couinaud's liver segmentation. All VOIs were registered to the ^{99m}Tc-MAA SPECT and ^{90}Y SPECT images. The ^{99m}Tc-MAA SPECT and ^{90}Y SPECT activity counts were normalized to the total administered activity of ^{90}Y. For each VOI, this practice resulted in a predictive amount of ^{90}Y (MBq/cm^3) based on ^{99m}Tc-MAA SPECT in comparison with an actual amount of ^{90}Y based on ^{90}Y SPECT. Bland–Altman analysis was used to investigate the agreement of the activity distribution between ^{99m}Tc-MAA SPECT and ^{90}Y-SPECT.

Introduction

Radioembolization with ^{90}Y microspheres is widely used for treatment of primary or metastatic liver malignancies. Selective injection of these microspheres in the hepatic artery results in high absorbed tumor doses while largely sparing the surrounding normal liver parenchyma, which is dependent mainly on the portal vein for its blood supply.[1-3]

In a pretreatment angiographic procedure the anatomy of the liver vasculature is evaluated, and hepatico-enteric anastomoses that may lead to extrahepatic deposition of activity are occluded by coil embolization.[4] Thereafter ^{99m}Tc-macroaggregated albumin particles (^{99m}Tc-MAA) are injected in the liver artery supplying the target volume, and the distribution of ^{99m}Tc-MAA is visualized by scintigraphy. Most centers that perform radioembolization use the distribution of ^{99m}Tc-MAA to calculate the lung shunt fraction and to detect any extrahepatic deposition of activity.[5,6] Furthermore, it is assumed that ^{99m}Tc-MAA can also be used to predict the intrahepatic distribution of ^{90}Y-microspheres, and as such, ^{99m}Tc-MAA is sometimes used for individualized treatment planning by the so-called partition model.[7-9]

In most of the patients, the prescribed activities for radioembolization are calculated with methods based on liver weight or on a combination of body surface area and

act

Results

A total of 39 procedures (225 VOIs) in 31 patients were included for analysis. The overall mean difference between pretreatment and post-treatment distribution of activity concentration for all segments was -0.022 MBq/cm^3 with 95% limits of agreement of -0.581 to 0.537 MBq/cm^3 (-28.9 to 26.7 Gy absorbed dose). A difference of >10%, >20%, and >30% of the mean activity per milliliter was found in, respectively, 153 (68%), 97 (43%), and 72 (32%) of the 225 segments. In every ^{99m}Tc-MAA procedure, at least 1 segment showed an under- or overestimation of >10%. The position of the catheter tip during administrations, as well as the tumor load of the liver segments, significantly influenced the disagreement.

Conclusion

In current clinical practice, ^{99m}Tc-MAA distribution does not accurately predict final ^{90}Y activity distribution. Awareness of the importance of catheter positioning and adherence to specific recommendations may lead to optimization of individualized treatment planning based on pretreatment imaging.

tumor liver involvement.[10] The absorbed dose to the tumor and any accompanying toxicity effects to the normal liver parenchyma may be observed only after the actual treatment. Dosimetry can be used for individualized treatment planning and aims to optimize treatment efficacy with acceptable toxicity. Pretreatment dosimetry, however, requires a scout or safety dose as a reference for the treatment, for example by using the ^{99m}Tc-MAA distribution as a reference for post-treatment dose distribution.

The partition model is suggested as an alternative means of activity calculation in patients with a limited number of hypervascular liver tumors, optimizing the administered activity in individual patients.[5] Tumor-to-non-tumor activity ratios on pretreatment ^{99m}Tc-MAA SPECT are used to calculate activities that better reflect the intrahepatic dose distribution. In clinical practice, this means that the partition-model–based activity may be much higher than prescribed activities that are based on the more conventional methods, especially in patients with hypervascular tumors, having high tumor-to-non-tumor activity ratios.[11]

The partition model relies on ^{99m}Tc-MAA as a predictor for ^{90}Y-microsphere distribution. However, the predictive value of ^{99m}Tc-MAA for the distribution of ^{90}Y-microspheres in the liver is still a matter of debate.[12] Parameters that may influence distribution

differences between ^{99m}Tc-MAA and ^{90}Y-microspheres include interval differences in catheter position, physiologic variances in hepatic blood flow, size and morphology differences between ^{99m}Tc-MAA particles and ^{90}Y-microspheres, tumor histopathology, and tumor load. These and other factors may all limit the agreement between ^{99m}Tc-MAA and ^{90}Y-microsphere distribution.

The aim of this study was to investigate the value of ^{99m}Tc-MAA to predict ^{90}Y-microsphere distribution. Insight on this matter is essential for further development of any dose calculation method based on pretreatment ^{99m}Tc-MAA distribution.

Materials and Methods

Patients

All patients who were treated with radioembolization from the start of our program in February 2009 up to February 2012 were retrospectively analyzed. The institutional review board approved this study and waived the requirements for patient informed consent. Patients who had received both the pretreatment administration of ^{99m}Tc-MAA and the treatment with ^{90}Y-microspheres were included. Exclusion criteria were missing data, malregistration of imaging data, and procedures with multiple administrations, rendering it impossible to relate individual administrations to specific target volumes. In some patients, two separate lobar procedures were included in the study analysis. Subsegmental administrations were not performed.

Radioembolization

All procedures were performed according to international consensus.[13] In short, during a pretreatment angiographic procedure, a 5-French catheter was used to evaluate hepatic vascular anatomy and to identify non-target vessels leading to organs other than the liver. In general, the gastroduodenal artery and the right gastric artery were coil-embolized to prevent extrahepatic deposition of activity. Any other vessels branching off near the injection site and leading to non-target organs were embolized as well. The cystic artery was not prophylactically embolized. Consecutively, a scout dose of ^{99m}Tc-MAA (150 MBq, 0.8 mg in 3.0 mL, TechneScan LyoMaa; Mallinckrodt Medical B.V.) was injected via a slow-pulsed injection, followed by planar imaging and SPECT, to check for inadvertent extrahepatic deposition. ^{99m}Tc-MAA was prepared immediately before administration; imaging was performed immediately after administration. If the ^{99m}Tc-MAA was not distributed to any non-target area (including a hepatopulmonary shunt ≤20%), the patient was scheduled for treatment (mean interval, 12 d; range, 0–23 d). However, in the case of inadvertent ^{99m}Tc-MAA distribution, a second pretreatment procedure was performed to embolize the culprit vessels. In those cases, only the most

recent ^{99m}Tc-MAA SPECT study was used for analyses. No vessels were coil-embolized after final ^{99m}Tc-MAA administration. Resin microspheres (SIR-Spheres; Sirtex) were used for treatment. Activity calculations were based on the body surface area method (prescribed activity in GBq, body surface area – 0.2 + 1 fractional tumor involvement). Patients with a lung shunt fraction of >20% were excluded from treatment, and in patients with a lung shunt fraction of 10%–15% or 15%–20% a reduction of 20% and 40% was applied, respectively. Per protocol, the interventional radiologist placed the catheter tip in the same position during both procedures. The microspheres were infused slowly, with intermittent contrast injection and digital subtraction angiography to check for stasis. All administered activity was corrected for any residual activity after treatment.

Imaging

Pre- and post-treatment imaging was performed on a dual-head γ-camera (Forte [Philips] for 7 procedures and Symbia [Siemens Health Care] for 32 procedures). Pretreatment ^{99m}Tc-MAA planar and SPECT images were acquired on a 128 x 128 matrix using a 129.5- to 150.5-keV energy window and a low-energy general-purpose collimator. For post-treatment ^{90}Y-bremsstrahlung SPECT imaging, the combination of a high-energy general-purpose collimator and a wide 50- to 250-keV energy window was used, which yields images with a favorable combination of sensitivity and contrast.[14] SPECT imaging was performed with 120 projections over a noncircular orbit of 180° (Forte; 30 s/projection) or 360° (Symbia; 20 s/projection). Data were reconstructed using ordered-subsets expectation maximization (5 iterations, 8 subsets) including attenuation correction and a Gaussian post-reconstruction filter of 5 mm in full width at half maximum. The reconstructed voxel size was 4.7 x 4.7 x 4.7 mm, 3.9 x 3.9 x 3.9 mm, and 4.8 x 4.8 x 4.8 mm, for Forte images, Symbia ^{99m}Tc-MAA images, and Symbia ^{90}Y images, respectively.

Analysis

Contrast-enhanced CT or MR pretreatment images were used for liver segmentation according to the Bismuth adaptation of Couinaud's classification of liver anatomy.[15] Software was developed at our institution for this purpose (Research Volumetool, version 1.3.3).[16] A maximum of 8 segments (volumes of interest, or VOIs) were delineated per patient. Prior liver resection and lobar procedures resulted in fewer segments. All delineated VOIs were manually registered to the ^{99m}Tc-MAA SPECT and ^{90}Y SPECT images (*Figure 1*). Procedures for which coregistration was impossible or inaccurate because of differences in liver position between the different scans were excluded from analysis. The pretreatment ^{99m}Tc-MAA SPECT and the post-treatment ^{90}Y SPECT ima-

ges were converted into units of ^{90}Y-activity concentration by normalization of the total number of reconstructed counts in the VOIs to the total administered activity of ^{90}Y. For each VOI, this practice resulted in a predictive amount of ^{90}Y (MBq/cm^3) based on ^{99m}Tc-MAA SPECT in comparison with an actual amount of ^{90}Y based on ^{90}Y SPECT. A homogeneous distribution of the activity inside a VOI, no activity distribution outside the liver, and no interval change in liver morphology were assumed. To illustrate the clinical implications of the disagreement, a map of the absorbed dose in grays was also calculated, using a conversion factor of 49.7 Gy/(MBq/cm^3).[17] The injection positions of ^{99m}Tc-MAA and ^{90}Y-microspheres were retrospectively analyzed. Three observers independently reviewed the agreement between the 2 injection positions (per procedure) on fluoroscopy images on a 4-point scale (1, very poor agreement, difference >10 mm; 2, poor agreement, difference >5–10 mm; 3, good agreement, difference >3–5 mm; 4, very good agreement, difference ≤3 mm). A subgroup of patients with suboptimal agreement between the injection positions (average score ≤2.5) was selected. The injection positions were also classified as close to a major bifurcation (<10 mm) or not close to a major bifurcation, and segments were classified as having >25% tumor involvement or ≤25%.

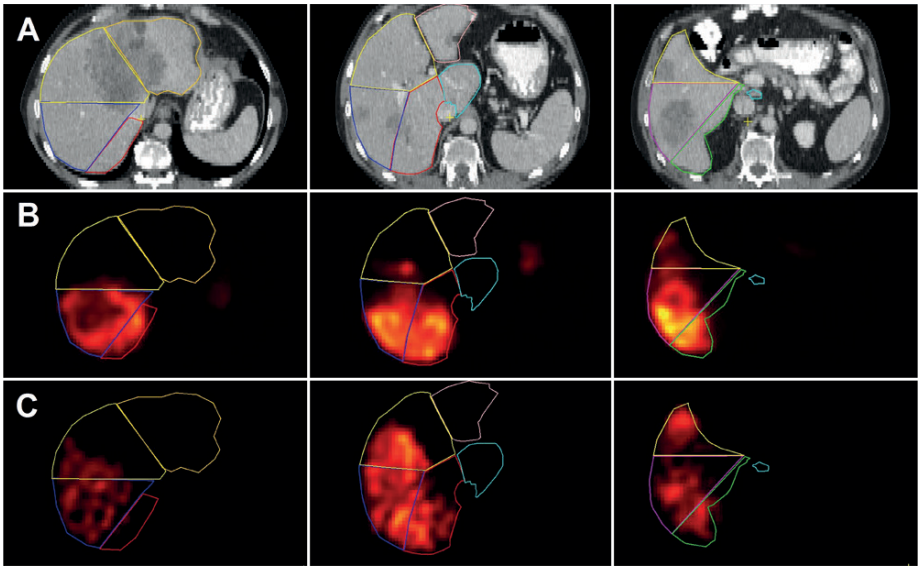

Figure 1. *Segmentation on CT (A) and co-registration of the segments on ^{99m}Tc-MAA-SPECT (B) and ^{90}Y-SPECT (C) after injection of activity in the right hepatic artery. Note the clear differences in intrahepatic activity distribution in this patient. There is also diffuse uptake of free pertechnetate in the stomach on ^{99m}Tc-MAA-SPECT, also evidenced by thyroid gland and kidney uptake (not shown).*

Statistical Analysis

A commercial statistical software package (SPSS for Windows, version 20.0; SPSS Inc.) was used for data analysis. Bland–Altman plots were used for evaluating agreement between pre- and post-treatment activity distributions.[18,19] A Bland–Altman graph is the preferred method to test for agreement between two instruments that are intended to measure the same parameter, in our case: ^{99m}Tc-MAA SPECT and ^{90}Y SPECT to measure final ^{90}Y-microsphere distribution. In a Bland–Altman plot, the difference between the 2 methods is plotted against the mean of the 2 methods. The error was estimated by the mean difference (d_m) and the SD of the differences (s). The 95% limits of agreement were calculated by $d_m \pm 2s$. Because the ^{99m}Tc-MAA was normalized to the ^{90}Y-activity, the expected mean difference is zero. In Bland–Altman analysis, the width of the distribution (*i.e.* 95% limits of agreement) is a measurement of the agreement between the 2 methods. An absorbed dose map in grays was calculated for translation to clinical practice. Cutoff levels (10%, 20%, and 30%) for the difference from the mean were used to evaluate variability in activity distribution. The Fisher exact test was used to test differences between subgroups with differences in tumor involvement, tumor cell type, and catheter positions.

Results

Eighty patients were evaluated for radioembolization (*Figure 2*). In 18 patients, contraindications to therapy were found during or after the ^{99m}Tc-MAA procedure. The remaining 62 patients underwent 73 treatment procedures. Multiple injections of activity in the same procedure led to exclusion of 27 procedures, and missing data led to exclusion of four procedures. In another three procedures, technical difficulties were encountered during coregistration because of substantial differences in liver position between the different scans ($n = 2$) or because of segmentation problems ($n = 1$). In the latter patient, extensive disease in the liver made it impossible to delineate the individual liver segments. A total of 39 procedures in 31 patients were included for analysis (*Table 1*). The mean administered activity of ^{90}Y-microspheres was 1,002 MBq per procedure (range, 207–1,912 MBq). In 8 patients, 2 separate procedures were included, one for the left liver lobe and one for the right lobe. A total of 225 liver segments were analyzed.

The overall mean difference between pretreatment and post-treatment distribution of activity concentration for all segments was -0.022 MBq/cm^3, with an SD of the mean of 0.285 MBq/cm^3. A Bland–Altman plot was constructed with the absolute differences against their mean (*Figure 3*). The 95% limits of agreement of the differences were -0.581 and 0.537 MBq/cm^3, which correspond to 95% limits of agreement of -28.9 and 26.7 Gy absorbed dose.

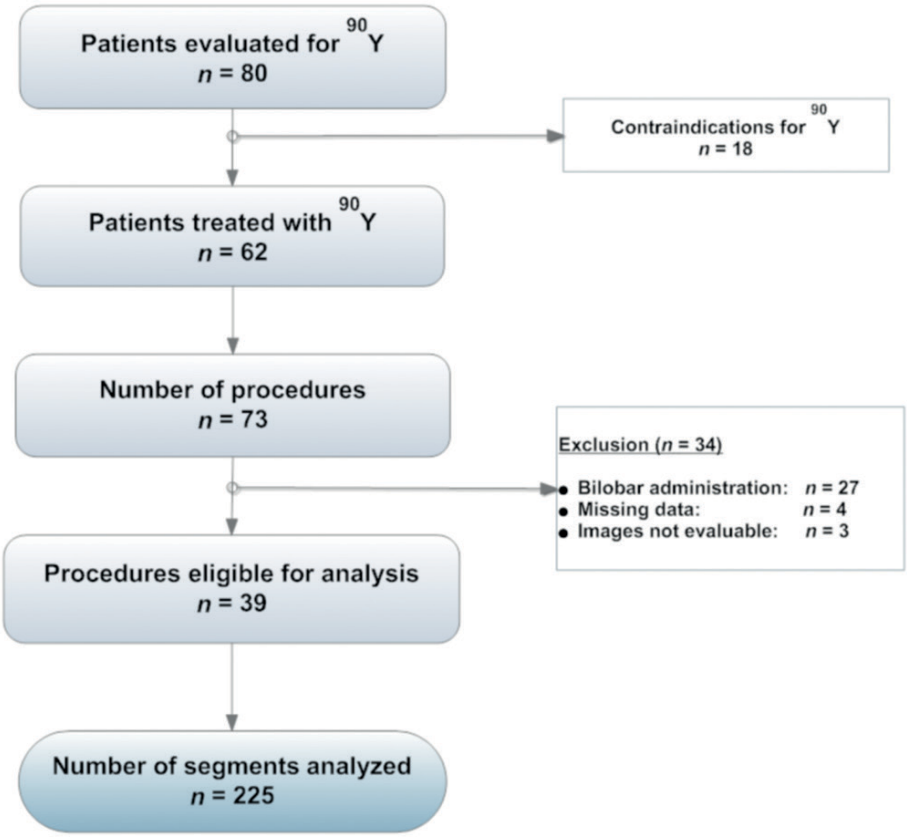

Figure 2. *Inclusion flowchart.*

A difference of >10%, >20%, and >30% of the mean activity per milliliter was found in, respectively, 153 (68%), 97 (43%), and 72 (32%) of the 225 segments (*Figure 4*). In every ^{99m}Tc-MAA procedure, at least 1 segment showed an under- or overestimation of >10%. A >20% and >30% difference in at least 1 segment was found for 35 (90%) and 32 (82%) of 39 procedures, respectively (*Figure 5*). A substantial difference in agreement between ^{99m}Tc-MAA and ^{90}Y activity distribution was found for every procedure (*Figure 6*). Interestingly, the distribution differences were found to be smaller for segments with greater tumor involvement. The mean difference and 95% limits of agreement were -0.027 ± 0.603 and 0.007 ± 0.381 MBq/cm^3 for segments with ≤25% and >25% tumor involvement, respectively. In grays, the 95% limits of agreement (-18.6 to 19.3 Gy) for segments with >25% tumor involvement had a smaller width than the 95% limits of agreement for segments with ≤25% tumor involvement (-31.3 to 28.6 Gy). A relative difference of >10%, >20%, and >30% was found in, respectively, 18 (51%), 9 (26%), and

Table 1. *Baseline characteristics*

Characteristic	Patients, *n* (%)
Sex, Male / Female	19 / 12
Age, year: median (range)	60.3 (35 – 76)
Primary tumor	
Colorectal	17 (55%)
Hepatocellular	4 (13%)
Neuroendocrine	3 (10%)
Cholangiocarcinoma	2 (6%)
Other *	5 (16%)
SIR-Spheres® activity in MBq: mean (range)	1002 (207 – 1912)
Liver tumor involvement	
< 25%	21 (68%)
25 – 50%	9 (29%)
50 – 75%	1 (3%)
75 – 100%	0 (0%)
Treatment	
Whole liver in one administration (one session)	6 (19%)
Whole liver in two lobar administrations (two sessions)	10 (31%)
Lobar left only	2 (6%)
Lobar right only	13 (44%)
Injection position	
Common or proper hepatic artery	6 (15%)
Right hepatic artery	22 (57%)
Left hepatic artery	11 (28%)
Total included procedures	39
Total included liver segments	225
Segment volume in mL: mean (range)	320 (5 – 1393)
Previous liver-directed treatment	
Trans-arterial embolization	1 (3%)
Partial liver resection	3 (10%)
Radiofrequency ablation (RFA)	5 (16%)
External beam radiotherapy	0 (0%)
Radioembolization	0 (0%)
Previous systemic treatment †	21 (68%)

** Uveal melanoma (2); Pancreatic (2); Insulinoma (1); Unknown primary (1). † Most patients were chemo-refractory, except those patients with chemoresistant tumors (hepatocellular, cholangiocarcinoma, neuroendocrine, melanoma, etc.)*

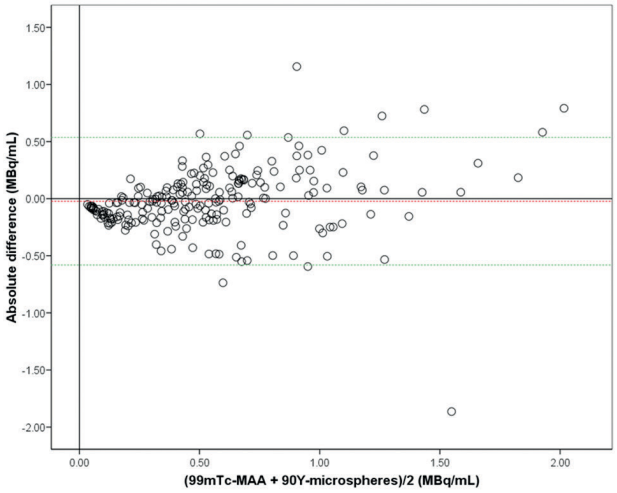

Figure 3. *Bland-Altman plot. The difference between ^{99m}Tc-MAA and ^{90}Y-microspheres activity in each segment is plotted against the mean activity in each segment. The 95% limits of agreement (LoA) are plotted as gren dotted lines. The mean bias is plotted as a red dotted line.*

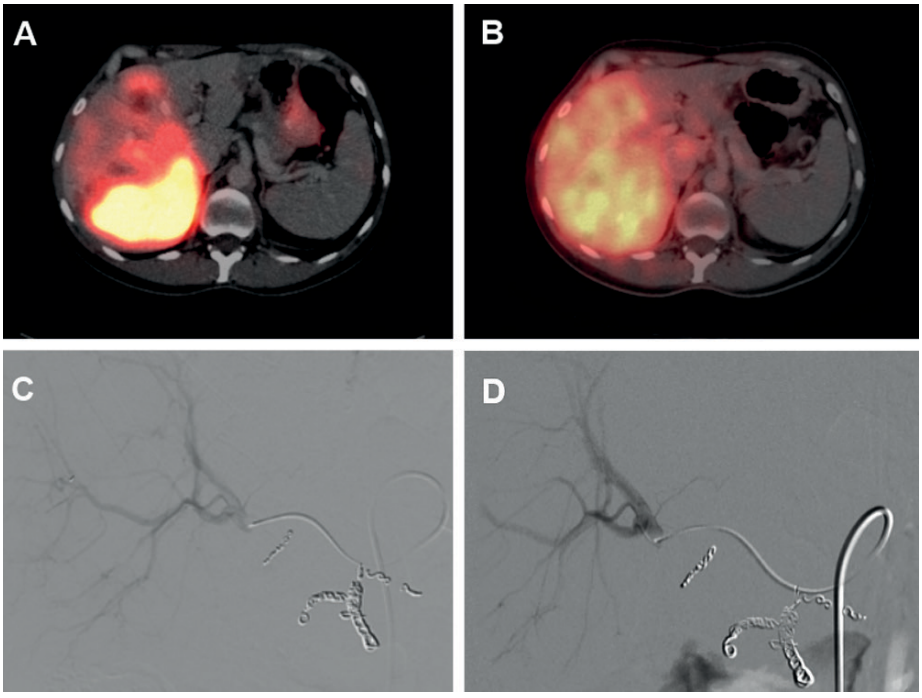

Figure 4. *Right-sided treatment of a 36-year-old patient with colorectal liver metastases. The pre-treatment ^{99m}Tc-MAA SPECT images (A) showed substantial distribution differences in comparison with the post-treatment ^{90}Y SPECT images (B). Digital subtraction angiography images show the identical position of the catheter tip in the right hepatic artery (C and D). The gastroduodenal artery, the right gastric artery and supraduodenal arteries were coil embolized. Diffuse uptake of free pertechnetate in the stomach on ^{99m}Tc-MAA-SPECT was also seen (A).*

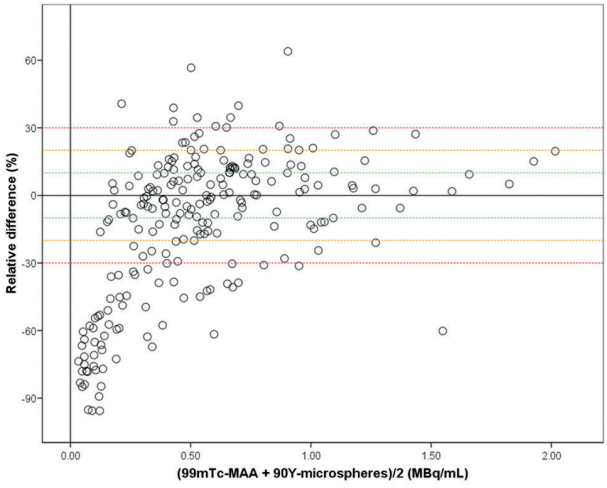

Figure 5. *Relative difference plot. The relative difference between ^{99m}Tc-MAA and ^{90}Y-microspheres activity in percentage of the mean activity is plotted against the mean activity, according to Bland-Altman. The dotted lines indicate the 95% limits of agreement for three categories representing > 10% (green), > 20% (orange), and > 30% (red) difference in activity.*

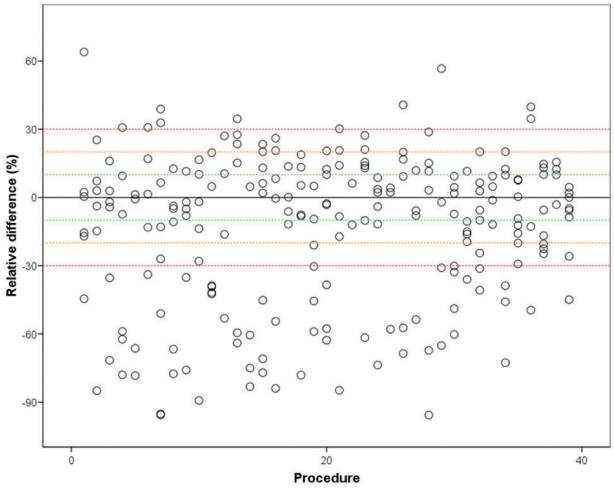

Figure 6. *Agreement per procedure. The relative difference between ^{99m}Tc-MAA and ^{90}Y-microspheres activity for each VOI is plotted per procedure. The dotted lines indicate the 95% limits of agreement for three categories representing > 10% (green), > 20% (orange), and > 30% (red) difference in activity.*

7 (20%) of the 35 segments with >25% tumor involvement and in 136 (72%), 88 (47%), and 64 (34%) of the 190 segments with ≤25% tumor involvement. This proved significant for the cutoff values of >10% (P = 0.028) and >20% (P = 0.026), but significance was not reached for a cutoff value of >30% (P = 0.118).

A suboptimal agreement on catheter tip position was found for 9 patients (11 procedures). The mean difference and 95% limits of agreement were -0.008 ± 0.622 MBq/cm^3 for procedures with a suboptimal agreement on catheter tip position (*Figure 7*) and -0.026 ± 0.556 MBq/cm^3 for procedures with an optimal agreement on catheter tip

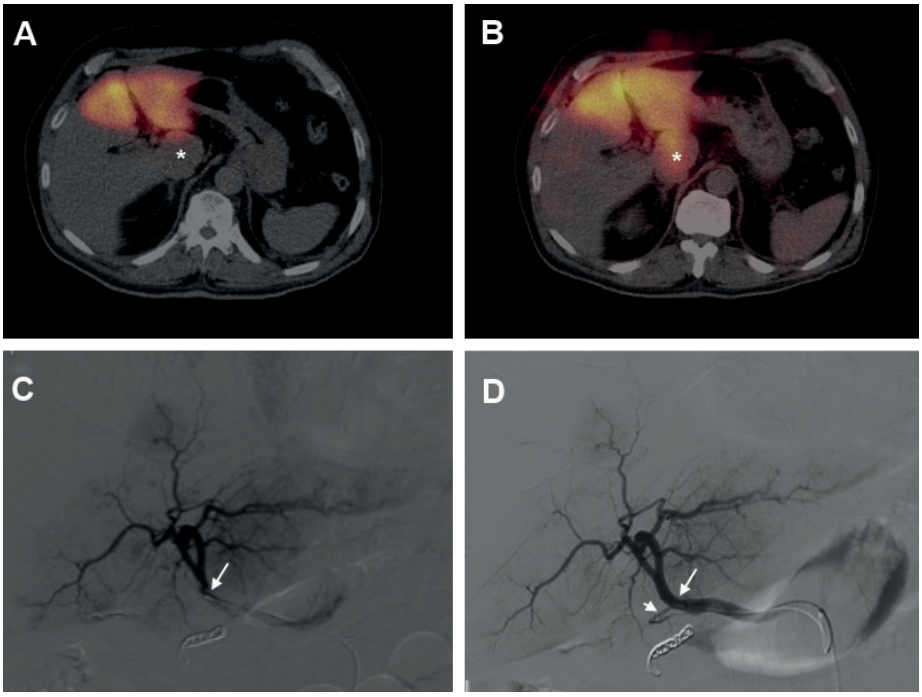

Figure 7. *Left-sided treatment of a 72-year-old patient with uveal melanoma liver metastases. The pre-treatment ^{99m}Tc-MAA SPECT images (A) showed substantial distribution differences in comparison with the post-treatment ^{90}Y SPECT images (B), especially in the caudate lobe (*). The injection position during ^{99m}Tc-MAA administration (C) and ^{90}Y administration (D) was also different. Digital subtraction angiography images show the catheter tip (long arrow) positioned in the left hepatic artery. At ^{90}Y administration the catheter tip was located proximal to a significant side branch (short arrow) probably supplying the caudate lobe. The catheter was distal to this branch during ^{99m}Tc-MAA administration.*

position. A relative difference of >10%, >20%, and >30% was found in, respectively, 54 (79%), 33 (49%), and 24 (35%) of the 68 segments for procedures with a suboptimal agreement on catheter tip position and in 100 (64%), 64 (41%), and 47 (30%) of the 157 segments for procedures with an optimal agreement on catheter tip position (Fig.7). This reached significance for the cutoff value of >10% (P = 0.020) but not for >20% (P = 0.307) and >30% (P = 0.438). Significant differences were not found between procedures with the catheter tip near a major bifurcation (<10 mm) and procedures without, as long as the position was the same during the ^{99m}Tc- MAA and the ^{90}Y injection. In procedures with the catheter tip close to a major bifurcation, as well as suboptimal agreement in catheter position between the ^{99m}Tc-MAA and the ^{90}Y injection, a significant difference in activity distribution was found. A relative difference of >10%, >20%, and >30% was found in, respectively, 19 (95%), 12 (60%), and 9 (45%) of the 20

segments for procedures with these 2 characteristics, and in 133 (65%), 85 (41%), and 62 (31%) of the 205 segments for procedures without. This reached significance for the cutoff value of >10% (P = 0.005) but not for >20% (P = 0.155) and >30% (P = 0.209). Evaluation of other parameters, including other combinations of parameters, did not yield any significant results. Procedures in patients with colorectal metastases (relatively hypovascular tumors) did not show any difference from procedures in patients with more hypervascular tumors, nor did treatment approach with regard to left lobar versus right lobar treatments.

Discussion

It is expected that patients can benefit from individualized treatment planning.[10] Most promising in this regard is the so-called partition model. This method was previously shown to accurately predict treatment response and survival.[11,20] The expected absorbed dose to the tumor is calculated on ^{99m}Tc-MAA SPECT. The tumors are delineated on morphologic images, whereas the dose distribution is estimated by calculation of ^{99m}Tc-MAA in the tumors, the normal liver, and the lungs. The prescribed activity may be calculated such that it does not exceed the maximum safe absorbed dose to the normal liver and lungs. Agreement between ^{99m}Tc-MAA and subsequent ^{90}Y is therefore crucial for the accuracy of the partition method.

The presented data, however, show a substantial disagreement between ^{99m}Tc- MAA and ^{90}Y activity distribution. In 68% of all segments, a difference of >10% between ^{99m}Tc-MAA and ^{90}Y activity distribution was found. In every procedure, at least 1 segment showed a >10% difference. These findings raise concern about the validity of the partition method. However, regardless of the found disagreement, early studies were able to show the accuracy of the partition method nevertheless, although dose–effect relationships with regard to toxicity on the normal liver parenchyma were ignored.[11,20] Knowledge of the existence, the magnitude, and the etiology of disagreement between ^{99m}Tc-MAA and ^{90}Y activity distribution should ultimately lead to the improved validity of these methods. Specific technical and methodological recommendations may help to overcome this issue. Knesaurek *et al.* visually assessed the correlation between ^{99m}Tc-MAA and ^{90}Y-distribution and found that correlation could vary from poor to relatively good (voxel-based Spearman rank correlation varied from 0.451 to 0.818).[21] However, their methodology is questionable. Their correlations indicate that ^{90}Y activity is higher when ^{99m}Tc-MAA is higher. This does not imply that for individual measurements, the distributions are equal to (or close approximations of) each other. Agreement as described by Bland and Altman[18] is a more appropriate method of comparing two measurements of the same variable (*i.e.* activity distribution).

There are several factors that may have caused the disagreement in ^{99m}Tc-MAA and ^{90}Y distribution. First, difference in catheter position between the two procedures seems to be a key factor. Although the catheter tip was positioned at the same location, small deviations (approximately 5–10 mm) were still found. A significantly increased disagreement between ^{99m}Tc-MAA and ^{90}Y distribution was found in these procedures. In another study with more substantial differences in catheter tip position between the ^{99m}Tc-MAA and subsequent ^{90}Y procedure, investigators found that position differences ($P < 0.001$) and a catheter position close to important side branches or bifurcations ($P < 0.01$) led to significant visually assessed distribution differences between ^{99m}Tc- MAA and ^{90}Y.[12] In the current study, we confirmed this finding quantitatively. In particular, patients with a mismatch in catheter tip position and injections close to a bifurcation showed significant disagreement. Selective administration of microspheres distal to the proper hepatic artery may largely overcome this issue. It was already shown that selective administrations are beneficial to prevent extrahepatic deposition of microsphere activity.[22] In addition, differences in the intraluminal cross-sectional position of the catheter tip may have influenced the disagreement (*Figure 7*). These differences are known to cause substantial differences in preferential flow.[23-25] Innovative catheter designs with spacers to keep the catheter tip centered in the arterial lumen during injection may lead to more comparable injection positions and subsequent improved agreement between ^{99m}Tc-MAA and ^{90}Y activity distribution.[26]

Second, differences in the number, density, size, and morphology of the radiopharmaceuticals may also have resulted in a different activity distribution. The number of ^{99m}Tc-MAA particles (1–2 x 10^5 particles) is significantly lower than the number of ^{90}Y microspheres applied (resin: 40–80 x 10^6; glass: 1.2–8 x 10^6 particles), whereas the density of ^{99m}Tc- MAA particles (1.1 g/mL) is lower than that of ^{90}Y microspheres (resin: 1.6 g/mL; glass: 3.3 g/mL).[27-29] The particle size distribution of ^{99m}Tc-MAA is such that over 90% are within 10–90 mm in size (mean, 15 mm). The mean size of ^{90}Y microspheres is 32 ± 10 mm, and the morphology of the spheric ^{90}Y microspheres is also considerably different from the macro-aggregated random shape of ^{99m}Tc-MAA particles.[27] The embolization effect of the much larger number of ^{90}Y-microspheres may result in flow alterations that alter the distribution of the particles.

Third, the use of bremsstrahlung ^{90}Y SPECT after treatment leads to a degree of blurring and quantitative uncertainty. To overcome this methodological problem, we chose to evaluate larger segment-based volumes instead of using a voxel-based analysis. The uncertainty in stochastic effects that are responsible for the measurement accuracy is far less in larger volumes. Larger VOIs were also useful to overcome quantification errors caused by coregistration artifacts. As a consequence, we were able to study quan-

titative distribution differences on only a segmental level. Any existing disagreement will be underestimated, since differences in certain areas of the segment may level out differences in other areas. One way to improve part of the methodology may be the use of ^{90}Y-PET imaging instead of SPECT. PET facilitates more accurate quantification based on improved spatial resolution and may aid in the study of distribution on a subsegmental or tumor level.[30-32] And lastly, the studied population was a heterogeneous group with regard to the histopathology of the primary tumor. We could not differentiate whether histopathologic features had any influence on the results. Remarkable was the finding that a larger degree of tumor involvement was associated with a better agreement between ^{99m}Tc-MAA and ^{90}Y. This finding may be due to a lesser degree of random distribution of activity.

On one hand, the results lead to concerns about the agreement between ^{99m}Tc-MAA and ^{90}Y distribution and, consequently, the validity of activity calculation methods that are based on the assumption of agreement, such as the partition method. On the other hand, it has been shown that, although based on the false assumption of agreement, the partition method still offers huge advantages over existing methods with regard to the prediction of treatment outcome and individualized treatment planning. This may be explained by the fact that the partition method is prescribed only for patients with a limited number of hypervascular tumors. Our results show that the agreement between ^{99m}Tc-MAA and ^{90}Y distribution in segments with a high tumor involvement is considerably better. Moreover, these patients are generally treated super-selectively, beyond the major bifurcation of the proper hepatic artery, and also with fewer embolic glass microspheres. All these factors seem to contribute to a better agreement between ^{99m}Tc- MAA and ^{90}Y distribution.

On the basis of the current study, the following two recommendations may lead to optimization of the predictive value of a pretreatment scout dose. First, the catheter tip should be placed in exactly the same position during both procedures, possibly augmented by the use of catheters that center the tip within the lumen; second, for each administration, the catheter tip should be placed distal to major bifurcations, with selective administration in each branch to prevent preferential flow. In patients with large hypervascular tumors limited to a single lobe, the agreement between ^{99m}Tc-MAA and ^{90}Y distribution is best, but caution should be taken in patients with multiple small liver metastases in both lobes, especially when an embolic effect of the microspheres is anticipated. The latter could be the case in patients who are treated with high-dosage resin microspheres and have small livers and prior treatments with anti-angiogenic drugs such as bevacizumab. To overcome the limitations of ^{99m}Tc-MAA as a scout dose, our group has developed a new generation of microspheres for multimodality ima-

ge-guided radioembolization: ^{166}Ho-poly(L-lactic acid) microspheres.[33] The radioisotope ^{166}Ho is embedded in microspheres of poly(L-lactic acid). It emits β-radiation (half-life, 26.8 h; maximum energy, 1.77 and 1.85 MeV) and γ-radiation (γ-energy, 80.6 keV) and is paramagnetic, because the element holmium is chemically part of the lanthanide group, like gadolinium.[34-36] The microspheres can be visualized in vivo with several clinical imaging modalities, including SPECT and MR imaging.[14,37,38] The particles used for pretreatment evaluation and actual treatment are exactly the same, and SPECT and MR imaging are used to combine high sensitivity with high spatial-temporal resolution and superior soft-tissue contrast to optimize dosimetry before and after treatment. The performance of ^{166}Ho-microspheres as a scout dose to predict distribution of the therapy dose is currently under investigation.

Conclusion

Individualized treatment planning methods may be used for optimized safety and efficacy of radioembolization treatments. By definition, these methods are based on predictive scout dose distribution within the target volume. The limited agreement between ^{99m}Tc-MAA and ^{90}Y distribution in current clinical practice raises concern about the validity of these methods. Care should be taken to use proper administration techniques to overcome this limitation.

References

1. Kennedy A, Coldwell D, Sangro B, Wasan H, Salem R (2012) Radioembolization for the treatment of liver tumors general principles. American journal of clinical oncology 35: 91-99.
2. Sangro B, Salem R, Kennedy A, Coldwell D, Wasan H (2011) Radioembolization for hepatocellular carcinoma: a review of the evidence and treatment recommendations. Am J Clin Oncol 34: 422-431.
3. Coldwell D, Sangro B, Salem R, Wasan H, Kennedy A (2012) Radioembolization in the treatment of unresectable liver tumors: experience across a range of primary cancers. Am J Clin Oncol 35: 167-177.
4. Lewandowski RJ, Sato KT, Atassi B, Ryu RK, Nemcek AA, Jr., et al. (2007) Radioembolization with ^{90}Y microspheres: angiographic and technical considerations. Cardiovasc Intervent Radiol 30: 571-592.
5. Dezarn WA, Cessna JT, DeWerd LA, Feng W, Gates VL, et al. (2011) Recommendations of the American Association of Physicists in Medicine on dosimetry, imaging, and quality assurance procedures for ^{90}Y microsphere brachytherapy in the treatment of hepatic malignancies. Med Phys 38: 4824-4845.
6. Lenoir L, Edeline J, Rolland Y, Pracht M, Raoul JL, et al. (2012) Usefulness and pitfalls of MAA SPECT/CT in identifying digestive extrahepatic uptake when planning liver radioembolization. Eur J Nucl Med Mol Imaging 39: 872-880.
7. Ho S, Lau WY, Leung TW, Chan M, Ngar YK, et al. (1996) Partition model for estimating radiation doses from yttrium-90 microspheres in treating hepatic tumours. Eur J Nucl Med 23: 947-952.
8. Ho S, Lau WY, Leung TW, Chan M, Chan KW, et al. (1997) Tumour-to-normal uptake ratio of ^{90}Y microspheres in hepatic cancer assessed with 99Tcm macroaggregated albumin. Br J Radiol 70: 823-828.
9. Ho S, Lau WY, Leung TW, Chan M, Johnson PJ, et al. (1997) Clinical evaluation of the partition model for estimating radiation doses from yttrium-90 microspheres in the treatment of hepatic cancer. Eur J Nucl Med 24: 293-298.
10. Lau WY, Kennedy AS, Kim YH, Lai HK, Lee RC, et al. (2012) Patient selection and activity planning guide for selective internal radiotherapy with yttrium-90 resin microspheres. Int J Radiat Oncol Biol Phys 82: 401-407.
11. Kao YH, Hock Tan AE, Burgmans MC, Irani FG, Khoo LS, et al. (2012) Image-guided personalized predictive dosimetry by artery-specific SPECT/CT partition modeling for safe and effective ^{90}Y radioembolization. J Nucl Med 53: 559-566.
12. Jiang M, Fischman A, Nowakowski FS (2012) Segmental Perfusion Differences on Paired Tc-99m Macroaggregated Albumin (MAA) Hepatic Perfusion Imaging and Yttrium-90 (Y-^{90}) Bremsstrahlung Imaging Studies in SIR-Sphere Radioembolization: Associations with Angiography. Journal of Nuclear Medicine & Radiation Therapy 03.
13. Kennedy A, Nag S, Salem R, Murthy R, McEwan AJ, et al. (2007) Recommendations for radioembolization of hepatic malignancies using yttrium-90 microsphere brachytherapy: a consensus panel report from the radioembolization brachytherapy oncology consortium. Int J Radiat Oncol Biol Phys 68: 13-23.

14. Elschot M, Nijsen JF, Dam AJ, de Jong HW (2011) Quantitative evaluation of scintillation camera imaging characteristics of isotopes used in liver radioembolization. PLoS One 6: e26174.

15. Bismuth H (1982) Surgical anatomy and anatomical surgery of the liver. World J Surg 6: 3-9.

16. Bol GH, Kotte AN, van der Heide UA, Lagendijk JJ (2009) Simultaneous multi-modality ROI delineation in clinical practice. Comput Methods Programs Biomed 96: 133-140.

17. Gulec SA, Mesoloras G, Stabin M (2006) Dosimetric techniques in ^{90}Y-microsphere therapy of liver cancer: The MIRD equations for dose calculations. J Nucl Med 47: 1209-1211.

18. Bland JM, Altman DG (1986) Statistical methods for assessing agreement between two methods of clinical measurement. Lancet 1: 307-310.

19. Bland JM, Altman DG (1995) Comparing methods of measurement: why plotting difference against standard method is misleading. Lancet 346: 1085-1087.

20. Garin E, Lenoir L, Rolland Y, Edeline J, Mesbah H, et al. (2012) Dosimetry based on ^{99m}Tc-macroaggregated albumin SPECT/CT accurately predicts tumor response and survival in hepatocellular carcinoma patients treated with ^{90}Y-loaded glass microspheres: preliminary results. J Nucl Med 53: 255-263.

21. Knesaurek K, Machac J, Muzinic M, DaCosta M, Zhang Z, et al. (2010) Quantitative comparison of yttrium-90 (^{90}Y)-microspheres and technetium-99m (^{99m}Tc)-macroaggregated albumin SPECT images for planning ^{90}Y therapy of liver cancer. Technol Cancer Res Treat 9: 253-262.

22. Barentsz MW, Vente MA, Lam MG, Smits ML, Nijsen JF, et al. (2011) Technical solutions to ensure safe yttrium-90 radioembolization in patients with initial extrahepatic deposition of (^{99m})technetium-albumin macroaggregates. Cardiovasc Intervent Radiol 34: 1074-1079.

23. Kao YH, Tan EH, Teo TK, Ng CE, Goh SW (2011) Imaging discordance between hepatic angiography versus Tc-99m-MAA SPECT/CT: a case series, technical discussion and clinical implications. Ann Nucl Med 25: 669-676.

24. Kennedy AS, Kleinstreuer C, Basciano CA, Dezarn WA (2010) Computer modeling of yttrium-90-microsphere transport in the hepatic arterial tree to improve clinical outcomes. Int J Radiat Oncol Biol Phys 76: 631-637.

25. Basciano CA, Kleinstreuer C, Kennedy AS, Dezarn WA, Childress E (2010) Computer modeling of controlled microsphere release and targeting in a representative hepatic artery system. Ann Biomed Eng 38: 1862-1879.

26. Rose SC, Kikolski SG, Chomas JE (2012) Downstream Hepatic Arterial Blood Pressure Changes Caused by Deployment of the Surefire AntiReflux Expandable Tip. Cardiovasc Intervent Radiol: [Epub ahead of print].

27. Bult W, Vente MA, Zonnenberg BA, Van Het Schip AD, Nijsen JF (2009) Microsphere radioembolization of liver malignancies: current developments. Q J Nucl Med Mol Imaging 53: 325-335.

28. Sirtex (2013) SIR-Spheres Yttrium-90 Resin Microspheres Package Insert.

29. Lewandowski RJ, Riaz A, Ryu RK, Mulcahy MF, Sato KT, et al. (2009) Optimization of radioembolic effect with extended-shelf-life yttrium-90 microspheres: results from a pilot study. J Vasc

Interv Radiol 20: 1557-1563.

30. Lhommel R, van Elmbt L, Goffette P, Van den Eynde M, Jamar F, et al. (2010) Feasibility of ^{90}Y TOF PET-based dosimetry in liver metastasis therapy using SIR-Spheres. Eur J Nucl Med Mol Imaging 37: 1654-1662.
31. Gates VL, Esmail AA, Marshall K, Spies S, Salem R (2011) Internal pair production of ^{90}Y permits hepatic localization of microspheres using routine PET: proof of concept. J Nucl Med 52: 72-76.
32. Kao YH, Tan EH, Ng CE, Goh SW (2011) Yttrium-90 time-of-flight PET/CT is superior to Bremsstrahlung SPECT/CT for postradioembolization imaging of microsphere biodistribution. Clin Nucl Med 36: e186-187.
33. Smits ML, Nijsen JF, van den Bosch MA, Lam MG, Vente MA, et al. (2012) Holmium-166 radioembolisation in patients with unresectable, chemorefractory liver metastases (HEPAR trial): a phase 1, dose-escalation study. Lancet Oncol 13: 1025-1034.
34. Nijsen JF, Zonnenberg BA, Woittiez JR, Rook DW, Swildens-van Woudenberg IA, et al. (1999) Holmium-166 poly lactic acid microspheres applicable for intra-arterial radionuclide therapy of hepatic malignancies: effects of preparation and neutron activation techniques. Eur J Nucl Med Mol Imaging 26: 699-704.
35. Zielhuis SW, Nijsen JF, Seppenwoolde JH, Zonnenberg BA, Bakker CJ, et al. (2005) Lanthanide bearing microparticulate systems for multi-modality imaging and targeted therapy of cancer. Current medicinal chemistry Anti-cancer agents 5: 303-313.
36. Zielhuis SW, Nijsen JF, de Roos R, Krijger GC, van Rijk PP, et al. (2006) Production of GMP-grade radioactive holmium loaded poly(L-lactic acid) microspheres for clinical application. Int J Pharm 311: 69-74.
37. Seevinck PR, Seppenwoolde JH, de Wit TC, Nijsen JF, Beekman FJ, et al. (2007) Factors affecting the sensitivity and detection limits of MRI, CT, and SPECT for multimodal diagnostic and therapeutic agents. Anticancer Agents Med Chem 7: 317-334.
38. van de Maat GH, Seevinck PR, Elschot M, Smits ML, de Leeuw H, et al. (2013) MRI-based biodistribution assessment of holmium-166 poly(L-lactic acid) microspheres after radioembolisation. Eur Radiol 23: 827-835.

Chapter 9

Value of ^{99m}Tc-Macroaggregated Albumin SPECT for Radioembolization Treatment Planning

MGEH Lam, MLJ Smits

Journal of Nuclear Medicine 2013

The recent work by Ulrich *et al.*[1] discussed the value of intratumoral ^{99m}Tc-macroaggregated albumin (MAA) distribution to predict treatment outcome after ^{90}Y-radioembolization in patients with colorectal cancer liver metastasis. Their results demonstrated that response was independent of the degree of intratumoral ^{99m}Tc-MAA uptake. This is an important and interesting finding, but it should be interpreted with caution. Several studies have shown that pretherapeutic dosimetric calculations based on ^{99m}Tc-MAA distribution may lead to improved treatment planning methods based on tumor dosimetry.[2,3] Because these developments are expected to lead to a paradigm shift in radioembolization treatment planning, from empiric methods to individualized treatment planning, it is critical that we carefully evaluate all aspects of scout dose imaging for radioembolization treatment planning. It is imperative to emphasize the importance of optimized scout dose imaging. Some additional comments may therefore be relevant to their research.

The presented study confirmed previous findings on the questionable prognostic value of pretherapeutic ^{99m}Tc-MAA distribution.[4] In our series we found a difference in activity distribution between ^{99m}Tc-MAA and ^{90}Y of at least 10% in as many as 153 (68%) of 225 segments in 39 procedures.[5] However, instead of correlating ^{99m}Tc-MAA distribution to post-therapeutic ^{90}Y distribution, the presented study correlated pretherapeutic ^{99m}Tc-MAA directly with parameters of efficacy. This methodology lacks an important stepwise approach.

First, the predictive value of pretherapeutic ^{99m}Tc-MAA should be evaluated to predict post-therapeutic ^{90}Y distribution, and subsequently, post-therapeutic ^{90}Y distribution should be compared with treatment outcome, both quantitatively. Otherwise, ^{90}Y distribution poses a significant confounding factor. Technical aspects of radioembolization are especially important for step 1, whereas clinical and biologic aspects of dose–response will influence step 2. Distribution differences between ^{99m}Tc-MAA and ^{90}Y are influenced by catheter tip position differences during the administration of both agents. This should be looked at in detail. Very small subcentimeter differences, as well as positioning the tip close to major bifurcations and side branches, may cause substantial differences in distribution.[4,5] But also the in-plane cross-sectional position of the catheter tip causes distribution variations.[6] Close attention to catheter tip positioning, possibly augmented by special catheters designed to fix the centriluminal positioning of the tip [7], will likely improve the predictive value of ^{99m}Tc-MAA scout dose imaging. Besides, an agent that better resembles the treatment device may replace ^{99m}Tc-MAA. For this purpose our group recently introduced new-generation microspheres for hepatic radioembolization: ^{166}Ho microspheres.[8] These microspheres offer accurate pre- and post-therapeutic quantitative imaging by SPECT (81 keV) and MR imaging (pa-

ramagnetic properties) but also offer effective treatment by b-radiation (half-life, 27 h; 1.8 MeV).

Second, dose–response relationships have not been fully established yet. The previously mentioned publications on partition modeling were among the first to show such effects, but these studies were limited to hepatocellular carcinoma only. Interestingly, it was shown that the pattern of activity uptake around the tumor influenced the response to radioembolization.[3] This was caused by variations in tumor perfusion, depending on location, and should be accounted for during treatment planning. Establishing such methods for multiple lesions in both liver lobes, such as colorectal cancer liver metastasis, is a great challenge because each tumor needs to be evaluated separately. The reported response in this cell type is very low (in the presented study only 10.4% at 3 months). It is not yet clear whether this is caused by resistance to radiation or by underdosing, but proper dosimetry should further elucidate these issues. Nevertheless, it is expected that individualized treatment planning based on pretherapeutic dosimetry will ultimately lead to improved efficacy and toxicity. Because the response in the presented study was too little to reveal any relation with activity distribution, the authors used a suboptimal response parameter (*i.e.* size change). It is also important that we stick to validated endpoints, including survival, for future investigation.[9]

Negative results should not lead to cessation of our quest for optimized dosimetry, since these results do not necessarily imply that no relation exists. They merely, but importantly, tell us that we should overcome the limitations that lead to these negative findings, in order to establish validated methods for individualized pretherapeutic treatment planning.

References

1. Ulrich G, Dudeck O, Furth C, Ruf J, Grosser OS, et al. (2013) Predictive value of intratumoral ^{99m}Tc-macroaggregated albumin uptake in patients with colorectal liver metastases scheduled for radioembolization with ^{90}Y-microspheres. J Nucl Med 54: 516-522.
2. Garin E, Lenoir L, Rolland Y, Edeline J, Mesbah H, et al. (2012) Dosimetry based on ^{99m}Tc-macroaggregated albumin SPECT/CT accurately predicts tumor response and survival in hepatocellular carcinoma patients treated with ^{90}Y-loaded glass microspheres: preliminary results. J Nucl Med 53: 255-263.
3. Kao YH, Hock Tan AE, Burgmans MC, Irani FG, Khoo LS, et al. (2012) Image-guided personalized predictive dosimetry by artery-specific SPECT/CT partition modeling for safe and effective ^{90}Y radioembolization. J Nucl Med 53: 559-566.
4. Jiang M, Fischman A, Nowakowski FS (2012) Segmental Perfusion Differences on Paired Tc-99m Macroaggregated Albumin (MAA) Hepatic Perfusion Imaging and Yttrium-90 (Y-90) Bremsstrahlung Imaging Studies in SIR-Sphere Radioembolization: Associations with Angiography. Journal of Nuclear Medicine & Radiation Therapy 03.
5. Wondergem M, Smits ML, Elschot M, de Jong HW, Verkooijen HM, et al. (2013) ^{99m}Tc-Macroaggregated Albumin Poorly Predicts the Intrahepatic Distribution of ^{90}Y Resin Microspheres in Hepatic Radioembolization. J Nucl Med.
6. Kennedy AS, Kleinstreuer C, Basciano CA, Dezarn WA (2010) Computer modeling of yttrium-90-microsphere transport in the hepatic arterial tree to improve clinical outcomes. Int J Radiat Oncol Biol Phys 76: 631-637.
7. Rose SC, Kikolski SG, Chomas JE (2012) Downstream Hepatic Arterial Blood Pressure Changes Caused by Deployment of the Surefire AntiReflux Expandable Tip. Cardiovasc Intervent Radiol: [Epub ahead of print].
8. Smits ML, Nijsen JF, van den Bosch MA, Lam MG, Vente MA, et al. (2012) Holmium-166 radioembolisation in patients with unresectable, chemorefractory liver metastases (HEPAR trial): a phase 1, dose-escalation study. Lancet Oncol 13: 1025-1034.
9. Salem R, Lewandowski RJ, Gates VL, Nutting CW, Murthy R, et al. (2011) Research reporting standards for radioembolization of hepatic malignancies. J Vasc Interv Radiol 22: 265-278.

Chapter 10

Imageable radioactive holmium-166 microspheres for treatment of liver malignancies: in vivo dosimetry based on SPECT and MRI

MLJ Smits, M Elschot, MAAJ van den Bosch, GH van de Maat, AD van het Schip, BA Zonnenberg, PR Seevinck, HM Verkooijen, CJ Bakker, HWAM de Jong, MGEH Lam, JFW Nijsen

Journal of Nuclear Medicine 2013

Holmium-166 (^{166}Ho) poly(L-lactic acid) microspheres allow for quantitative imaging with magnetic resonance imaging (MRI) and/or Single Photon Emission Computed Tomography (SPECT) for microsphere biodistribution assessment post radioembolization (RE). The purpose of this study was to evaluate SPECT- and MRI-based dosimetry in the first patients treated with ^{166}Ho-RE.

Materials and Methods

Fifteen patients with unresectable, chemorefractory liver metastases of any origin were enrolled in this phase 1 study and were treated with ^{166}Ho-RE according to a dose escalation protocol (20 Gy – 80 Gy). The contours of all liver segments and all discernible tumors were manually delineated on T_2-weighted post-treatment MRI and registered to the post-treatment SPECT images (n = 9) or SPECT-CT images (n = 6) and MRI-based R_2*-maps (n = 14). Dosimetry was performed based on SPECT (n = 15) and MRI (n = 9) for all volumes of interest, tumor-to-non-tumor activity concentration (T/N) ratios were calculated and correlation and agreement of MRI- and SPECT-based measurements were evaluated.

Introduction

Radioembolization (RE) is an interventional oncologic treatment during which radioactive microspheres are administered in the arterial vessels supplying the liver and its tumors. The rationale behind this and some other intra-arterial liver cancer treatments is that liver tumors are predominantly supplied by arterial blood, in contrast to the non-tumorous liver, which relies mainly on the portal vein for its blood supply. Injection of a substance in the hepatic artery will therefore selectively reach the tumorous tissue.[1] Currently, the microspheres used for radioembolization that are commercially available are labeled with yttrium-90 (^{90}Y). In order to be able to quantitatively evaluate the optimal and selective distribution of microspheres to the liver tumors, post-treatment imaging is indispensable. For that reason, optimization of post-treatment imaging of ^{90}Y-microspheres with bremsstrahlung Single Photon Emission Computed Tomography (SPECT) and Positron Emission Tomography (PET) has recently gained interest.[2-5]

Holmium-166 poly(L-lactic acid) (^{166}Ho) microspheres have been developed at our institute as an alternative to ^{90}Y-microspheres specifically in order to be able to visualize the in vivo biodistribution of microspheres after radioembolization. ^{166}Ho-microspheres have the advantage to be quantitatively imageable with both SPECT and magnetic

act

Results

The median overall T/N ratio was 1.4 based on SPECT (range 0.9 – 2.8) and 1.4 based on MRI (range 1.1 – 3.1). In six of fifteen patients (40%) all tumors had received an activity-concentration equal to or higher than the normal liver (T/N ratio ≥1). Analysis of SPECT and MRI-measurements for dose to liver segments yielded a high correlation (R^2 = 0.91) and a moderate agreement (mean bias: 3.7 Gy, 95% limits of agreement: -11.2 – 18.7).

Conclusion

Using ^{166}Ho-microspheres, in-vivo dosimetry is feasible based on both SPECT and MRI, which enables personalized treatment by selectively targeting of inadequately treated tumors.

resonance imaging (MRI), utilizing the emission of gamma-photon radiation and the paramagnetic properties of holmium, respectively.[6-10] Exploiting these qualities, multimodal dosimetry becomes feasible with a range of possibilities.

We performed a phase 1 clinical trial, purposed to assess the safety and toxicity of ^{166}Ho-RE in patients for the first time[11] and to investigate the feasibility of quantitative imaging of the biodistribution of microspheres within the liver based on SPECT and MRI. We now present the results of dosimetry based on SPECT and MR imaging of ^{166}Ho-microspheres in the patients of this phase 1 trial.

Materials and Methods

Microspheres

Ho-poly(L-lactic acid) microspheres with a mean diameter of 30 μm (range 20 – 50 μm) were produced at the University Medical Center Utrecht compliant with good manufacturing practice regulations, as described previously.[12,13] The holmium, which was homogeneously incorporated into these microspheres (18.7% weight/weight ratio), was used as a radioactive isotope for tumor destruction using its beta-radiation ($E_{\beta max}$

= 1.77 MeV and $E_{\beta max}$ = 1.85 MeV, I_{β} = 48.7% and 50.0%, respectively; $T_{1/2}$ = 26.8 h) and for SPECT imaging using its gamma-radiation (E_{γ} = 80.6 keV; I_{γ} = 6.7%), and as a contrast agent for MRI. For each treatment, a total of approximately 600mg of non-radioactive Ho-microspheres were packed in high-density polyethylene vials (Posthumus Plastics, Beverwijk, the Netherlands). The Ho-microspheres were then activated by neutron-irradiation in the nuclear reactor of the Reactor Institute Delft (Delft University of Technology, Delft, the Netherlands) during the night before a treatment session. After irradiation, the vials were shipped back to the University Medical Center where, prior to treatment, the total amount of activity was measured (using a dose calibrator: VDC-404, Veenstra Instrumenten, Joure, the Netherlands) and the quality of microspheres was checked (particle integrity assessment and particle size measurement).

Patients

Patients with unresectable, chemorefractory liver metastases of any origin were included in this phase 1 dose-escalation study on ^{166}Ho-RE. The design[14], and clinical results (patient characteristics, toxicity and adverse events)[11] of this study have been described previously. In short, patients needed to be at least 18 years of age, have an estimated life expectancy of at least 3 months, a World Health Organization (WHO) performance status of 0 – 2, at least one measurable lesion of ≥ 10 mm on CT, and a negative pregnancy test for women. Exclusion criteria were: an impaired hematological function (leukocytes < 4.0 10^9/l, platelet count < 150 10^9/l), an impaired renal function (serum creatinine > 185 μmol/l), an impaired cardiac function (relevant morphology on electrocardiography or New York Heart Association classification of heart disease ≥ 2), an impaired hepatic function (alanine aminotransferase, aspartate aminotransferase, or alkaline phosphatase > 5 times the upper limit of normal, or serum bilirubin > 1.5 times the upper limit of normal), having received chemotherapy or abdominal surgery within four weeks prior to inclusion, incompletely healed surgical incision, and contraindications for MRI. All patients provided written informed consent before enrolment. The study was approved by the institutional review board and the study was registered with Clinicaltrials.gov, number NCT01031784.

Study Design and Treatment

Patients were treated in four consecutive cohorts of 3 – 6 patients (depending on the occurrence of any dose limiting toxicity). Each cohort was scheduled for treatment with escalating desired whole-liver absorbed doses of ^{166}Ho-RE (20 Gy, 40 Gy, 60 Gy, and 80 Gy). The required amount of activity was calculated according to the following formula[9]:

A_{Ho166} (MBq) = D_{liver} (Gy) x 63 (MBq/J) x LW (kg)

Where A_{Ho166} is the administered activity, LW is the liver weight calculated by delineation on contrast-enhanced CT-images (assuming a tissue density of 1.06 g/cm^3)[15], and D_{liver} is the desired whole-liver absorbed dose.

Lesion vascularity, guided by arterial enhancement patterns as described in "Spiral and Multislice Computed Tomography of the Body"[16], was evaluated on baseline 3-phasic CT imaging by one of the investigators (MS). Patients underwent a standard work-up angiography during which the hepatic arterial vasculature was investigated and several non-target vessels, arising from the hepatic artery and leading to organs other than the liver, were coil-embolized. Subsequently, 150 MBq of ^{99m}Tc-MAA (0.8 mg, TechneScan LyoMaa, Mallinckrodt Medical B.V., Petten, the Netherlands) was administered through a microcatheter in the hepatic artery and the distribution was checked with (planar) scintigraphy and SPECT(/CT). If there was no extrahepatic distribution of activity, except for a lung shunt fraction of maximally 20%, the patients were scheduled for treatment generally one to two weeks after the work-up angiography. On the day of treatment, a microcatheter was angiographically placed as close as possible to the position of the ^{99m}Tc-MAA injection. Subsequently, a scout dose (60 mg, approximately 250 MBq) and a therapy dose of ^{166}Ho-microspheres (540 mg, varying activities, see *Table 1*) were injected with MR-imaging and scintigraphy and SPECT(/CT) in between. The scout dose was used to increase the safety of the procedure.

SPECT Imaging

SPECT images of the ^{166}Ho-microsphere distribution were acquired three to six days after administration of ^{166}Ho-microspheres, using a FORTE™ SPECT system (Philips Medical Systems, Milpitas, CA, USA) system (n = 9) or a Symbia T16 SPECT-CT system (Siemens Healthcare, Erlangen, Germany) (n = 6). The FORTE dual-headed gamma camera was equipped with ^{153}Gd scanning line-sources for transmission CT for attenuation correction. Medium energy collimators were used on both systems. Energy windows were set to 80.6 keV (15% window width) for the ^{166}Ho-photopeak and 118 keV (12%) for correction for down-scattered high-energy photons. 120 projections of 30 seconds were acquired in a 180° (FORTE) or 360° (Symbia T16) orbit around the liver. Data were reconstructed to a 128 x 128 x 128 matrix with an isotropic voxel size of 4.7 mm (FORTE) or 4.8 mm (Symbia T16), using an ordered subsets expectation maximization (OSEM) algorithm including resolution recovery and a hybrid method for scatter and attenuation correction.[6]

MRI

MRI was performed shortly before and 1 week after ^{166}Ho-RE, using a 1.5-T whole body system (Achieva, Philips Healthcare, Best, the Netherlands) equipped with a

16-element torso coil. For quantitative measurements of the ^{166}Ho-microsphere-biodistribution, a multi-slice multi-gradient echo (MGE) sequence was used, sampling the MRI signal of the free induction decay. Sixteen gradient echoes with a time spacing of 1.15 ms (first echo time = 1.33 ms) were acquired during breath hold with an in-plane voxel size of 2.0 x 2.0 mm^2 and a slice thickness of 6.0 mm. Other imaging parameters included: field of view: 288 x 384 mm^2, number of slices: 45, repetition time (TR): 440 ms, flip angle: 50°. Sensitivity encoding (SENSE) with a factor of 2.5 was used for acquisition acceleration resulting in an imaging time of 3 x 19 s during breath hold. For anatomical information and delineation of liver segments and tumors, T_2-weighted turbo spin echo (TSE) images were acquired with a FOV and voxel size identical to the previous sequence. Imaging parameters included: TR: 830 ms, echo time: 80 ms, SENSE factor: 2, imaging time: 2 x19 s during breath hold.

Delineation of Volumes of Interest

In order to perform dosimetry on specific liver regions and to be able to validate MRI-based dosimetry with SPECT-based dosimetry as a reference standard, each patient's liver was carefully segmented into a number of VOIs using the in-house developed radiotherapy-planning software package Volumetool, which has been validated and published elsewhere.[17] The T_2-weighted MR images of each patient's liver were used to manually segment the liver into approximately the eight (functionally independent) liver segments according to Bismuth's adaptation of the Couinaud classification[18] and to segment the contours of all discernible tumors at baseline and post treatment (*Figure 1*). Subsequently, the segmented contour of the liver was manually registered to the contour of the liver on post-treatment SPECT images (n = 9) or SPECT-CT images (n = 6) and baseline and post-treatment MRI-derived R_2*-maps.

Quantitative Analysis and Dosimetry

MRI-based absorbed dose maps were generated using previously described and validated methods.[8, 19] In short, R_2^* values were estimated voxelwise from the MGE data using a mono-exponential fitting algorithm weighting all signal amplitudes equally. In order to determine the microsphere-induced change in R_2^* (ΔR_2^*) after therapy, a baseline R_2^* value was subtracted from the post-therapy R_2^* values. This baseline value was, in contrast to the previously described method[19], determined for each VOI separately by the mean R_2^* value of that VOI prior to therapy. Voxelwise concentrations of ^{166}Ho-microspheres were determined from the ΔR_2^* maps by the relationship [^{166}Ho-microspheres] = $\Delta R_2^* / r_2^*$, with $r_2^* = 103\ s^{-1}mL^{-1}mg$ for ^{166}Ho-microspheres with holmium content of 18.9% by weight.[19] Using the voxel volume the total amount of ^{166}Ho-microspheres (mg) in each voxel was determined. This amount of ^{166}Ho-microspheres was then con-

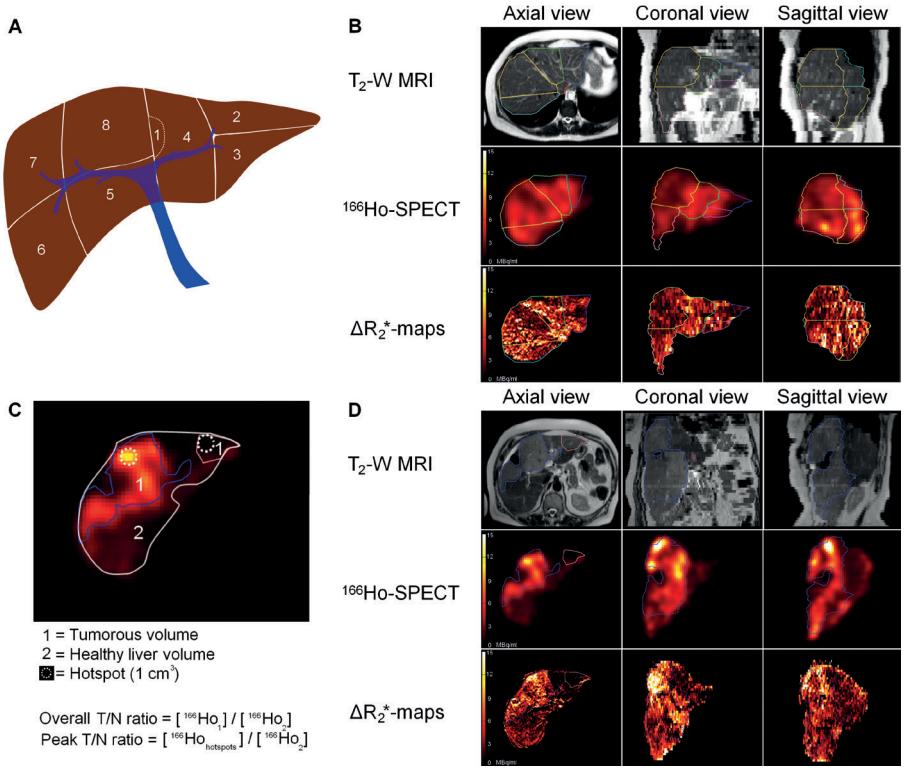

Figure 1. *Delineations distribution assessment. (A) Schematic overview of the volumes of interest (VOIs) that were created of each liver segment (1 – 8) according to Bismuth's adaptation of the Couinaud classification. (B) Top row: delineation of the liver segments on T_2-weighted Magnetic Resonance (MR) images. Middle row: VOIs registered to the holmium-166-Single Photon Emission Computed Tomography (^{166}Ho-SPECT) activity maps. Bottom row: ΔR_2*-based activity maps for the same set of VOIs. The delineation between rows may appear different due to rotation in multiple planes for registration across modalities. (C) Schematic overview of the tumor VOIs that were created for calculation of tumor-to-non-tumor (T/N) ratios and fine distribution assessment. (D) delineation of tumors. Orientation is the same as for (B). The hotspots for calculation of the peak T/N ratio are not depicted.*

verted into units of activity (MBq) by multiplication with the specific activity of the microspheres. Patients with surgical clips were excluded from analysis of MRI dosimetry because it has been demonstrated that MRI dosimetry is not reliable in these patients.[19]

SPECT-reconstructed counts were converted into units of activity using a calibration factor obtained from a phantom experiment with a uniformly filled cylinder with ^{166}Ho-chloride solution. Absorbed dose maps were calculated by convolution of the SPECT and MRI activity images with a ^{166}Ho 3D dose-point kernel with the appropriate voxel size[8], in accordance with MIRD Pamphlet No. 17.[20] The SPECT and MRI

dose-point kernels were calculated using the Monte Carlo engine MCNPX 2.5.0.[21] Volume, mean/maximum/minimum/peak activity, mean/maximum/minimum/peak radiation absorbed doses, and cumulative dose-volume-histograms were calculated for all VOIs using MATLAB (MathWorks, Natick, MA, USA). The definition of the peak values was derived from the PERCIST criteria, defining it as the mean activity concentration in the 1 cm^3 volume (within a VOI) with the highest activity concentration.[22] Mean tumor-to-non-tumor (T/N) activity concentration ratios, defined as the mean activity concentration in the tumor divided by the mean activity concentration in the non-tumorous liver, and peak T/N activity concentration ratios, defined as the peak activity concentration in the tumor divided by the mean activity concentration in the non-tumorous liver, were calculated per tumor and per patient. CT of the abdomen was performed at 6 and 12 weeks post-treatment for tumor response assessment according to RECIST 1.1.[23] The change in longest diameter of all index lesions (up to five lesions per patient) was plotted against the mean and maximum dose on those lesions for assessment of a dose-response relationship.

SPECT Activity Recovery

To correct for activity spill-in and spill-out effects in SPECT-based dosimetry, activity recovery coefficients (ARCs) for the FORTE-system and the Symbia-system were determined using a cylindrical water phantom with five hot spheres in a cold background (volume = 2.0, 4.1, 8.0, 24.1, and 106.2 mL; [A] = 700 kBq mL^{-1}). The ARCs were calculated as the fraction of the true activity in the sphere that was recovered in the spherical VOI on the SPECT image. Activity recovery curves were created by fitting the ARCs with a dual-exponential function of the shape $ARC = a_1+a_2*\exp(a_3*volume)+a_4*\exp(a_5*volume)$. For each tumor VOI, the corrected T/N ratio was subsequently calculated from the uncorrected (measured) T/N ratio using the following formula:
$T/N_{corrected} = (T/N_{uncorrected} - (1\text{-}ARC)) / ARC$

Statistical Analysis

Activities were expressed in MBq, absorbed doses in Gy, and quantitative values as mean ± SD or median plus range. T/N ratios were stratified for primary tumor type, liver tumor involvement, and tumor vascularity. Linear regression analysis was performed to investigate correlation and Bland Altman analysis was used to express agreement between measurements of two modalities.[24] High agreement was arbitrarily defined as both 95% limits of agreement <10 Gy and >-10 Gy; low agreement as one or more 95% limits of agreement ≥20 Gy or ≤-20 Gy. All other results were defined as moderate agreement.

Results

Treatment

Fifteen patients, mean age 55 y (range 38 – 87 y), with unresectable liver metastases originating from uveal melanoma (n = 6), colorectal cancer (n = 6), cholangiocarcinoma (n = 2), and breast carcinoma (n = 1), were treated with ^{166}Ho-RE. The first cohort (20 Gy) consisted of six patients. The other cohorts (40 Gy, 60 Gy, and 80 Gy) consisted of three patients each. Patient demographics and treatment details are listed in *Table 1*.

Dose to Normal Liver and Tumor

Figure 2 displays a flowchart of the analyses performed in this study. Post-treatment SPECT imaging was performed in all fifteen patients. Tumor dosimetry based on SPECT showed that, on average, the tumorous liver tissue in these patients received a dose of 16.6 Gy (20 Gy-cohort), 44.4 Gy (40 Gy-cohort), 44.7 Gy (60 Gy-cohort), and 59.2 Gy (80 Gy-cohort), whereas the non-tumorous liver tissue received an average dose of 9.6 Gy (20 Gy-cohort), 20.4 Gy (40 Gy-cohort), 33.5 Gy (60 Gy-cohort), and 43.9 Gy (80 Gy-cohort) (*Figure 3*).

The biodistribution of ^{166}Ho-microspheres was heterogeneous (see example of the biodistribution and implications on outcome in *Figure 4*), with the dose to the tumor region varying between and within patients. In thirty-one of the 107 delineated tumors (29%), the activity concentrations were less than the activity concentrations in the normal liver (*i.e.* T/N ratio <1.0). In only six of the fifteen patients (40%), it was found that all tumors had a T/N ratio ≥1.0. The median fraction of the net injected amount of activity lodging in the tumorous tissue as calculated based on SPECT, was 14.8% (range: 1.4 % – 60.7 %). This fraction was linearly related to the fraction of the liver involved by tumor (R^2 = 0.89).

The median overall tumor-to-non-tumor (T/N) ratio for the fifteen included patients was 1.4 (range 0.9 – 2.8). The median peak T/N ratio was 2.0 (range 0.9 – 10.3). Overall T/N ratios were highest for metastases from uveal melanoma (2.2), followed by colorectal cancer (1.5), breast carcinoma (1.4), and cholangiocarcinoma (1.2). Patients with a liver tumor involvement ≥25% had higher median overall- and peak T/N ratios (1.8 overall, 3.6 peak) than patients with liver tumor involvement <25% (1.3 overall, 1.5 peak). Patients with hypervascular tumors as scored on 3-phasic CT imaging had higher median overall T/N ratios (2.6 overall, 3.3 peak) than patients with non-hypervascular tumors (1.3 overall, 1.5 peak) (*Table 2*). From the phantom set-up, activity recovery curves for both SPECT systems were assessed and fitted to a dual-exponential function (*Figure 5*). Corrected for incomplete activity recovery, the median overall T/N ratio was 1.6 (range 1.1 – 3.6).

Table 1. *Demographics, treatment and imaging details*

Baseline characteristics	*n*
No. of patients that underwent ^{166}Ho-RE	15
Gender	
Male	9
Female	6
Age (y)	55 (38-87)
Tumor type (primary)	
Ocular melanoma	6
Colorectal carcinoma	6
Cholangiocarcinoma	2
Breast carcinoma	1
Tumor vascularity	
Hypervascular	3
Hypovascular	10
Centrally hypovascular and peripherally hypervascular	2
Liver tumor involvement	
Absolute fraction	14% (2%-52%)
0% - 25%	10
25% - 50%	4
>50%	1
No. of tumors per patient	5 (1 - 21)
Desired whole-liver absorbed dose	
20 Gy	6
40 Gy	3
60 Gy	3
80 Gy	3
Treatment details	
Bilobar treatment (whole liver treatment in one session)	
Injection from proper or common hepatic artery	7
Sequential injection from left and right hepatic artery	5
Lobar treatment*	
Injection from right hepatic artery	2
Injection from left hepatic artery	1
Net administered amount of microspheres (mg)	484 ± 53
Net administered ^{166}Ho-activity (MBq)	5,085 ± 2,876
Whole-liver absorbed dose (Gy) †	40 ± 23
Quantitative imaging	
Eligible for SPECT dosimetry	
Yes	15
No	0
Eligible for MRI-dosimetry	
Yes	9
No	6 (claustrophobia *n* = 1, metal clips *n* = 5)

*Data are number, median (range), or mean (SD). ^{166}Ho-RE = holmium-166 radioembolization; MRI = magnetic resonance imaging; SPECT = Single Photon Emission Computed Tomography; * Unilobar treatment because of unilateral disease (n = 1) or previous hemihepatectomy (n = 2); † Assuming all the energy of the net administered activity was absorbed in the liver*

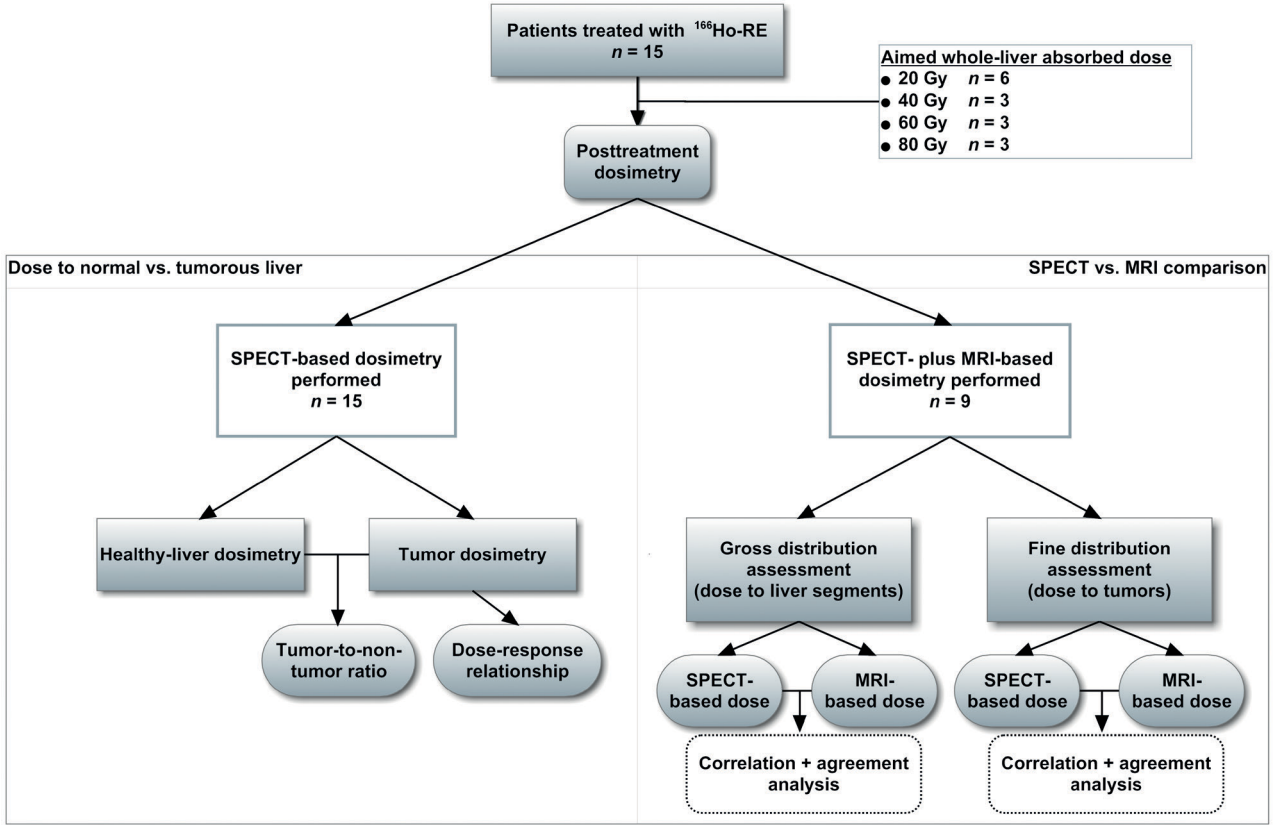

Figure 2. *Flowchart of study design and dosimetric analyses performed in this study. These analyses were aimed to determine the dose to the normal and the tumorous liver (left column) and to compare the dosimetric results based on Single Photon Emission Computed Tomography (SPECT) and Magnetic Resonance Imaging (MRI) (right column). [166]Ho-RE = holmium-166 radioembolization.*

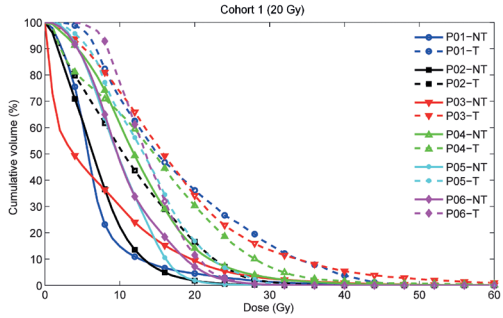

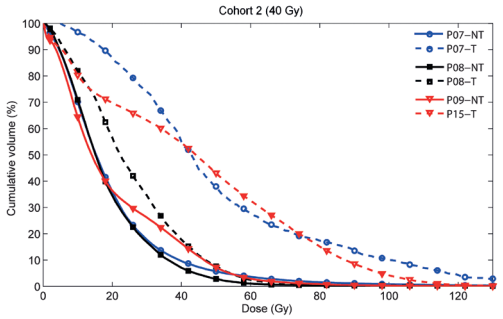

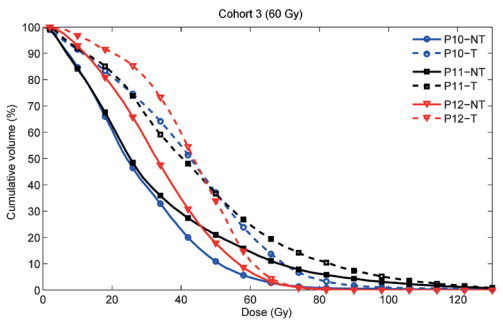

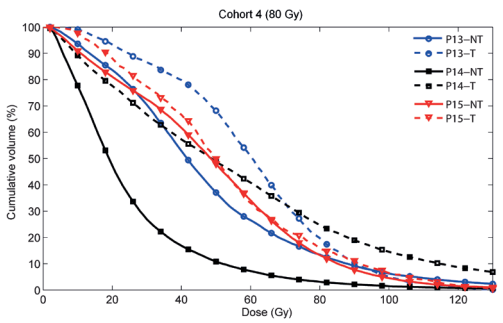

Figure 3. *Cumulative dose volume histograms per dose cohort (20 Gy, 40 Gy, 60 Gy, and 80 Gy). The lines represent the cumulative dose per volume fraction on the non-tumorous (NT) liver tissue (continuous lines) and on the tumorous (T) tissue (dotted lines) in each of the study patients.*

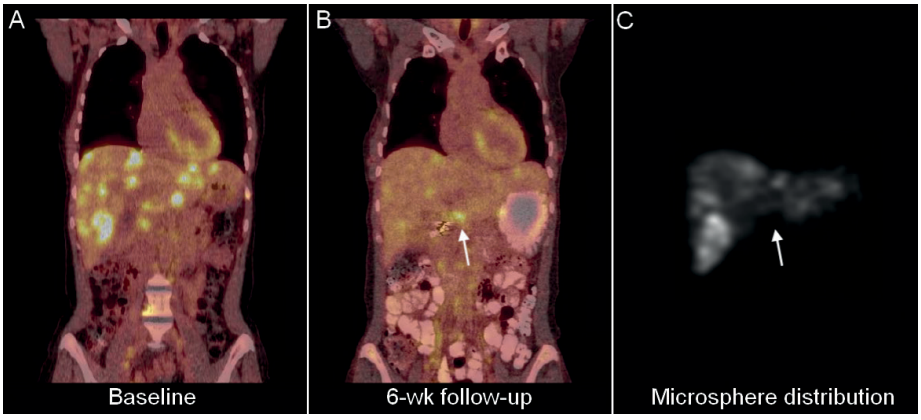

Figure 4. *Example of clinical implication of inadequate microsphere distribution. ^{18}F-Fludeoxyglucose Positron Emission Tomography (^{18}F-FDG-PET) at baseline (A) and at 6-weeks post treatment (B) shows substantial reduction of FDG-uptake in all but one liver lesion (arrow). Single Photon Emission Computed Tomography post ^{166}Ho-radioembolisation showed that only a very small amount of ^{166}Ho-microspheres had arrived at this lesion (C). The calculated mean absorbed dose to this lesion was 4.8 Gy versus 19.6 Gy on the normal liver and 27.7 Gy on the entire tumorous volume.*

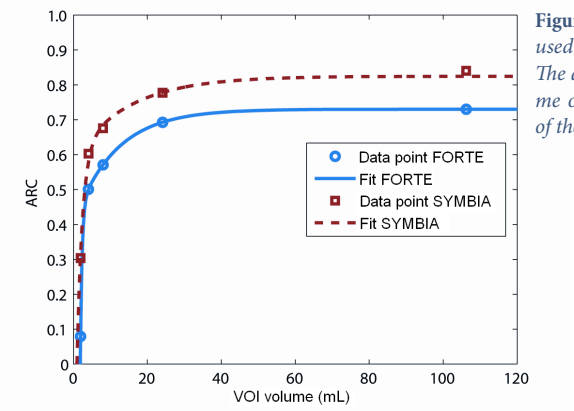

Figure 5. *Activity recovery curves for the two used SPECT-systems (SYMBIA and FORTE). The activity recovery coefficient (ARC) per volume of interest (VOI) increases with the volume of the VOI.*

Table 2. *Tumor dosimetry based on SPECT*

Descriptive statistics	SPECT			
	Median	range		
Volumes of interest				
Whole liver volume (mL)	2120	(1467 - 3650)		
Tumorous liver volume (mL)	333	(28 - 1809)		
Non-tumorous liver volume (mL)	1677	(1320 - 2477)		
Calculated radiation absorbed doses*				
Whole liver dose (Gy)	21.8	(8.4 - 54.2)		
Tumorous liver dose (Gy)	43.7	(13.2 - 64.9)		
Non-tumorous liver dose (Gy)	20.7	(7.1 - 54.3)		
Fraction of the injected activity arriving at the tumorous liver*	14.8%	(1.4% - 60.7%)		
T/N ratios	**Overall T/N ratio**		**Peak T/N ratio**	
Overall T/N ratio	1.4	(0.9 - 2.8)	2.0	(0.9 - 10.3)
T/N ratio for two largest lesions per patient	1.7	(0.8 - 3.2)	4.0	(0.5 - 10.3)
T/N ratio for the 'hottest' lesion per patient	2.3	(1.2 - 3.4)	5.1	(1.3 - 12.1)
Stratified for primary tumor type				
Ocular melanoma patients (n = 6)	2.2	(0.9 - 2.8)	2.1	(0.9 - 3.6)
Colorectal carcinoma patients (n = 6)	1.5	(1.2 - 2.4)	3.6	(1.3 - 10.3)
Cholangiocarcinoma patients (n = 2)	1.2	(1.2 - 1.2)	1.7	(1.6 - 1.8)
Breast carcinoma patients (n = 1)	1.4	N.A.	1.5	
Stratified for liver tumor involvement				
Liver tumor involvement ≥25% (n = 5)	1.8	(1.1 - 2.6)	3.6	(2.1 - 4.2)
Liver tumor involvement 0% - 25% (n = 10)	1.3	(0.9 - 2.8)	1.5	(0.9 - 10.3)
Stratified for lesion vascularity				
Patients with hypervascular lesions (n = 3)	2.6	(1.8 - 2.8)	3.3	(2.1 - 3.6)
Patients with non-hypervascular lesions (n = 12)	1.3	(0.9 - 2.7)	1.5	(0.9 - 10.3)

*Data are number or median (range). N.A. = Not applicable; T/N ratio = tumor-to-non-tumor ratio; * As calculated with quantitative SPECT*

Based on SPECT dosimetry, there was a weak correlation (R^2 = 0.09 at 6-week and R^2 = 0.04 at 12-week follow-up) between the change in longest diameter and mean dose on each index lesion. There was a stronger dose-response relationship when looking at the maximum dose (R^2 = 0.34 at 6-week and R^2 = 0.19 at 12-week follow-up) (*Figure 6*).

Comparison of MRI- and SPECT-Based Dosimetry

Five patients with surgical clips in the liver region were excluded from MRI-dosimetric analysis and one patient did not undergo MRI because of claustrophobia. In the remai-

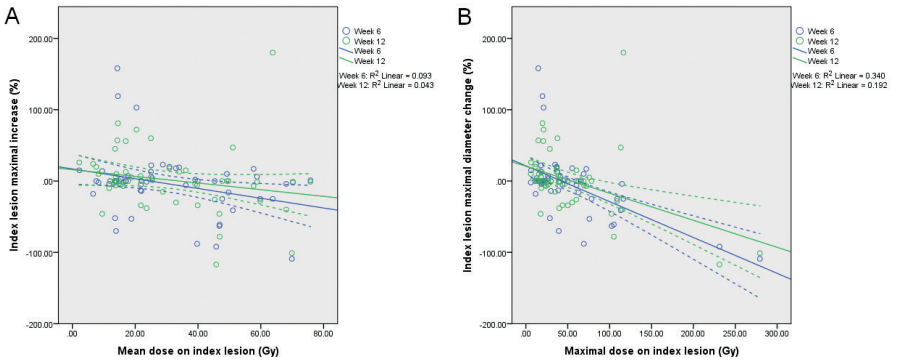

Figure 6. *Dose response analysis. The mean (A) and maximal (B) dose on all index lesions (up to five per patient) were plotted against the change in maximal diameter of the index lesions at six-week and twelve-week follow-up. Maximal diameters were measured on CT according to RECIST 1.1 and dose was measured with SPECT. There is a weak correlation between dose and change in tumor diameter.*

ning nine patients who were eligible for both SPECT- and MRI-based dosimetry, gross (dose to each liver segment, n = 72) and fine (dose to each tumor, n = 86) distribution assessment were compared. The gross distribution assessment comparison yielded a high correlation (R^2=0.91) and a moderate agreement between the estimated absorbed dose in each segment as estimated based on MRI and SPECT (mean bias: 3.7 Gy, 95% limits of agreement: -11.2 – 18.7) (*Figure 7*). The fine distribution assessment comparison yielded a good correlation (R^2 = 0.72) and a low agreement (mean bias: 8.4 Gy, 95% limits of agreement: -22.2 – 38.9 Gy) between the absorbed dose in each tumor as estimated based on MRI and SPECT.

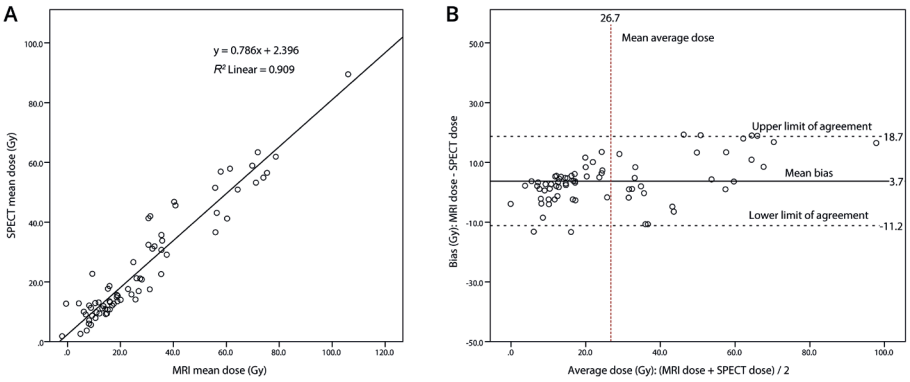

Figure 7. *Gross distribution assessment with Magnetic Resonance Imaging (MRI) and Single Photon Emission Computed Tomography (SPECT) for 72 liver segments in nine patients. (A) Linear regression analysis (correlation). (B) Bland Altman plot visualizing agreement between both measurements.*

The higher resolution of MRI allowed for more detailed evaluation of microsphere biodistribution (*Figure 8*). In the nine MRI-evaluated patients, the peak T/N ratios were notably higher for MRI (median peak T/N ratio = 2.8) than for SPECT (median peak T/N ratio = 1.8). These results are presented in *Table 3*.

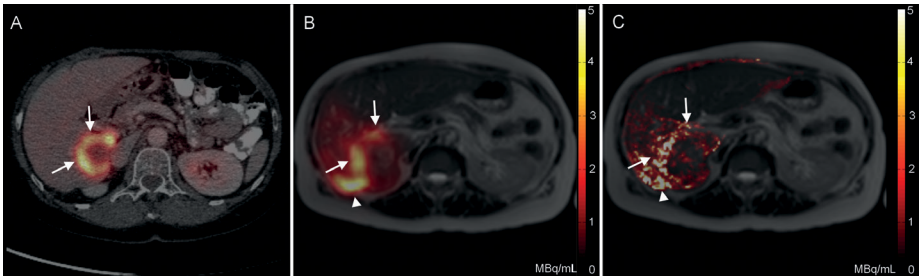

Figure 8. *Intrahepatic biodistribution on SPECT and MRI. (A) Baseline ^{18}F-fluorodeoxyglucose-Positron Emission Tomography (^{18}F-FDG-PET) fused with CT depicting a peripherally FDG-enhancing colorectal liver metastasis (arrows). (B) Single Photon Emission Computed tomography fused with Magnetic Resonance imaging (MRI) of the liver shows ^{166}Ho-microsphere-deposition primarily in the FDG-avid region of the same tumor and in a non-FDG-avid region (arrow head). (C) The MRI-based ΔR_2*-map shows a more detailed map of the microsphere-distribution due to the higher resolution of MR.*

Discussion

This study describes the results of SPECT- and MRI-based dosimetry in the first patients treated with ^{166}Ho-RE. We were able to visualize and quantify the distribution of microspheres within the liver and reliably perform dosimetry based on SPECT and MRI. The ability to perform dosimetry can benefit the patient because RE can now be performed in a more controlled fashion, knowing the amount of microspheres arriving in the tumor(s) and in the normal liver and being able to adjust the treatment plan accordingly.

The theoretical advantage of intra-arterial liver therapies is based on the assumption that the hepatic artery selectively feeds tumors and not the normal liver, which would consequently lead to high T/N ratios. We were now able to determine the amount of microspheres that arrived in the tumor and the amount of microspheres that arrived in the normal liver (T/N ratio) for patients treated with ^{166}Ho-RE. T/N ratios achieved in RE have previously been investigated in several series in which metastatic patients were reported to have a wide variety of T/N ratios ranging from 0.4 – 15.4.[25-29] However, these T/N ratios were often estimated using pre-treatment ^{99m}Tc-MAA-distributions[25, 26, 28, 29], and/or tumors were not delineated based on anatomy but were assumed to lie exactly there where a MAA-hotspot was visible.[28] In other cases, T/N ratios were only

Table 3. *Tumor dosimetry based on SPECT and MRI*

	SPECT				MRI			
Descriptive statistics								
Volumes of interest								
Whole liver volume (mL)	2120	(1467 - 3650)			2041	(1528 - 3433)		
Tumorous liver volume (mL)	443	(28 - 1809)			443	(35 - 1851)		
Non - tumorous liver volume (mL)	1549	(1320 - 2477)			1509	(1339 - 2271)		
Calculated radiation absorbed doses †								
Whole liver dose (Gy)	27.9	(9.7 - 54.2)			20.7	(13.0 - 68.3)		
Tumorous liver dose (Gy)	27.7	(13.2 - 64.9)			32.5	(14.8 - 75.4)		
Non - tumorous liver dose (Gy)	21.0	(7.7 - 54.3)			18.9	(9.1 - 68.2)		
T/N ratios	**Overall T/N ratio**		**Peak T/N ratio**		**Overall T/N ratio**		**Peak T/N ratio**	
Overall T/N ratio	1.4	(0.9 - 2.7)	1.8	(0.9 - 4.2)	1.4	(1.1 - 3.1)	2.8	(1.2 - 5.4)
T/N ratio for two largest lesions per patient	1.6	(0.8 - 2.7)	3.7	(0.5 - 6.5)	1.6	(0.8 - 2.5)	4.7	(1.5 - 9.7)
T/N ratio for the 'hottest' lesion per patient	2.1	(1.5 - 2.9)	4.3	(1.3 - 12.1)	1.9	(1.1 - 3.5)	5.6	(1.9 - 16.5)

*Data are number or median (range). T/N ratio = tumor-to-non-tumor ratio; * Only the nine patients eligible for MRI dosimetry were compared; † As calculated with quantitative SPECT / MRI*

calculated based on a selection of tumors or based on the 'hot spots' within a tumor and/or compared with an arbitrarily chosen 'normal liver' region in the rest of the liver.[25] The median overall T/N ratio found in our study population was only 1.4, ranging from 0.9 – 2.8. However, when calculating a peak T/N ratio for the 'hottest' tumor per patient, these figures were considerably higher (median peak T/N ratio 5.1, range 1.3 – 12.1). This shows that peak T/N ratios can be misleading since one may interpret the activity concentration in the entire volume of tumor(s) to be as high as 5.1 times the activity concentration in the entire non-tumorous liver, whereas this was actually only 1.4 times as high. On the other hand, when taking the entire tumor volume into account for calculation of overall T/N ratios, a tumor receiving little activity in its non-viable core but a tumoricidal dose to its viable parts may still display an overall T/N ratio <1. Peak T/N ratios are not affected this way. Another factor that may be of influence in T/N ratio assessment is the occurrence of activity spill-in or spill-out. We know from the phantom set-ups that the accuracy of the calculated SPECT-based activity concentration in a VOI is hindered by spill-in or spill-out of activity. This effect may lead to over- or underestimation of the true activity in a VOI, the degree of which depends on the size of the VOI and the activity concentration ratio between the VOI and it's surrounding. Corrected for these effects, the median overall T/N ratio in this population was slightly higher (1.6).

In this study, patients with uveal melanoma metastases had the highest T/N ratios, which is in line with the, in general, more pronounced arterial vascularity of these tumors.[30] T/N ratios may be influenced by microsphere-specific characteristics such as microsphere size and number of microspheres injected. We do, however, not believe that the specific properties of ^{166}Ho-PLLA-microspheres caused the T/N ratios to be lower than the reported T/N ratios for ^{90}Y-microspheres. Catheter position during administration is in our opinion a more important factor. In this study microspheres were administered from the proper, common, right or left hepatic artery. Administration from a more selective catheter position might lead to higher T/N ratios.

SPECT- and MRI-based dosimetry on liver segments showed a high correlation and a moderate agreement, which supports the validity of both modalities for gross intrahepatic dosimetry. The correlation for tumor dosimetry was also high and equivalent T/N ratios (median 1.4) were obtained with both modalities. However, the agreement for tumor dosimetry was low according to our predefined criteria, which means that there is a significant uncertainty in the bias between MRI- and SPECT-based doses on a specific tumor. These criteria may be too strict for tumor dosimetry since the uncertainty on this smaller level is intrinsically higher. The low agreement on this level may be caused in part by registration errors, since there were many small lesions, but also by differences between the modalities. Both SPECT and MRI have their specific advanta-

ges, such as, for SPECT, a superior sensitivity and accuracy[10]; and, for MRI, anatomical reference, the high soft tissue contrast in combination with high resolution quantitative imaging, potentially eliminating the need for registration. These two independent modalities may complement each other when combined. MRI does for instance not rely on radioactivity but on differences in susceptibility. This property enables assessment of the biodistribution of decayed microspheres long after therapy or the distribution of a non-radioactive scout dose, but makes intrahepatic dosimetry also sensitive to susceptibility artifacts. Furthermore, SPECT remains crucial for assessment of any extrahepatic distribution because MRI-based dose assessment is hampered by susceptibility artifacts around air containing organs such as the lungs and intestines. MRI-dosimetry may be locally more accurate than SPECT-dosimetry because of the high resolution of MRI, which provides a high level of detail and is less susceptible to partial volume effects. This is probably the reason that higher peak T/N ratios were found for MRI.

A great amount of imaging was involved in this study for dosimetric purposes: 3x MRI, 3x scintigraphy and SPECT(/CT). This amount of imaging is not desirable for clinical practice since these exams are costly and a burden for the patient. Therefore, future research will need to facilitate the decision whether to continue with ^{99m}Tc-MAA or with ^{166}Ho-microspheres to predict biodistribution, which will eliminate part of the imaging, and whether to use SPECT or MRI for dosimetry. At this point, SPECT is the most obvious modality to use for dosimetry since SPECT-based dosimetry is very sensitive and specific and MRI-based dose assessment is limited by artifacts and patients may have contraindications for MRI (claustrophobia, metal devices/shrapnel, etc.). However, MRI-based dosimetry continues to improve and might prove valuable for future purposes such as real-time dosimetry during MRI-guided radioembolization.[31]

This study is limited by the small number of patients and the variation of primary tumor types. The heterogeneity of this study population is, however, a true reflection of the population of patients that is referred to our institute for radioembolization. Furthermore, tumor delineation was performed manually and distinguishing tumor and normal liver tissue on MRI leaves room for subjective interpretation. Using functional imaging such as FDG-PET for tumor delineation may be more appropriate since it can be used to separate non-viable tumor tissue from viable tumor tissue. Whether liver segments were precisely delineated according to Bismuth's adaptation of the Couinaud classification was not essential for this study's analyses. We sought to divide the liver into several sub-regions to assess SPECT- and MRI-based dosimetry and we chose the Bismuth's adaptation of the Couinaud classification because it is well known by clinicians, is based on anatomical landmarks and divides the liver in parts of approximately 100 – 500 mL, which is large enough to compare the gross intrahepatic biodistribution assessment based on SPECT and MRI. The calculated absorbed doses on SPECT and

MRI were consistently lower than the desired liver absorbed doses of 20 – 80 Gy. This is due to residual activity in the administration system, lung shunting, and activity in the liver hilus, which was excluded on segmentation.
Now that in vivo post-treatment dosimetry of ^{166}Ho-microspheres and early recognition of inadequately treated tumors is feasible with both SPECT and MRI, a personalized approach in which inadequately treated tumors receive additional, selective treatment is advised. These next-generation microspheres for radioembolization are therapeutic and imaging agents in one, and provide the opportunity to see what one is treating. Sub-optimal treatment can be detected by MRI and SPECT and a retreatment plan can be elaborated to ensure full efficacy of the treatment. To date, dose-response relationships reported for RE are mainly based on the distribution of ^{99m}Tc-MAA particles and not on the actual microsphere distribution[3, 32]. In the current study we found a weak to moderate dose-response relationship when looking at decrease in tumor diameter. We think that decrease in tumor diameter as used for response assessment is a too indirect measure of response for individual tumors. Using an indicator of functional tumor response such as the apparent diffusion coefficient on diffusion weighted MR imaging or an FDG-PET-marker might show a closer dose-response relationship.[22, 34] Investigating if a higher tumor dose leads to better functional tumor response and prolonged patient survival will be the focus of future studies on ^{166}Ho-RE. The value of a scout dose of a small number of ^{166}Ho-microspheres to predict the post-treatment absorbed dose distribution in the liver will have to be studied and compared to the conventional ^{99m}Tc-MAA-scout dose. If predictive, a scout dose of ^{166}Ho-microspheres might allow pre-treatment dosimetry and identification of patients who will not benefit from treatment due to an unfavorable biodistribution or patients who need extra precautions due to a high normal-liver absorbed dose. In addition, the favorable MRI-characteristics of ^{166}Ho-microspheres may allow for administration under real-time MRI-guidance with direct visualization of the distribution of microspheres (*i.e.* per-treatment dosimetry).[31]

Conclusion

The purpose of this study was to evaluate SPECT- and MRI-based dosimetry in the first patients treated with ^{166}Ho-RE. Dose to the tumorous and non-tumorous liver were quantitatively determined and median T/N ratios were found to be only 1.4 (overall) and 2.0 (peak). Many tumors had received a lower concentration of activity than the non-tumorous liver. Using ^{166}Ho-microspheres, in-vivo dosimetry based on SPECT and MRI correlated well for dose to liver segments and dose to tumors. These results may enable personalized treatment by selective targeting of inadequately treated tumors.

References

1. Bierman HR, Byron RL, Jr., Kelley KH, Grady A. Studies on the blood supply of tumors in man. III. Vascular patterns of the liver by hepatic arteriography in vivo. *J Natl Cancer Inst.* 1951;12:107-131.
2. Elschot M, Nijsen JF, Dam AJ, de Jong HW. Quantitative evaluation of scintillation camera imaging characteristics of isotopes used in liver radioembolization. *PLoS One.* 2011;6:e26174.
3. Garin E, Lenoir L, Rolland Y, et al. Dosimetry based on ^{99m}Tc-macroaggregated albumin SPECT/CT accurately predicts tumor response and survival in hepatocellular carcinoma patients treated with ^{90}Y-loaded glass microspheres: preliminary results. *J Nucl Med.* 2012;53:255-263.
4. Walrand S, Flux GD, Konijnenberg MW, et al. Dosimetry of yttrium-labelled radiopharmaceuticals for internal therapy: ^{86}Y or ^{90}Y imaging? *Eur J Nucl Med Mol Imaging.* 2011;38 Suppl 1:S57-68.
5. Rong X, Du Y, Ljungberg M, Rault E, Vandenberghe S, Frey EC. Development and evaluation of an improved quantitative (90) Y bremsstrahlung SPECT method. *Med Phys.* 2012;39:2346-2358.
6. de Wit TC, Xiao J, Nijsen JF, et al. Hybrid scatter correction applied to quantitative holmium-166 SPECT. *Phys Med Biol.* 2006;51:4773-4787.
7. Nijsen JF, Seppenwoolde JH, Havenith T, Bos C, Bakker CJ, van het Schip AD. Liver tumors: MR imaging of radioactive holmium microspheres - phantom and rabbit study. *Radiology.* 2004;231:491-499.
8. Seevinck PR, van de Maat GH, de Wit TC, Vente MA, Nijsen JF, Bakker CJ. Magnetic resonance imaging-based radiation-absorbed dose estimation of ^{166}Ho microspheres in liver radioembolization. *Int J Radiat Oncol Biol Phys.* 2012;83:e437-444.
9. Vente MA, Nijsen JF, de Wit TC, et al. Clinical effects of transcatheter hepatic arterial embolization with holmium-166 poly(L-lactic acid) microspheres in healthy pigs. *Eur J Nucl Med Mol Imaging.* 2008;35:1259-1271.
10. Seevinck PR, Seppenwoolde JH, de Wit TC, et al. Factors affecting the sensitivity and detection limits of MRI, CT, and SPECT for multimodal diagnostic and therapeutic agents. *Anticancer Agents Med Chem.* 2007;7:317-334.
11. Smits ML, Nijsen JF, van den Bosch MA, et al. Holmium-166 radioembolisation in patients with unresectable, chemorefractory liver metastases (HEPAR trial): a phase 1, dose-escalation study. *Lancet Oncol.* 2012.
12. Zielhuis SW, Nijsen JF, de Roos R, et al. Production of GMP-grade radioactive holmium loaded poly(L-lactic acid) microspheres for clinical application. *Int J Pharm.* 2006;311:69-74.
13. Nijsen JF, Zonnenberg BA, Woittiez JR, et al. Holmium-166 poly lactic acid microspheres applicable for intra-arterial radionuclide therapy of hepatic malignancies: effects of preparation and neutron activation techniques. *Eur J Nucl Med.* 1999;26:699-704.
14. Smits ML, Nijsen JF, van den Bosch MA, et al. Holmium-166 radioembolization for the treatment of patients with liver metastases: design of the phase I HEPAR trial. *J Exp Clin Cancer Res.* 2010;29:70.

15. Vente MA, de Wit TC, van den Bosch MA, et al. Holmium-166 poly(L-lactic acid) microsphere radioembolisation of the liver: technical aspects studied in a large animal model. *Eur Radiol.* 2010;20:862-869.

16. Prokop M, Galanski M, Schaefer-Prokop C. Spiral and Multislice Computed Tomography of the body. Stuttgart: Thieme; 2003:421-425.

17. Bol GH, Kotte AN, van der Heide UA, Lagendijk JJ. Simultaneous multi-modality ROI delineation in clinical practice. *Comput Methods Programs Biomed.* 2009;96:133-140.

18. Bismuth H. Surgical anatomy and anatomical surgery of the liver. *World journal of surgery.* 1982;6:1:3-9.

19. van de Maat GH, Seevinck PR, Elschot M, et al. MRI-based biodistribution assessment of holmium-166 poly(L-lactic acid) microspheres after radioembolisation. *Eur Radiol.* 2012.

20. Bolch WE, Bouchet LG, Robertson JS, et al. MIRD pamphlet No. 17: the dosimetry of nonuniform activity distributions--radionuclide S values at the voxel level. Medical Internal Radiation Dose Committee. *J Nucl Med.* 1999;40:11S-36S.

21. Hendricks JS, McKinney GW, Waters LS, et al. MCNPX Extensions, Version 2.5.0. Los Alamos, CA: Los Alamos National Laboratory Report LA-UR-05-2675, http://mcnpx.lanl.gov/. 2005.

22. Wahl RL, Jacene H, Kasamon Y, Lodge MA. From RECIST to PERCIST: Evolving Considerations for PET response criteria in solid tumors. *J Nucl Med.* 2009;50 Suppl 1:122S-150S.

23. Eisenhauer EA, Therasse P, Bogaerts J, et al. New response evaluation criteria in solid tumours: revised RECIST guideline (version 1.1). *Eur J Cancer.* 2009;45:228-247.

24. Bland JM, Altman DG. Statistical methods for assessing agreement between two methods of clinical measurement. *Lancet.* 1986;1:307-310.

25. Dhabuwala A, Lamerton P, Stubbs RS. Relationship of 99m-technetium labelled macroaggregated albumin (^{99m}Tc-MAA) uptake by colorectal liver metastases to response following Selective Internal Radiation Therapy (SIRT). *BMC Nucl Med.* 2005;5:7.

26. Gulec SA, Mesoloras G, Dezarn WA, McNeillie P, Kennedy AS. Safety and efficacy of Y-90 microsphere treatment in patients with primary and metastatic liver cancer: the tumor selectivity of the treatment as a function of tumor to liver flow ratio. *J Transl Med.* 2007;5:15.

27. Kennedy AS, Nutting C, Coldwell D, Gaiser J, Drachenberg C. Pathologic response and microdosimetry of (90)Y microspheres in man: review of four explanted whole livers. *Int J Radiat Oncol Biol Phys.* 2004;60:1552-1563.

28. Gyves JW, Ziessman HA, Ensminger WD, et al. Definition of hepatic tumor microcirculation by single photon emission computerized tomography (SPECT). *J Nucl Med.* 1984;25:972-977.

29. Ho S, Lau WY, Leung TW, et al. Tumour-to-normal uptake ratio of ^{90}Y microspheres in hepatic cancer assessed with 99mTc-macroaggregated albumin. *Br J Radiol.* 1997;70:823-828.

30. Namasivayam S, Martin DR, Saini S. Imaging of liver metastases: MRI. *Cancer Imaging.* 2007;7:2-9.

31. Seppenwoolde JH, Bartels LW, van der Weide R, Nijsen JF, van het Schip AD, Bakker CJ.

Fully MR-guided hepatic artery catheterization for selective drug delivery: a feasibility study in pigs. *J Magn Reson Imaging.* 2006;23:123-129.

32. Flamen P, Vanderlinden B, Delatte P, et al. Multimodality imaging can predict the metabolic response of unresectable colorectal liver metastases to radioembolization therapy with Yttrium-90 labeled resin microspheres. *Phys Med Biol.* 2008;53:6591-6603.
33. Strigari L, Sciuto R, Rea S, et al. Efficacy and toxicity related to treatment of hepatocellular carcinoma with ^{90}Y-SIR spheres: radiobiologic considerations. *J Nucl Med.* 2010;51:1377-1385.
34. Cui Y, Zhang XP, Sun YS, Tang L, Shen L. Apparent diffusion coefficient: potential imaging biomarker for prediction and early detection of response to chemotherapy in hepatic metastases. *Radiology.* 2008;248:894-900.

Chapter 11

Radiation emission from patients treated with holmium-166 radioembolization

MLJ Smits, JF Prince, GC Krijger, MGEH Lam, BA Zonnenberg,
MAAJ van den Bosch, JFW Nijsen

Submitted

Purpose

Holmium-166 (^{166}Ho) microspheres have been developed for radioembolization (RE) of liver tumors. The gamma rays of ^{166}Ho-microspheres reaching outside the body are useful for imaging purposes, but could necessitate contact restrictions for patients treated with ^{166}Ho-RE. The purpose of this study was to assess the potential dose to other individuals from patients treated with ^{166}Ho-RE and to evaluate what radiation safety precautions are necessary post treatment.

Materials and methods

Fifteen patients with unresectable, chemorefractory liver metastases received ^{166}Ho-RE with escalating aimed-whole liver doses of 20, 40, 60, and 80 Gy. Dose rates from patients were measured at 1.0 m distance from a right lateral and frontal position at 0, 3, 6, 24, and 48 h after infusion. Total effective dose equivalent (TEDE) to a maximally exposed contact was calculated in accordance with published guidelines of the U.S. Nuclear Regulatory Commission (NRC). Results were recalculated to an aimed-whole liver dose of 60 Gy and compared with current NRC regulations in order to evaluate after how much time patients can be released and whether or not they require contact restrictions.

Introduction

Radioactive microspheres can be used for radioembolization of liver tumors. The two most commonly used types of microspheres are resin microspheres that chelate yttrium-90 (^{90}Y) (SIR-Spheres, Sirtex Medical Limited, Australia), and glass microspheres containing ^{90}Y (Theraspheres, BTG International Ltd., London, UK). At our institute, we have developed a different kind of microsphere for radioembolization, consisting of a poly(L-lactic acid) matrix containing holmium-166 (^{166}Ho), that can be visualized in vivo with both SPECT and MRI.[1]

All three microsphere products are loaded with a high-energy beta-emitting isotope. For SIR-Spheres® and TheraSphere® the used isotope ^{90}Y emits a beta particle with a maximum energy of 2.28 MeV with an intensity of 99%. The half-life is 64.1 hours. ^{166}Ho, on the other hand, emits beta-radiation at two main energies (Eb- max = 1.74 and 1.85 MeV, Intensity = 48.7% and 50.0%, respectively) and has a half-life of 26.8 hours. Since the beta energy of ^{166}Ho is somewhat lower than ^{90}Y and its physical half-life is significantly shorter, the energy released per unit of activity is 15.87 J/GBq for ^{166}Ho and 49.67 J/GBq for ^{90}Y.[2] Therefore, an approximate three times higher amount of ^{166}Ho is required to obtain an absorbed dose similar to the dose from a given activity of ^{90}Y. For both ^{90}Y and ^{166}Ho, low energy photons (bremsstrahlung) are also emitted

act

Results

The median dose rate at discharge, 48 hours after infusion, measured from 1.0 m distance from a right lateral position was 26 μSv/h (range 7 – 45 μSv/h). Recalculated to 60 Gy, none of the dose rates for the NRC contact scenario, at any time, frontal or lateral, would lead to a TEDE exceeding 5 mSv and all patients would have been releasable directly after treatment according to the NRC regulations. Release without contact restrictions 24 h after treatment was appropriate for all patients who received up to 11 GBq.

Conclusions

In the NRC contact scenario, TEDE to a contact of patients treated with ^{166}Ho-RE aimed at a 60 Gy whole-liver absorbed dose, will not exceed the NRC limit of 5 mSv: not even when discharged immediately after treatment. Contact restrictions 24 h after treatment are not necessary for infused activities <11 GBq according to the NRC contact scenario.

indirectly due to deceleration of the beta particles in the body. The direct gamma radiation of ^{166}Ho-microspheres (81 keV, abundance 6.2%) can be used for dosimetry with SPECT.[1,3] However, from a radiation safety point of view, the direct gamma emission of ^{166}Ho, including a low intensity (abundance 0.93%) 1379 keV gamma emission, increases the radiation exposure to individuals surrounding the patient in the first days after treatment.

The nuclear regulatory commission (NRC) of the United States has set regulations for the release of patients after administration of radioactive materials. Using the scenario described by the NRC, the limit of the total effective dose equivalent (TEDE) to individuals surrounding patients treated with radioactive materials is 5 mSv, above which patients cannot be discharged.[4] When the TEDE to surrounding individuals will exceed 1 mSv, the patients should be given written instructions how to keep exposure to other individuals as low as reasonably achievable (*i.e.* contact restrictions).

The purpose of this study was to assess the potential dose to other individuals from patients treated with ^{166}Ho-RE and to evaluate what radiation safety precautions are necessary post treatment.

Methods

Phase 1 study

In this phase 1 study, the safety and toxicity profile of ^{166}Ho-microspheres were evaluated in patients with unresectable, chemorefractory liver metastases. The primary endpoint was the maximum tolerated radiation dose (MTRD) to the liver. Patients were treated in four cohorts, with escalating radioactivity of ^{166}Ho-microspheres, to accomplish an aimed whole liver dose of respectively 20, 40, 60 and 80 Gy. All patients provided written informed consent prior to study enrolment. This trial was approved by the institutional review board and is registered with ClinicalTrials.gov, number NCT01031784.

Production of microspheres

^{166}Ho-microspheres were made by incorporating holmium-165 into poly(L-lactic acid) (PLLA) microspheres and exposing them to neutron irradiation.[5] In short, holmium-acetylacetonate crystals (Ho-AcAc) were prepared from a continuously stirred aqueous solution of acetylacetone by addition of ammonium hydroxide and holmium chloride. The formed Ho-AcAc was then added to PLLA, chloroform, and polyvinyl alcohol, after which the chloroform was allowed to evaporate. The formed microspheres were washed and sieved, after which they were neutron irradiated in high-density polyethylene vials at the Reactor Institute in Delft, The Netherlands (thermal neutron flux 5 x 10^{12} cm^{-2} s^{-1}). Neutron irradiation time was customized to the activity needed for each patient. This way, 600 mg of ^{166}Ho-microspheres was administered to each patient but with a different amount of radioactivity. The GMP-grade production of the ^{166}Ho-microspheres was described in detail in prior work.[6]

Treatment procedure

Patients eligible for treatment were discussed in a multidisciplinary liver tumor board. After baseline imaging, patients were admitted for a pre-treatment angiography. After coil-embolization of non-hepatic vessels, technetium-99m-macro-aggregated albumin (^{99m}Tc-MAA) was administered in relevant arteries leading to liver parenchyma. If no significant lung shunting or extrahepatic deposition was observed, patients received a second angiography during which they received a scout dose of ^{166}Ho-microspheres (approximately 60 mg, 250 MBq) to assess microsphere distribution. After imaging of the scout dose, a therapy dose (approximately 540 mg, varying activities) was given several hours after infusion of the scout dose.

Release and follow-up

Patients had to stay in the nuclear medicine ward for 48 h post treatment. After discharge, patients were given contact restrictions for another 48 h (*see Appendix 1*). Patients returned to the outpatient department for weekly follow-up visits during which physical examination was performed and blood was drawn for hematological and biochemical tests. PET-CT and MRI were performed at 6 and 12 weeks for tumor response assessment.

Planning the activity to be administered

Dosimetry to the liver was calculated using a method analogous to the medical internal radiation dosimetry (MIRD) pamphlet number 17.[7] Aimed whole liver radiation absorbed doses were 20 Gy, 40 Gy, 60 Gy, and 80 Gy. For calculation of necessary radioactivity of ^{166}Ho-microspheres, the following formula was used:

$$A_{Ho166}(\mathrm{MBq}) = Dose_{\,Liver}(\mathrm{Gy}) \times 63 \left(\frac{\mathrm{MBq}}{\mathrm{J}}\right) \times \mathrm{M}_{Liver}\ (\mathrm{kg}) \quad [Equation\ 1]$$

Where A_{Ho166} is the activity of ^{166}Ho-microspheres in MBq to be administered, the Absorbed energy is the activity-to-dose conversion of ^{166}Ho assuming that all energy of the emitted beta particles is absorbed in the liver, and the M_{Liver} is the mass calculated by delineating the liver on CT using the in-house developed software Volumetool[8], assuming a liver tissue density of 1.0 g/cm^3. As such, activities for each cohort were respectively 1.3, 2.5, 3.8 and 5.0 GBq/kg (liver weight).

Net administered activity measurement

Before treatment, the activity of the vial containing the microspheres was measured using a validated dose calibrator (VDC 405 or 404, Veenstra Instruments, the Netherlands). Upon completion of therapy, the remnant radioactivity in the vial was measured again. The difference was used as the net activity with which the patient was treated and used in further dose calculations.

Post treatment radiation emission

The radiation emitted by the patient after treatment was studied in three ways. First, the potential dose to other individuals was estimated based on the net administered activity. Second, the dose rates at 1.0 m distance from the patient were measured after treatment and transformed to absorbed doses. Third, the calculated absorbed doses were recalculated for a scenario where each patient receives an aimed-whole liver absorbed dose of 60 Gy.

1. Estimated dose to others

Using the net administered activity and the gamma ray constant, the TEDE to others from the direct gamma radiation after discharge can be estimated. All ^{166}Ho was assumed to remain in the liver. Biological half-life was thus neglected and only radioactive half-life was taken into account. The bremsstrahlung and the fraction of metastable ^{166}Ho were neglected for the estimated dose to others. In the rest of this paper, the term "effective dose" will be used instead of TEDE. The effective dose was calculated using the following formula:[4]

$$D(\infty) = \frac{34.6\ \Gamma\ Q_0\ t_{1/2}\ E}{(1.0)^2} \qquad [Equation\ 2]$$

Where D(∞) is the effective dose (mSv), 34.6 is a conversion factor (24h/day * 1/ln(2)), Γ the specific gamma ray dose constant (mSv/GBq-h at 1.0 m), Q_0 is the activity at time of release (GBq), $t_{1/2}$ the half-life time (days), E the occupancy factor, and 1.0 the average distance from the patient (m). The specific gamma ray dose constant for ^{166}Ho is 0.00627 mSv/GBq-hr at 1.0 m.[9] The half-life for ^{166}Ho is 26.8 hours. No significant beta emission is expected outside of the human body due to the maximal tissue penetration of 8.7 mm and mean tissue penetration of 2.5 mm of beta radiation from ^{166}Ho.[10,11] Given the above, the formula can be rewritten as:

$$D(\infty) = 0.242\ Q_0\ E \quad [Equation\ 3]$$

Where D(∞) is the effective dose (mSv) from activity Q_0 (GBq) until final decay, with a presence E (range 0-100%) at 1.0 m. E was conservatively set to 1 (continuous presence) for the analyses of this study because the half-life of ^{166}Ho is relatively short. Effective dose was calculated for the four most relevant time points that were also used for measurements in this study, *i.e.* 0, 6, 24, 48 h after infusion.

2. Measurements of dose rates and effective doses

External radiation dose rates from patients were measured after treatment with ^{166}Ho-RE from two positions at five different times. Measurements were performed from a right lateral and frontal position from the patient at 1.0 m distance, in line from the center of the liver, perpendicular to the liver surface. A wooden stick of 1.00 m was used to keep the appropriate distance. The dose rate meter was aimed at the center of the liver. The measurements were performed shortly after infusion of microspheres (called t_0), and at t_3, t_6, t_{24}, and t_{48} hours after infusion. The exact times of the measurements were noted, to allow correction for decay. Immediately after the angiography

procedure, patients were required to remain in the supine position in order to allow the vascular access site to heal, and thus frontal measurements were not performed at t_0. A portable dose rate meter was used (Radiagem 2000, CANBERRA, Meriden, Ct.). This calibrated dose rate meter was sensitive for gamma radiation only (range 40 keV – 1.5 MeV).

Dose rates were measured at different times, so to allow comparison, all dose rates from the same patient and position were transformed back to dose rate at time of infusion. The mean of these dose rates was used to calculate effective doses. To assess the validity of these values, the mean of the decay-corrected dose rate measurements and effective dose of each patient was examined for a correlation with the infused activity. Pearson's correlation coefficient (R^2) was calculated. The slope of the correlation line between dose rate and infused activity was used to determine a new constant that includes attenuation to replace the hypothetical constant of 0.242 mSv/GBq in equation 3. The newly determined constant was then used to determine whether contact restrictions are necessary for different release times and varying amounts of infused activity.

The effective dose to other individuals was calculated from measured dose rates in accordance with published guidelines of the U.S. NRC.[4] The following equation, which is also used by McCann *et al.*,[12] was used to calculate the effective dose to others:

$$D(\infty) = 34.6\ R_0\ T_p\ E \qquad \text{[Equation 4]}$$

Where D(∞) is the effective dose (in mSv), 34.6 is the conversion factor of 24 hours / day time the total integration of decay (1/ln(2) = 1.44), R_0 is the dose rate measured at 1.0 m from the patient (in mSv/h), T_p is the physical half-life in days (1.115 days for ^{166}Ho), and E is the occupancy factor.

3. Recalculation to a 60-Gy aimed dose

In the current dose-escalation study the whole-liver absorbed doses ranged from 14.7 Gy to 78.3 Gy. Based on the maximum tolerated radiation dose established in this study, 60 Gy will be the aimed-whole liver dose for future ^{166}Ho-RE treatments (equivalent to 3.8 GBq/kg).[13] Since the liver absorbed doses in the patients of this study varied widely, dose rates could be recalculated to a scenario where each patient receives a whole liver dose of 60 Gy, assuming a good correlation between infused activity and measured dose rates (as described above). In order to do so, the mean dose rate for each patient was multiplied by the ratio between the aimed-whole liver absorbed dose for future treatments (*i.e.* 60 Gy) and the actual whole liver absorbed dose (range 14.7 – 78.3 Gy). Using equation 3, the effective dose for different contact scenarios was calculated, as

suggested by Gulec and Siegel.[14] Besides the basic scenario in which the occupancy factor (E) is 1 (continuous presence) and the distance (d) is 1.0 m, scenarios for household members (E=0.25, d=1), caregivers (E=0.25, d=0.3), givers of significant care (E=0.5, d=0.3), and for infants, children or pregnant women (E=0.042, d=0.1) were calculated. The applied distance correction factor was not the inverse square but a multiplication of 3/d, where d is the distance in meters. This correction factor is more appropriate for distances closer than 1.0 m due to the source of radiation (*i.e.* the liver) more resembling a line than a point source.[14]

Results

Fifteen patients were treated with ^{166}Ho-RE. The primary tumor was ocular melanoma in six patients, colorectal cancer in six patients, cholangiocarcinoma in two patients and breast cancer in one patient. Mean liver volume for each cohort was 2234 mL (SD 756), 1884 mL (SD 530), 2236 mL (SD 498), and 1771 mL (SD 497). The mean infused activity for each of the cohorts was 2532 MBq (SD 1039), 4145 MBq (SD 1161), 8099 MBq (SD 1378), 8120 MBq (SD 1900), with a mean actual whole-liver absorbed dose of 18 Gy (1.1 GBq/kg), 35 Gy (2.2 GBq/kg), 58 Gy (3.7 GBq/kg), and 78 Gy (4.6 GBq/kg).

1. Estimated dose to others

Based on the net administered activity, the estimated median effective dose to other individuals from patients treated with ^{166}Ho-RE was 0.31 mSv (range 0.11 – 0.72 mSv)

Table 1a. *Estimated effective dose to others from patients treated with holmium-166 radioembolization starting from different time points*

	Dose T_0 (mSv)	Dose T_6 (mSv)	Dose T_{24} (mSv)	Dose T_{48} (mSv)
Cohort 20 Gy	0.52 (0.39-1.09)	0.45 (0.33-0.93)	0.28 (0.21-0.59)	0.15 (0.11-0.31)
Cohort 40 Gy	0.84 (0.84-1.33)	0.72 (0.72-1.14)	0.45 (0.45-0.71)	0.24 (0.24-0.38)
Cohort 60 Gy	1.92 (1.65-2.31)	1.64 (1.41-1.98)	1.03 (0.89-1.24)	0.55 (0.48-0.67)
Cohort 80 Gy	1.74 (1.66-2.49)	1.49 (1.42-2.13)	0.94 (0.89-1.34)	0.50 (0.48-0.72)

Table 1b. *Measured effective dose to others from patients treated with holmium-166 radioembolization starting from different time points*

	Dose T_0 (mSv)	Dose T_6 (mSv)	Dose T_{24} (mSv)	Dose T_{48} (mSv)
Cohort 20 Gy	0.32 (0.27-0.65)	0.27 (0.24-0.55)	0.17 (0.15-0.35)	0.09 (0.08-0.19)
Cohort 40 Gy	0.62 (0.56-0.85)	0.53 (0.48-0.73)	0.33 (0.30-0.46)	0.18 (0.16-0.25)
Cohort 60 Gy	1.25 (1.18-1.32)	1.07 (1.01-1.13)	0.67 (0.64-0.71)	0.36 (0.34-0.38)
Cohort 80 Gy	1.56 (0.93-1.82)	1.34 (0.80-1.56)	0.84 (0.50-0.98)	0.45 (0.27-0.52)

Reported data are median (range)

assuming an occupancy factor of 1 (continuous presence at 1.0 m during total decay) starting at from the moment that patients were discharged in this study (48 hours post treatment). The effective dose for the other time points are presented in *Table 1*.

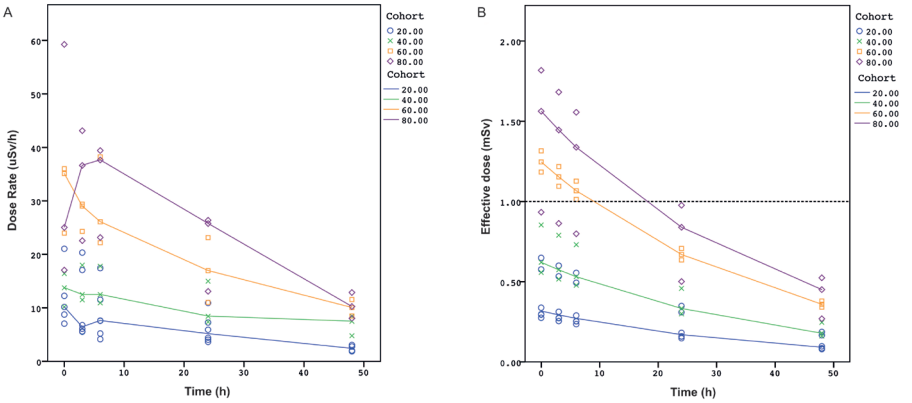

Figure 1. *Measured dose rates for each patient categorized per cohort (A) and subsequently calculated effective dose rates (B). The median dose rates and median effective doses per cohort are connected by lines. The black reference line in B represents the 1.0 mSv threshold above which contact restrictions are necessary for release.*

2. Measured dose rates and calculated doses

Six of 135 dose rate measurements were missing (4.4%, one lateral, five frontal measurements). These measurements were missing in 5 different patients. The median lateral dose rates at discharge, 48 hours after infusion, measured from 1.0 m distance were 8 µSv/h (range 7 - 11 µSv/h), 26 µSv/h (17 – 29 µSv/h), 35 µSv/h (29 – 40 µSv/h), and 36 µSv/h (28 – 45 µSv/h) for the 20-Gy, 40-Gy, 60-Gy and 80-Gy cohort, respectively. The dose rates and effective doses for each cohort are presented in *Figure 1*.

After correction for decay, there was a strong correlation between mean dose rate at t0 for each patient and the infused activity for the lateral measurements (R^2=0.94, $p < 0.01$) and for the frontal measurements (R^2=0.92, $p < 0.01$) (*Figure 2A*). Since the lateral dose rates measurements correlated slightly better with infused activity than the frontal measurements, the lateral dose rates were used for further calculations. The median effective dose to other individuals assuming an occupancy factor of 1 starting 48 h post treatment was 0.19 mSv range (0.08 – 0.52 mSv) The effective doses for the other time points are displayed in *Table 1*.

The calculated effective dose for a person standing at 1.0 m distance on the right side of the patient for continuous presence from t0 correlated well with the infused activity (R^2=094) with a constant of 0.161 mSv/GBq (*Figure 2B*). This constant was used to create a chart that indicates whether contact restrictions are necessary for different release times (*Figure 3*). According to these calculations, for the basic contact scenario, release without contact restrictions 24h after treatment is appropriate for all patients

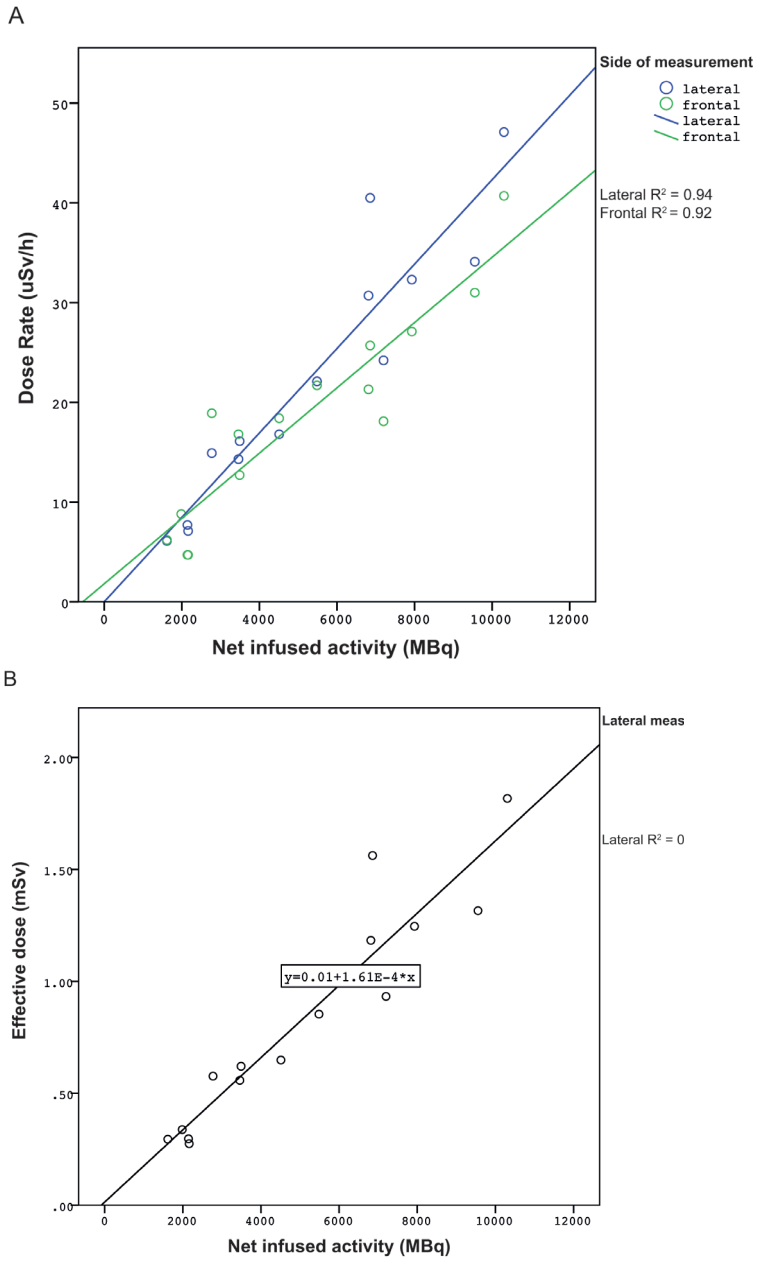

Figure 2. *Scatter plots of the infused activity versus (A) the lateral and frontal dose rates, and (B) the effective dose based on the lateral dose rates. The constant of 0.161 mSv/GBq was derived from the trendline in B. Reported R^2 values are Pearson's correlation coefficients.*

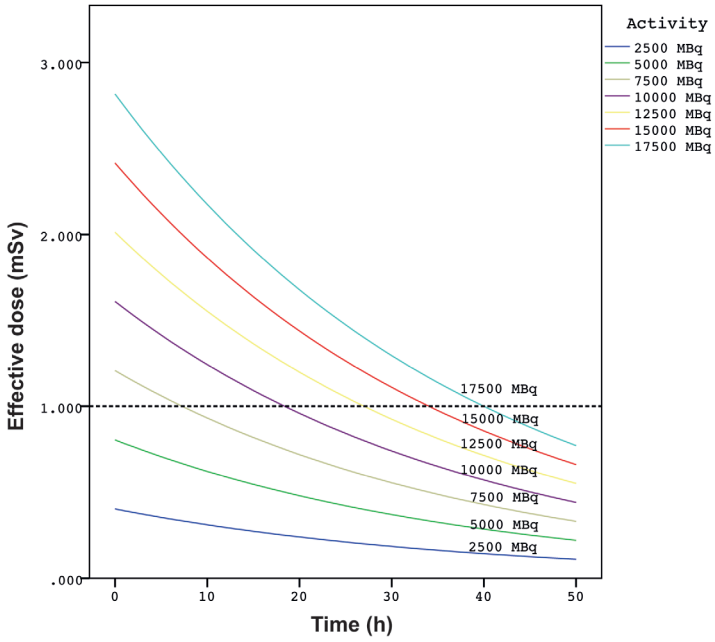

Figure 3. *Total effective dose equivalent (TEDE) for different infused activities and release times. Contact restrictions are necessary if the TEDE exceeds 1.0 mSv (dashed reference line). Whether release without contact restrictions is appropriate can be checked by following the line for the activity administered to the patient and the time of release on the x-axis. If the value is below 1.0 mSv, the release without contact restrictions is appropriate.*

who receive up to 11 GBq of ^{166}Ho. All patients who receive up to 21 GBq of ^{166}Ho are releasable without instructions 48 h post therapy.

3. Recalculation to a 60 Gy aimed dose

Recalculation of the measured radiation dose rates to the future aimed whole-liver dose of 60 Gy (3.8 GBq/kg), resulted in median dose rates of 31 µSv/h, 30 µSv/h, 28 µSv/h, 19 µSv/h, and 10 µSv/h for the lateral measurements, at 0h, 3h, 6h, 24h, and 48 h, respectively. Assuming continuous presence (occupancy factor = 1) starting 48 hours after infusion, the median dose to a person standing at 1.0 m in the right lateral position was estimated to be 0.35 mSv (range 0.21-0.59 mSv). The median dose to a person at 1.0 m distance, lateral from the patient, starting immediately after treatment is 1.20 mSv (range 0.71-2.06 mSv). None of the recalculated dose rates for the basic scenario, at any time, frontal or lateral, would lead to a effective dose exceeding 5 mSv. For the caregivers and givers of significant care scenarios, the effective dose could exceed 5 mSv unless waited for 6 or 48 h, respectively. The mean effective dose to individuals for other contact scenarios is displayed in *Table 2*.

Table 2. *Maximum effective doses for a 60-Gy whole liver absorbed dose scenario combined with different contact scenarios*

	Dose T_0 (mSv)	Dose T_6 (mSv)	Dose T_{24} (mSv)	Dose T_{48} (mSv)
Basic scenario (E=1, d=1)	1.20 (0.71-2.06)	1.03 (0.61-1.76)	0.64 (0.38-1.11)	0.35 (0.21-0.59)
NRC contact scenario: Household members (E=0.25, d=1)	0.30 (0.18-0.51)	0.26 (0.15-0.44)	0.16 (0.10-0.28)	0.09 (0.05-0.15)
Caregivers (E=0.25, d=0.3)	3.00 (1.79-5.15)	2.57 (1.53-4.41)	1.61 (0.96-2.76)	0.87 (0.52-1.48)
Givers of significant care (E=0.5, d=0,3)	6.00 (3.57-10.29)	5.13 (3.06-8.81)	3.22 (1.92-5.53)	1.73 (1.03-2.97)
Infants / children / pregnant women (E=0.042, d=0.1)	1.51 (0.90-2.59)	1.29 (0.77-2.22)	0.81 (0.48-1.39)	0.44 (0.26-0.75)

Reported data are median (range)

Discussion

The gamma radiation emitted by ^{166}Ho is beneficial for imaging purposes[1,3] but can raise concerns regarding radiation exposure to others. This study describes the radiation emitted from patients treated with ^{166}Ho-RE and the subsequent potential dose to others. The doses to others were first estimated using the gamma ray constant and were then calculated based on the measured dose rates. As expected, the estimated doses were higher than the calculated doses, since attenuation was not taken into account for the estimated doses. There was an excellent correlation between the infused activity and the effective doses based on the lateral measurements at 1.0 m distance (R^2=0.94) with a constant of 0.161 mSv/GBq of ^{166}Ho. We used this constant to recalculate the measured values to a whole-liver dose of 60 Gy (3.8 GBq/kg) in order to gain insight in the radiation exposure of future patients who will be treated with aimed whole-liver absorbed doses of 60 Gy. Potential effective doses for a range of contact scenarios were calculated, of which some posed a concern (significant caregivers).[15]

A similar study has been performed in patients treated with resin or glass ^{90}Y-microspheres.[12] In that study there was a poor correlation between infused activity of resin microspheres and dose rates at 1.0 m (R^2=0.21). This discrepancy may be due to the fact that the measured dose rate in patients treated with ^{90}Y consists of bremsstrahlung only and the amount of bremsstrahlung leaving the body is highly dependent on distribution and attenuation. This is of less influence to the direct gamma radiation coming

from ^{166}Ho. As expected, because of the gamma-emission of holmium, the dose rates and effective doses to others from patients treated with ^{166}Ho are higher than for ^{90}Y-RE shortly after treatment.[12] Nevertheless, patients treated with ^{166}Ho-RE can still be discharged directly after treatment according to the NRC contact scenario. Furthermore, contact restrictions might only be necessary for patients who are discharged within 24 h after treatment or who received more than 11 GBq. Discharge within 48 h after treatment is however uncommon. A recent review demonstrated that most centers keep patients in a nuclear medicine ward for 2-3 days after treatment with RE.[16] After a stay of 48 h post therapy, patients treated with the recommended whole liver absorbed dose of 60 Gy can be released without restrictions in all cases. We chose to use the NRC guidelines for the U.S. as a reference since these regulations apply to the entire U.S. where a large number of RE-treatments are performed. The threshold for release of patients and need for contact restrictions may be different in other countries. After how much time patients can be released respecting other thresholds can be read out from the graph in *Figure 3*.

Although contact restrictions are not required in most cases, the effective doses should still be minimized by employing all reasonable methods according to the radiation safety 'as low as reasonably achievable' (ALARA) principle. One must however recognize that the safety restrictions recommended to patients may have a negative influence on their quality of life in, perhaps, the last months of their lives. Avoiding physical contact and not sleeping in the same bed as a partner – which are recommended restrictions at our center and by the NRC (*see Appendix 1 and 2*) – can weigh heavily on for instance an elderly couple. In a recent study on quality of life in patients treated with ^{166}Ho-RE, social functioning was found to decrease after treatment with improvement at 12 weeks post treatment.[17] The reasons for this decrease in social functioning are not fully identifiable using the standard quality of life questionnaires, but it may have partly been caused by the set of restrictions given to the patients after treatment. For this reason, we think physicians should always give written instructions to patients as to how to minimize the dose to others and discuss the potential harms of radiation, but also provide a pragmatic advice on how to personally determine what restrictions are reasonable.

Despite the limited number of patients in this study, the measurements consistently showed a strong correlation between infused activity and dose rate and effective dose. Also, as part of this phase 1 dose-escalation study, patients received a range of activities in our study. We did not consider this a limitation. The range in infused activities helped to establish the relationship between infused activity and effective dose and to recalculate more accurately to higher amounts of activity.

The estimated effective dose to others (part 1) was limited by the fact that we neglected bremsstrahlung radiation and metastable ^{166}Ho. These components were expected to be far smaller than the dose from the direct gamma radiation. Bremsstrahlung and metastable ^{166}Ho were part of the measured dose rates and calculated effective doses (part 2). True dose rates were nevertheless somewhat underestimated by these measurements due to the limited range of the dose rate meter (range 40 keV – 1.5 MeV), especially in the 0-40 keV range. This lower limit is especially relevant for measuring bremsstrahlung, since low-energy photons constitute a significant part of the bremsstrahlung spectrum.[18]

Both lateral and frontal dose rate measurements were performed. For the frontal measurements, the patient needs to sit up in bed, which is not possible shortly after closure of the arterial access site for angiography. The lateral dose rate measurements are easier to perform, more comfortable for the patient and proved to be more accurate. Therefore, we have decided to perform only lateral dose rate measurements in future studies.

Another limitation of this study was the assumption that all radiation was emitted by ^{166}Ho from inside the liver. Just as with resin ^{90}Y-microspheres, it is known that trace amounts of ^{166}Ho may leach into the system.[13,19] Body fluids, especially the urine, can thus be contaminated. We are currently collecting urine from a larger number of patients to determine what amounts of radioactivity can be found in the urine after treatment and whether patients need to stay in a nuclear medicine ward for this reason.

Even before and during treatment, persons other than the patient may absorb radiation from ^{166}Ho. One concern is the dose to personnel handling the radioactive microspheres. At this moment, a vial with ^{166}Ho-microspheres at the right activity for each specific patient is delivered to the hospital in the morning of the treatment day. The vial is placed in a lead-glass container inside a poly(methyl methacrylate) box and brought to the angiography room. During the time that the administration system is set up and microspheres are administered, up to the time that the patient leaves the room, the personnel in the angiography room (interventional radiologists, technicians, nuclear medicine physicians) are exposed to gamma-radiation from ^{166}Ho. Preliminary measurements from our institution's radiation safety committee have indicated that the dose to the operators in the angiography room from ^{166}Ho is far less than the dose coming from scattered radiation from the c-arm. It is however complex to exactly determine the contribution of ^{166}Ho to the entire dose absorbed by operators during an RE-procedure. This will be the focus of a future mock-up study.

In conclusion, according to the NRC contact scenario, the effective dose to a contact of patients treated with ^{166}Ho-RE aimed at a 60 Gy whole-liver absorbed dose, will not exceed the NRC limit of 5 mSv. Not even when discharged immediately after treatment.

Contact restrictions 24 h after treatment are not necessary for infused activities <11 GBq according to the NRC contact scenario. Other radiation safety aspects concerning ^{166}Ho-RE such as the dose to personnel and release through body fluids need to be studied further.

Appendix 1.

List of instructions given at our center to patients for 48 hours after treatment with ^{166}Ho-RE

- Keep roommates at a distance of at least 1 m
- Avoid physical contact with children up to 10 years old. Others should take care of them. Maximize the distance to children. If these precautions are not possible, let the children stay with family or friends during the period that the contact restrictions apply.
- Keep at least 2 m distance from a partner or roommate during when sleeping, if possible in separate rooms. Pay attention that the beds in the separate rooms are not placed adjacent to the same wall. Direct physical contact like cuddling and sexual intercourse should be limited to 30 minutes a day.
- Maximize the distance to pregnant women in order to minimize the dose to the unborn child.
- In case you die within 20 days after treatment, one of your relatives should contact the nuclear medicine department.
- In case you have an appointment with a physician outside the nuclear medicine department of this hospital within 13 days after treatment, please notify that physician about the radioactivity present in your body.

Appendix 2.

Example of additional instructions that may be given to patients with permanent implants as provided by the Nuclear Regulatory Commission:[4]

"A small radioactive source has been placed (implanted) inside your body. The source is actually many small metallic pellets or seeds, which are each about 1/3 to 1/4 of an inch long, similar in size and shape to a grain of rice. To minimize exposure to radiation to others from the source inside your body, you should do the following for _____ days.

- Stay at a distance of _____ feet from _____.
- Maintain separate sleeping arrangements.
- Minimize time with children and pregnant women.
- Do not hold or cuddle children.
- Avoid public transportation.
- Examine any bandages or linens that come into contact with the implant site for any pellets or seeds that may have come out of the implant site.
- If you find a seed or pellet that falls out:

- Do not handle it with your fingers. Use something like a spoon or tweezers to place it in a jar or other container that you can close with a lid.
- Place the container with the seed or pellet in a location away from people.
- Notify one of the persons listed in this instruction."

References

1. Smits ML, Elschot M, Van Den Bosch MA, van de Maat GH, van het Schip AD, et al. (2013) Imageable radioactive holmium-166 microspheres for treatment of liver malignancies: *in vivo* dosimetry based on SPECT and MRI. Journal of Nuclear Medicine *[in press]*.
2. Vente MA, Nijsen JF, de Wit TC, Seppenwoolde JH, Krijger GC, et al. (2008) Clinical effects of transcatheter hepatic arterial embolization with holmium-166 poly(L-lactic acid) microspheres in healthy pigs. Eur J Nucl Med Mol Imaging 35: 1259-1271.
3. Elschot M, Nijsen JF, Dam AJ, de Jong HW (2011) Quantitative evaluation of scintillation camera imaging characteristics of isotopes used in liver radioembolization. PLoS One 6: e26174.
4. Nuclear Regulatory Commission, Regulatory Guide 8.39, April 1997. Accesible at http://pbadupws.nrc.gov/docs/ML0833/ML083300045.pdf.
5. Nijsen JF, Zonnenberg BA, Woittiez JR, Rook DW, Swildens-van Woudenberg IA, et al. (1999) Holmium-166 poly lactic acid microspheres applicable for intra-arterial radionuclide therapy of hepatic malignancies: effects of preparation and neutron activation techniques. Eur J Nucl Med Mol Imaging 26: 699-704.
6. Zielhuis SW, Nijsen JF, de Roos R, Krijger GC, van Rijk PP, et al. (2006) Production of GMP-grade radioactive holmium loaded poly(L-lactic acid) microspheres for clinical application. Int J Pharm 311: 69-74.
7. Bolch WE, Bouchet LG, Robertson JS, Wessels BW, Siegel JA, et al. (1999) MIRD pamphlet No. 17: the dosimetry of nonuniform activity distributions--radionuclide S values at the voxel level. Medical Internal Radiation Dose Committee. J Nucl Med 40: 11S-36S.
8. Bol GH, Kotte AN, van der Heide UA, Lagendijk JJ (2009) Simultaneous multi-modality ROI delineation in clinical practice. Comput Methods Programs Biomed 96: 133-140.
9. Radiation-related consulting and services from Integrated Environmental Management, Inc. Gamma Ray Dose Constant http://www.iem-inc.com/toolgam.html.
10. Bult W, Kroeze SG, Elschot M, Seevinck PR, Beekman FJ, et al. (2013) Intratumoral administration of holmium-166 acetylacetonate microspheres: antitumor efficacy and feasibility of multimodality imaging in renal cancer. PLoS One 8: e52178.
11. Breitz HB, Wendt RE, 3rd, Stabin MS, Shen S, Erwin WD, et al. (2006) ^{166}Ho-DOTMP radiation-absorbed dose estimation for skeletal targeted radiotherapy. J Nucl Med 47: 534-542.
12. McCann JW, Larkin AM, Martino LJ, Eschelman DJ, Gonsalves CF, et al. (2012) Radiation emission from patients treated with selective hepatic radioembolization using yttrium-90 microspheres: are contact restrictions necessary? J Vasc Interv Radiol 23: 661-667.
13. Smits ML, Nijsen JF, van den Bosch MA, Lam MG, Vente MA, et al. (2012) Holmium-166 radioembolisation in patients with unresectable, chemorefractory liver metastases (HEPAR trial): a phase 1, dose-escalation study. Lancet Oncol 13: 1025-1034.
14. Gulec SA, Siegel JA (2007) Posttherapy radiation safety considerations in radiomicrosphere

treatment with ^{90}Y-microspheres. J Nucl Med 48: 2080-2086.

15. Gulec SA, Suthar RR, Barot TC, Pennington K (2011) The prognostic value of functional tumor volume and total lesion glycolysis in patients with colorectal cancer liver metastases undergoing ^{90}Y selective internal radiation therapy plus chemotherapy. Eur J Nucl Med Mol Imaging 38: 1289-1295.
16. Powerski MJ, Scheurig-Munkler C, Banzer J, Schnapauff D, Hamm B, et al. (2012) Clinical practice in radioembolization of hepatic malignancies: a survey among interventional centers in Europe. Eur J Radiol 81: e804-811.
17. Smits ML, Prince JF, Pronk AA, Nijsen JF, Zonnenberg B, et al. (2013) Quality of life in liver metastases patients treated with holmium-166 radioembolization. [submitted].
18. Rault E, Staelens S, Van Holen R, De Beenhouwer J, Vandenberghe S (2010) Fast simulation of yttrium-90 bremsstrahlung photons with GATE. Med Phys 37: 2943-2950.
19. Lambert B, Sturm E, Mertens J, Oltenfreiter R, Smeets P, et al. (2011) Intra-arterial treatment with (90)Y microspheres for hepatocellular carcinoma: 4 years experience at the Ghent University Hospital. Eur J Nucl Med Mol Imaging 38: 2117-2124.

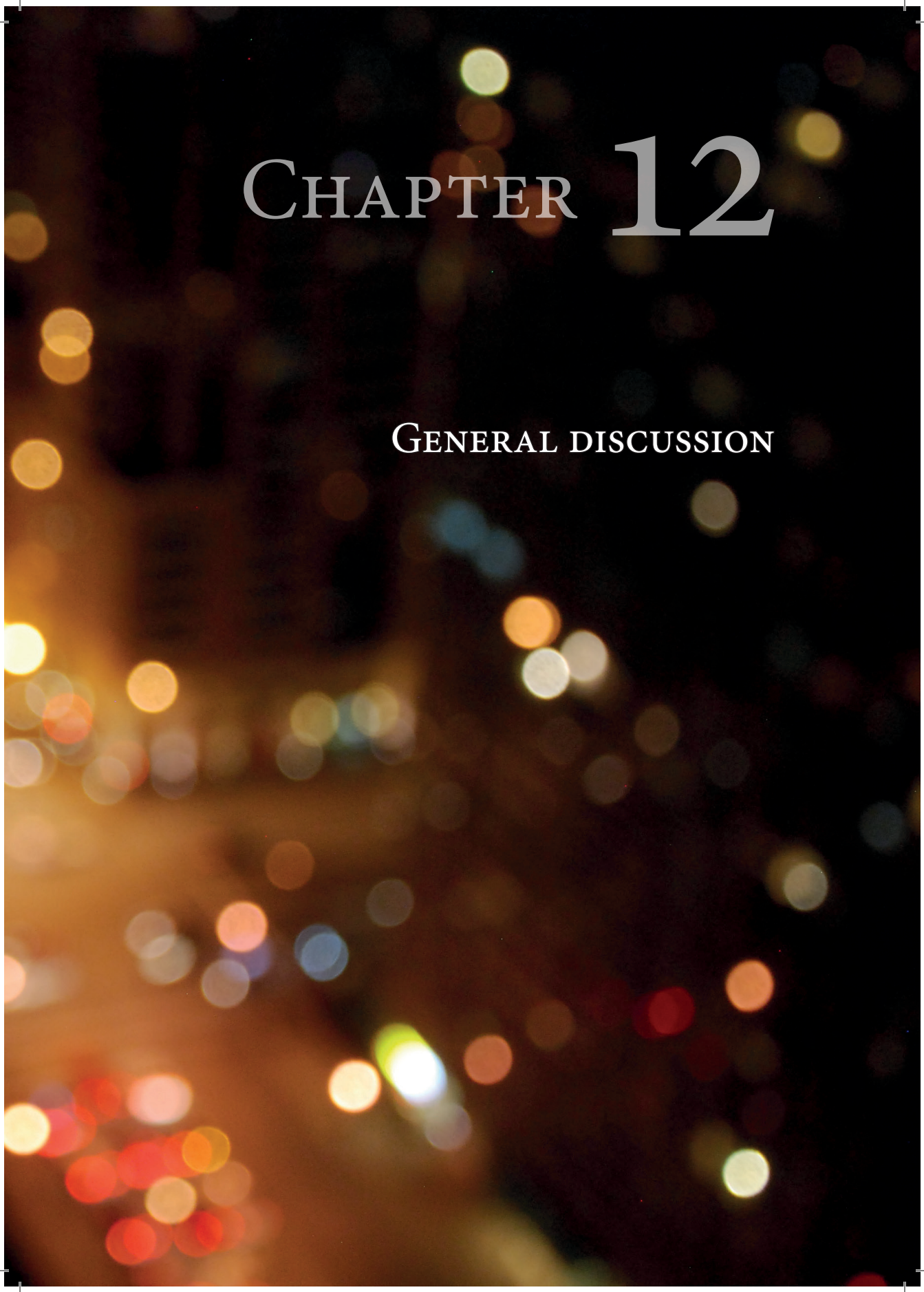

Chapter 12

General discussion

In this thesis, the first clinical trial on holmium-166 (^{166}Ho) radioembolization in human patients is described. The first part of this thesis describes the clinical outcomes of radioembolization in terms of response and toxicity. The main distinguishing characteristics of ^{166}Ho-microspheres are the possibilities for imaging and dosimetry, which is the focus of the second part.

Part I Response and Toxicity

^{90}Y-radioembolization

The University Medical Center Utrecht was the first center in the Netherlands to perform ^{90}Y-radioembolization. The first patient was treated in February 2009, while thousands of patients worldwide had already received ^{90}Y-radioembolization. Our institution had a lot to catch up with compared to high-volume centers. Data from all patients that were scheduled for ^{90}Y-radioembolization outside the prospective RADAR study[1] between February 2009 and March 2012 was retrospectively studied, as described in **Chapter 2**. Safety was the main priority of this retrospective analysis: what complications and adverse effects occurred in these patients and what kind of toxicity can we expect for future patients? Besides safety, efficacy in terms of tumor response and survival were evaluated. The clinical toxicity after ^{90}Y-radioembolization was in line with the literature, consisting mainly of low-grade post-embolization symptoms that were well manageable with outpatient medication.[2-5] Liver enzymes levels significantly increased after ^{90}Y-radioembolization in 38% of patients. These patients showed no signs of radiation induced liver disease and it was concluded that liver enzyme elevations are part of the physiological reaction of the liver to ^{90}Y-radioembolization. Disease control in the liver (complete or partial tumor response and stable disease) was obtained in only 21% of patients at 3 months follow-up. The majority of patients had progressive disease shortly after treatment. These figures differed a lot from the disease control rates reported in the literature ranging from 63 – 100%.[6] Part of this discrepancy is likely due to the methodology of dose response assessment. Tumor response was assessed blindly in our trial in order to increase objectivity and response rates were reported for different levels (target lesions only, whole-liver, and whole body). The methods of response assessment (*i.e.* responsimetry) were often not clearly described in the literature, which may have resulted in higher response rates.

Phase 1 clinical trial, design and limitations

A phase 1 clinical trial on ^{166}Ho-radioembolization was also started in 2009. The rationale and full design of this trial are presented in **Chapter 3**. The trial was designed to determine the maximum tolerated radiation dose in end-stage liver metastases patients

by escalating the dose after each cohort of 3-6 patients. Since these were the first patients to be treated with ^{166}Ho-radioembolization, the starting dose was set relatively low at 20 Gy. The dose increased linearly in steps of 20 Gy per dose cohort up to an absorbed dose of 80 Gy. 80 Gy was chosen as the highest dose since it is approximately two times the whole-liver absorbed dose that is delivered with ^{90}Y-radioembolization using the empirical or body surface area method, which is generally in the range of 20-60 Gy.[2,7]

A dose-escalation trial is always a compromise between exposing a minimum number of patients to an ineffective or toxic dose and accurately determining the optimum dose.[8] For this reason the HEPAR (Holmium Embolization Particles for Arterial Radiotherapy) trial was performed with a limited number of patients. Due to the limited number of patients in each cohort and conservative stopping rules, it cannot be excluded that chance may have played a role in determining the maximum tolerated radiation dose. Furthermore, the future dose was only determined based on maximum tolerated toxicity, not on efficacy. Maximum efficacy may be obtained already at a lower dose or at a higher dose. In a phase 1 trial, however, these aspects need to be balanced against practical and safety aspects.

Phase 1 clinical trial, outcomes

Chapter 4 presents the main outcomes of the phase 1 clinical trial. The maximum tolerated radiation dose was determined to be 60 Gy due to dose-limiting toxicities in the 80-Gy cohort. However, one can argue whether these toxicities were truly dose-related. The first of the patients in the 80-Gy cohort was readmitted with abdominal pain after a part of the radioactivity had inadvertently been deposited in the duodenum. The pain gradually disappeared over a period of four weeks. This event had to be interpreted as dose-limiting toxicity since it was a non-expected serious adverse event, although there seems to be no relation to the dose given. The second patient of the 80-Gy cohort developed signs of liver failure several weeks after treatment that can point to an overdose of radioactivity to the healthy liver. The patient died 15 weeks after radioembolization. At autopsy, however, no signs of radiation-induced liver disease were found and the entire liver was seeded with metastases. Liver failure was most likely due to tumor progression and the amount of radioactivity administered during radioembolization seemed unrelated. A third patient was treated at 80 Gy and did not experience any serious adverse events. Considering these findings together with the inherent limitations of the phase 1 clinical trial design, 60 Gy is probably not the absolute maximum tolerated radiation dose for end-stage liver metastases patients, if an absolute maximum tolerated radiation dose even exists for a group of patients.

Non-dose limiting toxicity was also thoroughly evaluated in this phase 1 clinical trial. Abdominal pain and nausea were the most frequent clinical toxicities, each reported in 80% of patients. Laboratory toxicity consisted mainly of liver enzyme levels elevations. The measured laboratory toxicities seemed in large part due to disease progression.

Comparison of ^{90}Y with ^{166}Ho

The aforementioned results on toxicity are in line with the toxicity from ^{90}Y-radioembolization as described in **Chapter 2**. The clinical adverse events consisted mainly of symptoms belonging to the post-embolization syndrome (*e.g.* abdominal pain, nausea, fatigue, loss of appetite). No new toxicities were found for ^{166}Ho-radioembolization that are not known to ^{90}Y-radioembolization. However, incidence rates of toxicity in our phase 1 clinical trial (**Chapter 4**) did differ from the toxicity as observed in clinical practice with ^{90}Y-radioembolization as presented in **Chapter 2**. We would like to stress that the results of the phase 1 clinical trial cannot be compared directly to ^{90}Y-radioembolization studies with completely different study designs. In a comment to our article describing the results of the phase 1 clinical trial, prof. Cosimelli, from the Regina Elena National Cancer Institute (Rome, Italy), stated that ^{166}Ho-radioembolization comes with a new range of adverse events, referring to the 80% lymphocytopenia and elevated gamma-glutamyl transpeptidase rate reported in this study.[9] In response to his comments (**Chapter 5)** we explained that these adverse events have been reported for ^{90}Y-radioembolization as well, and we highlighted the pitfalls of comparing the results of a phase 1 clinical trial – performed in a limited number of patients, that were treated at various doses and followed extensively with weekly blood analysis analysis and outpatient visits, where the main goal was to identify side effects – with dissimilar studies on ^{90}Y-radioembolization.

Quality of life

There is an increasing trend to look beyond the obvious outcomes like toxicity, tumor response and survival, when evaluating new treatment options.[10] To approximately 90% of cancer patients quality of life (QoL) is at least as important as length of life.[11,12] The effect of ^{166}Ho-radioembolization on QoL was presented in **Chapter 6**. Despite that ^{166}Ho-radioembolization comes with relatively little adverse events, especially compared to the systemic therapies that many of these patients had had, QoL decreased moderately and consistently after treatment. Similar results have been reported for ^{90}Y-radioembolization in patients with end-stage disease. QoL may benefit from higher response rates, since disease progression had a negative impact on QoL. Tumor response rates are likely to be higher when patients receive radioembolization in an earlier phase of treatment.[6]

Part II Imaging and Dosimetry

An overview of the imaging and dosimetry aspects of radioembolization is provided in **Chapter 7**. Dosimetry can be categorized into pre-treatment dosimetry, dosimetry during treatment, and post-treatment dosimetry. There are various techniques and particles used for each of these categories that are discussed in detail in this chapter. Dosimetry can be further divided into extrahepatic and intrahepatic dosimetry. Extrahepatic dosimetry is crucial to prevent complications due to non-target radioembolization. The main goal of intrahepatic dosimetry is to get or verify a therapeutic dose on the tumorous tissue and an as low as possible dose on the healthy liver. An overview of studies on dose-response relations in radioembolization is presented in order to get an indication of what a therapeutic tumor dose might be. This chapter provides insight into the latest developments on imaging and dosimetry for radioembolization and how these can be used for individualized treatment planning.

Pre-treatment dosimetry with ^{99m}Tc-MAA

Technetium-99m-macroaggretated albumin (^{99m}Tc-MAA) is the widely used surrogate particle for ^{90}Y-microspheres. The amount of ^{99m}Tc-MAA arriving in the lungs, and/or in the different compartments of the liver is taken into account for calculating the amount of activity administered at radioembolization. The underlying assumption is that the biodistribution of ^{99m}Tc-MAA is equal to the biodistribution of ^{90}Y-microspheres. **Chapter 8**, however, demonstrates that this is not the case for the intrahepatic biodistribution, and a recent study demonstrated that this is not the case for biodistribution to the lungs either.[13] In **Chapter 9**, we discussed why the literature is so divided when it comes to the value of ^{99m}Tc-MAA, and what role the methods of administration (*e.g.* catheter tip position) and methods of dosimetry may play.[14-17]

Post-treatment dosimetry of ^{166}Ho-microspheres

^{166}Ho-microspheres can be visualized with single photon emission computed tomography (SPECT) and MRI. In **Chapter 10**, data from the first patients treated with ^{166}Ho-radioembolization were used to demonstrate the feasibility of performing intrahepatic dosimetry with SPECT and MRI post treatment. MRI-based dosimetry could not be performed in 6 of 15 patients due to claustrophobia (n=1) or due to the presence of surgical clips in the liver distorting the images (n=5). SPECT-based dosimetry was performed in all patients. The agreement and correlation between both modalities on assessing the dose to liver segments and dose to tumors was assessed in the nine patients that received both SPECT and MRI-based dosimetry. There was a low to moderate agreement and high correlation between both modalities.
Accurate intrahepatic dosimetry allows for dosimetry on tumor level and calculating so

called tumor-to-non-tumor (T/N) ratios. The concept of radioembolization is founded on the assumption that the tumors in the liver are selectively fed by the hepatic artery and that arterially injected microspheres will thus end up in much higher concentrations in the tumor than in the normal liver tissue. T/N ratios for liver metastases patients have been reported to be up to 15.[18] In the study described in **Chapter 10**, however, mean T/N ratios ranged from 0.9 – 2.8, which is far lower than often assumed. T/N ratios can even be below 1.0, which means that there is a higher concentration of activity in the normal part of the liver than in the tumorous liver. However, determining exactly what is 'normal' liver and what is tumor is subject to error as well as dosimetry on the level of multiple small tumors. Tumor dosimetry is likely to benefit from ongoing developments like automatic functional liver delineation using sulfur colloid as described in **Chapter 7**. Various efforts have been made to improve T/N ratios in order to enhance tumor response and decrease toxicity. Vasoactive agents like angiotensin-II have been used for this purpose since the early days of radioembolization, with promising effects on T/N ratios.[19,20] Unfortunately, the limited availability of angiotensin II plus the lack of guidelines on how and how much of these agents should be administered and the systemic side effects seem to have hampered the application in clinical practice.[21,22]

Radiation safety

The gamma radiation that comes with ^{166}Ho and renders it imageable with SPECT, has downsides as well. The beta-radiation is absorbed in the patient's body, but a major part of the gamma-dose leaves the body, exposing other individuals. **Chapter 11** is a study on the radiation emission from patients treated with ^{166}Ho-RE. The total dose to others from patients treated with ^{166}Ho-RE was 1) estimated using the gamma-ray constant for ^{166}Ho, 2) calculated based on the dose rate measurements from the 15 patients, and 3) recalculated to the whole liver absorbed dose that future treatments will be aimed at (*i.e.* 60 Gy) and evaluated according to the U.S. Nuclear Regulatory Commission (NRC) regulations.[23] As expected the conservatively estimated total doses were higher than the total doses calculated based on the dose rate measurements. Also, the total doses to others were higher than total doses for ^{90}Y-radioembolization reported in the literature, which is caused by the gamma-radiation. All patients receiving ^{166}Ho-radioembolization can nevertheless be discharged from the hospital directly after treatment with contact restrictions according to the NRC regulations. According to these guidelines patients cannot be released if the calculated total dose to others in a basic scenario of 1 m distance and invariable presence exceeds 5 mSv. Contact restrictions are required in case the calculated total dose exceeds 1 mSv. The data from this study shows that contact restriction are not required in any patients with an administered activity up to 21 GBq when released 48 h post treatment.

Future perspectives

SPECT or MRI

In the phase 1 clinical trial, patients received ^{99m}Tc-MAA, a ^{166}Ho-scout dose, and a ^{166}Ho-therapy dose. Imaging was performed after each administration with SPECT and/or MRI. As described in **Chapter 10**, this amount of imaging is not desirable for clinical practice and future studies should help to make clear in what situations SPECT or MRI is most useful for dosimetry. Some factors that should be considered are the higher resolution of MRI compared to SPECT and that MRI does not rely on radioactivity.[24] MRI is, however, more susceptible to artifacts from metallic implants or air-containing organs (like the stomach, intestines and lungs) and MRI is limited to intrahepatic dosimetry. SPECT remains the preferred modality for extrahepatic dosimetry.
MRI-dosimetry is potentially useful for real-time MRI guidance during radioembolization. The feasibility of this concept was demonstrated in pigs.[25] The scarcity of dedicated materials for MRI-guided endovascular interventions and the lack of real-time dosimetry software have prevented us from performing MRI-guided radioembolization, but this remains an interesting topic for future research.

Scout dose

There are several reasons why ^{99m}Tc-MAA is not the ideal particle for biodistribution prediction. We have presented a scout dose consisting of a small amount (60 mg, 10% of therapy dose) of ^{166}Ho-microspheres with a lower specific activity than the treatment dose (250 MBq). Both the ^{166}Ho-scout dose and ^{99m}Tc-MAA were used in this phase 1 clinical trial since administration of ^{99m}Tc-MAA is the accepted method for pre-treatment safety assessment. Our goal is, however, to replace ^{99m}Tc-MAA with the scout dose of ^{166}Ho-microspheres. There are several hurdles that have to be taken before ^{99m}Tc-MAA can be replaced. First of all, although the specific activity of microspheres in the ^{166}Ho-scout dose is substantially lower than microspheres in the treatment dose, these microspheres still emit beta-radiation next to the gamma-radiation. Beta-radiation in non-target organs is undesirable and potentially harmful. Low amounts of beta radiation concentrated on a small part of the stomach or duodenum may for instance result in ulceration and even perforation. Our research group is currently investigating these safety aspects by looking at 1) what amounts of beta-radiation are tolerable in non-target organs, 2) how techniques like c-arm CT may help to reduce the chance of extrahepatic deposition of a scout dose, and 3) whether the activity of the scout dose can be reduced while still maintaining a satisfactory image quality. The scout dose of ^{166}Ho-microspheres has already shown to be superior to ^{99m}Tc-MAA for lung shunt prediction.[13] Similarly, the intrahepatic biodistribution of the ^{166}Ho-scout dose should ideally approach the biodistribution of the ^{166}Ho-treatment dose.

The position of radioembolization in the Netherlands

In the year of 2013, there is a growing number of centers in the Netherlands offering ^{90}Y-radioembolization. Those centers mainly perform ^{90}Y-radioembolization for primary liver cancer, since the college of health insurance companies has approved the reimbursement of ^{90}Y-radioembolization for patients with hepatocellular carcinoma only. The reimbursement of ^{90}Y-radioembolization for end-stage liver metastases and in particular for colorectal cancer liver metastases, has not yet been approved because of a shortage of evidence for treatment benefit. The body of evidence is, however, increasing and this year, ^{90}Y-radioembolization has been included in the concept Dutch national Colorectal liver metastases guidelines.[26]

As with many novel treatment options in oncology, radioembolization is currently mostly applied in patients with end-stage disease. End-stage disease means in general that patients had at least had the standard lines of systemic or locoregional treatments, or were not eligible for those treatments, or explicitly wished not to deviate from the standard treatment options due to toxicity. In that stage, ^{90}Y-radioembolization has shown a significant time-to-liver-progression benefit when added to 5-fluorouracil treatment for colorectal cancer liver metastases.[27] Other studies have found promising results as well, with an estimated pooled any-response rate of 79% in patients with end-stage disease.[6]

Radioembolization may, however, be more effective in earlier stages of disease. Radioembolization is a liver-directed therapy and is thus best suited for patients with metastasis confined to the liver. As the disease progresses, the metastasis becomes systemic and radioembolization alone may not be sufficiently effective. Not surprisingly, there is a trend to investigate whether there is a place for radioembolization in earlier stages of disease in combination with systemic treatment options. Systemic treatment options are relatively effective in colorectal cancer patients with liver metastases since metastases are often not confined to the liver only. However, systemically administered chemotherapy may not reach a high enough dose on the liver metastases. Complementing systemic treatment with a locoregional therapy that only targets the liver metastases seems therefore promising. Figure 1 shows the current position of radioembolization in relation to the systemic treatment lines for colorectal cancer liver metastases as well as the position of radioembolization in ongoing studies. The largest of these studies are the FOXFIRE and SIRFLOX trials and these aim at the top of the treatment algorithm.[28,29] These studies are targeted at more than 1000 patients (combined) and compare the overall survival of patients who receive first-line therapy with oxaliplatin-based treatment with patients who receive oxaliplatin-based treatment plus ^{90}Y-radioembolization. In the inSIRT trial, patients who are progressive on first-line oxaliplatin-based treatment receive ^{90}Y-radioembolization shortly before second-line

chemotherapy.[30] Combining ^{90}Y-radioembolization with second-line chemotherapy is also under investigation in the EPOCH study, which uses glass microspheres.[31] The results of these studies are eagerly awaited and may result in a shift from applying radioembolization for end-stage disease only, towards treatment of early-stage disease as well.

HEPAR trial phases

Clinical trials on new drugs or medical devices are often described in four temporal phases. According to the guidelines provided by the International Conference on Harmonization[32], phase 1 studies provide information on the short-term safety and tolerability in a limited number of patients and the information from those studies can be used to chose a suitable dosage range or administration schedule for further studies. The sequential studies are usually larger and have a longer follow-up time. Phase 2 trials should aim to select which of all the new drugs, devices etc., are worth it to be taken to a phase 3 trial.

These general guidelines apply well to the clinical trials on ^{166}Ho-radioembolization. The HEPAR phase 1 clinical trial was performed in 15 end-stage patients with a follow-up of three months. The main purpose of this study was to establish the maximum dose that could be safely given to end-stage disease patients.[33] Tumor response was also looked at in the phase 1 clinical trial, but a larger number of patients is necessary to tell whether holmium-radioembolization can induce tumor response. This will be answered in a phase 2 trial in which a larger number (n = 30 - 48) of the same category of patients will receive holmium-radioembolization with a follow-up time up to a year. The (interim) results of the HEPAR phase 2 trial should thus be used to make a decision on whether or not to embark on a much larger, and resource consuming, phase 3 trial. Design of a phase 3 trial is ongoing. This trial will aim at colorectal cancer patients in an earlier phase of disease, adding ^{166}Ho-radioembolization to second-line chemotherapy (*Figure 1*).

Valorization

Valorization is the process of creating value out of knowledge.[34] As mentioned in the Introduction of this thesis, the development of holmium-microspheres at our institute began more than 20 years ago and research and development has continued uninterruptedly ever since with an increasing number of people working on this project. Now, the first trial in human patients has been completed and a phase 2 trial is recruiting. Research and publishing of scientific data is important, but the impact for society increases when the knowledge obtained through research can be translated to clinical practice.

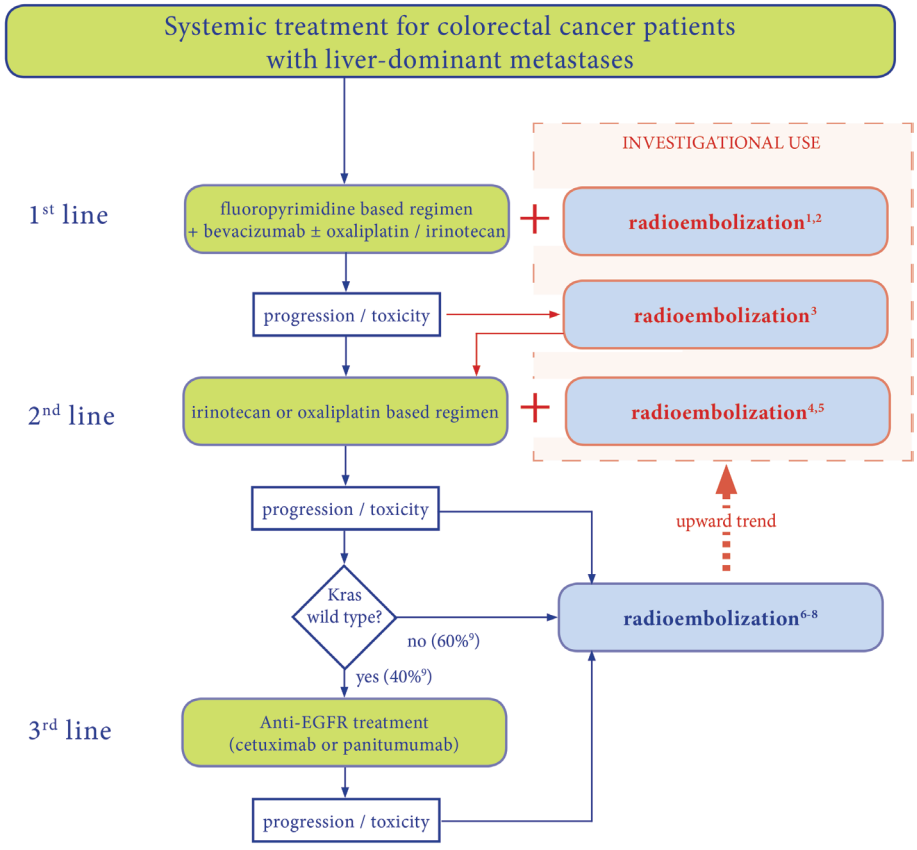

References
1. FOXFIRE study, Sharma et al., Clin Oncol 2008; 20: 261-3
2. SIRFLOX study, www.sirflox.com
3. inSIRT study, Reid et al., JVIR 2012; WCIO abstracts poster 42
4. EPOCH study, clinicaltrials.gov, NCT01483027
5. HEPAR III study
6. Hendlisz et al., J Clin Oncol, 2010; 28: 3687-94
7. Cosimelli et al., Br J Cancer, 2010; 103: 324-31
8. HEPAR study, Smits et al., Lancet Oncol, 2012; 13: 1025-35
9. De Roock et al., Lancet Oncol, 2010; 11: 753-63

Figure 1. *Algorithm for the current and investigational position of radioembolization (blue boxes) displayed against the systemic treatment lines (green boxes) for colorectal cancer patients. Radioembolization is currently predominantly performed in patients who have received first and second line therapy, but radioembolization can also be performed after third line therapy. The red quad indicates the position of radioembolization in ongoing studies in which radioembolization is combined with oxaliplatin-or irinotecan-based treatment (+ sign) or in between (arrows). Kras = v-Ki-ras2 Kirsten rat sarcoma viral oncogene homologue gene; EGFR = epidermal growth factor receptor.*

Several grants have been invested in the development of holmium-microspheres and related studies. *Inter alia* the Dutch Technology Foundation (Stichting Technische Wetenschappen), the Dutch Cancer society (Koningin Wilhelmina Kankerbestrijdingsfonds), the Sacha Swarttouw Heijmans Foundation, Maurits and Anna de Kock Foundation, Netherlands Genomics Initiative, and the University Medical Center have funded this process. We are very grateful for this broad support that enabled us to develop the product and perform the studies described in this thesis. Valorizing the resources invested in holmium microspheres by making holmium radioembolization available for a broad public is one of the future goals.

We believe that making holmium microspheres commercially available contributes to reaching patients with liver tumors worldwide. The need for commercialization led to the foundation of Quirem Medical in 2013.[35] Obtaining CE-marking is one of the next steps in the valorization of holmium-microspheres, since this will enable other centers to use holmium microspheres as well, which makes it available to patients with liver malignancies. Further steps that are essential for successful valorization include up-scaling the production / preparation of microspheres, marketing the product, performing further studies, assuring integration of the treatment in international treatment guidelines, and reimbursement by insurance companies. These steps should assure that holmium radioembolization will become available on a large scale for patients in and outside the Netherlands within a few years.

References

1. (2013) The RADAR study http://www.radioembolisatie.nl/wp-content/uploads/2013/08/RADAR studie.pdf.
2. Smits ML, van den Hoven AF, Rosenbaum CE, Zonnenberg BA, Lam MG, et al. (2013) Clinical and laboratory toxicity after intra-arterial radioembolization with (90)y-microspheres for unresectable liver metastases. PLoS One 8: e69448.
3. Van Hazel G, Blackwell A, Anderson J, Price D, Moroz P, et al. (2004) Randomised phase 2 trial of SIR-Spheres plus fluorouracil/leucovorin chemotherapy versus fluorouracil/leucovorin chemotherapy alone in advanced colorectal cancer. J Surg Oncol 88: 78-85.
4. Kennedy AS, Coldwell D, Nutting C, Murthy R, Wertman DE, Jr., et al. (2006) Resin ^{90}Y-microsphere brachytherapy for unresectable colorectal liver metastases: modern USA experience. Int J Radiat Oncol Biol Phys 65: 412-425.
5. Piana PM, Gonsalves CF, Sato T, Anne PR, McCann JW, et al. (2011) Toxicities after radioembolization with yttrium-90 SIR-spheres: incidence and contributing risk factors at a single center. J Vasc Interv Radiol 22: 1373-1379.
6. Vente MA, Wondergem M, van der Tweel I, van den Bosch MA, Zonnenberg BA, et al. (2009) Yttrium-90 microsphere radioembolization for the treatment of liver malignancies: a structured meta-analysis. Eur Radiol 19: 951-959.
7. Kennedy AS, McNeillie P, Dezarn WA, Nutting C, Sangro B, et al. (2009) Treatment parameters and outcome in 680 treatments of internal radiation with resin ^{90}Y-microspheres for unresectable hepatic tumors. Int J Radiat Oncol Biol Phys 74: 1494-1500.
8. Le Tourneau C, Lee JJ, Siu LL (2009) Dose escalation methods in phase I cancer clinical trials. J Natl Cancer Inst 101: 708-720.
9. Cosimelli M (2012) The evolution of radioembolisation. Lancet Oncol 13: 965-966.
10. Goodwin PJ, Black JT, Bordeleau LJ, Ganz PA (2003) Health-related quality-of-life measurement in randomized clinical trials in breast cancer--taking stock. J Natl Cancer Inst 95: 263-281.
11. Meropol NJ, Egleston BL, Buzaglo JS, Benson AB, 3rd, Cegala DJ, et al. (2008) Cancer patient preferences for quality and length of life. Cancer 113: 3459-3466.
12. Meropol NJ, Weinfurt KP, Burnett CB, Balshem A, Benson AB, 3rd, et al. (2003) Perceptions of patients and physicians regarding phase I cancer clinical trials: implications for physician-patient communication. J Clin Oncol 21: 2589-2596.
13. Elschot M, Lam MG, Nijsen JF, Smits ML, Prince JF, et al. (2013) Tc-99m-MAA overestimates the absorbed dose to the lungs in radioembolization: a quantitative evaluation in patients treated with Ho-166 microspheres. [submitted].
14. Ulrich G, Dudeck O, Furth C, Ruf J, Grosser OS, et al. (2013) Predictive value of intratumoral ^{99m}Tc-macroaggregated albumin uptake in patients with colorectal liver metastases scheduled for radioembolization with ^{90}Y-microspheres. J Nucl Med 54: 516-522.
15. Knesaurek K, Machac J, Muzinic M, DaCosta M, Zhang Z, et al. (2010) Quantitative comparison of yttrium-90 (^{90}Y)-microspheres and technetium-99m (^{99m}Tc)-macroaggregated albumin SPECT images for planning ^{90}Y therapy of liver

cancer. Technol Cancer Res Treat 9: 253-262.

16. Jiang M, Fischman A, Nowakowski FS (2012) Segmental Perfusion Differences on Paired Tc-^{99m} Macroaggregated Albumin (MAA) Hepatic Perfusion Imaging and Yttrium-90 (Y-^{90}) Bremsstrahlung Imaging Studies in SIR-Sphere Radioembolization: Associations with Angiography. Journal of Nuclear Medicine & Radiation Therapy 03.

17. Garin E, Lenoir L, Rolland Y, Edeline J, Mesbah H, et al. (2012) Dosimetry based on ^{99m}Tc-macroaggregated albumin SPECT/CT accurately predicts tumor response and survival in hepatocellular carcinoma patients treated with ^{90}Y-loaded glass microspheres: preliminary results. J Nucl Med 53: 255-263.

18. Gulec SA, Mesoloras G, Dezarn WA, McNeillie P, Kennedy AS (2007) Safety and efficacy of Y-90 microsphere treatment in patients with primary and metastatic liver cancer: the tumor selectivity of the treatment as a function of tumor to liver flow ratio. J Transl Med 5: 15.

19. Burke D, Davies MM, Zweit J, Flower MA, Ott RJ, et al. (2001) Continuous angiotensin II infusion increases tumour: normal blood flow ratio in colo-rectal liver metastases. Br J Cancer 85: 1640-1645.

20. Goldberg JA, Thomson JA, Bradnam MS, Fenner J, Bessent RG, et al. (1991) Angiotensin II as a potential method of targeting cytotoxic-loaded microspheres in patients with colorectal liver metastases. Br J Cancer 64: 114-119.

21. Dhabuwala A, Lamerton P, Stubbs RS (2005) Relationship of ^{99m}technetium labelled macroaggregated albumin (^{99m}Tc-MAA) uptake by colorectal liver metastases to response following Selective Internal Radiation Therapy (SIRT). BMC Nucl Med 5: 7.

22. Sasaki Y, Imaoka S, Hasegawa Y, Nakano S, Ishikawa O, et al. (1985) Changes in distribution of hepatic blood flow induced by intra-arterial infusion of angiotensin II in human hepatic cancer. Cancer 55: 311-316.

23. Nuclear regulatory commission, § 35.75 Release of individuals containing unsealed byproduct material or implants containing byproduct material. http://www.nrc.gov/reading-rm/doc-collections/cfr/part035/part035-0075.html

24. van de Maat GH, Seevinck PR, Elschot M, Smits ML, de Leeuw H, et al. (2012) MRI-based biodistribution assessment of holmium-166 poly(L-lactic acid) microspheres after radioembolisation. Eur Radiol.

25. Seppenwoolde JH, Bartels LW, van der Weide R, Nijsen JF, van het Schip AD, et al. (2006) Fully MR-guided hepatic artery catheterization for selective drug delivery: a feasibility study in pigs. J Magn Reson Imaging 23: 123-129.

26. (2006) Colorectal liver metastases, Dutch guideline, Version: 1.0, Oncoline, Integraal Kankercentrum Nederland,.

27. Hendlisz A, Van den Eynde M, Peeters M, Maleux G, Lambert B, et al. (2010) Phase III trial comparing protracted intravenous fluorouracil infusion alone or with yttrium-90 resin microspheres radioembolization for liver-limited metastatic colorectal cancer refractory to standard chemotherapy. J Clin Oncol 28: 3687-3694.

28. (2008) FOLFOX Plus SIR-SPHERES MICROSPHERES Versus FOLFOX Alone in Patients With Liver Mets From Primary Co-

lorectal Cancer (SIRFLOX), ClinicalTrials.gov Identifier: NCT00724503.

29. Sharma RA, Wasan HS, Love SB, Dutton S, Stokes JC, et al. (2008) FOXFIRE: a phase III clinical trial of chemo-radio-embolisation as first-line treatment of liver metastases in patients with colorectal cancer. Clin Oncol (R Coll Radiol) 20: 261-263.

30. Reid TR, Roeland E, Dad S, Shimabukuro KA, Fanta PT (2012) inSIRT trial: Single-center phase II study of yttrium-90 radioactive resin microspheres in the treatment of liver- predominant metastatic colorectal adenocarcinoma after failure of first-line combination chemotherapy. Journal of Clinical Oncology, 2012 ASCO Annual Meeting Proceedings (Post-Meeting Edition) 30.

31. (2011) Efficacy Evaluation of TheraSphere Following Failed First Line Chemotherapy in Metastatic Colorectal Cancer (EPOCH). ClinicalTrials.gov Identifier: NCT01483027.

32. (1997) General Considerations for Clinical Trials E8, International Conference on Harmonisation of Technical Requirements for Registration of Pharmaceuticals for Human Use.

33. Smits ML, Nijsen JF, van den Bosch MA, Lam MG, Vente MA, et al. (2012) Holmium-166 radioembolisation in patients with unresectable, chemorefractory liver metastases (HEPAR trial): a phase 1, dose-escalation study. Lancet Oncol 13: 1025-1034.

34. (2013) Rathenau Institute, Foundation STW, and Technopolis. Valuable - Indicators for valorisation, http://www.rathenau.nl/uploads/tx_tferathenau/ReportValuable.pdf, accessed August 25th 2013.

35. Quirem Medical, http://quiremmedical.com.

Chapter 13

Nederlandse samenvatting

In dit proefschrift wordt de eerste toepassing van holmium-166 radioembolisatie in de mens beschreven. Deel 1 van dit proefschrift beschrijft de klinische uitkomsten van radioembolisatie. Deel 2 behandelt de onderscheidende eigenschappen van holmium-166 microsferen, namelijk de mogelijkheden tot beeldvorming en dosimetrie bij radioembolisatie.

Inleiding

Gedeeltelijk gebaseerd op "Radioembolisatie van levermetastasen", door Smits MLJ, Nijsen JFW. Oncologie-Up-To-Date, 2012, vol 3, nummer 4

Principe van radioembolisatie

Radioembolisatie bestaat uit het toedienen van enkele miljoenen radioactieve microsferen (bolletjes met een diameter van ongeveer 30 micrometer) in de leverslagader waarmee bestraling binnen in de lever tot stand wordt gebracht. Deze behandeling kan worden gebruikt om patiënten met tumoren in de lever te behandelen. Het woord radioembolisatie is een samenvoeging van de woorden 'radio' en 'embolisatie' die de voornaamste componenten van deze behandeling omschrijven. 'Radio' slaat op het feit dat er radioactiviteit wordt gebruikt om de tumoren van binnenuit te bestralen en 'embolisatie' (het afsluiten van een bloedvat door inbrenging van een bepaalde substantie) slaat op de (gedeeltelijke) afsluiting van de bloedvaten richting de tumor door de microsferen. Bij radioembolisatie wordt gebruik gemaakt van de unieke bloedvoorziening van de lever: gezond leverweefsel wordt voornamelijk gevoed door de poortader, terwijl levertumoren hoofdzakelijk gevoed worden door de leverslagader. Door microsferen toe te dienen in de leverslagader kunnen de tumoren selectief worden behandeld met hoge doses zonder het gezonde leverweefsel overmatig te schaden. Het belangrijkste voordeel van radioembolisatie ten opzichte van andere lokale behandelopties is dat er weinig beperkingen zijn wat betreft de maximum toelaatbare grootte, aantal en verdeling van de tumoren in de lever.

Microsferen

Op dit moment wordt voor radioembolisatie gebruik gemaakt van microsferen geladen met het element yttrium-90 (^{90}Y). Deze microsferen zenden bèta-straling uit waarmee schade aan de tumoren wordt bereikt. Als alternatief voor de yttrium-microsferen zijn in het Universitair Medisch Centrum (UMC) Utrecht microsferen ontwikkeld die het element holmium-166 (^{166}Ho) bevatten. Deze microsferen zenden behalve bèta- ook gamma-straling uit. Daarnaast is holmium een paramagnetisch element. Deze eigenschappen zorgen er voor dat holmium-microsferen met meerdere methoden in beeld kunnen worden gebracht (*zie Figuur 1*). Doordat in kaart kan worden gebracht waar

de microsferen zich precies bevinden in de lever, kan men vaststellen of elke tumor een adequate dosis heeft gehad en of er nog aanvullende behandeling nodig is. Dit aspect wordt verder belicht onder "Deel II, Beeldvorming en Dosimetrie".

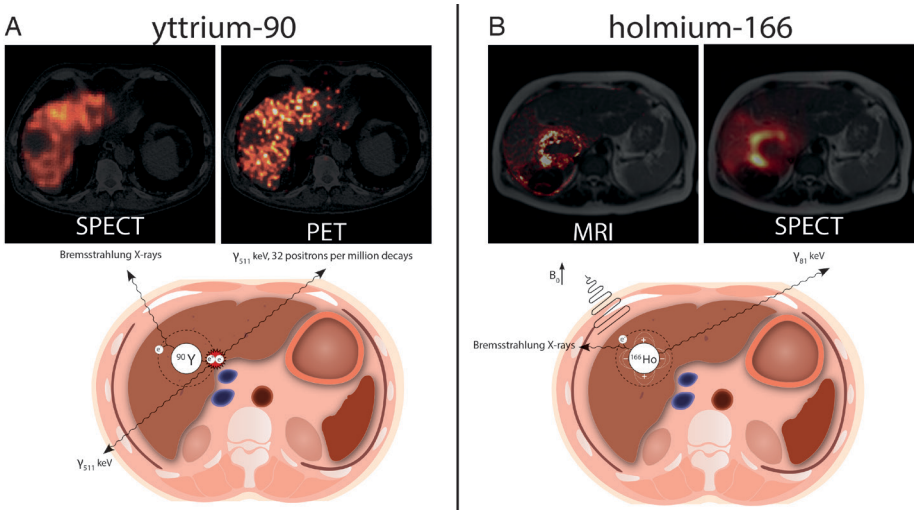

Figuur 1. *Beeldvorming van yttrium-microsferen (A) en holmium-microsferen (B). Yttrium-microsferen zijn zichtbaar met Single Photon Emission Computed Tomography (SPECT) via indirecte gamma-straling (Bremsstrahlung) en Positron Emission Tomography (PET). Holmium-microsferen zijn zichtbaar met Magnetic Resonance Imaging (MRI) vanwege het paramagnetisme van holmium en middels SPECT via directe gamma-straling.*

Productie

^{166}Ho is een radioactief isotoop, waarvan 166 het massagetal is (som van aantal protonen en neutronen). ^{166}Ho is instabiel en vervalt met een half-waarde tijd van 27 uur naar erbium-166. Tijdens dit verval komt er bèta- en gamma-straling vrij. Gamma-straling heeft een veel langere dracht dan bèta-straling en wordt in aanzienlijk mindere mate door het lichaam geabsorbeerd. Deze straling kan buiten het lichaam worden waargenomen door middel van een gamma-camera. Holmium microsferen – opgebouwd uit holmium-165 in een melkzuurmatrix – worden gemaakt in de radionucliden apotheek van het UMC Utrecht. Deze niet-radioactieve microsferen worden afgewogen, verpakt en vervolgens gedurende enkele uren met neutronen bestraald in de kernreactor van het Reactor Instituut Delft. De radioactieve ^{166}Ho-microsferen worden tot slot naar het UMC Utrecht vervoerd waar ze dezelfde dag nog worden gebruikt voor behandeling van een patiënt.

Deel I Respons en Toxiciteit

^{90}Y-radioembolisatie

Het UMC Utrecht was het eerste centrum in Nederland dat startte met 90Y-radioembolisatie. De eerste patiënt werd behandeld in februari 2009, terwijl al duizenden patiënten wereldwijd ^{90}Y-radioembolisatie hadden gehad. Ons instituut had daarom een achterstand in te halen vergeleken met internationale hoge-volume-centra. We hebben data van alle patiënten die buiten de RADAR-studie[1] tussen februari 2009 en maart 2012 in aanmerking kwamen voor ^{90}Y-radioembolisatie verzameld en beschreven in **Hoofdstuk 2**. Veiligheid was de voornaamste prioriteit van deze retrospectieve analyse: welke complicaties en bijwerkingen treden op in deze patiënten en welke toxiciteit kunnen we voor toekomstige patiënten verwachten? Behalve veiligheid werd effectiviteit geëvalueerd in termen van tumor respons en overleving. De klinische toxiciteit na ^{90}Y-radioembolisatie was in lijn met de literatuur en bestond met name uit laag-gradige post-embolisatie symptomen die goed te controleren waren met medicatie.[2-5] Leverenzym-spiegels stegen significant na ^{90}Y-radioembolisatie in 38% van de patiënten. Deze patiënten lieten geen tekenen zien van radiatie-geïnduceerd leverfalen en er werd geconcludeerd dat leverenzym stijgingen onderdeel zijn van de fysiologische reactie van de lever op ^{90}Y-radioembolisatie. Tumor controle (complete tumor respons, partiële tumor respons of stabiele ziekte) na drie maanden werd bereikt in slechts 21% van de patiënten. De meerderheid van de patiënten ontwikkelde kort na behandeling progressieve ziekte. Deze cijfers verschillen aanzienlijk van de respons-cijfers die in de literatuur worden gerapporteerd, waarbij tumor controle werd bereikt in 63% – 100%.6 Deze discrepantie zou gedeeltelijk veroorzaakt kunnen zijn door verschillen in de methoden van tumor-respons meting. Tumor respons werd in onze studie blind gemeten om de objectiviteit te maximaliseren en respons ratio's werden uitgesplitst voor verschillende niveaus (doel-laesies, gehele lever en geheel lichaam). De methoden van respons meting en rapportage worden vaak niet duidelijk omschreven in de literatuur, wat tot hogere respons ratio's kan hebben geleid.

Fase 1 studie, ontwerp en beperkingen

In 2009 werd ook een fase 1 klinische studie gestart naar ^{166}Ho-radioembolisatie. De rationale en volledig ontwerp van deze studie worden gepresenteerd in **Hoofdstuk 3**. De studie was ontworpen om de maximum tolereerbare stralingsdosis vast te stellen in patiënten met eind-stadium levermetastasen (uitzaaiingen), door middel van het verhogen van de dosis na elk cohort van 3-6 patiënten. Aangezien dit de eerste keer was dat patiënten met ^{166}Ho-radioembolisatie werden behandeld, was een relatief lage startdosering van 20 Gray (Gy) gekozen. Gy is de eenheid voor geabsorbeerde ioni-

serende straling. De dosis nam lineair toe in stappen van 20 Gy per dosis-cohort tot een geabsorbeerde dosis van 80 Gy. 80 Gy was gekozen als de hoogste dosis omdat dit ongeveer twee keer de geabsorbeerde dosis op de hele lever is na ^{90}Y-radioembolisatie volgens de empirische- of lichaamsoppervlakte methode, welke in het algemeen varieert van 20 Gy tot 60 Gy.[2,7]

Het ontwerp van een dosis-escalatie studie bevat vaak de afweging tussen enerzijds zo min mogelijk patiënten blootstellen aan een ineffectieve of toxische dosis en anderzijds zo accuraat mogelijk bepalen wat de optimale dosis is.[8] Om deze reden was de HEPAR (Holmium Embolisatie Partikels voor Arteriële Radiotherapie) uitgevoerd in een beperkt aantal patiënten. Gezien het beperkte aantal patiënten in elk cohort en de conservatieve stopregels, kan niet worden uitgesloten dat toeval een grote rol heeft gespeeld in het bepalen van de maximaal tolereerbare stralingsdosis. Bovendien werd de toekomstige dosis in deze studie alleen bepaald op basis van maximaal tolereerbare toxiciteit en niet op basis van effectiviteit. Maximale effectiviteit zou in principe al bij een lagere dosis of pas bij een hogere dosis kunnen worden bereikt. In een fase 1 studie moeten deze aspecten echter worden afgewogen tegenover praktische- en veiligheidsoverwegingen.

Fase 1 studie uitkomsten

In **Hoofdstuk 4** worden de voornaamste uitkomsten van de fase 1 studie gepresenteerd. De maximum-tolereerbare stralingsdosis werd vastgesteld op 60 Gy nadat er dosis-limiterende toxiciteit was opgetreden in het 80-Gy cohort. Men kan zich echter afvragen of deze toxiciteiten daadwerkelijk gerelateerd waren aan de dosis. De eerste patiënt uit het 80-Gy cohort werd heropgenomen met buikpijn nadat een deel van de radioactiviteit onbedoeld in de twaalfvingerige darm terecht was gekomen. De pijn nam geleidelijk af gedurende vier weken. Ondanks dat er geen relatie leek te zijn met de dosis, moest deze gebeurtenis toch worden geïnterpreteerd als dosis-limiterende toxiciteit omdat het ging om een onverwachte ernstige bijwerking. De tweede patiënt van het 80-Gy cohort ontwikkelde enkele weken na behandeling tekenen van leverfalen. Deze tekenen kunnen wijzen op een overdosis aan radioactiviteit op het gezonde leverweefsel. Deze patiënt overleed 15 weken na radioembolisatie. Bij autopsie werden echter geen tekenen van radiatie-geïnduceerd leverfalen geconstateerd. Daarentegen was de gehele lever bezaaid met uitzaaiingen. Het leverfalen werd waarschijnlijk veroorzaakt door tumorprogressie en leek niet gerelateerd aan de hoeveelheid toegediende radioactiviteit. Een derde patiënt werd ook behandeld met 80 Gy en ontwikkelde geen ernstige bijwerkingen. Deze bevindingen in overweging nemend samen met de inherente beperkingen van het fase 1 studie design, is 60 Gy waarschijnlijk niet de absolute, maximaal tolereerbare stralingsdosis voor patiënten met eind-stadium leverme-

tastasen. Men kan zich afvragen of een absolute, maximaal tolereerbare stralingsdosis voor een groep patiënten überhaupt bestaat, hierover meer in **Hoofdstuk 7**.
Niet-dosis-limiterende toxiciteit was ook uitvoerig geëvalueerd in deze fase 1 studie. Buikpijn en misselijkheid waren de meest frequente symptomen, elk gerapporteerd in 80% van de patiënten. Laboratorium toxiciteit bestond met name uit leverenzym stijgingen. Er waren aanwijzingen dat de gemeten laboratorium toxiciteit in groot deel werd veroorzaakt door progressie van tumoren.

Vergelijking ^{90}Y en ^{166}Ho

De bovengenoemde resultaten met betrekking tot toxiciteit zijn in lijn met de toxiciteit van ^{90}Y-radioembolisatie zoals beschreven in Hoofdstuk 2. De klinische bijwerkingen bestonden voornamelijk uit symptomen van het post-embolisatie syndroom (*e.g.* buikpijn, misselijkheid, moeheid, verminderde eetlust). Er werden geen nieuwe toxiciteiten vastgesteld bij ^{166}Ho-radioembolisatie die niet al beschreven waren na ^{90}Y-radioembolisatie. De incidentie van toxiciteit in onze fase 1 studie (Hoofdstuk 4) verschilde echter wel van de incidentie van toxiciteit zoals die veelal wordt gerapporteerd na ^{90}Y-radioembolisatie. Het is belangrijk om te benadrukken dat de resultaten van deze prospectieve fase 1 studie niet rechtstreeks kunnen worden vergeleken met compleet verschillend ontworpen studies naar ^{90}Y-radioembolisatie. In een brief naar aanleiding van ons artikel waarin de resultaten van deze fase 1 studie worden beschreven, noemt prof. Cosimelli van het Regina Elena National Cancer Institute (Rome, Italië) dat ^{166}Ho-radioembolisatie gepaard gaat met een scala aan nieuwe bijwerkingen, verwijzend naar de lymfocytopenie en gamma-glutamyl transpeptidase stijging in 80% van de studiepatienten.[9] In antwoord op dit commentaar (**Hoofdstuk 5**) leggen we uit dat deze bijwerkingen ook na ^{90}Y-radioembolisatie zijn beschreven en we benoemen de valkuilen van het vergelijken van resultaten van een fase 1 studie – uitgevoerd in een beperkt aantal patiënten die behandeld werden met variërende doses en intensief werden gevolgd met wekelijkse bloed analyses en polikliniek bezoeken – met studies naar ^{90}Y-radioembolisatie die een totaal andere opzet hadden.

Kwaliteit van Leven

Bij het evalueren van nieuwe behandelopties voor kanker is er tegenwoordig een trend om verder te kijken dan de voor de hand liggende uitkomstmaten zoals toxiciteit, tumor respons en overleving.[10] Zo'n 90% van de patiënten met kanker geeft aan dat kwaliteit van leven voor hen minstens zo belangrijk is als overlevingswinst.[11,12] Het effect van ^{166}Ho-radioembolisatie op kwaliteit van leven is beschreven in **Hoofdstuk 6**. Ondanks dat ^{166}Ho-radioembolisatie met relatief weinig bijwerkingen gepaard gaat, met name in vergelijking met de systemische therapieën die veel van deze patiënten hebben

gehad, was er een (matige) daling in kwaliteit van leven. Vergelijkbare resultaten zijn gerapporteerd voor ^{90}Y-radioembolisatie in patiënten met eind-stadium ziekte. Kwaliteit van leven zou wellicht kunnen verbeteren door meer tumor respons te verkrijgen, aangezien ziekte progressie een negatieve invloed had op kwaliteit van leven. Mogelijk kan tumor respons in een groter aantal patiënten behaald worden als de behandeling in een eerdere fase wordt uitgevoerd.[6]

Deel II Beeldvorming en Dosimetrie

Hoofdstuk 7 beschrijft een overzicht van de beeldvorming en dosimetrie aspecten van radioembolisatie. Dosimetrie is het meten van de (radioactieve) dosis op een bepaald object of weefsel. Dosimetrie kan worden gecategoriseerd in dosimetrie voorafgaand aan behandeling, gedurende behandeling en na behandeling. Dit hoofdstuk behandelt de verschillende technieken en partikels die gebruikt worden voor dosimetrie. Dosimetrie kan verder worden onderverdeeld in extra-hepatische en intra-hepatische dosimetrie. Extra-hepatische dosimetrie is cruciaal om te voorkomen dat radioactiviteit buiten de lever terecht komt en voor ernstige complicaties zorgt. Het hoofddoel van intra-hepatische dosimetrie is om een therapeutische dosis op het tumorweefsel te verkrijgen / verifiëren en een zo laag mogelijke dosis op het gezonde leverweefsel. Om een indruk te krijgen van wat een therapeutische dosis is, is in dit hoofdstuk een overzicht toegevoegd van studies die naar dosis-respons relaties bij radioembolisatie hebben gekeken. Samenvattend biedt dit hoofdstuk inzicht in de laatste ontwikkelingen op het vlak van beeldvorming en dosimetrie voor radioembolisatie en hoe deze kunnen worden gebruikt om de behandeling toe te spitsen op iedere individuele patiënt.

Dosimetrie voorafgaand aan behandeling met ^{99m}Tc-MAA

Voorafgaand aan elke radioembolisatie behandeling krijgt elke patiënt een proefbehandeling waarbij technetium-99m-macro-albumine aggregaten (^{99m}Tc-MAA) worden toegediend als surrogaat partikel voor ^{90}Y-microsferen. De hoeveelheid ^{99m}Tc-MAA dat in de longen en/of de verschillende compartimenten van de lever terecht komt wordt meegenomen bij het berekenen van de toe te dienen hoeveelheid ^{90}Y-activiteit. De onderliggende aanname is dat de verdeling van ^{99m}Tc-MAA in het lichaam en in de lever gelijk is aan de verdeling van ^{90}Y-microsferen. In **Hoofdstuk 8** wordt aangetoond dat dit niet het geval is voor de intra-hepatische verdeling en recent is aangetoond dat dit ook niet het geval is voor de verdeling in de longen.[13] In **Hoofdstuk 9** wordt bediscussieerd waarom de literatuur zo verdeeld is als het gaat over de waarde van ^{99m}Tc-MAA en welke rol de toedieningsmethoden (*e.g.* kathetertip positie) en methoden van dosimetrie kunnen spelen.[14-17]

Dosimetrie na behandeling met ^{166}Ho-microsferen

^{166}Ho-microsferen kunnen in beeld worden gebracht met SPECT en MRI (zie *Figuur 1*). In **Hoofdstuk 10** wordt in de eerste patiënten die behandeld waren met ^{166}Ho-radioembolisatie aangetoond dat intra-hepatische dosimetrie na behandeling mogelijk is met SPECT en MRI. Dosimetrie op basis van MRI kon niet worden uitgevoerd in 6 van de 15 patiënten door claustrofobie (1 patiënt) of door de aanwezigheid van metalen clips na een operatie aan de lever (5 patiënten). Op SPECT gebaseerde dosimetrie was in alle patiënten uitgevoerd. De overeenkomst en correlatie tussen beide modaliteiten voor het inschatten van de dosis op elk lever segment en de dosis op de tumoren werd bepaald in negen patiënten die geschikt waren voor dosimetrie op basis van zowel SPECT als MRI. De overeenkomst was laag tot matig, de correlatie was hoog.

Accurate intra-hepatische dosimetrie maakt dosimetrie op niveau van de tumor en het berekenen van de zogenaamde tumor-tot-non-tumor (T/N) ratio's mogelijk. Het concept radioembolisatie is gebaseerd op de aanname dat de tumoren in de lever selectief worden voorzien van bloed door de leverslagader en dat microsferen die in de leverslagader worden toegediend in veel hogere concentraties in de tumoren terecht komen dan in het gezonde leverweefsel. Er zijn zelfs T/N ratio's van 15 gerapporteerd in patiënten met levermetastasen, wat betekent dat de concentratie microsferen in de tumoren 15 keer zo hoog is als de concentratie in het gezonde leverweefsel.[18] Echter, in de studie beschreven in Hoofdstuk 10 varieerden de T/N ratio's van 0.9 tot 2.8, wat een stuk lager is dan vaak wordt aangenomen. T/N ratio's kunnen zelfs kleiner zijn dan 1.0, wat betekent dat er een hogere concentratie activiteit in het gezonde leverweefsel terecht is gekomen dan in de tumoren. Het blijft echter lastig en foutgevoelig om dosimetrie uit te voeren op meerdere kleine tumoren en om precies te bepalen welk deel van de lever 'gezond' is en wat tumor is. Dosimetrie op tumor-niveau zou kunnen profiteren van lopende ontwikkelingen zoals automatische omlijning van functioneel leverweefsel (beschreven in Hoofdstuk 7). Vanaf het begin van radioembolisatie zijn er pogingen ondernomen om T/N ratio's te verbeteren met als doel het effect op de tumoren te versterken en de bijwerkingen te verminderen. Voor dit doel zijn in het verleden verscheidene vaso-actieve stoffen zoals angiotensine-II bij radioembolisatie toegepast.[19,20] Helaas worden deze stoffen niet routinematig gebruikt in de praktijk vanwege slechte verkrijgbaarheid van deze middelen, gebrek aan gebruiksrichtlijnen en het risico op systemische bijwerkingen.[21,22]

Stralingshygiëne

De gamma-straling waarmee ^{166}Ho gepaard gaat zorgt er voor dat de microsferen zichtbaar zijn met SPECT, maar er zijn ook nadelen aan verbonden. De bèta-straling wordt geabsorbeerd in het lichaam van de patiënt, maar een groot deel van de gam-

ma-straling verlaat het lichaam waardoor anderen aan radioactieve straling worden blootgesteld. **Hoofdstuk 11** is een studie naar de straling die wordt uitgezonden door patiënten die behandeld zijn met ^{166}Ho-radioembolisatie. De totale effectieve dosis aan derden werd op drie manieren bepaald. Ten eerste werd deze geschat door middel van de gamma-straling constante voor ^{166}Ho. Ten tweede werd deze berekend op basis van exposie-tempo metingen in 15 patiënten, en ten derde werd deze herberekend naar een scenario waarin alle patiënten behandeld zouden zijn met de toekomstige hoeveelheid activiteit (*i.e.* hele-lever geabsorbeerde dosis van 60 Gy), en werd geëvalueerd volgens het reglement van de U.S. Nuclear Regulatory Commission (NRC).[23] Zoals verwacht waren de conservatief-geschatte totale effectieve doses hoger dan de berekende totale effectieve dosis op basis van de exposie-tempo metingen. De totale effectieve doses aan derden waren hoger dan de waarden gerapporteerd voor ^{90}Y-radioembolisatie, wat kan worden verklaard door de gamma-straling van ^{166}Ho. Alle patiënten die behandeld worden met ^{166}Ho-radioembolisatie kunnen desondanks direct na behandeling worden ontslagen uit het ziekenhuis met leefregels volgens het reglement van de NRC. Volgens dit reglement mogen patiënten niet worden ontslagen als de ingeschatte totale effectieve dosis aan derden, volgens een basis-scenario van onafgebroken aanwezigheid op 1m afstand, 5 millisievert (mSv) overschrijdt. Leefregels zijn noodzakelijk als de ingeschatte totale effectieve dosis 1 mSv overschrijdt. Deze studie laat zien dat leefregels niet nodig zijn als patiënten tenminste 48 uur worden opgenomen en niet meer dan 21 giga-becquerel (GBq), aan ^{166}Ho hebben ontvangen. Becquerel is de SI-eenheid voor radioactiveit, waarbij 1 becquerel gelijk is aan het verval van één atoomkern per seconde.

Toekomst perspectieven

SPECT of MRI

In de fase 1 studie werd zowel ^{99m}Tc-MAA, als een speurdosis ^{166}Ho-microsferen, als een therapeutische dosis ^{166}Ho-microsferen toegediend aan iedere patiënt. Na elke toediening werd er beeldvorming uitgevoerd met SPECT en/of MRI. Zoals beschreven in Hoofdstuk 10, is deze hoeveelheid beeldvorming niet wenselijk voor de klinische praktijk en daarom moeten toekomstige studies duidelijk maken in welke situaties SPECT of MRI de meest bruikbare modaliteit voor dosimetrie is. Enkele factoren die in die overweging mee moeten worden genomen zijn de hogere resolutie van MRI ten opzichte van SPECT en het gegeven dat MRI niet gebaseerd is op radioactiviteit.[24] MRI is echter gevoelig voor beeldverstoringen van metalen implantaten of lucht-houdende (organen zoals de maag, darmen en longen)en MRI is beperkt tot intra-hepatische dosimetrie. SPECT blijft daarom voorlopig de voorkeursmodaliteit voor extra-hepatische dosimetrie.

Dosimetrie op basis van MRI is potentieel bruikbaar voor MRI-geleide radioembolisatie. Dit concept is reeds aangetoond in varkens.[25] Het gebrek aan toegewijde materialen voor MRI-geleide endovasculaire interventies en het gebrek aan de vereiste software hebben ons er van weerhouden om MRI-geleide radioembolisatie in mensen uit te voeren, maar dit blijft een interessant onderwerp voor toekomstig onderzoek.

Speurdosis

Er zijn verschillende redenen waarom ^{99m}Tc-MAA niet het ideale partikel is voor voorspelling van de verdeling van microsferen. In de fase 1 studie hebben we een speurdosis gebruikt bestaande uit een kleine hoeveelheid (60 mg, 10% van de totale hoeveelheid microsferen) ^{166}Ho-microsferen met een lagere activiteit per microsfeer dan de therapie dosis (250 MBq). Zowel de speurdosis met ^{166}Ho-microsferen als ^{99m}Tc-MAA zijn in deze fase 1 studie gebruikt aangezien toediening van ^{99m}Tc-MAA op dit moment de aangewezen methode is om de behandeling voor te bereiden. Het is ons streven om ^{99m}Tc-MAA op den duur te vervangen met een speurdosis van ^{166}Ho-microsferen, maar voor het zo ver is, moeten er nog enkele hindernissen genomen worden. Ondanks de lagere activiteit per microsfeer zenden de ^{166}Ho-microsferen in de speurdosis potentieel schadelijke bèta-straling uit. Het is uiterst onwenselijk en schadelijk als bèta-straling terecht komt in niet-doel organen. Lage hoeveelheden bèta-straling, geconcentreerd in een klein volume van bijvoorbeeld de maag of twaalfvingerige darm kan resulteren in een ulcus of perforatie van de maag- of darmwand. Enkele vraagstukken die van belang zijn, zijn: 1) welke hoeveelheid bèta-straling verdraagbaar is voor niet-doel organen, 2) hoe technieken zoals c-arm CT het risico op extra-hepatische depositie van de speurdosis kunnen voorkomen, en 3) of de activiteit van de scout dosis kan worden gereduceerd met behoud van beeldkwaliteit. Het is al aangetoond dat een speurdosis met 166Ho-microsferen superieur is in het voorspellen van de hoeveelheid activiteit die in de longen terecht komt.[13] Op een zelfde wijze moet worden aangetoond dat de intra-hepatische verdeling van de speurdosis ^{166}Ho-microsferen vergelijkbaar is met de verdeling van de therapeutische dosis.

De positie van radioembolisatie in Nederland

Anno 2013 biedt een groeiend aantal centra in Nederland ^{90}Y-radioembolisatie aan. ^{90}Y-radioembolisatie wordt in deze centra met name toegepast voor de behandeling van primaire levertumoren (tumoren die zijn ontstaan in de lever), omdat het college van zorgverzekeraars ^{90}Y-radioembolisatie op dit moment alleen nog vergoedt voor deze categorie patiënten. De vergoeding voor ^{90}Y-radioembolisatie voor eind-stadium levermetastasen en colorectale levermetastasen in het bijzonder is nog niet goedgekeurd vanwege een tekort aan bewijs dat deze behandeling voordelen oplevert voor de

patiënt. De hoeveelheid bewijs neemt echter toe en dit jaar is ^{90}Y-radioembolisatie voor het eerst opgenomen in de Nederlandse concept richtlijnen voor colorectale levermetastasen.[26] Zoals met vele nieuwe oncologische therapieën wordt radioembolisatie op dit moment voornamelijk toegepast in patiënten met eind-stadium ziekte. Eind-stadium ziekte betekent in het algemeen dat patiënten de standaard chemotherapie en/of loco-regionale behandelingen hebben ondergaan, of niet geschikt waren voor deze behandelingen, of de expliciete wens hadden om af te wijken van de standaard behandeling vanwege bijvoorbeeld bijwerkingen. In dit stadium is aangetoond dat ^{90}Y-radioembolisatie een significante verlengde tijd-tot-lever-progressie teweeg kan brengen bij patiënten met colorectale levermetastasen, in combinatie met 5-fluorouracil behandeling.[27] Andere studies hebben ook veelbelovende resultaten gevonden, met een geschatte gewogen tumor-controle ratio van 97% in patiënten met eind-stadium ziekte.[6] Radioembolisatie zou echter effectiever kunnen zijn in eerdere fases van de ziekte. Radioembolisatie is een behandeling gericht exclusief op de lever en is dus het beste geschikt voor patiënten met metastasen beperkt tot de lever. Terwijl de ziekte voortschrijdt, wordt de kans groter dat er systemische uitzaaiing optreedt en dan is radioembolisatie alleen niet meer voldoende effectief. Het is daarom ook niet verrassend dat er een toenemende trend is om te onderzoeken of er een plaats is voor radioembolisatie in eerdere fases van de ziekte in combinatie met systemische chemotherapie. Systemische chemotherapie is relatief effectief in patiënten met colorectale levermetastasen omdat deze metastasen vaak niet tot de lever beperkt zijn. Systemisch toegediende chemotherapie lijkt echter niet altijd te resulteren in een adequate dosis op de tumoren in de lever. Het lijkt daarom veelbelovend om systemische behandeling aan te vullen met een locoregionale behandeling die alleen de lever metastasen aanpakt. *Figuur 1* laat de huidige positie van radioembolisatie in verhouding tot de systemische behandelingen zien voor colorectale levermetastasen evenals de positie van radioembolisatie in huidige studies. De grootste van deze studies zijn de FOXFIRE en SIRFLOX studies, welke gericht zijn op de top van het behandelalgoritme.[28,29] Deze studies zijn samen gericht op meer dan 1000 patiënten en vergelijken de algehele overleving van patiënten die eerstelijns oxaliplatin-bevattende behandeling hebben ontvangen, met patiënten die oxaliplatin-bevattende chemotherapie hebben ontvangen in combinatie met ^{90}Y-radioembolisatie. In een andere studie, de inSIRT trial genaamd, worden patiënten die progressief waren onder eerstelijns oxaliplatin-bevattende chemotherapie behandeld met ^{90}Y-radioembolisatie kort voorafgaand aan tweedelijns chemotherapie.[30] Het combineren van ^{90}Y-radioembolisatie met tweedelijns chemotherapie wordt ook onderzocht in de EPOCH studie, welke glas microsferen gebruikt.[31] Er wordt hoopvol uitgekeken naar de resultaten van deze studies welke zouden kunnen leiden tot een verandering

van de positie van radioembolisatie: van toepassing alleen in eind-stadium ziekte naar toepassing in eerdere fases van de ziekte.

HEPAR-studie fases

Klinische studies naar een nieuw geneesmiddel of medisch hulpmiddel worden vaak beschreven in vier fasen. Volgens de richtlijnen van de internationale conferentie op het gebied van harmonisatie[32], verstrekken fase 1 studies in het algemeen informatie met betrekking tot de verdraagbaarheid en veiligheid op korte termijn in een beperkt aantal patiënten. De informatie van deze studies kan worden gebruikt om een geschikte dosis of toedieningsschema voor toekomstige studies te bepalen. De daaropvolgende studies worden gewoonlijk in een groter aantal patiënten uitgevoerd en patiënten worden langer gevolgd. Fase 2 studies zouden zich moeten richten op het selecteren van nieuwe geneesmiddelen / medische hulpmiddelen etc., die het waard zijn om verder te worden onderzocht in een fase 3 studie. Vanwege beperkte middelen kan niet elk nieuw geneesmiddel / medisch hulpmiddel dat veilig blijkt in een fase 1 studie door gaan naar een fase 3 studie.
Deze algemene richtlijnen zijn goed toepasbaar op de klinische studies naar ^{166}Ho-radioembolisatie. De HEPAR fase 1 studie werd uitgevoerd in 15 eind-stadium patiënten met een volgperiode van drie maanden. Het hoofddoel van deze studie was om vast te stellen wat de maximale dosis is die veilig aan patiënten met eind-stadium levermetastasen kan worden gegeven.[33] In deze fase 1 studie werd tumor respons ook geanalyseerd, maar er is een groter aantal patiënten nodig om vast te kunnen stellen of ^{166}Ho-radioembolisatie daadwerkelijk in staat is om tumor respons te induceren. Dit zal worden beantwoord in een fase 2 studie waarin een groter aantal (n = 30 – 48) vergelijkbare patiënten zal worden behandeld met ^{166}Ho-radioembolisatie met een volgperiode van maximaal een jaar. De (tussentijdse) resultaten van de HEPAR fase 2 studie worden gebruikt om te bepalen of gestart wordt met een grotere, kostbare fase 3 studie. Er wordt op dit moment gewerkt aan het ontwerp van een dergelijke fase 3 studie, die zich bijvoorbeeld zou kunnen richten op het toevoegen van ^{166}Ho-radioembolisatie aan tweedelijns chemotherapie in patiënten met colorectale levermetastasen.

Valorisatie

Valorisatie is het proces van het creëren van waarde uit kennis.[34] De ontwikkeling van holmium-microsferen begon meer dan 20 jaar geleden in ons instituut en sindsdien is het onderzoek en de ontwikkeling ononderbroken doorgegaan met een toenemend aantal personen werkzaam op dit project. De eerste studie in patiënten is nu afgerond en een tweede studie loopt. Natuurlijk is het belangrijk om gedegen onderzoek uit te voeren en de resultaten te publiceren in de vorm van wetenschappelijke artikelen, maar

dit project kan met name waarde toevoegen aan de samenleving als de opgedane kennis kan worden vertaald naar de praktijk.
Er is vanuit verschillende bronnen geïnvesteerd in de ontwikkeling van holmium-microsferen en de gerelateerde studies. Onder andere de Stichting Technische Wetenschappen, het Koningin Wilhelmina Kankerbestrijdingsfonds, de Sacha Swarttouw Heijmans stichting, de Maurits en Anna de Kock stichting, het Netherlands Genomics Initiative, en het Universitair Medisch Centrum Utrecht hebben dit proces gesteund. We zijn zeer dankbaar voor deze brede steun dat ons in staat heeft gesteld om het product te ontwikkelen en de studies uit te voeren die onder andere in dit proefschrift zijn beschreven. Een belangrijk doel voor de toekomst is dan ook om de middelen die in holmium-microsferen zijn geïnvesteerd te valoriseren door holmium-radioembolisatie beschikbaar te maken voor breed publiek.
In onze opinie draagt het commercieel beschikbaar maken van holmium-microsferen bij aan het bereiken van patiënten met levertumoren wereldwijd. De behoefte aan commercialisatie heeft geleid tot de oprichting van Quirem Medical in 2013.[35] Het verkrijgen van CE-markering is een van de volgende stappen in de valorisatie van holmium-microsferen, omdat dit andere centra in staat moet stellen om holmium-microsferen te gebruiken. Overige stappen die belangrijk zijn voor succesvolle valorisatie zijn onder andere het opschalen van de productie / bereiding van de microsferen, product marketing, het uitvoeren van vervolgstudies, het positioneren van de behandeling in internationale richtlijnen, en het verkrijgen van vergoeding voor therapie van de zorgverzekeraars. Deze stappen moeten er voor zorgen dat holmium-radioembolisatie binnen enkele jaren op grote schaal beschikbaar komt voor patiënten binnen en buiten Nederland.

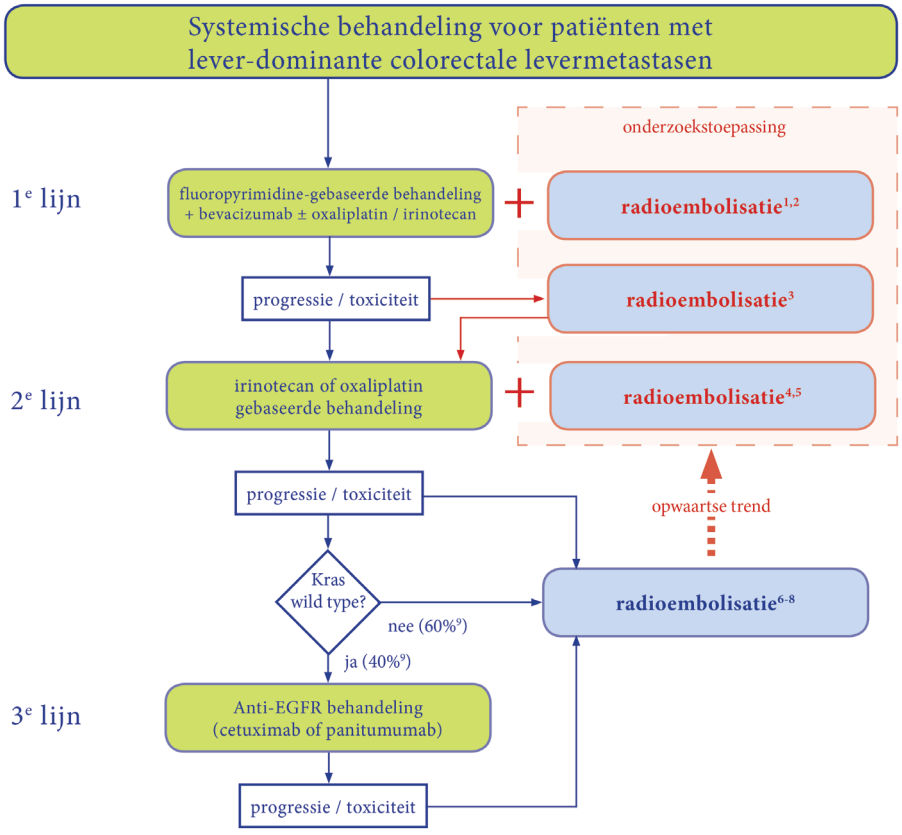

Referenties
1. FOXFIRE study, Sharma et al., Clin Oncol 2008; 20: 261-3
2. SIRFLOX study, www.sirflox.com
3. inSIRT study, Reid et al., JVIR 2012; WCIO abstracts poster 42
4. EPOCH study, clinicaltrials.gov, NCT01483027
5. HEPAR III study
6. Hendlisz et al., J Clin Oncol, 2010; 28: 3687-94
7. Cosimelli et al., Br J Cancer, 2010; 103: 324-31
8. HEPAR study, Smits et al., Lancet Oncol, 2012; 13: 1025-35
9. De Roock et al., Lancet Oncol, 2010; 11: 753-63

Figuur 2. *Algoritme voor de huidige positie en onderzoekstoepassing van radioembolisatie (blauwe kaders) tegenover de systemische behandel-lijnen (groene kaders) in het behandelschema van patiënten met colorectale levermetastasen. Radioembolisatie wordt op dit moment voornamelijk uitgevoerd in patiënten die reeds eerste- en tweedelijns chemotherapie hebben ontvangen, maar radioembolisatie kan ook worden uitgevoerd na derde lijn systemische therapie. Het rode kader indiceert de positie van radioembolisatie zoals deze op dit moment wordt onderzocht in studies die radioembolisatie ofwel combineren met eerste of tweede lijns therapie (+ teken) of radioembolisatie tussen deze behandelingen in geven (pijlen). Kras = v-Ki-ras2 Kirsten rat sarcoom viraal oncogeen homoloog gen; EGFR = epidermale groei factor receptor*

Referenties

1. (2013) The RADAR study http://www.radioembolisatie.nl/wp-content/uploads/2013/08/RADAR studie.pdf.
2. Smits ML, van den Hoven AF, Rosenbaum CE, Zonnenberg BA, Lam MG, et al. (2013) Clinical and laboratory toxicity after intra-arterial radioembolization with (90)y-microspheres for unresectable liver metastases. PLoS One 8: e69448.
3. Van Hazel G, Blackwell A, Anderson J, Price D, Moroz P, et al. (2004) Randomised phase 2 trial of SIR-Spheres plus fluorouracil/leucovorin chemotherapy versus fluorouracil/leucovorin chemotherapy alone in advanced colorectal cancer. J Surg Oncol 88: 78-85.
4. Kennedy AS, Coldwell D, Nutting C, Murthy R, Wertman DE, Jr., et al. (2006) Resin 90Y-microsphere brachytherapy for unresectable colorectal liver metastases: modern USA experience. Int J Radiat Oncol Biol Phys 65: 412-425.
5. Piana PM, Gonsalves CF, Sato T, Anne PR, McCann JW, et al. (2011) Toxicities after radioembolization with yttrium-90 SIR-spheres: incidence and contributing risk factors at a single center. J Vasc Interv Radiol 22: 1373-1379.
6. Vente MA, Wondergem M, van der Tweel I, van den Bosch MA, Zonnenberg BA, et al. (2009) Yttrium-90 microsphere radioembolization for the treatment of liver malignancies: a structured meta-analysis. Eur Radiol 19: 951-959.
7. Kennedy AS, McNeillie P, Dezarn WA, Nutting C, Sangro B, et al. (2009) Treatment parameters and outcome in 680 treatments of internal radiation with resin 90Y-microspheres for unresectable hepatic tumors. Int J Radiat Oncol Biol Phys 74: 1494-1500.
8. Le Tourneau C, Lee JJ, Siu LL (2009) Dose escalation methods in phase I cancer clinical trials. J Natl Cancer Inst 101: 708-720.
9. Cosimelli M (2012) The evolution of radioembolisation. Lancet Oncol 13: 965-966.
10. Goodwin PJ, Black JT, Bordeleau LJ, Ganz PA (2003) Health-related quality-of-life measurement in randomized clinical trials in breast cancer--taking stock. J Natl Cancer Inst 95: 263-281.
11. Meropol NJ, Egleston BL, Buzaglo JS, Benson AB, 3rd, Cegala DJ, et al. (2008) Cancer patient preferences for quality and length of life. Cancer 113: 3459-3466.
12. Meropol NJ, Weinfurt KP, Burnett CB, Balshem A, Benson AB, 3rd, et al. (2003) Perceptions of patients and physicians regarding phase I cancer clinical trials: implications for physician-patient communication. J Clin Oncol 21: 2589-2596.
13. Elschot M, Lam MG, Nijsen JF, Smits ML, Prince JF, et al. (2013) Tc-99m-MAA overestimates the absorbed dose to the lungs in radioembolization: a quantitative evaluation in patients treated with Ho-166 microspheres. [submitted].
14. Ulrich G, Dudeck O, Furth C, Ruf J, Grosser OS, et al. (2013) Predictive value of intratumoral ^{99m}Tc-macroaggregated albumin uptake in patients with colorectal liver metastases scheduled

for radioembolization with 90Y-microspheres. J Nucl Med 54: 516-522.

15. Knesaurek K, Machac J, Muzinic M, DaCosta M, Zhang Z, et al. (2010) Quantitative comparison of yttrium-90 (^{90}Y)-microspheres and technetium-99m (^{99m}Tc)-macroaggregated albumin SPECT images for planning 90Y therapy of liver cancer. Technol Cancer Res Treat 9: 253-262.
16. Jiang M, Fischman A, Nowakowski FS (2012) Segmental Perfusion Differences on Paired Tc-99m Macroaggregated Albumin (MAA) Hepatic Perfusion Imaging and Yttrium-90 (Y-90) Bremsstrahlung Imaging Studies in SIR-Sphere Radioembolization: Associations with Angiography. Journal of Nuclear Medicine & Radiation Therapy 03.
17. Garin E, Lenoir L, Rolland Y, Edeline J, Mesbah H, et al. (2012) Dosimetry based on 99mTc-macroaggregated albumin SPECT/CT accurately predicts tumor response and survival in hepatocellular carcinoma patients treated with 90Y-loaded glass microspheres: preliminary results. J Nucl Med 53: 255-263.
18. Gulec SA, Mesoloras G, Dezarn WA, McNeillie P, Kennedy AS (2007) Safety and efficacy of Y-90 microsphere treatment in patients with primary and metastatic liver cancer: the tumor selectivity of the treatment as a function of tumor to liver flow ratio. J Transl Med 5: 15.
19. Burke D, Davies MM, Zweit J, Flower MA, Ott RJ, et al. (2001) Continuous angiotensin II infusion increases tumour: normal blood flow ratio in colo-rectal liver metastases. Br J Cancer 85: 1640-1645.
20. Goldberg JA, Thomson JA, Bradnam MS, Fenner J, Bessent RG, et al. (1991) Angiotensin II as a potential method of targeting cytotoxic-loaded microspheres in patients with colorectal liver metastases. Br J Cancer 64: 114-119.
21. Dhabuwala A, Lamerton P, Stubbs RS (2005) Relationship of 99mtechnetium labelled macroaggregated albumin (^{99m}Tc-MAA) uptake by colorectal liver metastases to response following Selective Internal Radiation Therapy (SIRT). BMC Nucl Med 5: 7.
22. Sasaki Y, Imaoka S, Hasegawa Y, Nakano S, Ishikawa O, et al. (1985) Changes in distribution of hepatic blood flow induced by intra-arterial infusion of angiotensin II in human hepatic cancer. Cancer 55: 311-316.
23. Nuclear regulatory commission, § 35.75 Release of individuals containing unsealed byproduct material or implants containing byproduct material. http://www.nrc.gov/reading-rm/doc-collections/cfr/part035/part035-0075.html.
24. van de Maat GH, Seevinck PR, Elschot M, Smits ML, de Leeuw H, et al. (2012) MRI-based biodistribution assessment of holmium-166 poly(L-lactic acid) microspheres after radioembolisation. Eur Radiol.
25. Seppenwoolde JH, Bartels LW, van der Weide R, Nijsen JF, van het Schip AD, et al. (2006) Fully MR-guided hepatic artery catheterization for selective drug delivery: a feasibility study in pigs. J Magn Reson Imaging 23: 123-129.
26. (2006) Colorectal liver metastases, Dutch guideline, Version: 1.0, Oncoline, Integraal Kankercentrum Nederland,.
27. Hendlisz A, Van den Eynde M, Peeters M, Maleux G, Lambert B, et al. (2010) Phase III trial comparing protracted intravenous fluorouracil

infusion alone or with yttrium-90 resin microspheres radioembolization for liver-limited metastatic colorectal cancer refractory to standard chemotherapy. J Clin Oncol 28: 3687-3694.

28. (2008) FOLFOX Plus SIR-SPHERES MICROSPHERES Versus FOLFOX Alone in Patients With Liver Mets From Primary Colorectal Cancer (SIRFLOX), ClinicalTrials.gov Identifier: NCT00724503.
29. Sharma RA, Wasan HS, Love SB, Dutton S, Stokes JC, et al. (2008) FOXFIRE: a phase III clinical trial of chemo-radio-embolisation as first-line treatment of liver metastases in patients with colorectal cancer. Clin Oncol (R Coll Radiol) 20: 261-263.
30. Reid TR, Roeland E, Dad S, Shimabukuro KA, Fanta PT (2012) inSIRT trial: Single-center phase II study of yttrium-90 radioactive resin microspheres in the treatment of liver- predominant metastatic colorectal adenocarcinoma after failure of first-line combination chemotherapy. Journal of Clinical Oncology, 2012 ASCO Annual Meeting Proceedings (Post-Meeting Edition) 30.
31. (2011) Efficacy Evaluation of TheraSphere Following Failed First Line Chemotherapy in Metastatic Colorectal Cancer (EPOCH). ClinicalTrials.gov Identifier: NCT01483027.
32. (1997) General Considerations for Clinical Trials E8, International Conference on Harmonisation of Technical Requirements for Registration of Pharmaceuticals for Human Use.
33. Smits ML, Nijsen JF, van den Bosch MA, Lam MG, Vente MA, et al. (2012) Holmium-166 radioembolisation in patients with unresectable, chemorefractory liver metastases (HEPAR trial): a phase 1, dose-escalation study. Lancet Oncol 13: 1025-1034.
34. (2013) Rathenau Institute, Foundation STW, and Technopolis. Valuable - Indicators for valorisation, http://www.rathenau.nl/uploads/tx_tferathenau/ReportValuable.pdf, accessed August 25th 2013.
35. Quirem Medical, http://quiremmedical.com.

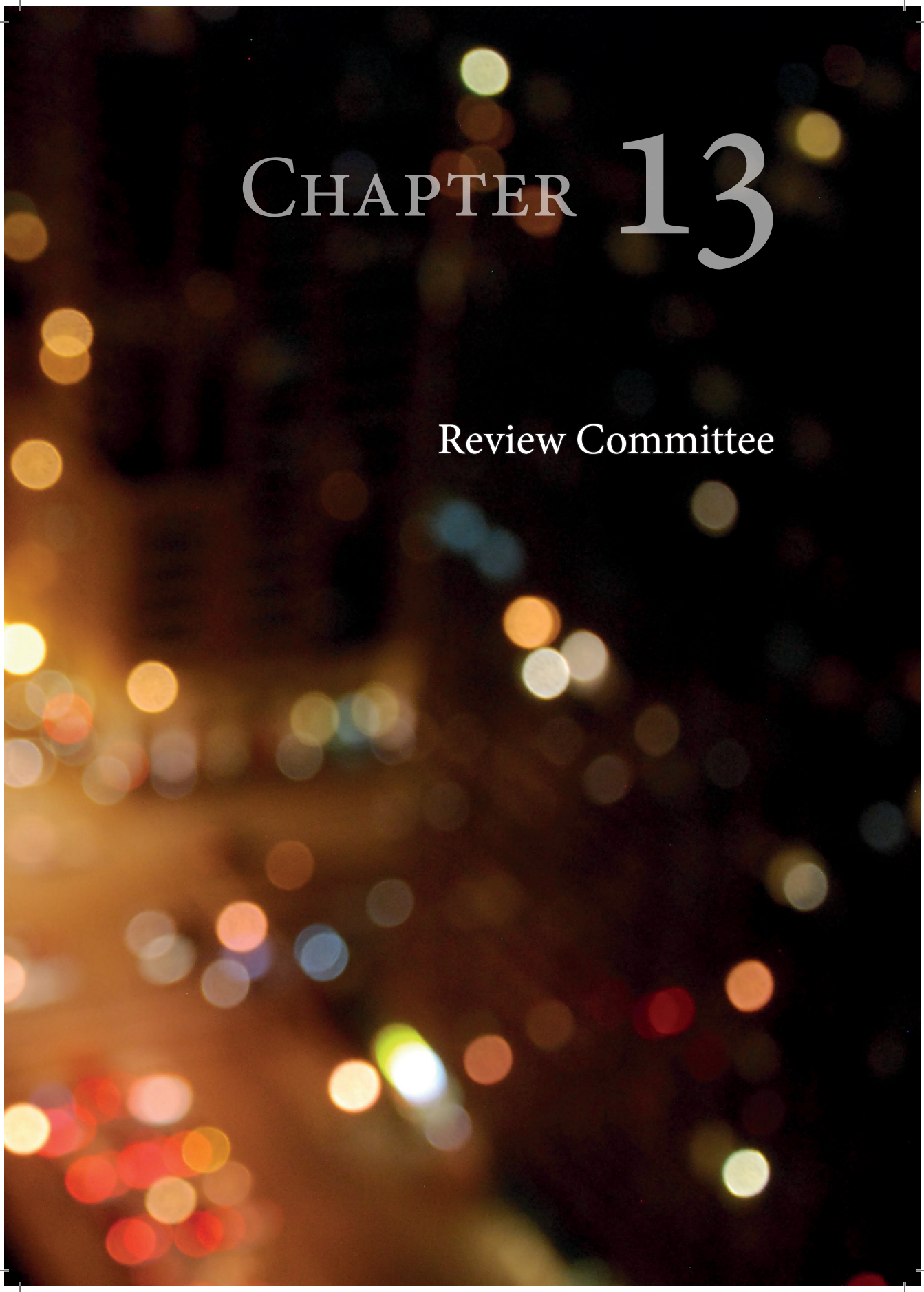

Chapter 13

Review Committee

Prof. Dr. P. J. van Diest
Professor in Pathology
Division of Laboratories and Pharmacy, University Medical Center Utrecht

Prof. Dr. P. R. Luijten
Professor of Functional Medical Imaging
Imaging Division, University Medical Center Utrecht

Prof. Dr. M. van Vulpen
Professor of Radiotherapy
Imaging Division, University Medical Center Utrecht

Prof. Dr. J. A. Reekers
Professor of Interventional Radiology
Department of Radiology, Academic Medical Center Amsterdam

Prof. Dr. I. H. M. Borel Rinkes
Professor in Surgical Oncology
Division of Surgical Specialties, University Medical Center Utrecht

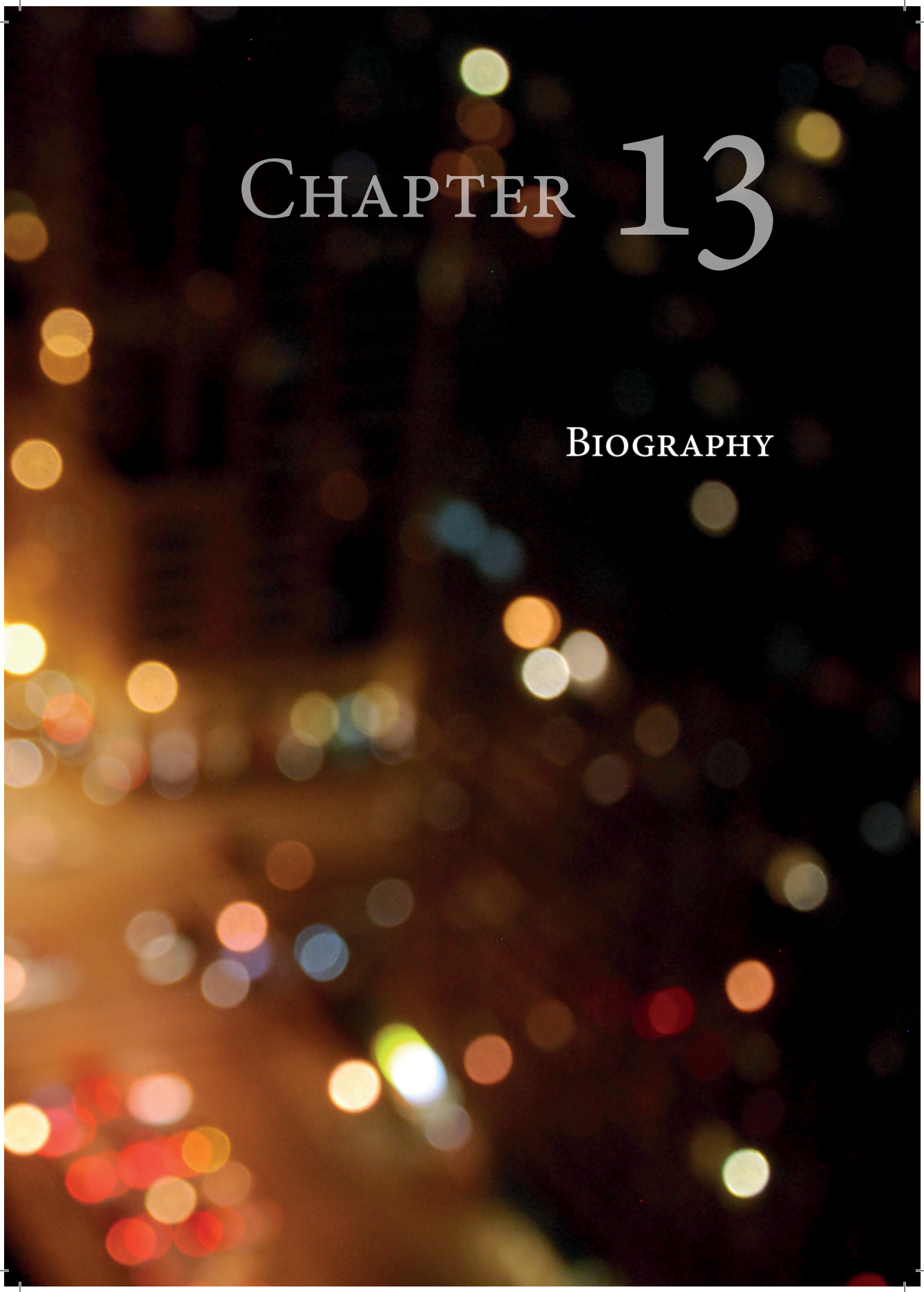

Chapter 13

Biography

Maarten Smits was born on the 24th of November 1987 in Amsterdam, the Netherlands. Soon after his birth, his family moved to Deventer (Overijssel) and eight years later to Veghel (Noord-Brabant). He graduated cum laude in 2005 at the Gymnasium Bernrode in Heeswijk-Dinther and started medical school at the Utrecht University in the same year.

In 2007, he started an undergraduate research project on MRI of ductal carcinoma in situ of the breast at the Radiology department of the University Medical Center (UMC) Utrecht under supervision of prof. dr. Willem Mali and prof. dr. Maurice van den Bosch. In 2009, he received a student scholarship by the Dutch Cancer Society for a research internship at the University Hospital of Gent, Belgium, under supervision of prof. dr. Luc Defreyne. The author graduated from medical school in August 2011 and was awarded an Alexandre Suerman stipendium: a personal grant to facilitate an MD, PhD project.

This MD, PhD project was performed at the Radiology department of the UMC Utrecht based on a phase 1 study on holmium-radioembolization. In November 2012, he left the Netherlands for a half-year research internship on MRI-guided treatment of prostate cancer at Stanford University in California. In January 2014, he will start his Radiology training at the Gelre Ziekenhuizen Apeldoorn and UMC Utrecht.

Chapter 13

List of Publications

Peer-reviewed publications

Elschot M, **Smits MLJ**, Nijsen JFW, Lam MGEH, van den Bosch MAAJ, Viergever MA, de Jong HWAM. Quantitative Monte Carlo-based holmium-166 SPECT reconstruction. *Medical Physics, accepted Sept 2013*

Smits MLJ, Elschot M, van den Bosch MAAJ, van de Maat GH, van het Schip AD, Zonnenberg BA, Seevinck PR, Verkooijen HM, Bakker CJ, de Jong HWAM, Lam MGEH, Nijsen JFW. Imageable radioactive holmium-166 microspheres for treatment of liver malignancies: *in vivo* dosimetry based on SPECT and MRI
The Journal of Nuclear Medicine, 2013 [Epub]

Prince JF, **Smits MLJ**, van Herwaarden JA, Arntz MJ, Vonken EJ, van den Bosch MA, de Borst GJ. Endovascular treatment of internal iliac artery stenosis in patients with buttock claudication.
PLoS One. 2013;8(8):e73331.

Smits MLJ, van den Hoven AF, Rosenbaum CENM, Zonnenberg BA, Lam MGEH, Nijsen JFW, van den Bosch MAAJ. Clinical and laboratory toxicity after intra-arterial radioembolization with ^{90}Y-microspheres for unresectable liver metastases.
Plos One, 2013 Jun Jul 24;8(7):e69448.

Rosenbaum CENM, Verkooijen HM, Lam MGEH, **Smits MLJ**, Koopman M, van Seeters T, Vermoolen MA, van den Bosch MAAJ. Radioembolisation for treatment of salvage patients with colorectal cancer liver metastases: A systematic review
Journal of Nuclear Medicine, 2013 [Epub]

Lam MGEH, **Smits MLJ**.
Value of ^{99m}Tc-macroaggregated albumin SPECT for radioembolization treatment planning *[Letter to the editor].*
Journal of Nuclear Medicine, 2013 [Epub]

Wondergem M, **Smits MLJ**, Elschot M, de Jong HWAM, Verkooijen HM, van den Bosch MAAJ, Nijsen JFW, Lam MGEH. Technetium-99m-MAA poorly predicts the intrahepatic distribution of yttrium-90 resin microspheres in hepatic radioembolization
Journal of Nuclear Medicine, 2013 [Epub]

Smits MLJ, Prince JF, Rosenbaum CENM, van den Hoven AF, Nijsen JFW, Zonnenberg BA, Seinstra BA, Lam MGEH, van den Bosch MAAJ. Intra-arterial radioembolization of breast cancer liver metastases: A structured review.
Eur J Pharmacol. 2013 Jun 5;709(1-3):37-42.

Smits MLJ, van den Bosch MAAJ, Nijsen JFW, Zonnenberg BA.
The evolution of radioembolisation. *[Letter to the editor]*
Lancet Oncol. 2012 Dec;13(12):e519.

Van de Maat GH, Seevinck PR, Elschot M, **Smits MLJ**, de Leeuw H, van het Schip AD, Vente MAD, Zonnenberg BA, de Jong HWAM, Lam MGEH, Viergever MA, van den Bosch MAAJ, Nijsen JFW, Bakker CJG. MRI-based biodistribution assessment of Holmium-166 poly(L-lactic acid) microspheres after radioembolisation. *Eur Radiol. 2013 Mar;23(3):827-35.*

Smits MLJ, Nijsen JFW, van den Bosch MAAJ, Lam MGEH, Vente MAD, Mali WPThM, van het Schip AD, Zonnenberg BA. Holmium-166 radioembolisation: results of a phase 1, dose escalation study in patients with unresectable, chemorefractory liver metastases – the HEPAR trial.
Lancet Oncol. 2012 Oct;13(10):1025-34.

Smits MLJ, Vanlangenhove P, Sturm EJC, van den Bosch MAAJ, Hav M, Praet M, Vente MAD, Snaps FR, Defreyne L. Transsinusoidal portal vein embolization with ethylene vinyl alcohol copolymer (Onyx): a feasibility study in pigs.
Cardiovasc Intervent Radiol 2012 Oct;35(5):1172-80.

Wijlemans JW, van Erpecum KJ, Lam MGEH, Seinstra BA, **Smits MLJ**, Zonnenberg BA, van den Bosch MAAJ. Trans-arterial 90yttrium radioembolization for patients with unresectable tumors originating from the biliary tree.
Ann Hepatol 2011; 10(3) 349-54

Barentsz MW, Vente MAD, Lam MGEH, **Smits MLJ**, Nijsen JFW, Seinstra BA, Rosenbaum CENM, Verkooijen HM, Zonnenberg BA, van den Bosch MAAJ. Technical solutions to Ensure Safe Yttrium-90 Radioembolization in Patients with Initial Extrahepatic Deposition of (99m)Technetium-Albumin-Macroaggregates.
Cardiovasc Inter Rad 2010; 34(5) 1074-9

Smits MLJ, Nijsen JFW, van den Bosch MAAJ, Lam MGEH, Vente MAD, Huijbregts JE, van het Schip AD, Elschot M, Bult W, de Jong HWAM, Meulenhoff PCW, Zonnenberg BA. Holmium-166 radio-embolization for the treatment of patients with liver metastases: design of the phase I HEPAR trial.
J Exp Clin Canc Res 2010, 29:70

Schmitz AC, **Smits MLJ**, Veldhuis W, van der Wall E, van Hillegersberg R, Borel-Rinkes IHM, Mali WPThM, van den Bosch MAAJ. Breast MR-imaging of ductal carcinoma in situ: a systematic review.
Imaging Decisions 2009;13 (3-4):112–121

Vente MAD, **Smits MLJ**, Zonnenberg BA, Nijsen JFW, van den Bosch MAAJ. Radioembolisatie met Yttrium-90 microsferen ter behandeling van niet-resectabele colorectale lever metastasen.
Nederlands Tijdschrift voor Oncologie 2008;5(8): 370-376

Non-peer reviewed publications

Smits MLJ, Nijsen JFW.
Holmiumradio-embolisatie voor levermetastasen
Kanker Breed 2011;3(3): 20-22

Smits MLJ, Nijsen JFW, van den Bosch MAAJ
Radio-embolisatie van levermetastasen
Oncologie up to date 2012;3(4): 18

Book Chapter

Cursusboek klinische hepatologie. Behandeling van maligne levertumoren door de radioloog. **Smits MLJ**, Seinstra BA, van den Bosch MAAJ. *Haarlem 2010, ISBN 978-90-79014-04-0*

Conference presentations

Smits MLJ, Pronk AA, Nijsen JFW, *et al.* Quality of life in patients with hepatic malignancies treated with holmium-166 radioembolization.
Society of Interventional Radiology, New Orleans, 2013 (oral presentation)

Smits MLJ, Nijsen JFW, van den Bosch MAAJ, *et al.* Resultaten van een fase 1, dosis escalatie studie naar holmium-radioembolisatie in patiënten met irresectabele, chemorefractaire lever metastasen: de HEPAR trial.
Nederlandse Radiologendagen, 's Hertogenbosch, 2012 (oral presentation)

Smits MLJ, van de Maat G, Elschot M, *et al.* Assessment of holmium-166 microsphere biodistribution after radioembolization in patients with liver metastases: comparison between MRI and SPECT.
Society of Interventional Radiology, San Francisco, 2012 (oral presentation)

Smits MLJ, Elschot M, van de Maat G, *et al.* Intrahepatic holmium-166 microsphere biodistribution assessment in patients with liver metastases using MRI and SPECT.
Annual Meeting of the Radiology Society of North America, Chicago, 2011 (poster presentation)

Smits MLJ, Elschot M, van de Maat G, *et al.* Intrahepatic holmium-166 microsphere biodistribution assessment in patients with liver metastases using MRI and SPECT.
Nederlandse Radiologendagen, Maastricht, 2011 (oral presentation)

Smits MLJ, Vente MAD, Lam MGEH, *et al.* Yttrium-90 radioembolization associated liver toxicity and potential implications for retreatment of paients.
15th Asean Association of Radiology Congress, Singapore 2011 (oral presentation)

Smits MLJ, Nijsen JFW, van den Bosch MAAJ, *et al.* Holmium-166 radioembolization for the treatment of patients with liver metastases: design and initial results of the phase I HEPAR trial.
Nederlandse Radiologendagen, Veldhoven, 2010 (oral presentation)

Smits MLJ, Nijsen JFW, van den Bosch MAAJ, *et al.* Holmium-166 Microsphere Radioembolization for the Treatment of Patients with Liver Metastases: The HEPAR Trial, Study Announcement and Initial Results.
Annual meeting of the IRIST（the International Research group in Immuno-Scintigraphy and Therapy), Groningen, 2010 (oral presentation)

Smits MLJ, Lam MGEH, Vente MAD, *et al.* Yttrium-90 radioembolization for the treatment of patients with liver malignancies: first experiences in the Netherlands.
'Jong talent in Beeld', department of Radiology UMC Utrecht, Utrecht, 2010 (oral presentation)

Smits MLJ, Lam MGEH, Zonnenberg BA, van den Bosch MAAJ. Radioembolization of colorectal liver metastases.
68e Oncologiedag 'Colorectal cancer' (Nederlandse Vereniging voor Oncologie), Utrecht, 2010 (oral presentation)

Smits MLJ, Hav M, Vanlangenhove P, *et al*. Transsinusoidal Portal Vein Embolization with Onyx: a feasibility study in pigs.
European Congress of Radiology, Vienna, 2009 (poster presentation)

Smits MLJ, Hav M, Vanlangenhove P, *et al*. Transsinusoidal Portal Vein Embolization with Onyx: a feasibility study in pigs.
Nederlandse Radiologendagen, Amsterdam, 2009 (poster presentation)

Smits MLJ, Prevoo W, Teertstra HJ, *et al*. Hepatic intra-arterial chemoinfusion as salvage therapy for patients with unresectable liver metastases from breast cancer.
Nederlandse Radiologendagen, Rotterdam, 2008 (oral presentation)

Chapter 13

Acknowledgements

Dankwoord

Met dit dankwoord sluit ik dit proefschrift af en tevens ook een periode van zo'n vier jaar waarin ik hoofdzakelijk aan dit onderzoek heb gewerkt. Mijn promotietijd heb ik met veel plezier beleefd dankzij de mensen om mij heen. De onderstaande woorden vormen een poging om mijn dank voor jullie uit te drukken.

Promotoren en co-promotoren

Prof dr. van den Bosch, beste Maurice, ik ben je erg dankbaar. Toen ik per e-mail voor het eerst aan "the Bosch" werd voorgesteld werkte jij aan Stanford en ik had nog geen idee wat jij voor mijn toekomst in de Radiologie zou gaan betekenen. Je hebt buitengewoon veel in mij geïnvesteerd, zelfs toen ik nog student was, en je hebt als mentor altijd mijn toekomst in het vizier gehouden. Op die manier heb jij er voor gezorgd dat ik al tijdens mijn studie kon beginnen aan een zeer gewild promotietraject. Ik wil je bedanken voor het vertrouwen dat je in mij hebt getoond en de daarbij horende vrijheden. Hopelijk kunnen we ook na dit proefschrift blijven samenwerken!

Prof. dr. Mali, beste Willem, mijn onderzoekstijd is bij u begonnen. Zonder doel voor ogen kon de studie Geneeskunde mij nauwelijks uitdagen. U wist mij al in mijn tweede studiejaar te interesseren voor de Radiologie en u bood mij de kans om onderzoek te doen. Sindsdien bent u altijd zeer begaan geweest met mijn ontwikkeling en ik ben trots dat ik als tweede generatie Smits bij u mag promoveren.

Dr. Zonnenberg, beste Bernard, als principle investigator van de HEPAR studie werd jij talloze malen door mij om handtekeningen gevraagd, waarbij jij uren de tijd nam om mij te vertellen over diverse maatschappelijke, carrière-technische en geneeskundige onderwerpen. Jouw schijnbaar onuitputtelijke kennis heeft mij zeer geïnspireerd. De introductie van dit proefschrift is grotendeels tot stand gekomen tijdens een van deze sessies.

Dr. Nijsen, beste Frank, dank dat je mij in het holmium-team hebt opgenomen. We hebben vaak gesproken over de geschiedenis, het heden en de toekomst van radioembolisatie. Al jaren zet jij je in voor de ontwikkeling van een nieuwe generatie microsferen en ik ben blij dat ik daaraan heb mogen bijdragen.

Beoordelingscommissie

De leden van de beoordelingscommissie, prof. dr. van Diest, prof. dr. van Vulpen, prof. dr. Luijten, prof. dr. Borel Rinkes en prof. dr. Reekers. Ik ben u zeer dankbaar voor de tijd en aandacht die u heeft gestoken in het beoordelen van mijn proefschrift.

Holmium-team

Het 'holmium-team' bestaat uit een groot aantal personen zonder wie niets van dit proefschrift tot stand zou zijn gekomen. Enkele van deze personen wil ik hieronder persoonlijk noemen.

Marnix Lam, ik heb goede herinneringen aan onze tijd aan Stanford. Tussen al het onderzoek naar MRI van de prostaat door was ik opgelucht om tijdens de lunch 'gewoon' over radioembolisatie te kunnen filosoferen met jou. Ik bewonder je moed om in een zaal vol preutse Amerikanen jouw werk af te doen als "academische masturbatie". Wellicht heeft dit geleid tot je gerespecteerde plek in het internationaal rondreizend circus.

Tjitske Bosma, organisatorische ruggengraat van de HEPAR studie. Door jouw inzet heb jij er voor gezorgd dat de studie op rolletjes liep, iedereen zich aan zijn afspraken hield en ik mij kon concentreren op de wetenschap. Dank.

Fred van het Schip, Gerard Krijger, Remmert de Roos, dank voor al het werk dat jullie achter de schermen verrichten voor de behandeling van patiënten en jullie hulp bij het onderzoek.

Mattijs Elschot, ik denk dat wij een zeer prettige en vruchtbare samenwerking hebben gehad waarbij we het klinische en technische aspect van holmium radioembolisatie bij elkaar wisten te brengen. Dank voor de talloze keren waarop je mij geduldig de technische principes van jouw werk hebt uitgelegd. Ik geloof dat ik het begin te snappen.

Peter Seevinck, Gerrit van de Maat, mogelijk gehinderd door de fysieke afstand verliep de communicatie tussen ons aanvankelijk wat stroef. Gelukkig hebben we dit kunnen overbruggen en zijn we tot een aantal mooie ontwikkelingen gekomen.

Chris Oerlemans, niet te vergeten, ik bewonder hoe jij aan de basis stond van de creatie van verschillende typen microsferen. Het was me dan ook een genoegen om samen een van deze veelbelovende creaties te testen.

Maarten Vente, het is een voorrecht geweest om jou als leermeester te hebben gehad. Hopelijk blijkt uit dit proefschrift dat de decimal mark en de Oxford comma er nu wel in zijn geslepen. Ik heb altijd het gevoel gehad dat jij het meeste verstand had van radioembolisatie, in Utrecht en wellicht ver daarbuiten. Na vele jaren heb jij afscheid genomen van het holmium-team om de 'concurrent' te versterken. Ik gun het jou en

hen, en ben blij voor de radioembolisatie-community dat jouw kennis en inzicht in het vak is gebleven.

Overige collega's en betrokkenen

Ik wil graag alle laboranten, radiologen, nucleair geneeskundigen, en assistenten bedanken die op welke manier dan ook hebben bijgedragen aan dit onderzoek.

Miriam Koopman, Maurits Wondergem, Julia Huijbregts, Hugo de Jong, dank voor jullie bijdrage aan dit proefschrift.

Angioteam, ik realiseer me dat de holmium behandelingen tijdrovend waren en het programma in de war gooiden. Bedankt voor jullie geduld. Jan, Rutger, Alexander, ik waardeer de manier waarop jullie je open hebben gesteld voor de arts-onderzoekers, blijkend uit de mogelijkheid tot laagdrempelig overleg over studie-interventies en het samen sjouwen met bakstenen als training voor de Urbanathlon.

Trial bureau, Anneke, Lenny, Shanta, Saskia, jullie werk is essentieel voor de kwaliteit van de wetenschap binnen onze divisie. Cees Haaring, jij verdient aparte vermelding vanwege al het werk dat jij voor ons hebt verricht rondom datamanagement.

Fotografie, onderzoekers van andere afdelingen zijn jaloers op 'onze' eigen fotografie afdeling. Ik kwam vaak bij jullie terecht voor hulp met figuren, foto's, scans, prints. Karin van Rijnbach, bedankt voor de hulp bij de verschillende figuren in dit proefschrift. Roy Sanders, bedankt voor het opmaken van dit proefschrift en je hulp bij de organisatie van het symposium.

Stafsecretariaat Radiologie, Annet, Marja, bedankt dat jullie altijd klaar staan om ons te helpen. Annet, bedankt voor jouw inzet rondom de organisatie van deze promotie en het symposium.

Akke Pronk, jij hebt je als student ingezet om kwaliteit van leven na radioembolisatie in kaart te brengen. Hopelijk gaan we meer van jou zien!

Stichting Beeldgestuurde Behandelingen van Kanker, beste Martha, dank voor de interesse en vertrouwen die jij en Wilt in mij hebben getoond. Wilt heeft een stichting nagelaten om trots op te zijn!

Alexandre Suerman stipendium, prof. Paul Coffer, Lucette Teurlings, en de selectiecommissie, mijn dank voor dit genereuze stipendium waarmee medisch studenten worden aangemoedigd een wetenschappelijke carrière te beginnen. Mijn dank gaat ook uit naar mijn Alexandre Suerman collega's voor het delen van ervaringen en vermakelijke masterclasses.

Quirem Medical, beste Jan, Jan-Remt en Frank, dank voor de ondersteuning van dit proefschrift met mede daardoor een ongekende oplage. Ik merk dat de voortgang van holmium microsferen in een stroomversnelling is gekomen sinds de oprichting van Quirem Medical. Ik wens jullie veel succes met de valorisatie van holmium microsferen.

Collega arts-onderzoekers

Jip Prince en Andor van den Hoven, ik ben blij dat de toekomst van het holmium-onderzoek in goede handen is en ik hoop dat we de aankomende jaren op dit vlak kunnen blijven samenwerken. Marnix van Herwaarden, eeuwige verhalenverteller, bedankt voor de gezellig tijd en adviezen op allerlei vlakken. Joris Niesten, Thijs Braber, in deze zin wil ik jullie graag bedanken voor nooit een saai moment. Ik kijk met plezier terug op de tafelvoetbalcompetitie met jullie allen. Ik vraag me nog steeds over sommige schoten af of ze überhaupt wel konden. Ik zal het missen!

Joost Wijlemans, Charlotte Rosenbaum, Merel Huisman, Susanne Diepstraten, kamergenoten. Floor, Dominica, Wouter, Anouk & Anouk, Martin, Pushpa, Richard, Arthur, Alexander, Gisela, Erika, Marleen, Hamza, Laura, Jill, Marlijne, Hanke, Bertine, Björn & Alexandra, en alle andere arts-onderzoekers van onze divisie. Ik denk dat we trots op mogen zijn op de collegialiteit binnen onze groep. Ik kijk terug op een mooie periode en ik wens jullie alle succes.

International colleagues

Prof. dr. L. Defreyne, beste Luc, hartelijk dank voor de gastvrijheid tijdens mijn stage in Gent. U heeft mij geleerd door te zoeken naar de ware oorzaak van een fenomeen. Ik zal ook de kalfsniertjes van onze culinaire expedities in Luik niet vergeten! Mijn dank gaat ook uit naar alle andere VINRAD-collega's in Gent, in het bijzonder dr. Peter van Langenhoven.

Prof. dr. B. Daniel, dear Bruce, I was honored to work under your supervision at Stanford University. Your great insight and knowledge were inspiring. I also learned

the value of collaborating with non-medical disciplines like mechanical- and electrical engineering. I would like to thank the numerous people at Stanford who helped me a lot and made my time very enjoyable, especially: Elena Kaye, Shanthi Elayaperumal, Andrew Holbrook, prof. dr. Graham Sommer, Andrew Wentland, Wendy Gardner, and Yamil Saenz.

Vrienden en familie

Tot slot wil ik graag van deze unieke gelegenheid gebruik maken om mijn vrienden en familie te bedanken.

Vrienden, team- en studiegenoten: Ivo Tanis, Thijs Campschroer, Sander Barentsz, Stefan Coppens, Bert van Enter, Daan Bäckes, Frank van Schendel, Peter-Paul Zwetsloot, Dino Colo, en de mannen van Phoenix Heren 3. Jullie hebben voor de nodige ontspanning en vermaak gezorgd tijdens mijn studie- en promotietijd.

Ian Charles, Steve Baran, Mark Wossidlo, Julia Arand, Cesar Corona, R.J. Davis, and Sarah Loesby, thanks for the wonderful time during my stay in the States!

Maarten Barentsz en Michel Teuben, paranimfen, bedankt dat jullie mij op deze belangrijke dag willen ondersteunen. Michel, er is niemand met wie ik zo veel weddenschappen ben aangegaan als met jou. Afgezien van de vele kratjes die zijn uitgewisseld, denk ik dat dit tot de goede eigenschap heeft geleid dat we nu allebei niet snel meer iets beweren als we het niet zeker weten. Onderzoek doen naast de studie was onze common ground. Dat we dezelfde onderzoeksbeurs hebben ontvangen is misschien geen toeval. Maarten, jij en je broer Sander zijn zo verschillend, toch heb ik met jullie beiden een sterke vriendschap opgebouwd. Als collega's met naastgelegen bureaus hielden we het vrij goed uit met elkaar uit dus besloten we ook samen te gaan hockeyen. Het doet me deugd dat jij nu ook voor een half jaar naar Stanford bent gegaan.

Familie de Wilde: Roeland, Pauline, Roeland, Wies en Sofieke. Dank voor jullie gezelligheid en oprechte interesse in mijn onderzoek.

Bovenal wil ik mijn familie bedanken: Opa en oma Smits, opa en oma Retera, ooms, tantes, neefjes en nichten. Jullie hebben altijd veel belangstelling getoond in mijn onderzoek.

Papa en Mama, bedankt voor de interesse die jullie altijd in mijn wetenschappelijke carrière hebben getoond en de bijhorende raad. Gelukkig kan ik altijd bij jullie terecht. Papa, ik kon me geen betere raadgever bedenken dan iemand wiens loopbaan zoveel gelijken vertoont en altijd het beste met mij voor heeft.
Zus en broers, lieve Cathelijne, Laurent en Roeland, jullie zijn mijn beste vrienden, ik koester onze sterke gezinsband.

Liefste Marlieke, ik heb je lang geplaagd dat dit proefschrift ondanks jou tot stand is gekomen, maar het tegengestelde is waar. In naam van de wetenschap heb jij mij voor lange tijd naar het buitenland zien vertrekken en heb ik vele avonden en zaterdagen gewerkt. Samen met jou zijn is voor mij het grootste geluk en ik ben je zeer dankbaar voor je eindeloze liefde!